Stabilised Finite Element Approximation for Degenerate Convex Minimisation Problems

D I S S E R T A T I O N

zur Erlangung des akademischen Grades

Dr. rer. nat.
im Fach Mathematik

eingereicht an der
Mathematisch-Naturwissenschaftlichen Fakultät II
Humboldt-Universität zu Berlin

von
Dipl.-Math. Wolfgang Josef Boiger

Präsident der Humboldt-Universität zu Berlin:
Prof. Dr. Jan-Hendrik Olbertz

Dekan der Mathematisch-Naturwissenschaftlichen Fakultät II:
Prof. Dr. Elmar Kulke

Gutachter:
1. Prof. Dr. Carsten Carstensen, HU Berlin
2. Prof. Dr. Sören Bartels, Universität Freiburg
3. Prof. Dr. Eun-Jae Park, Yonsei University Seoul

Tag der mündlichen Prüfung: 04. Juli 2013

Abstract

Infimising sequences of nonconvex variational problems often do not converge strongly in Sobolev spaces due to fine oscillations. These oscillations are physically meaningful; finite element approximations, however, fail to resolve them in general. Relaxation methods replace the nonconvex energy with its (semi)convex hull. This leads to a macroscopic model which is degenerate in the sense that it is not strictly convex and possibly admits multiple minimisers. The lack of control on the primal variable leads to difficulties in the a priori and a posteriori finite element error analysis, such as the reliability-efficiency gap and no strong convergence.

To overcome these difficulties, stabilisation techniques add a discrete positive definite term to the relaxed energy. Bartels et al. (IFB, 2004) apply stabilisation to two-dimensional problems and thereby prove strong convergence of gradients. This result is restricted to smooth solutions and quasi-uniform meshes, which prohibit adaptive mesh refinements.

This thesis concerns a modified stabilisation term and proves convergence of the stress and, for smooth solutions, strong convergence of gradients, even on unstructured meshes. Furthermore, the thesis derives the so-called flux error estimator and proves its reliability and efficiency. For interface problems with piecewise smooth solutions, a refined version of this error estimator is developed, which provides control of the error of the primal variable and its gradient and thus yields strong convergence of gradients. The refined error estimator converges faster than the flux error estimator and therefore narrows the reliability-efficiency gap. Numerical experiments with five benchmark examples from computational microstructure and topology optimisation complement and confirm the theoretical results.

Zusammenfassung

Infimalfolgen nichtkonvexer Variationsprobleme haben aufgrund feiner Oszillationen häufig keinen starken Grenzwert in Sobolevräumen. Diese Oszillationen haben eine physikalische Bedeutung; Finite-Element-Approximationen können sie jedoch im Allgemeinen nicht auflösen. Relaxationsmethoden ersetzen die nichtkonvexe Energie durch ihre (semi)konvexe Hülle. Das entstehende makroskopische Modell ist degeneriert: es ist nicht strikt konvex und hat eventuell mehrere Minimalstellen. Die fehlende Kontrolle der primalen Variablen führt zu Schwierigkeiten bei der a priori und a posteriori Fehlerschätzung, wie der Zuverlässigkeits-Effizienz-Lücke und fehlender starker Konvergenz.

Zur Überwindung dieser Schwierigkeiten erweitern Stabilisierungstechniken die relaxierte Energie um einen diskreten, positiv definiten Term. Bartels et al. (IFB, 2004) wenden Stabilisierung auf zweidimensionale Probleme an und beweisen dabei starke Konvergenz der Gradienten. Dieses Ergebnis ist auf glatte Lösungen und quasi-uniforme Netze beschränkt, was adaptive Netzverfeinerungen ausschließt.

Die vorliegende Arbeit behandelt einen modifizierten Stabilisierungsterm und beweist auf unstrukturierten Netzen sowohl Konvergenz der Spannungstensoren, als auch starke Konvergenz der Gradienten für glatte Lösungen. Ferner wird der sogenannte Fluss-Fehlerschätzer hergeleitet und dessen Zuverlässigkeit und Effizienz gezeigt. Für Interface-Probleme mit stückweise glatter Lösung wird eine Verfeinerung des Fehlerschätzers entwickelt, die den Fehler der primalen Variablen und ihres Gradienten beschränkt und so starke Konvergenz der Gradienten sichert. Der verfeinerte Fehlerschätzer konvergiert schneller als der Fluss-Fehlerschätzer, und verringert so die Zuverlässigkeits-Effizienz-Lücke. Numerische Experimente mit fünf Benchmark-Tests der Mikrostruktursimulation und Topologieoptimierung ergänzen und bestätigen die theoretischen Ergebnisse.

Contents

1 Introduction

The calculus of variations addresses the minimisation of energy functionals which are mappings from a suitable space of functions into the real numbers. This thesis aims at the numerical solution of minimisation problems in computational microstructure and topology optimisation.

The first well-known problem of the calculus of variations is probably the brachistochrone curve problem posed by Johann Bernoulli in 1696. Its goal is to determine a curve between two points such that a mass, starting at the first point and travelling on the curve under the influence of gravity, reaches the second point in minimal time. The solution, i.e., the curve which minimises a time functional, is the cycloid illustrated in Figure 1.1. After several centuries of intense mathematical research, today problems in the calculus of variations arise naturally in the context of scientific and industrial simulations. Examples thereof include phase transitions in shape-memory alloys, elastoplastic deformations (Martin, 1975), computational microstructure (Luskin, 1996; Dolzmann, 2003), micromagnetism (Prohl, 2001), topology optimisation problems (Kohn and Strang, 1986), to name but a few. The mathematical models behind such problems are, in general, nonlinear and do not permit for an explicit solution. Therefore one employs numerical methods to obtain an approximate solution. However, even the simplest model problems of the aforementioned classes are not (quasi-)convex in general, which causes severe difficulties (Carstensen, 2001): infimising sequences develop strong oscillations with no classical limit in the sense of Sobolev functions (see below for an explanation of the term "infimising"). A finite element discretisation can exhibit clusters of local solutions, which might lead the numerical solver astray. Furthermore, fine grids are required to resolve the oscillations.

Figure 1.1: A cycloid, the solution of the brachistochrone curve problem

This thesis concerns relaxed variational problems. While the measure-valued minimiser of a nonconvex problem describes *microscopic* properties of the solution, minimisers of a convexified version of the problem describe the *macroscopic* behaviour. In contrast to the nonconvex model, the convexified model in general admits a weak minimiser in the sense of Sobolev functions. The convexification of a nonconvex energy functional is not at all strictly convex, which causes difficulties for finite element discretisations: the solution of such a problem is possibly not unique. Furthermore, solution algorithms based on Newton-Raphson schemes rely on the Hessian matrix of a discrete energy functional. The lack of strict convexity can lead to situations where the Hessian is singular and may cause the solver to fail (Bartels et al., 2004b). As a remedy, this thesis proposes stabilisation methods which regularise the energy functional with an additional, strictly convex term. Error estimators are required to control the error and the mesh refinements of adaptive finite element algorithms. However, well-established error estimators are not compatible with stabilisation methods. This thesis develops new error estimators which are suitable

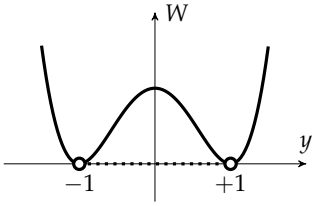

Figure 1.2: Two-well energy density W of the one-dimensional minimisation problem (1.1), and its convex hull (dotted)

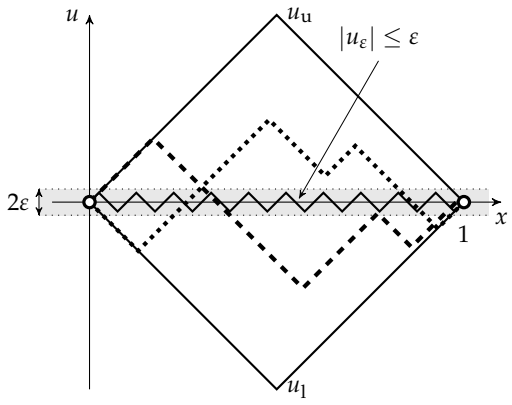

Figure 1.3: Illustration of solutions of the one-dimensional minimisation problem (1.1). For $\alpha = 0$ all depicted functions are solutions, e.g., u_u, u_l, u_ε, as well as functions represented by the dashed and dotted lines. For $\alpha > 0$ highly oscillating functions like u_ε form infimising sequences for $\varepsilon \to 0$.

to control the adaptivity in the presence of stabilisation.

Microstructure in One Dimension

To illustrate the implications of nonconvex minimisation problems we consider a simple example in one dimension which is essentially due to Bolza (1902), see also Young (1969) and Carstensen (2006, Examples 1.7–1.8).

Given the open interval $\Omega :=]0,1[$, let $\mathcal{A} := W_0^{1,4}(\Omega)$ be the space of absolutely continuous L^4 functions v on Ω which satisfy $v(0) = 0 = v(1)$ and $v' \in L^4(\Omega)$. Note that the derivative of an absolutely continuous function exists almost everywhere in the sense of Lebesgue measures. Let further $W(y) := (y^2-1)^2$ for $y \in \mathbb{R}$. The example problem reads for $\alpha \geqslant 0$

$$\text{minimise } E(u) := \int_0^1 \left(W(u'(x)) + \alpha u(x)^2\right) \mathrm{d}x \quad \text{amongst } u \in \mathcal{A}. \tag{1.1}$$

Figure 1.2 illustrates the energy density W. Clearly W prefers functions u with a derivative $u'(x)$ which is approximately ± 1 ("prefer" meaning that W rewards such functions with low energy values). A sequence of functions $\left(u_j\right)_{j\in\mathbb{N}} \subset \mathcal{A}$ is called an *infimising sequence* if

$$\lim_{j\to\infty} E(u_j) = \inf_{u\in\mathcal{A}} E(u).$$

An infimising sequence $\left(u_j\right)_{j\in\mathbb{N}}$ is called *minimising sequence* if the infimum is actually attained by the energy, i.e., if there exists a $u_0 \in \mathcal{A}$ such that

$$\lim_{j\to\infty} E(u_j) = \inf_{u\in\mathcal{A}} E(u) = \min_{u\in\mathcal{A}} E(u) = E(u_0).$$

Assume $\alpha = 0$. By the construction of E and of W we have $E(u) \geqslant 0$ for all $u \in \mathcal{A}$. The functions $u_\mathrm{l}(x) = |x| - 1$ and $u_\mathrm{u}(x) = 1 - |x|$ are solutions of (1.1) as they are in $\mathcal{A}$ with $E(u_\mathrm{l}) = E(u_\mathrm{u}) = 0$. This also holds for any Lipschitz continuous function u with $u_\mathrm{l} \leqslant u \leqslant u_\mathrm{u}$ and $|u'| = 1$ almost everywhere in Ω. Figure 1.3 depicts some examples of such solutions u together with u_l and u_u.

The situation is quite different for $\alpha > 0$. Clearly the energy satisfies

$$E(u) \geqslant \alpha \|u\|^2_{L^2(\Omega)} \geqslant 0.$$

For a sufficiently small $\varepsilon > 0$ we define the zig-zag function $u_\varepsilon \in \mathcal{A}$ via

$$u_\varepsilon \coloneqq \min\{u_\mathrm{u}, \max\{u_\mathrm{l}, w_\varepsilon\}\} \quad \text{with } w_\varepsilon(x) \coloneqq \begin{cases} x & \text{for } -\varepsilon \leqslant x \leqslant \varepsilon, \\ 2\varepsilon - x & \text{for } \varepsilon \leqslant x \leqslant 3\varepsilon \text{ and} \\ w_\varepsilon(x - 4\varepsilon) & \text{for } x \geqslant 3\varepsilon. \end{cases}$$

Figure 1.3 illustrates u_ε. We have $W(u_\varepsilon(x)) = 0$ for almost every $x \in \Omega$, and furthermore

$$E(u_\varepsilon) = \alpha \|u_\varepsilon\|^2_{L^2(\Omega)} \leqslant \alpha\varepsilon^2 \to 0 \text{ as } \varepsilon \to 0.$$

Hence $(u_\varepsilon)_{\varepsilon \to 0}$ forms an infimising sequence which exhibits increasingly fine oscillations called microstructure. However, the limit $u_\infty \equiv 0$ of u_ε in $L^4(\Omega)$ attains the energy $E(u_\infty) = 1$ and is therefore *not* a minimiser of E. The derivative u'_ε does not have a limit in $L^4(\Omega)$. This means u_ε attains the weak limit $u_\infty \equiv 0$ as $\varepsilon \to 0$, but no strong limit of the derivatives in the sense of Sobolev spaces. In fact, its limit is a measure-valued function which reflects the oscillations between the values ± 1. This is due to the nonconvexity of W.

A numerical approximation of (1.1) is obtained as follows. For a given $N \in \mathbb{N}$ and $h \coloneqq 1/N$ the space

$$\mathcal{A}_h \coloneqq \left\{ v \in \mathcal{C}([0,1]) \,:\, v|_{[(j-1)h, j]} \text{ is affine for } j = 1, \dots, N, \text{ and } v(0) = 0 = v(1) \right\}$$

is a $(N-1)$-dimensional vector space. For $\alpha > 0$, the discrete problem

$$\text{minimise } E(u_h) \text{ amongst } u_h \in \mathcal{A}_h$$

admits two separate global minimisers u_h which are characterised by $u'_h = \pm\sqrt{1 - \alpha h^2/3}$ almost everywhere with alternating sign (Carstensen, 2001, Theorem 8.1). Hence the minimisers reconstruct the oscillations as far as the discrete space $\mathcal{A}_h$ permits. To obtain a fine resolution of the oscillations, the discrete problem therefore requires a high number N of nodes. Apart from the global solutions, the discrete problem allows for multiple local minimisers, which pose an additional difficulty to the numerical solver as it might not be able to detect a global minimum at all.

As a remedy for the difficulties which stem from the lack of convexity, we consider the relaxed problem

$$\text{minimise } E^{\star\star}(u) \coloneqq \int_0^1 \left(W^{\star\star}(u'(x)) + \alpha u(x)^2 \right) \mathrm{d}x \text{ amongst } u \in \mathcal{A}.$$

The convex hull $W^{\star\star}$ of the two-well energy density W reads

$$W^{\star\star}(y) = \begin{cases} 0 & \text{for } |y| \leqslant 1, \\ W(y) & \text{for } |y| \geqslant 1. \end{cases}$$

Figure 1.2 illustrates $W^{\star\star}$. In contrast to the observations above the relaxed problem admits a unique minimiser $u \equiv 0 \in \mathcal{A}$, which is also the (weak) limit of infimising sequences of (1.1). Moreover, $u_h \equiv 0$ is also a unique solution of the discrete relaxed problem

$$\text{minimise } E^{\star\star}(u_h) \text{ amongst } u_h \in \mathcal{A}_h.$$

Note that the condition number of the mass matrix scales with α, hence the problem is ill-conditioned for small α. Nicolaides and Walkington (1995) observed that, under general assumptions, the discrete minimisers of the one-dimensional relaxed problem converge strongly to a solution of the relaxed problem. As it turns out, this observation heralds the effect of stabilisation techniques even in higher dimensions where these methods lead to strong convergence of the gradients.

Historical Outline

In his famous lecture "Mathematical Problems", Hilbert (1900, Problem 23) encouraged his colleagues to further research the calculus of variations, a branch of mathematics which, in his opinion, received less attention than it deserves. The field of nonconvex variational problems gained more attention with the observations of Bolza (1902). That publication shows with a simple one-dimensional example, similar to the example above, that nonconvex energy densities may lead to oscillations in minimising functions. The pioneering work of Young (1938, 1942, 1969) investigates this phenomenon and proposes an extension of the notion of a solution to measure-valued function, so-called Young measures. Such a measure defines a statistic of the gradients of infimising sequences with oscillations.

Dacorogna (1989) provides an exhaustive collection of the state-of-the-art methods in the calculus of variations and dedicates a chapter to nonconvex problems. In this context, Dacorogna's book also presents the various notions of semi-convex hulls and relaxation theorems. The book of Roubíček (1997) concentrates specifically on relaxation methods for problems in the calculus of variations, as well as in optimal control and game theory. Pedregal (1997) presents a systematic analysis of Young measures as a tool to represent oscillations in the solutions of variational problems. Finally, we refer to Luskin (1996) for a survey article on microstructure phenomena with the direct method in the calculus of variations.

Principal Results

This thesis proposes stabilisation methods to overcome the difficulties which arise from degenerate convex problems. To aid adaptive mesh refinements, it also concerns error estimators for stabilised discrete problems. For the remaining part of the introduction, we

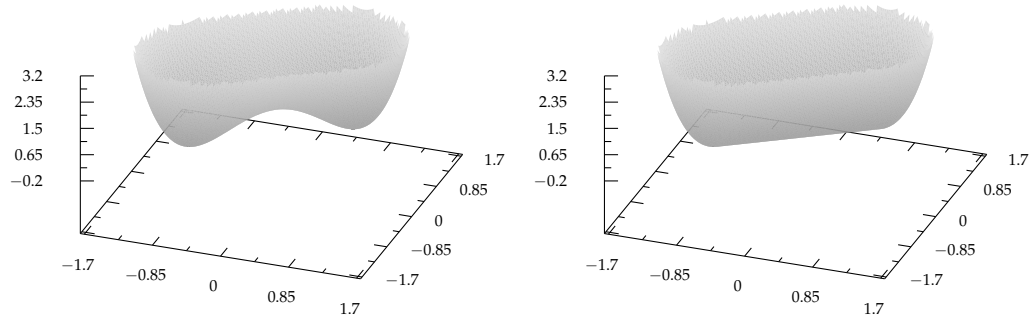

Figure 1.4: Graphs of the energy density functions W (left) and $W^{\star\star}$ (right) of the two-well benchmark of Carstensen and Jochimsen (2003). The convexified energy density $W^{\star\star}$ lacks strict convexity.

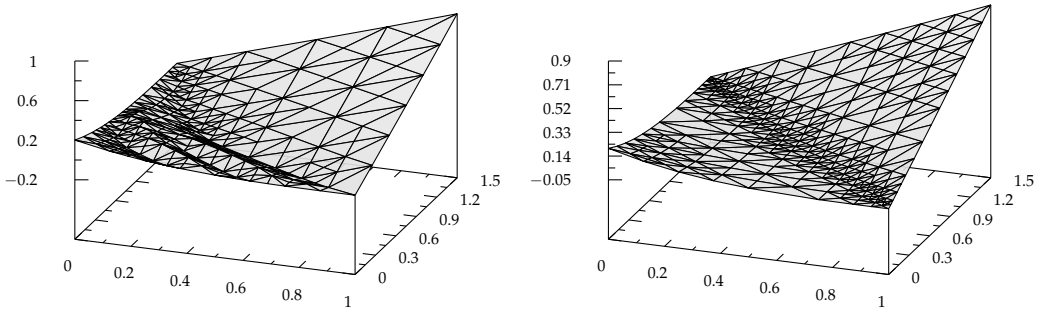

Figure 1.5: Numerical solutions of the two-well benchmark of Carstensen and Jochimsen (2003), with nonconvex (left) and convexified (right) energy density. The adaptive mesh refinements are based on the residual-based error estimator of Section 3.3.

consider the general minimisation problem

$$\text{minimise } E^{\star\star}(v) \coloneqq \int_\Omega W^{\star\star}(\mathrm{D}v(x))\mathrm{d}x + \text{lower-order terms} \;\; \text{amongst } v \in H^1_0(\Omega) \quad (1.2)$$

with a (possibly degenerate) convex energy density $W^{\star\star}$. Figure 1.4 depicts graphs of the nonconvex two-well energy density W and its convexification $W^{\star\star}$ from the two-dimensional benchmark examples of Carstensen and Jochimsen (2003) (cf. Section 2.3).

A discrete version of (1.2) replaces the set $H^1_0(\Omega)$ of admissible functions with the finite-dimensional space of conforming P_1 finite element functions $\mathcal{S}_1(\mathcal{T}_\ell)$, given on the triangulation $\mathcal{T}_\ell$ of Ω. Stabilisation methods add a positive definite bilinear form $a_\ell(\cdot,\cdot)$ (which depends on the triangulation $\mathcal{T}_\ell$) to the energy of the discrete problem and lead to the stabilised problem

$$\text{minimise } E^{\star\star}_\ell(v_\ell) \coloneqq E^{\star\star}(v_\ell) + \frac{1}{2}a_\ell(v_\ell, v_\ell) \;\; \text{amongst } v_\ell \in \mathcal{A}_\ell \coloneqq H^1_0(\Omega) \cap \mathcal{S}_1(\mathcal{T}_\ell). \quad (1.3)$$

See Chapter 2 for a rigorous introduction of Sobolev spaces and of the model problem (1.2), and Chapter 3 for a formal definition of triangulations and a presentation of the discrete problem. Figure 1.5 shows numerically obtained solutions of the two-dimensional benchmark examples of Carstensen and Jochimsen (2003) with the two-well energy

density of Figure 1.4. The nonconvex energy density causes oscillations which are clearly visible in Figure 1.5.

Chapter 4 of the thesis investigates the particular stabilisation function

$$a_\ell(v,w) \coloneqq H_\ell^2 \sum_{F\in\mathcal{F}_\ell^\Omega} h_F^{-1} \int_F [\mathrm{D}v]_F : [\mathrm{D}w]_F \,\mathrm{d}s, \tag{1.4}$$

and derives error estimators for the stabilised problem. Here, H_ℓ denotes the global mesh size of the triangulation, $[\mathrm{D}v]_F$ is the jump of the gradient of v along the interior side F, and h_F is the diameter of the side F. For some $\alpha \geqslant 0$ which depends on the lower-order terms of (1.2), Theorem (4.2.3) provides the general convergence result

$$\|\sigma - \sigma_\ell\|_{L^2(\Omega)} + \alpha \|u - u_\ell\|_{L^2(\Omega)} \to 0 \;\text{ as } H_\ell \to 0,$$

where u and u_ℓ is the solution of the continuous problem (1.2) and the stabilised discrete problem (1.3), respectively, $\sigma \coloneqq \mathrm{D}W^{\star\star}(\mathrm{D}u)$ and $\sigma_\ell \coloneqq \mathrm{D}W^{\star\star}(\mathrm{D}u_\ell)$ are their stress tensors, and H_ℓ is the maximal diameter of all simplices in $\mathcal{T}_\ell$. This result, which does not require any additional smoothness assumptions on the solution u, indicates that the stabilisation term maintains convergence of the discrete problem.

For highly smooth solutions $u \in H^{3/2+\varepsilon}(\Omega)$ (with some $\varepsilon > 0$) which are $\mathcal{T}_\ell$-piecewise in H^2, Theorem (4.2.1) even guarantees convergence of the gradients

$$\|u - u_\ell\|_{H^1(\Omega)} \lesssim H_\ell^{1/2}, \tag{1.5}$$

where "$\lesssim$" means "$\leqslant$" up to a multiplicative constant which is independent of crucial values like the mesh size of the triangulation $\mathcal{T}_\ell$. The convergence result (1.5) extends Bartels et al. (2004b), who observe the same convergence behaviour for different choices of stabilisation functions a_ℓ, from quasi-uniform to general shape-regular triangulations. This extension is an important step towards adaptive finite element methods, which, in general, generate triangulations that lack quasi-uniformity.

Well-established error estimators for the discrete problem without stabilisation depend on an important property of the discrete problem, the so-called Galerkin orthogonality. The added stabilisation term annihilates the Galerkin orthogonality and thereby precludes a proof of reliability for these error estimators. Theorem (4.3.1) circumvents the lack of Galerkin orthogonality and proves that any $\tau \in H(\mathrm{div},\Omega)$ satisfies

$$\begin{gathered}\|\sigma - \sigma_\ell\|_{L^2(\Omega)}^2 + \alpha \|u - u_\ell\|_{L^2(\Omega)}^2 \lesssim m_2(\tau)\, |u - u_\ell|_{H^1(\Omega)} \lesssim m_2(\tau) \\ \text{with}\;\; m_2(\tau) \coloneqq \|\sigma_\ell - \tau\|_{L^2(\Omega)} + \|\Pi_\ell\Lambda_\ell + \mathrm{div}\,\tau\|_{L^2(\Omega)} + \text{h.o.t.}\end{gathered} \tag{1.6}$$

Here $\Pi_\ell\Lambda_\ell$ is essentially the L^2 projection of the lower-order terms of (1.2) and "h.o.t." abbreviates terms which are of higher order in general and therefore not significant to the estimate. Theorem (4.3.2) shows that a suitably chosen $\tau \in H(\mathrm{div},\Omega)$ also yields a lower bound on the error, which reads

$$\|\sigma_\ell - \tau\|_{L^2(\Omega)} + \|\Pi_\ell\Lambda_\ell + \mathrm{div}\,\tau\|_{L^2(\Omega)} \lesssim \|\sigma - \sigma_\ell\|_{L^2(\Omega)} + \alpha \|u - u_\ell\|_{L^2(\Omega)} + \text{h.o.t.}. \tag{1.7}$$

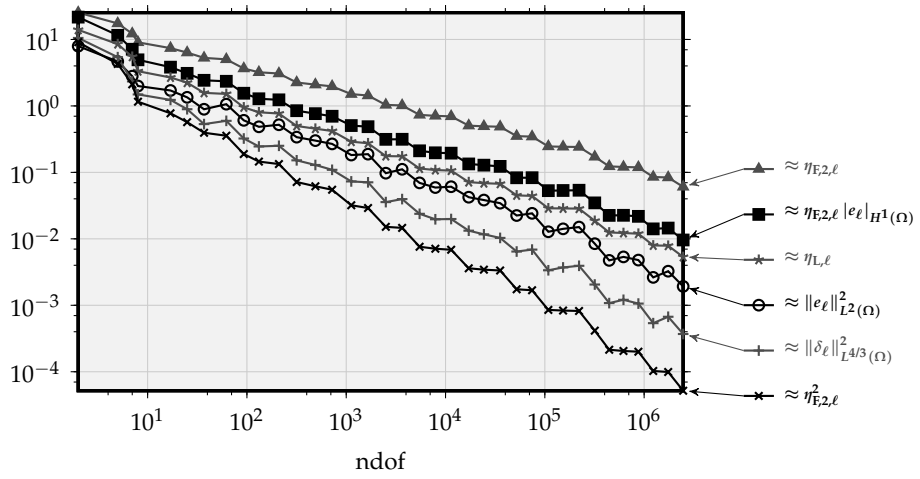

Figure 1.6: The errors $e_\ell \coloneqq u - u_\ell$ and $\delta_\ell \coloneqq \sigma - \sigma_\ell$ of the convexified two-well benchmark of Carstensen and Jochimsen (2003) are bounded from above by $\eta_{\mathrm{F},2,\ell}$ and from below by $\eta^2_{\mathrm{F},2,\ell}$. The reliability-efficiency gap between these bounds is narrowed with the improved error estimator $\eta_{\mathrm{L},\ell}$. The error δ_ℓ is measured in the $L^{4/3}$ norm, which fits the growth of the energy density $W^{\star\star}$. The symbol "$\approx$" indicates that the graphs are rescaled, i.e., shifted vertically, to prevent intersections and emphasise the difference of their slopes.

Thereby, Theorems (4.3.1) and (4.3.2) demonstrate that $m_2(\tau)$ is an upper and a lower bound on the error of the discrete solution. The minimum of $m_2(\tau)$ amongst all τ in the space $RT_0(\mathcal{T}_\ell)$ of Raviart-Thomas functions is the *flux error estimator*

$$\eta_{\mathrm{F},2,\ell} \coloneqq \min_{\tau_\ell \in RT_0(\mathcal{T}_\ell)} m_2(\tau_\ell)\,.$$

Carefully note the differing exponents of the errors in (1.6) and (1.7). A consequence of this difference is that the upper and the lower bound of the error converge to zero *with different convergence rates* for $H_\ell \to 0$. Figure 1.6 illustrates this phenomenon called *reliability-efficiency gap*. We have (1.5) for highly smooth solutions u. However, in the general case we can merely provide the pessimistic estimate $|u - u_\ell|_{H^1(\Omega)} \lesssim 1$ in (1.6). The lack of a better estimate is the source of the reliability-efficiency gap.

In order to narrow the reliability-efficiency-gap and thereby obtain tighter error control, this thesis investigates interface problems which are characterised by a piecewise smooth and globally Lipschitz continuous solution, and which appear naturally in phase transition scenarios. The class of interface problems contains the two-well benchmark of Carstensen and Jochimsen (2003) (see Figure 1.7) and the three-well benchmark of Bartels (2001) (see Figure 1.8), which is introduced in Section 2.4. Theorem (4.4.1) derives an improved upper bound on $|u - u_\ell|_{H^1(\Omega)}$ for interface problems, which in turn leads to the error estimators $\eta_{\mathrm{L},\ell}$ and $\eta_{\mathrm{H},\ell}$ which satisfy

$$\|u - u_\ell\|_{L^2(\Omega)} \lesssim \eta_{\mathrm{L},\ell} \lesssim \eta_{\mathrm{F},2,\ell} \quad \text{and} \quad |u - u_\ell|_{H^1(\Omega)} \lesssim \eta_{\mathrm{H},\ell}$$

and thereby lead to strong H^1 convergence. Figure 1.6 also depicts the graph of $\eta_{\mathrm{L},\ell}$ and indicates that it converges faster than $\eta_{\mathrm{F},2,\ell}$, narrowing the reliability-efficiency gap. Figure

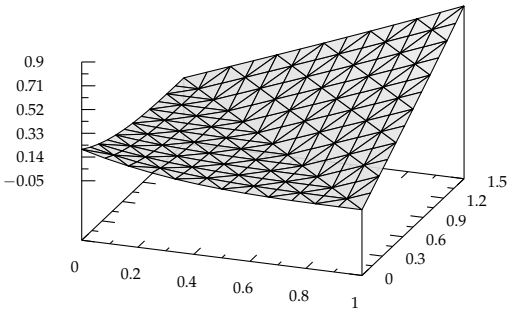

Figure 1.7: Nodal interpolation of the exact solution u of the convexified two-well problem of Carstensen and Jochimsen (2003). The derivative Du is discontinuous along the line $\{x \in \mathbb{R}^2 : x \cdot (3,2) = 3\}$.

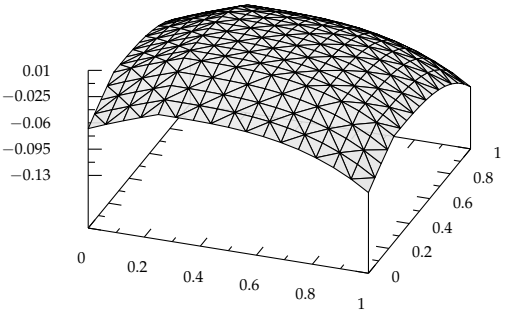

Figure 1.8: Nodal interpolation of the exact solution u of the convexified three-well problem of Bartels (2001). The derivative Du is discontinuous along the lines $\{x \in \mathbb{R}^2 : x_1 = 1/4\}$ and $\{x \in \mathbb{R}^2 : x_2 = 1/4\}$.

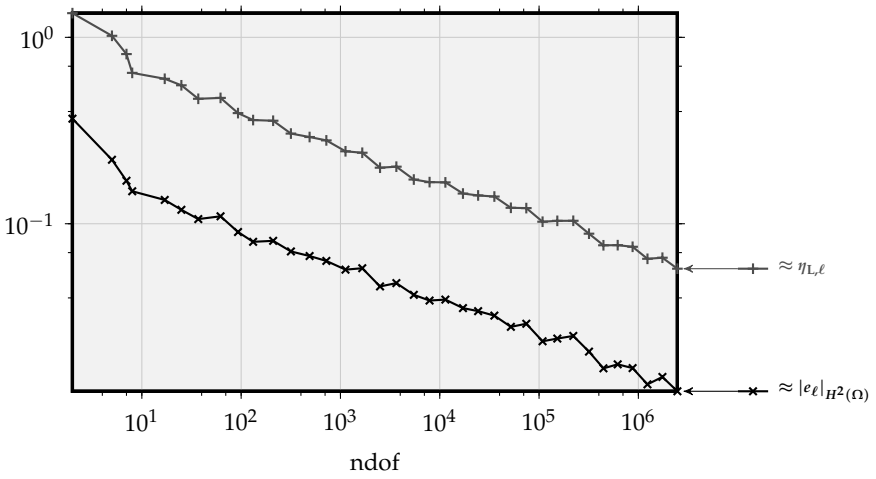

Figure 1.9: The error estimator $\eta_{\mathrm{H},\ell}$ is an upper bound of the error $e_\ell := u - u_\ell$ in the H^1 semi-norm. The symbol "$\approx$" indicates that the graphs are rescaled, i.e., shifted vertically, to emphasise the similarity of the slopes.

1.9 illustrates that $\eta_{\mathrm{H},\ell}$ is actually an excellent guess for the error $|u - u_\ell|_{H^1(\Omega)}$.

Conclusions and Outlook

The aforementioned theoretical results guarantee that the stabilisation methods yield a regularisation of degenerate convex problems and even enable strong convergence of the gradients under certain circumstances. The flux error estimator is a guaranteed upper bound of the error of the stabilised discrete problem. The error estimators for interface problems actually improve the flux error estimator and thereby narrow the reliability-efficiency gap. The numerical experiments of Chapter 5 provide striking numerical evidence in favour of these results. However, they also show that the convergence rates of the stabilised problem fall short of the convergence of the discrete problem without stabilisation (cf. Section 5.7). In particular, the convergence rates of the stabilised discrete

problem are *lower* with adaptive mesh refinements than with uniform mesh refinements. This suggests that, despite the local parameter h_F, the stabilisation function (1.4) is not well-suited for adaptive finite element methods. The a priori convergence theorems of this thesis depend on the assumption $H_\ell \to 0$, which is *not* guaranteed by adaptive mesh refinements. Future research is necessary to develop an adaptive algorithm and a stabilisation which ensure convergence even with adaptive mesh refinements. A possible approach are nonconforming finite element functions, such as Crouzeix-Raviart functions, and discontinuous Galerkin schemes. The stabilisation of (1.4) penalises jumps along the sides of a triangulation and can be interpreted as a penalty term for higher order derivatives. While (1.4) mimics an H^2 norm, a $W^{2,p}$ norm appears more appropriate, where p matches the growth of the energy density. Such research is, however, far beyond the scope of this thesis.

Structure of the Thesis

The content of the remaining parts of the thesis is structured as follows. Chapter 2 introduces the mathematical model which is at the heart of the thesis. Section 2.1 presents a concise definition of Sobolev spaces and collects well-known results which are used frequently in subsequent chapters. The definitions also encompass Sobolev spaces on surfaces and fractional Sobolev spaces. Amongst the results are well-established theorems like the trace theorem and Poincaré's and Friedrichs' inequalities. Section 2.2 presents a very general class of degenerate convex problems in two and three dimensions. This presentation includes the set of admissible functions with Dirichlet boundary conditions and, most importantly, growth conditions on the energy density. Note that the model problem of Section 2.2 is commonly called "continuous" problem to distinguish it from the "discrete" problem of Section 3.2. Section 2.2 also gives existence and uniqueness results for the continuous problem. Sections 2.3, 2.4 and 2.5 present three benchmark problems (plus two variations thereof) which comply with the general framework of Section 2.2. These problems exhibit several features which cause difficulties for numerical algorithms. They serve as example cases during the numerical experiments in Chapter 5.

Chapter 3 aims at a discretisation of the model problem of Section 2.2 with P_1 conforming finite elements. Section 3.1 defines regular triangulations in the sense of Ciarlet (2002) and introduces some notation which is necessary for the remaining sections. It also defines several discrete function spaces, like P_1 conforming functions and Raviart-Thomas functions, presents interpolation operators for these function spaces and derives interpolation error estimates. With the tools of Section 3.1 at hand, Section 3.2 establishes a discretisation of the continuous model problem of Section 2.2, based on P_1 conforming finite element functions. Akin to Section 2.2 we give existence and uniqueness results for the discrete problem. Sections 3.3 and 3.4 present the well-established residual-based a posteriori error estimator and the averaging a posteriori error estimator for the discrete problem and prove their reliability and efficiency. Furthermore, the theory of Section 3.3 yields an a priori error estimate. The arguments and observations of Section 3.3 are also significant for the error analysis of Chapter 4. Therefore this section provides full proofs of most of its results. Section 3.5 provides an introduction to stabilisation methods with the help of Tikhonov regularisation of linear systems. Bartels et al. (2004b) observed strong H^1 convergence for stabilised problems on two-dimensional quasi-uniform triangulations.

We state their results, then define the stabilisation function of Boiger and Carstensen (2010) which is at the core of Chapter 4. Finally, Section 3.5 establishes the *stabilised discrete* problem and proves existence and uniqueness results.

Chapter 4 is dedicated to the error analysis of the stabilised discrete problem. Sections 4.1 and 4.2 concern a priori error control. Section 4.1 presents the proof of H^1 convergence for stabilised problems with quasi-uniform triangulations and smooth solutions. The proof applies to a stabilisation of Bartels et al. (2004b) as well as the stabilisation of Boiger and Carstensen (2010) and generalises the result of Bartels et al. (2004b) to a larger class of problems. Section 4.2 proves that the stabilisation of Boiger and Carstensen (2010) ensures H^1 convergence even on triangulations which lack quasi-uniformity. This section also presents a convergence result for the L^2 error which does not depend on additional smoothness conditions of the solution.

The remaining part of the thesis concerns the effects of the stabilisation function of Boiger and Carstensen (2010). The proofs of reliability of the error estimators of Sections 3.3 and 3.4 fail for the stabilised problem, due to the lack of Galerkin orthogonality. Therefore Section 4.3 derives the *flux error estimator* and proves its reliability and efficiency for arbitrary discrete solutions. Since the flux error estimator suffers from the reliability-efficiency gap, Section 4.4 considers interface problems. Such problems are characterised by a piecewise smooth solution and permit a refinement of the flux error estimator, which leads to an a posteriori error estimate for the error of the primal variable in the L^2 and the H^1 norms.

Chapter 5 explains the algorithms which implement the discrete problems and evaluates the results of numerical experiments. Section 5.1 introduces the basic loop of the adaptive finite element method, which consists of the actual computation of a discrete solution as well as error estimation and refinement of the underlying triangulation. Section 5.2 details the error estimation. Thereby it references the error estimators of Sections 3.3, 3.4, 4.3 and 4.4. Section 5.2 also introduces the concept of refinement indicators and presents Dörfler marking as our strategy of choice to decide which elements of the current triangulation deserve refinement. Section 5.3 provides the algorithm for the refinement itself. Section 5.4 studies the effects of parameters which control the intensity of the stabilisation. Since the computation of the flux error estimator includes a nonlinear minimisation problem on its own, Section 5.5 describes an efficient algorithm to obtain an approximate solution of this problem. This algorithm reduces the computational costs of the minimisation to the solution process of at most three linear systems, and it guarantees that the resulting error estimator is an upper bound of the error. Section 5.6 explains the discrete setup for the benchmark examples, in particular the choice of the initial triangulation. It also collects the observations from the numerical experiments and comments on them in the light of the theoretical results of Chapter 4. Finally, Section 5.7 gives a critical analysis of the various observations. It turns out that the stabilisation actually improves the condition number of the discrete problem. However, in most cases the convergence behaviour appears to be inferior in comparison to the convergence of the unstabilised problems. The improved error estimators of Section 4.4 indeed lead to refined error control and narrow the reliability-efficiency gap.

The convergence graphs of the principal experiments are laid out in Appendix A. Appendix B introduces the MATLAB implementation which realises the experiments and visualisations of Chapter 5. Appendix C provides an index of common notational

symbols which are used throughout this thesis.

Acknowledgements

The author wishes to thank Prof. Carsten Carstensen and his working group, in particular Christian Merdon and Hella Rabus, for all the discussions which contributed new ideas and insights to this thesis. Moreover, the author thankfully acknowledges the support of the Deutsche Forschungsgemeinschaft (DFG) through the Research Training Group 1128 "Analysis, Numerics, and Optimization of Multiphase Problems" and Research Group 797 "Microplast", the support of National Research Foundation of Korea (NRF) through the World Class University (WCU) programme, as well as support of the Berlin Mathematical School (BMS).

2 Mathematical Model

This thesis concerns the model minimisation problem

$$\text{minimise } E^{\star\star}(v) \coloneqq \int_\Omega \Big(W^{\star\star}(\mathrm{D}v(x)) + \alpha \, |v(x) - f(x)|^2 - g(x) \cdot v(x) \Big) \, \mathrm{d}x$$

amongst some suitable set of admissible functions. The energy density $W^{\star\star}$ is assumed to be convex. Commonly it is the convex hull of some nonconvex energy density and therefore degenerate, at least in the example problems of the thesis. The goal of this chapter is to formally introduce the model problem together with important assumptions and results.

The chapter is structured as follows: Section 2.1 introduces the necessary functional analytic setting for the model problem as well as for the remaining chapters. It defines Sobolev spaces in a very general form and presents prominent results. An important prerequisite is familiarity with Lebesgue spaces. Section 2.2 presents the mathematical model which forms the basis of the analysis of the thesis. It states the model problem in its most general form, gives assumptions on parameters and proves existence and uniqueness results. The remaining sections 2.3, 2.4 and 2.5 offer three examples of degenerate convex minimisation problems which comply with the model of Section 2.2. Each of the benchmark examples is the result of the convexification of a nonconvex minimisation problem and is therefore degenerate convex. The experiments of Section 5.6 (page 102) use these problems to study the characteristics of various numerical methods.

2.1 Sobolev Spaces: Definitions and Facts

The goal of this section is to introduce Sobolev spaces and to present important results with minimal notational overhead. The definition of Sobolev spaces follows the trails of Carstensen (2009, Section 0.7) and Grisvard (1985, Chapter 1). See also Brenner and Scott (2002, Chapter 1) and Dacorogna (2004, Section 1.3–1.4) for detailed explanations and proofs.

2.1.1 Domains and Surfaces

To begin with, some concepts of domains and their boundaries are presented. This notation is not pivotal for subsequent chapters, but it is essential for the following definitions. A *domain* is an open connected subset of $\mathbb{R}^d$ for $d \in \mathbb{N}$. For some domain $\Omega \subset \mathbb{R}^d$ denote

$$\mathcal{C}^{k,1}(\Omega) \coloneqq \Big\{ u \in \mathcal{C}^k(\Omega) \,:\, k\text{-th derivative of } u \text{ is Lipschitz continuous} \Big\} \quad \text{for } k \in \mathbb{N}_0.$$

A $\mathcal{C}^{k,1}$-*surface* in $\mathbb{R}^d$ is a set which can locally be represented by (possibly rotated) graphs of $\mathcal{C}^{k,1}$-functions in $\mathbb{R}^{d-1}$. Particularly, a $\mathcal{C}^{0,1}$-surface is a *Lipschitz surface*. Refer to Grisvard (1985, Sections 1.2.1, 1.3.3, pages 5, 19) for a rigorous investigation of such surfaces in the context of Sobolev spaces. In this thesis, Ω is commonly assumed to be a *Lipschitz domain* in $\mathbb{R}^d$, that is, a nonempty, connected, open set such that its boundary $\partial\Omega$ is a Lipschitz surface. Note that due to Rademacher's Theorem (Evans, 1998, Theorem 6, page 281) the outer-pointing unit normal vector $n_{\partial\Omega}$ of a Lipschitz domain Ω exists almost everywhere on the surface $\partial\Omega$.

For the familiar concept of Lebesgue spaces $L^p(\Omega)$ on a domain $\Omega \subset \mathbb{R}^d$, where $1 \leqslant p \leqslant \infty$, recall the definition of the L^p norm

$$\|u\|_{L^p(\Omega;\mathbb{R}^n)} \coloneqq \begin{cases} \left(\int_\Omega |u(x)|_{\ell^2}^p \,\mathrm{d}x\right)^{1/p} & \text{for } p < \infty, \\ \operatorname{esssup}_{x\in\Omega} |u(x)|_{\ell^2} & \text{for } p = \infty \end{cases} \quad \text{for } u \in L^p(\Omega;\mathbb{R}^n).$$

The vector norm $|\cdot|_{\ell^2}$ denotes the usual Euclidian norm in $\mathbb{R}^n$, and esssup is the essential supremum, that is, the supremum up to sets of zero measure. In the following $|\cdot|_{\ell^2}$ is abbreviated with $|\cdot|$ and $\|\cdot\|_{L^p(\Omega;\mathbb{R}^n)}$ with $\|\cdot\|_{L^p(\Omega)}$. Also, while the definitions and results of this section are formulated for scalar valued functions $u \in L^p(\Omega)$, they apply verbatimly to vector-valued functions $u \in L^p(\Omega;\mathbb{R}^n)$.

2.1.2 Sobolev Spaces

Given a domain Ω, the space of *test functions* consists of

$$\mathcal{D}(\Omega) \coloneqq \left\{ u : \mathbb{R}^d \to \mathbb{R} \text{ infinitely differentiable with compact support in } \Omega \right\}.$$

(2.1.1) Definition (Sobolev Norms and Spaces)**.** *For a multi-index $\alpha = (\alpha_1, \ldots, \alpha_d) \in \mathbb{N}_0^d$ of order $|\alpha| \coloneqq \alpha_1 + \cdots + \alpha_d$ let D_α be the corresponding differential operator,*

$$\mathrm{D}_\alpha \coloneqq \frac{\partial^{|\alpha|}}{\partial x_1^{\alpha_1} \cdots \partial x_d^{\alpha_d}}.$$

Let $\Omega \subset \mathbb{R}^d$ be a Lipschitz domain, possibly $\Omega = \mathbb{R}^d$. Let further $1 \leqslant p \leqslant \infty$ and $k \in \mathbb{N}_0$. The Sobolev norms $\|\cdot\|_{W^{k,p}(\Omega)}$ *are given by*

$$\|u\|_{W^{k,p}(\Omega)}^p \coloneqq \sum_{\substack{\alpha\in\mathbb{N}_0^d \\ |\alpha|\leqslant k}} \|\mathrm{D}_\alpha u\|_{L^p(\Omega)}^p \quad \text{for } p < \infty, \quad \text{and} \quad \|u\|_{W^{k,\infty}(\Omega)} \coloneqq \max_{\substack{\alpha\in\mathbb{N}_0^d \\ |\alpha|\leqslant k}} \|\mathrm{D}_\alpha u\|_{L^\infty(\Omega)}.$$

The Sobolev spaces $W^{k,p}(\mathbb{R}^d)$ *and* $W_0^{k,p}(\Omega)$ *are defined as the closures*

$$W^{k,p}(\mathbb{R}^d) \coloneqq \overline{\mathcal{D}(\mathbb{R}^d)}^{\|\cdot\|_{W^{k,p}(\mathbb{R}^d)}} \quad \text{and} \quad W_0^{k,p}(\Omega) \coloneqq \overline{\mathcal{D}(\Omega)}^{\|\cdot\|_{W^{k,p}(\Omega)}}.$$

The Sobolev space $W^{k,p}(\Omega)$ is then defined by restriction to Ω,

$$W^{k,p}(\Omega) \coloneqq \left\{ u|_\Omega \,:\, u \in W^{k,p}(\mathbb{R}^d) \right\}.$$

Finally, assume $\Omega \subset \mathbb{R}^d$ *such that its interior* $\operatorname{int}\Omega$ *is a Lipschitz domain. Then*

$$W^{k,p}(\Omega) \coloneqq W^{k,p}(\operatorname{int}\Omega) \;\; \textit{and} \;\; W_0^{k,p}(\Omega) \coloneqq W_0^{k,p}(\operatorname{int}\Omega)$$

with the same norms.

For open sets Definition (2.1.1) is consistent with common definitions found in the references above (cf. Grisvard (1985, Theorem 1.4.3.1, page 25)).

(2.1.2) Definition (Fractional Sobolev Spaces and Semi-Norms)**.** *Let* $\Omega \subset \mathbb{R}^d$ *be a Lipschitz domain. Let further* $1 \leqslant p \leqslant \infty$ *and* $k \in \mathbb{N}_0$*. The* Sobolev semi-norms $|\cdot|_{W^{k,p}(\Omega)}$ *read*

$$|u|_{W^{k,p}(\Omega)}^p \coloneqq \sum_{\substack{\alpha\in\mathbb{N}_0^d \\ |\alpha|=k}} \|\mathrm{D}_\alpha u\|_{L^p(\Omega)}^p \;\; \textit{for } p<\infty, \;\; \textit{and} \;\; |u|_{W^{k,\infty}(\Omega)} \coloneqq \max_{\substack{\alpha\in\mathbb{N}_0^d \\ |\alpha|=k}} \|\mathrm{D}_\alpha u\|_{L^\infty(\Omega)}\,.$$

Let $0<s<1$*, then, for* $p<\infty$*, the* fractional Sobolev space $W^{k+s,p}(\Omega)$ *is given by*

$$W^{k+s,p}(\Omega) \coloneqq \left\{ u \in W^{k,p}(\Omega) \,:\, |u|_{W^{k+s,p}(\Omega)} < \infty \right\},$$

where the corresponding semi-norm and norm read

$$\begin{aligned} |u|_{W^{k+s,p}(\Omega)}^p &\coloneqq \sum_{\substack{\alpha\in\mathbb{N}_0^d \\ |\alpha|=k}} \int_\Omega \int_\Omega \frac{|\mathrm{D}_\alpha u(x) - \mathrm{D}_\alpha u(y)|^p}{|x-y|^{d+sp}} \mathrm{d}x\mathrm{d}y \;\; \textit{and} \\ \|u\|_{W^{k+s,p}(\Omega)}^p &\coloneqq \|u\|_{W^{k,p}(\Omega)}^p + |u|_{W^{k+s,p}(\Omega)}^p\,. \end{aligned}$$

Sobolev spaces are Banach spaces with respect to their corresponding norms. In the case $p=2$ the $W^{s,2}$ norm corresponds to a scalar product and hence $W^{s,2}$ is a Hilbert space which we abbreviate with H^s. Also note that $L^p = W^{0,p}$ and $L^2 = H^0$. Furthermore, we occasionally require the function spaces

$$\begin{aligned} H(\operatorname{div},\Omega) \coloneqq H(\operatorname{div},\Omega;\mathbb{R}^d) &\coloneqq \overline{\mathcal{D}(\Omega;\mathbb{R}^d)}^{\|\cdot\|_{H(\operatorname{div},\Omega)}} \\ &\qquad \text{with } \|u\|_{H(\operatorname{div},\Omega)}^2 \coloneqq \|u\|_{L^2(\Omega)}^2 + \|\operatorname{div} u\|_{L^2(\Omega)}^2\,, \\ L^{s+}(\Omega) &\coloneqq \bigcup_{\varepsilon>0} L^{s+\varepsilon}(\Omega) \;\; \text{for } s \geqslant 1, \\ H^{s+}(\Omega) &\coloneqq \bigcup_{\varepsilon>0} H^{s+\varepsilon}(\Omega) \;\; \text{for } s \geqslant 0. \end{aligned}$$

The space $H(\operatorname{div})$ is a weakened form of H^1 in that it does not require every first-order partial derivative to be in L^2, but only the divergence.

A remark on the notation of derivatives is necessary. In the remainder of this thesis the symbol $\mathrm{D}u$ (without multi-index α) refers to the Jacobian matrix of a function u, so $\mathrm{D}u(x) \in \mathbb{R}^{n\times d}$ for some $u : \mathbb{R}^d \to \mathbb{R}^n$ and $x \in \mathbb{R}^d$. The symbol D^2u refers to the Hessian of a function u, which is a $d \times d$ matrix for scalar valued functions u, however, it is an $(n \times d \times d)$-dimensional tensor in the case of $u : \mathbb{R}^d \to \mathbb{R}^n$. An unfortunate exception

is the proof of Lemma (3.3.10) (page 47) where excessive use of the chain rule requires an extension of this notation, which is explained there. For matrix valued functions $u \in H(\mathrm{div}, \Omega; \mathbb{R}^d)^n = H(\mathrm{div}, \Omega; \mathbb{R}^{n\times d})$ the divergence $\mathrm{div}\, u$ operates row-wise on u. The next definition formally defines derivatives of Sobolev functions.

(2.1.3) Definition/Theorem (Derivative of Sobolev Functions)**.** *Given a Lipschitz domain* $\Omega \subset \mathbb{R}^d$ *let* $1 \leqslant p \leqslant \infty$ *and* $s \geqslant 0$*, but* $p < \infty$ *for* $s \notin \mathbb{N}$*. The derivative operator* $\mathrm{D} : \mathcal{D}(\Omega) \to \mathcal{D}(\Omega, \mathbb{R}^d)$ *has a unique continuous extension* $\mathrm{D} : W^{s,p}(\Omega) \to W^{s-1,p}(\Omega, \mathbb{R}^d)$*.*

Proof. The assertion is clearly true for $s \in \mathbb{N}$. The general case is an implication of Grisvard (1985, Lemma 1.4.1.3, page 21). □

This thesis denotes the Lebesgue measure of a set $\Omega \subset \mathbb{R}^d$ with $|\Omega|$. The following lemma provides a well-known inclusion relation between Lebesgue spaces. It is presented together with its proof because the factor $|\Omega|^\xi$ is required later on.

(2.1.4) Lemma. *Let* $\Omega \subset \mathbb{R}^d$ *be a Lipschitz domain with* $|\Omega| < \infty$*, and let* $1 \leqslant p < q \leqslant \infty$*. Then* $L^q(\Omega) \subset L^p(\Omega)$ *and all* $u \in L^q(\Omega)$ *satisfy*

$$\|u\|_{L^p(\Omega)} \leqslant |\Omega|^\xi \, \|u\|_{L^q(\Omega)} \quad \text{with } \xi = \begin{cases} \frac{q-p}{qp} & \text{for } q < \infty, \\ \frac{1}{p} & \text{for } q = \infty. \end{cases}$$

In particular, this implies $W^{k,q}(\Omega) \subset W^{k,p}(\Omega)$ *for* $k \in \mathbb{N}_0$*.*

Proof. Set $v = u^p$. For $q = \infty$ we observe

$$\|u\|^p_{L^p(\Omega)} = \int_\Omega v(x)\mathrm{d}x \leqslant \|v\|_{L^\infty(\Omega)} \int_\Omega 1\mathrm{d}x = \|u\|^p_{L^\infty(\Omega)} \, |\Omega| \,.$$

For $q < \infty$ a Hölder inequality with exponent q/p and conjugate $q/(q-p)$ yields

$$\|u\|^p_{L^p(\Omega)} \leqslant \|1\|_{L^{q/(q-p)}(\Omega)} \, \|v\|_{L^{q/p}(\Omega)} = |\Omega|^{(q-p)/q} \, \|u\|^p_{L^q(\Omega)} \,. \qquad \square$$

(2.1.5) Lemma (Grisvard, 1985, Theorems 1.4.3.1, 1.4.4.1, pages 25, 27)**.** *Let* $\Omega \subset \mathbb{R}^d$ *be a bounded Lipschitz domain, and let* $1 < p \leqslant q < \infty$ *and* $0 \leqslant t \leqslant s$ *with* $s - d/p = t - d/q$*. Then* $W^{s,p}(\Omega) \subset W^{t,q}(\Omega)$*.*

In the context of Lebesgue exponents the fraction "$1/\infty$" is to be understood as 0 in the following.

(2.1.6) Lemma. *Let* $\Omega \subset \mathbb{R}^d$ *be a bounded Lipschitz domain and let* $1 < p \leqslant \infty$ *and* $s > d/p$*, but* $p < \infty$ *for* $s \notin \mathbb{N}$*. Then* $W^{s,p}(\Omega)$ *is continuously embedded in* $\mathcal{C}(\overline{\Omega})$*.*

Proof. This is a consequence of Grisvard (1985, Theorems 1.4.3.1, 1.4.4.1, pages 25, 27). □

(2.1.7) Lemma (Evans, 1998, Theorem 4, page 279)**.** *Given a bounded Lipschitz domain* Ω *in* $\mathbb{R}^d$ *it holds*

$$W^{1,\infty}(\Omega) = \{u \in \mathcal{C}(\Omega) \,:\, u \text{ is Lipschitz continuous}\} \,.$$

2.1.3 Sobolev Spaces on Surfaces

The following definition of Sobolev spaces on surfaces adheres to the concepts of Evans and Gariepy (1992) and Grisvard (1985). Here and in the remainder of the thesis the symbol $\fint_\Omega$ abbreviates the *mean value integral* $|\Omega|^{-1}\int_\Omega$.

(2.1.8) Definition/Theorem (Precise Representative (Evans and Gariepy, 1992, Sections 1.7, 4.3))**.** *For an $x \in \mathbb{R}^d$ denote the open ball with radius $r > 0$ around x with $B_r(x)$. Given a function $u : \Omega \to \mathbb{R}$ on a Lipschitz domain $\Omega \in \mathbb{R}^d$, its* precise representative *reads*

$$u^\star : \overline{\Omega} \to \mathbb{R}, u^\star(x) \coloneqq \begin{cases} \lim_{r\to 0} \fint_{\Omega\cap B_r(x)} u(y)\mathrm{d}y, & \text{or} \\ 0 \quad \text{if the limit does not exist.} \end{cases}$$

For $u \in L^1(\Omega)$ it holds $u = u^\star$ almost everywhere in Ω.

(2.1.9) Definition. *Given a Lipschitz domain $\Omega \subset \mathbb{R}^d$ and a Lipschitz surface $\Gamma \subset \overline{\Omega}$ let $1 \leqslant p \leqslant \infty$ and $s \geqslant 0$, but $p < \infty$ for $s \notin \mathbb{N}$. Define*

$$W^{s,p}_\Gamma(\Omega) \coloneqq \overline{\left\{u|_\Omega \,:\, u \in \mathcal{D}(\mathbb{R}^d\backslash\Gamma)\right\}}^{\|\cdot\|_{W^{s,p}(\Omega)}}.$$

Note that $W^{k,p}_0(\Omega) = W^{k,p}_{\partial\Omega}(\Omega)$ by Definitions (2.1.1) and (2.1.9).

The following gives a formal definition of Sobolev spaces on surfaces. If $\Gamma \subset \mathbb{R}^d$ is an affine surface, i.e., a rotated and translated subset of $\mathbb{R}^{d-1} \times \{0\}$, it is straightforward to define $W^{s,p}(\Gamma)$ with Definition (2.1.1) applied to said subset of $\mathbb{R}^{d-1}$. Otherwise, i.e., if Γ is curved, we define $W^{s,p}(\Gamma)$ as a quotient space as follows.

(2.1.10) Definition (Sobolev Spaces on Surfaces)**.** *Given a compact Lipschitz surface $\Gamma \subset \mathbb{R}^d$ with positive $(d-1)$-dimensional Hausdorff measure let $1 \leqslant p \leqslant \infty$ and $s \geqslant 0$, but $p < \infty$ for $s \notin \mathbb{N}$.*

(a) Assume Γ is an affine surface in the sense that there exist a bounded Lipschitz domain $\omega \subset \mathbb{R}^{d-1}$, an orthogonal matrix $Q \in \mathbb{R}^{d\times d}$ and a scalar $t \in \mathbb{R}$ such that

$$Q(\overline{\omega} \times \{t\}) = \Gamma. \tag{2.1}$$

Define the Sobolev space $W^{s,p}(\Gamma)$ and its norm by

$$W^{s,p}(\Gamma) \coloneqq \left\{v \circ \Phi \circ Q^{-1} \,:\, v \in W^{s,p}(\omega)\right\} \quad \text{and}$$
$$\|u\|_{W^{s,p}(\Gamma)} \coloneqq \left\|u \circ Q \circ \Phi^{-1}\right\|_{W^{s,p}(\omega)},$$

where $\Phi : \mathbb{R}^{d-1} \times \{t\} \to \mathbb{R}^{d-1}$, $(x_1, \ldots, x_{d-1}, t) \mapsto (x_1, \ldots, x_{d-1})$.

(b) If Γ is not an affine surface, i.e., if (2.1) cannot be satisfied, define $W^{s,p}(\Gamma)$ and its norm by the quotient space

$$W^{s,p}(\Gamma) \coloneqq W^{s+1/p,p}(\mathbb{R}^d) \Big/ W^{s+1/p,p}_\Gamma(\mathbb{R}^d) \quad \text{and}$$
$$\|u\|_{W^{s,p}(\Gamma)} \coloneqq \min_{v\in W^{s+1/p,p}_\Gamma(\mathbb{R}^d)} \|u - v\|_{W^{s+1/p,p}\left(\mathbb{R}^d\right)}.$$

Note that $W_\Gamma^{s+1/p,p}(\mathbb{R}^d)$ is closed in $W^{s+1/p,p}(\mathbb{R}^d)$ by Definition (2.1.9), therefore the quotient space of Definition (2.1.10) (b) is well-defined. In fact, Definition (2.1.10) (b) is equivalent to a definition of $W^{s,p}(\Gamma)$ via parametrised maps of Γ as long as Γ satisfies certain smoothness conditions and $s \notin \mathbb{N}_0$, see Remark (2.1.12) below for details.

(2.1.11) Lemma (Trace Theorem (Grisvard, 1985, Theorem 1.5.1.2, page 37))**.** *Given a bounded Lipschitz domain $\Omega \subset \mathbb{R}^d$ and a compact $\mathcal{C}^{k,1}$ surface $\Gamma \subset \overline{\Omega}$ with positive $(d-1)$-dimensional Hausdorff measure for $k \in \mathbb{N}_0$, let $1 < p < \infty$ and $0 < s \leqslant k + 1 - 1/p$ with $s \notin \mathbb{N}$. Then the mapping*

$$W^{s+1/p,p}(\Omega) \to W^{s,p}(\Gamma), \quad u \mapsto u^\star|_\Gamma$$

is continuous and admits a right-continuous inverse.

(2.1.12) Remark. *Definition (2.1.10) (a) can be extended to possibly curved surfaces by means of local parametrisation, similar to the common definition of Lebesgue spaces $L^p(\Gamma)$ on surfaces $\Gamma \in \mathbb{R}^d$. However, the maps which define a parametrisation of Γ need to be smooth enough such that the derivatives in Definitions (2.1.1) and (2.1.2) are well-defined. Such a definition can be found in Grisvard (1985, Section 1.3.3, page 19) and is actually equivalent to Definition (2.1.10) (b) in the situation of Lemma (2.1.11). As a consequence Lemmas (2.1.5) and (2.1.7) hold on surfaces as well.*

On the other hand, if one of the conditions of Lemma (2.1.11) on k, s and p is violated, this equivalence cannot be guaranteed anymore. In particular, the equivalence of (a) and (b) of Definition (2.1.10) is not clear *for $W^{s,p}(\Gamma)$ with $s \in \mathbb{N}$.*

(2.1.13) Definition (Jump)**.** *Given a domain $\Omega \subset \mathbb{R}^d$, a Lipschitz surface $\Gamma \subset \Omega$ and a point $x \in \Gamma$, the surface divides Ω locally into two subdomains $\omega_+, \omega_- \subset \Omega$ as illustrated in Figure 2.1. The* jump *of a function $u : \Omega \to \mathbb{R}$ in x along Γ is defined, up to a sign, by the difference of the precise representatives of u on any such subdomains,*

$$[u]_\Gamma \coloneqq [u]_\Gamma(x) \coloneqq u|^\star_{\omega_+}(x) - u|^\star_{\omega_-}(x).$$

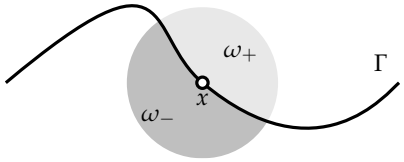

Figure 2.1: The surface Γ divides an open neighbourhood of x into two subdomains $\omega_\pm$

To avoid the somehow confusing notation "$[u]_\Gamma(x)$" the abbreviation "$[u]_\Gamma$" is preferred whenever it is clear at which point the jump function is actually evaluated. The sign of the jump depends on the choice of ω_+ and ω_- in Definition (2.1.13). However, this choice is not significant within this thesis as long as it remains fixed for a given surface Γ.

In the following, $\lfloor s \rfloor$ refers to the *floor* of a real number s, that is, the largest integer which is less or equal s. The *ceiling* $\lceil x \rceil$ of a real number s is the smallest integer which is greater or equal s.

(2.1.14) Lemma (Extended Trace Theorem)**.** *Given a bounded Lipschitz domain $\Omega \subset \mathbb{R}^d$ and a compact $\mathcal{C}^{k,1}$ surface $\Gamma \subset \Omega$ with positive $(d-1)$-dimensional Hausdorff measure for $k \in \mathbb{N}_0$, let $1 < p < \infty$ and $1/p < s \leqslant k + 1$ with $s - 1/p \notin \mathbb{N}$. Then $\left[\partial^j u / \partial n_\Gamma^j\right]_\Gamma = 0$ almost everywhere on Γ for all $u \in W^{s,p}(\Omega)$ and $j = 0, \ldots, \lfloor s - 1/p \rfloor$.*

Proof. The claim clearly holds for $u \in \mathcal{D}(\mathbb{R}^d)$. For $u \in W^{s,p}(\Omega)$ the assertion is a consequence of the density of $\mathcal{D}(\mathbb{R}^d)$ in $W^{s,p}(\Omega)$ and Lemma (2.1.11). □

2.1.4 Miscellaneous Results

The remaining part of this section collects several elementary results which are related to Sobolev spaces in one way or another, without a particular order. The notation $A \lesssim B$ is synonymous to $A \leqslant CB$ with a generic constant $C > 0$ which is independent of crucial values. The details are explained from case to case (see Lemma (2.1.16) below for an example). The notation $A \approx B$ means $A \lesssim B \lesssim A$.

(2.1.15) Lemma (Fundamental Lemma of the Calculus of Variations (Dacorogna, 2004, Theorem 1.24, page 23))**.** *Let $\Omega \subset \mathbb{R}^d$ be a Lipschitz domain and let $u \in L^1(\Omega)$. If*

$$\int_\Omega u(x)w(x)\mathrm{d}x = 0 \quad \textit{for all } w \in \mathcal{D}(\Omega)$$

then $u(x) = 0$ almost everywhere.

(2.1.16) Lemma (Poincaré Inequality)**.** *Given a bounded Lipschitz domain $\Omega \subset \mathbb{R}^d$ and $1 \leqslant p \leqslant \infty$,*

$$\|u - u_0\|_{L^p(\Omega)} \lesssim \operatorname{diam}(\Omega)\, |u|_{W^{1,p}(\Omega)} \quad \textit{for all } u \in W^{1,p}(\Omega) \quad \textit{with } u_0 = \fint_\Omega u(x)\mathrm{d}x.$$

The generic constant depends on p and the shape of Ω, but not on its size.

Here and in the following the *diameter* of a set $X \subset \mathbb{R}^d$ is the largest possible distance of two points in X, i.e., $\operatorname{diam}(X) \coloneqq \sup_{x,y\in X} |x - y|$.

Proof. Evans (1998, Theorem 1, page 275) formally proves the assertion for domains with a $\mathcal{C}^1$-boundary $\partial\Omega$. However, a close look at the proof reveals that a compact embedding $W^{1,p}(\Omega) \subset L^p(\Omega)$ is sufficient. Grisvard (1985, Theorem 1.4.3.2, page 26) implies that the embedding is indeed compact for Lipschitz domains. □

(2.1.17) Lemma (Friedrichs Inequality)**.** *Given a bounded Lipschitz domain $\Omega \subset \mathbb{R}^d$ and $1 \leqslant p \leqslant \infty$, let $\Gamma \subset \partial\Omega$ be a part of its boundary with positive $(d-1)$-dimensional Hausdorff measure. Then*

$$\|u\|_{L^p(\Omega)} \lesssim \operatorname{diam}(\Omega)\, |u|_{W^{1,p}(\Omega)} \quad \textit{for all } u \in W^{1,p}_\Gamma(\Omega).$$

The generic constant depends on p and the shape of Γ and Ω, but not on their size.

Notes on the proof. Brenner and Scott (2002, Proposition (5.3.5), page 136) prove the inequality for $\Gamma = \partial\Omega$. Braess (2007, Remark 1.6, page 30) observes that this result extends to functions with homogeneous boundary conditions on parts of the boundary. □

(2.1.18) Remark. *Lemma (2.1.17) is also valid if $d = 1$. In this case $\Omega =]a, b[\subset \mathbb{R}$ is an open and bounded interval and Γ is a nonempty subset of $\{a, b\}$. The proof of Lemma (3.3.3) (page 44) utilises this one-dimensional version of Friedrichs' inequality.*

The following Lemma extends the integration by parts formula, which is well-known for continuously differentiable functions, to Sobolev functions.

(2.1.19) Lemma (Integration by Parts)**.** *Let $1 < p < \infty$ and let p' be the* Hölder conjugate *of p, i.e., $1/p + 1/p' = 1$. Given a bounded Lipschitz domain $\Omega \subset \mathbb{R}^d$ it holds*

$$\int_\Omega (\mathrm{D}u(x)v(x) + u(x)\mathrm{D}v(x))\,\mathrm{d}x = \int_{\partial\Omega} u(x)v(x)n_{\partial\Omega}(x)\mathrm{d}s \qquad \text{for all } u \in W^{1,p}(\Omega), v \in W^{1,p'}(\Omega),$$

$$\int_\Omega (\mathrm{D}u(x)\cdot v(x) + u(x)\,\mathrm{div}\,v(x))\,\mathrm{d}x = \int_{\partial\Omega} u(x)v(x)\cdot n_{\partial\Omega}(x)\mathrm{d}s \qquad \text{for all } u \in H^1(\Omega), v \in H(\mathrm{div},\Omega).$$

Notes on the proof. The integrals on the boundary $\partial\Omega$ are well-defined by Lemma (2.1.11). Since the Lemma holds for continuously differentiable functions, the claimed equalities are a consequence of the density of $\mathcal{D}(\Omega)$ in the respective Sobolev spaces. □

(2.1.20) Lemma (Trace Theorem (Brenner and Scott, 2002, Theorem (1.6.6), page 39))**.** *Given a bounded Lipschitz domain $\Omega \subset \mathbb{R}^d$ and $1 \leqslant p \leqslant \infty$,*

$$\|u\|_{L^p(\partial\Omega)} \lesssim \|u\|^{1-1/p}_{L^p(\Omega)} \|u\|^{1/p}_{W^{1,p}(\Omega)} \quad \text{for all } u \in W^{1,p}(\Omega).$$

The generic constant depends on Ω and p.

The section concludes with some handy results which, although not being directly related to Sobolev spaces, round out the previous inequalities.

(2.1.21) Lemma (Jensen Inequality (Evans, 1998, Theorem 2, page 621))**.** *Given a bounded Lipschitz domain Ω in $\mathbb{R}^d$ and a convex $f : \mathbb{R} \to \mathbb{R}$,*

$$f\left(\fint_\Omega u(x)\mathrm{d}x\right) \leqslant \fint_\Omega f(u(x))\mathrm{d}x \quad \text{for } u \in L^1(\Omega).$$

Note that the right-hand side may assume ∞ for $f \circ u \notin L^1(\Omega)$.

(2.1.22) Lemma (Young Inequality (Evans, 1998, page 622))**.** *Given $1 < p < \infty$ and its Hölder conjugate p', i.e., $1/p + 1/p' = 1$, it holds*

$$ab \leqslant a^p/p + b^{p'}/p' \quad \text{for } a, b > 0.$$

In particular, it holds $ab \lesssim a^p + b^{p'}$, where the generic constant depends on p only.

An immediate consequence of Lemma (2.1.22) is the following technique.

(2.1.23) Lemma (Absorption)**.** *Given $1 < p < \infty$ and its Hölder conjugate p', i.e., $1/p + 1/p' = 1$, it holds for any $a, b, c \in \mathbb{R}$ with $a, b > 0$*

$$a^p \lesssim ab + c \Longrightarrow a^p \lesssim b^{p'} + c.$$

2.2 A Class of Convex Minimisation Problems

This section states the mathematical model of interest in its most general form. In this way it serves as a reference for the upcoming investigations. We also present results on the properties of the model problem and its solutions, however, we recite proofs only if the arguments are beneficial for the proofs in subsequent chapters.

2.2.1 Problem Statement

The thesis considers two- and three-dimensional problems only, so assume $d = 2$ or 3. Let $\Omega \subset \mathbb{R}^d$ be a bounded Lipschitz domain. Note that the numerical analysis in the forthcoming chapters requires Ω to be endowed with a polyhedral boundary in order to allow for an exact triangulation of the domain (see Section 3.1, page 32, for a definition of triangulations), however, the results of the present chapter do not require this assumption. Let p' be the Hölder conjugate of some fixed exponent $2 \leqslant p < \infty$, i.e., $1/p + 1/p' = 1$. Given a convex energy density $W^{\star\star} \in \mathcal{C}^1(\mathbb{R}^{n\times d})$, a real number $\alpha \geqslant 0$ and *lower-order terms* $f \in L^2(\Omega;\mathbb{R}^n)$ and $g \in L^{p'}(\Omega;\mathbb{R}^n)$, the *continuous convex model problem* reads

$$\begin{aligned} \text{minimise } E^{\star\star}(v) &\coloneqq \int_\Omega \Big(W^{\star\star}(\mathrm{D}v(x)) + \alpha \left|v(x) - f(x)\right|^2 - g(x)\cdot v(x) \Big) \,\mathrm{d}x \\ &\text{amongst } v \in \mathcal{A}. \end{aligned} \tag{2.2}$$

The adjective "continuous" in "continuous convex model problem" helps to distinguish (2.2) from the "*discrete* convex model problem" (3.10) on page 40. For a given $u_D \in W^{1,p}(\Omega;\mathbb{R}^n)$ the space of admissible functions reads $\mathcal{A} \coloneqq u_D + V$ with $V \coloneqq W^{1,p}_0(\Omega;\mathbb{R}^n)$. This ensures that $v = u_D$ almost everywhere on $\partial\Omega$ for all $v \in \mathcal{A}$. Put differently, u_D encodes Dirichlet boundary conditions. Note that stricter regularity assumptions on u_D are imposed in subsequent chapters to allow for the approximation error estimates of boundary values.

For a given fixed $u \in \mathcal{A}$ the derivatives of the energy density and the lower-order terms of (2.2) are frequently abbreviated with

$$\sigma(x) \coloneqq S(\mathrm{D}u(x)) \coloneqq \mathrm{D}W^{\star\star}(\mathrm{D}u(x)) \quad\text{and}\quad \Lambda(x) \coloneqq -2\alpha(u(x) - f(x)) + g(x). \tag{2.3}$$

The function σ is commonly called *stress field* or *stress tensor*, due to its meaning in modeling physical phenomena. This notation permits the *Euler-Lagrange equation* that corresponds to (2.2) to be stated as

$$\int_\Omega (\sigma(x) : \mathrm{D}v(x) - \Lambda(x)\cdot v(x)) \,\mathrm{d}x = 0 \quad \text{for all } v \in V. \tag{2.4}$$

2.2.2 Growth Conditions

The following assumptions on the energy density $W^{\star\star}$ are essential for several results ahead. The first one ensures that $W^{\star\star}$ exhibits a certain growth which is compatible with the Lebesgue exponent p.

(2.2.1) Assumption (Two-Sided Growth)**.** *The energy density $W^{\star\star}$ satisfies*

$$|y|^p - 1 \lesssim W^{\star\star}(y) \lesssim |y|^p + 1 \ \text{ for all } y \in \mathbb{R}^{n\times d}, \tag{2.5}$$

where the generic constants do not depend on y.

The second assumption states a strong kind of convexity.

(2.2.2) Assumption (Convexity Control)**.** *There exist real numbers r and s with*

$$p' \leqslant r \tag{2.6}$$

and

$$0 \leqslant s \leqslant rp - r - p \tag{2.7}$$

such that

$$|S(y_1) - S(y_2)|^r \lesssim \left(1 + |y_1|^s + |y_2|^s\right)(S(y_1) - S(y_2)) : (y_1 - y_2) \ \text{ for all } y_1, y_2 \in \mathbb{R}^{n\times d}. \tag{2.8}$$

The generic constant does not depend on y_1 and y_2.

The condition (2.6) differs from the cited literature (e.g. Bartels et al., 2004b, (H1)), where $1 < r$ is commonly assumed. However, (2.7) alone enforces $p' \leqslant r$, so there is no need to artificially extend the range of possible values for r.

2.2.3 Existence and Uniqueness of Solutions

Assumptions (2.2.1) and (2.2.2) lead to the following theorems concerning existence and uniqueness of solutions.

(2.2.3) Theorem (Existence of Solutions)**.** *Given the minimisation problem* (2.2) *let its energy density $W^{\star\star}$ satisfy Assumption (2.2.1). Then there exists a minimiser $u \in \mathcal{A}$ of* (2.2)*.*

Notes on the proof. The existence of minimisers $u \in \mathcal{A}$ is asserted by the direct method of the calculus of variations, which is outlined in the book of Dacorogna (2008). In particular it is a consequence of Theorem 1.1 (page 48) and Remark i) (page 75) in this book. Note that a requisite of the proof is $W^{1,p}$-boundedness of infimising sequences. The boundedness is a consequence of (2.10) below. □

The following result states the equivalency of the minimisation problem (2.2) and its Euler-Lagrange equation (2.4).

(2.2.4) Theorem. *Given the minimisation problem* (2.2) *let its energy density $W^{\star\star}$ satisfy Assumption (2.2.1). Then every minimiser u of* (2.2) *is a solution of the Euler-Lagrange equation* (2.4)*. Conversely, every solution $u \in \mathcal{A}$ of* (2.4) *is a minimiser of* (2.2)*.*

Notes on the proof. Dacorogna (2004, Theorem 3.11, page 92) proves the equivalence of (2.2) and (2.4), even for the vector-valued case ($n > 1$, see Dacorogna, 2004, Remark 3.12 (v), page 93). Note that the problem (2.2) formally does not satisfy condition (H3) of Theorem 3.11 by Dacorogna (2004), but instead (with the same notation)

$$|f_u(x,u,\xi)|, \left|f_{\tilde{\xi}}(x,u,\xi)\right| \leqslant \beta\left(a(x) + |u|^{p-1} + |\xi|^{p-1}\right) \ \text{ for some } a \in L^{p'}(\Omega).$$

However, this modification of (H3) does not invalidate the argumentation of Dacorogna (2004). □

The following uniqueness result concludes the section. A complete proof, based on the proof of Carstensen and Plecháč (1997, Theorem 2), is given because the upcoming sections on the stabilised discrete problem employ similar arguments.

(2.2.5) Theorem (Uniqueness)**.** *Assume that the energy density $W^{\star\star}$ of* (2.2) *complies with Assumptions (2.2.1) and (2.2.2). Then any two solutions u_1 and u_2 of* (2.2) *satisfy $S(\mathrm{D}u_1) = S(\mathrm{D}u_2)$ almost everywhere in Ω. If furthermore $\alpha > 0$, then also $u_1 = u_2$ almost everywhere in Ω.*

(2.2.6) Lemma. *Given the minimisation problem* (2.2) *let its energy density $W^{\star\star}$ satisfy Assumptions (2.2.1) and (2.2.2). Then the set of minimisers is bounded in $W^{1,p}(\Omega)$, i.e., $\|u\|_{W^{1,p}(\Omega)} \lesssim 1$ for all solutions $u \in \mathcal{A}$, with a generic constant independent of the choice of u.*

Proof. Given a solution u of (2.2), Friedrichs' inequality (Lemma (2.1.17)) for $v = u - u_D \in V$ shows

$$\|u\|_{L^p(\Omega)} \leqslant \|u_D\|_{L^p(\Omega)} + \|v\|_{L^p(\Omega)} \lesssim \|u_D\|_{L^p(\Omega)} + |v|_{W^{1,p}(\Omega)} \lesssim \|u_D\|_{W^{1,p}(\Omega)} + |u|_{W^{1,p}(\Omega)}\,. \tag{2.9}$$

The two-sided growth condition (Assumption (2.2.1)) and (2.9) lead to

$$\begin{aligned} E^{\star\star}(u) &\gtrsim \int_\Omega \Big(|\mathrm{D}u(x)|^p - 1 + \alpha\,|u(x) - f(x)|^2 - g(x)u(x) \Big)\,\mathrm{d}x \\ &\geqslant |u|^p_{W^{1,p}(\Omega)} - |\Omega| - \|g\|_{L^{p'}(\Omega)}\,\|u\|_{L^p(\Omega)} \gtrsim |u|^p_{W^{1,p}(\Omega)} - 1 - |u|_{W^{1,p}(\Omega)}\,. \end{aligned} \tag{2.10}$$

Clearly all solutions u of (2.2) attain the same energy $E^{\star\star}(u)$, therefore a constant $C > 0$ (independent of u) exists such that

$$|u|^p_{W^{1,p}(\Omega)} - |u|_{W^{1,p}(\Omega)} - 1 < C. \tag{2.11}$$

Hence $|u|_{W^{1,p}(\Omega)}$ is bound by the positive root of $X^p - X - C - 1 = 0$, which exists due to $p \geqslant 2$. This bound and (2.9) yield a bound on $\|u\|_{L^p(\Omega)}$ and thus prove the claim. □

(2.2.7) Lemma. *Let $u_1, u_2 \in W^{1,p}(\Omega;\mathbb{R}^n)$ with corresponding stresses $\sigma_1 = S(\mathrm{D}u_1)$ and $\sigma_2 = S(\mathrm{D}u_2)$. If the energy density $W^{\star\star}$ satisfies Assumptions (2.2.1) and (2.2.2) then*

$$\|\sigma_1 - \sigma_2\|^r_{L^{p'}(\Omega)} \lesssim \int_\Omega (\sigma_1(x) - \sigma_2(x)) : \mathrm{D}(u_1 - u_2)(x)\mathrm{d}x,$$

where the generic constant depends on $|\Omega|$, s, p, r, on the generic constants of (2.5)*, and on upper bounds of $|u_1|_{W^{1,p}(\Omega)}$ and $|u_2|_{W^{1,p}(\Omega)}$. In particular, the integral on the right-hand side is nonnegative.*

Note that Lemma (2.2.7) does not require boundary conditions, hence it also holds if u_1 and u_2 have different boundary values. Therefore the lemma also estimates the error of a discrete approximation u_ℓ of u which does not obey the boundary conditions of u_D exactly (see e.g. Lemma (3.3.8) on page 45, or Lemma (4.1.7) on page 70).

Proof. Let $e \coloneqq u_1 - u_2$, $\delta \coloneqq \sigma_1 - \sigma_2$ and $q \coloneqq 1 + s/p$. The q-th root of (2.8) with y_1 and y_2 replaced by $\mathrm{D}u_1$ and $\mathrm{D}u_2$ reads

$$|\delta(x)|^{r/q} \lesssim \left(1 + |\mathrm{D}u_1(x)|^s + |\mathrm{D}u_2(x)|^s\right)^{1/q} (\delta(x) : \mathrm{D}e(x))^{1/q} \quad \text{for } x \in \Omega.$$

Elementary algebra and (2.7) prove $1 < p' \leqslant r/q$ and $s < p$. The integral over Ω and a Hölder inequality (with exponents q and $q' = q/(q-1)$) yield

$$\begin{aligned}\|\delta\|^{r/q}_{L^{r/q}(\Omega)} &\lesssim \int_\Omega \left(1 + |\mathrm{D}u_1(x)|^s + |\mathrm{D}u_2(x)|^s\right)^{1/q} (\delta(x) : \mathrm{D}e(x))^{1/q} \,\mathrm{d}x \\ &\leqslant \left(\int_\Omega \left(1 + |\mathrm{D}u_1(x)|^s + |\mathrm{D}u_2(x)|^s\right)^{q'/q} \mathrm{d}x\right)^{1/q'} \left(\int_\Omega \delta(x) : \mathrm{D}e(x)\mathrm{d}x\right)^{1/q}.\end{aligned}$$

Another Hölder inequality (in $\mathbb{R}^3$ with exponents $p/(p-s)$ and $p/s = q'/q$) allows the estimation of the $L^{p/s}$ norm on the right hand side,

$$1 + |\mathrm{D}u_1(x)|^s + |\mathrm{D}u_2(x)|^s \leqslant 3^{(p-s)/p} \left(1 + |\mathrm{D}u_1(x)|^p + |\mathrm{D}u_2(x)|^p\right)^{s/p}.$$

Lemma (2.1.4) shows $\|\cdot\|_{L^{p'}(\Omega)} \lesssim \|\cdot\|_{L^{r/q}(\Omega)}$ where the generic constant depends on $|\Omega|$ and the Lebesgue exponents p' and r/q. Hence

$$\begin{aligned}\|\delta\|^r_{L^{p'}(\Omega)} \lesssim \|\delta\|^r_{L^{r/q}(\Omega)} &\lesssim \left(\int_\Omega \left(1 + |\mathrm{D}u_1(x)|^p + |\mathrm{D}u_2(x)|^p\right) \mathrm{d}x\right)^{s/p} \int_\Omega \delta(x) : \mathrm{D}e(x)\mathrm{d}x \\ &= \left(|\Omega| + |u_1|^p_{W^p(\Omega)} + |u_2|^p_{W^p(\Omega)}\right)^{s/p} \int_\Omega \delta(x) : \mathrm{D}e(x)\mathrm{d}x. \qquad \square\end{aligned}$$

Proof of Theorem (2.2.5). This proof adopts the notation of Lemma (2.2.7), i.e., σ_1 and σ_2 denote the stress tensors corresponding to u_1 and u_2, and the differences of the solutions and their stresses is denoted with $e \coloneqq u_1 - u_2$ and $\delta \coloneqq \sigma_1 - \sigma_2$. Furthermore, $\Lambda_j \coloneqq -2\alpha(u_j - f) + g$ denotes the derivatives of the energy's lower-order terms with respect to the solution u_j for $j = 1, 2$. Their difference is given by $\Lambda_1 - \Lambda_2 = -2\alpha e$. Hence the difference of the Euler-Lagrange equations (2.4) of both solutions reads

$$\int_\Omega (\delta(x) : \mathrm{D}v(x) + 2\alpha e(x) \cdot v(x)) \,\mathrm{d}x = 0 \quad \text{for all } v \in V.$$

With $v = e \in V$, this and Lemma (2.2.7) yield

$$\|\delta\|^r_{L^{p'}(\Omega)} \lesssim \int_\Omega \delta(x) : \mathrm{D}e(x)\mathrm{d}x = -2\alpha \|e\|^2_{L^2(\Omega)}$$

The nonnegativity of the norms proves both claims. $\square$

The remaining sections of this chapter offer a closer look at various example problems of the type (2.2). These problems also serve as benchmark examples in Chapter 5, in order to compare various numerical methods.

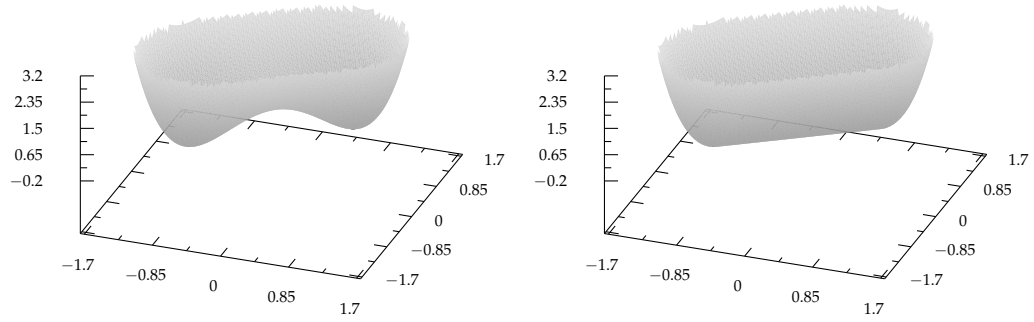

Figure 2.2: Graphs of the energy density functions W (left) and $W^{\star\star}$ (right) of Lemma (2.3.1)

2.3 Two-Well Benchmark

Carstensen and Jochimsen (2003) proposed a benchmark example for two-dimensional minimisation problems with microstructure which is based on the following nonconvex model problem. Given the vector $a := (3,2)/\sqrt{13}$ in $\mathbb{R}^2$ the nonconvex energy density reads

$$W(y) := |y-a|^2\,|y+a|^2\,. \tag{2.12}$$

For $x := (x_1, x_2) \in \Omega :=]0,1[\times]0, \frac{3}{2}[$ set $t := (3(x_1-1)+2x_2)/\sqrt{13}$ and

$$f(x) := -3t^5/128 - t^3/3 \;\text{ and }\; u_D(x) := \begin{cases} f(x) & \text{for } t \leqslant 0, \\ t^3/24 + t & \text{for } t \geqslant 0. \end{cases} \tag{2.13}$$

The resulting nonconvex problem

$$\text{minimise } E(v) = \int_\Omega \Big(W(\mathrm{D}v(x)) + |v(x) - f(x)|^2 \Big)\,\mathrm{d}x$$

does not admit a solution amongst $v \in \mathcal{A} = u_D + W_0^{1,4}(\Omega)$, cf. Carstensen and Jochimsen (2003, Theorem 2.1).

The following Lemma presents an explicit formula for the convex hull of W.

(2.3.1) Lemma (Carstensen and Plecháč, 1997, Proposition 1)**.** *The energy density W of* (2.12) *and its convexification $W^{\star\star}$ are given by*

$$W(y) = 4\Big(|y|^2 - (a\cdot y)^2\Big) + \Big(|y|^2 - 1\Big)^2, \;\; \textit{and}$$
$$W^{\star\star}(y) = 4\Big(|y|^2 - (a\cdot y)^2\Big) + \Big(|y|^2 - 1\Big)_+^2,$$

with the vector $a \in \mathbb{R}^2$ as in (2.12)*.*

Here and in the following the plus operator $(\cdot)_+ := \max\{0, \cdot\}$. is applied prior to an exponent, i.e., $(\cdot)_+^k = \big((\cdot)_+\big)^k$. Figure 2.2 depicts $3D$ plots of the energy densities W and $W^{\star\star}$.

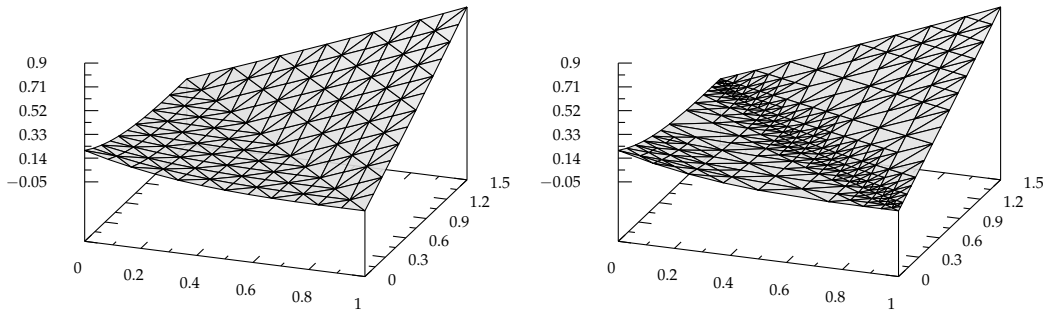

Figure 2.3: Nodal interpolation of the exact solution u_D from (2.13) of the two-well problem (left); numerical solution of the two-well problem (2.14) (right, based on the residual-based refinement indicator (5.5), page 94). Note the kink along the line $t = 0$ (with t as in (2.13)).

With $W^{\star\star}$ from Lemma (2.3.1) the convexified benchmark is given by

$$\text{minimise } E^{\star\star}(v) = \int_\Omega \Big(W^{\star\star}(\mathrm{D}v(x)) + |v(x) - f(x)|^2 \Big)\,\mathrm{d}x \;\text{ amongst } v \in \mathcal{A} \tag{2.14}$$

with f from (2.13), $W^{\star\star}$ from (2.3.1) and $\mathcal{A} = u_D + W_0^{1,4}(\Omega)$.

The following lemma proves that (2.14) fits into the framework of Section 2.2.

(2.3.2) Lemma (Carstensen and Plecháč, 1997, Corollary 4)**.** *The two-well minimisation problem* (2.14) *complies with Assumptions (2.2.1) and (2.2.2), with* $p = 4$ *and* $r = s = 2$*. Therefore Theorems (2.2.3), (2.2.4) and (2.2.5) apply to* (2.14)*.*

The following lemma by Carstensen and Jochimsen (2003) states uniqueness of the solution u of (2.14) and provides an explicit formula for it.

(2.3.3) Lemma (Carstensen and Jochimsen, 2003, Theorem 2.1)**.** *The two-well minimisation problem* (2.14) *has a unique solution, which is* $u = u_D$ *from* (2.13)*.*

Figure 2.3 displays the exact solution u_D as well as a numerical approximation, computed with the methods of Chapter 5.

Recall the abbreviation $S \coloneqq \mathrm{D}W^{\star\star}$. We also consider a modified version of the two-well problem (2.14) with linear lower-order terms, which reads

$$\text{minimise } E^{\star\star}(v) = \int_\Omega \big(W^{\star\star}(\mathrm{D}v(x)) - g(x)v(x) \big)\,\mathrm{d}x \;\text{ amongst } v \in \mathcal{A} \tag{2.15}$$

with $g \coloneqq -\operatorname{div}(S(\mathrm{D}u_D))$, which is defined in $\Omega\backslash\Gamma$ with $\Gamma \coloneqq \{x \in \Omega : t = 0\}$, and t as in (2.13).

We claim that u_D is also the unique solution of (2.15). Indeed, an integration by parts shows for $v \in V$

$$\begin{aligned} -\int_\Omega g(x)v(x)\mathrm{d}x = &\int_{\partial\Omega} S(\mathrm{D}u_D(x)) \cdot n_{\partial\Omega}(x)v(x)\mathrm{d}x \\ &+ \int_\Gamma [S(\mathrm{D}u_D)]_\Gamma \cdot n_\Gamma v(x)\mathrm{d}x - \int_\Omega S(\mathrm{D}u_D(x))\mathrm{D}v(x)\mathrm{d}x. \end{aligned} \tag{2.16}$$

The integral over Γ accounts for the discontinuity of g along Γ. However, direct computation shows that $S(\mathrm{D}u_D)$ is continuous along Γ and so this integral vanishes. The integral over $\partial\Omega$ also vanishes since $v = 0$ on $\partial\Omega$. Hence u_D is a solution of the corresponding Euler-Lagrange equation and thereby of (2.15). The uniqueness is a consequence of Theorem (4.2.3) (page 75, see also Remark (4.2.4) for an explanation).

(2.3.4) Remark. *Bolza's one-dimensional problem* (1.1) *(page 2) illustrates that nonconvex minimisation problems can lead to highly oscillating infimising sequences $(u_j)_{j\in\mathbb{N}}$ without a strong limit in $W^{1,p}(\Omega)$ and without a solution in the classical sense. The nonconvex two-well problem with the energy density of* (2.12) *suffers from the same difficulty. Instead, the limit of infimising sequences is in general a* Young measure *$(\nu_x)_{x\in\Omega}$, that is, a parametrised measure which describes the oscillations in the limit $\lim_{j\to\infty} \mathrm{D}u_j$ (Carstensen and Plecháč, 1997, Section 2). These oscillations, however, prevent an effective approximation of $(\nu_x)_x$ with finite element schemes. Under certain conditions, which are satisfied by the two-well benchmark, it is possible to recover the unique Young measure-valued solution $(\nu_x)_x$ of the nonconvex problem from the gradients of the solution of the convexified problem. The minutiae are outside of the scope of this thesis. Details on the computation of $(\nu_x)_x$ based on the convexified solution are contained in Carstensen and Jochimsen (2003, in particular Theorem 2.1). For a general introduction to parametrised measures refer to Pedregal (1997).*

The following lemma, which is essential to prove L^2 convergence of the discrete solutions $u_\ell \to u$ in Theorem (4.2.3) (page 75), concludes the section.

(2.3.5) Lemma. *Set $z = (-3,2)/\sqrt{13}$. Then any $y_1, y_2 \in \mathbb{R}^2$ satisfy*

$$8\,|(y_1 - y_2)\cdot z|^2 \leqslant (S(y_1) - S(y_2))\,(y_1 - y_2)\,.$$

Here and in the following the symbol "1" not only denotes the real number, but also refers to the unit element within any ring structure.

Proof. z is a unit vector and orthogonal to a from (2.12). Therefore a projection operator $\mathbb{P}$ defined by Carstensen and Plecháč (1997, Definition 4.2) reads $\mathbb{P} = 1 - aa^{\mathrm{T}} = zz^{\mathrm{T}}$, where $1 \in \mathbb{R}^{2\times 2}$ denotes the identity matrix. Carstensen and Plecháč (1997, Proposition 3) conjecture

$$8\,|(y_1 - y_2)\cdot z|^2 = 8\left|zz^{\mathrm{T}}\,(y_1 - y_2)\right|^2 \leqslant (S(y_1) - S(y_2))\,(y_1 - y_2)\,. \qquad \square$$

2.4 Three-Well Benchmark

The two-well benchmarks of (2.14) and (2.15) have both a unique solution, which is given in (2.13). In contrast, Bartels (2001, Example 5.6.4, page 58) presents a problem with three wells, for which uniqueness cannot be guaranteed.

The convexification of

$$W : \mathbb{R}^2 \to \mathbb{R},\quad y \mapsto \min\left\{|y|^2, |y-(1,0)|^2, |y-(0,1)|^2\right\}$$

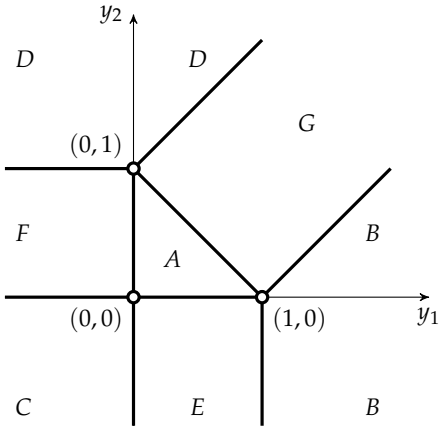

Figure 2.4: Subsets $A, B, C, D, E, F, G \subset \mathbb{R}^2$ of (2.17)

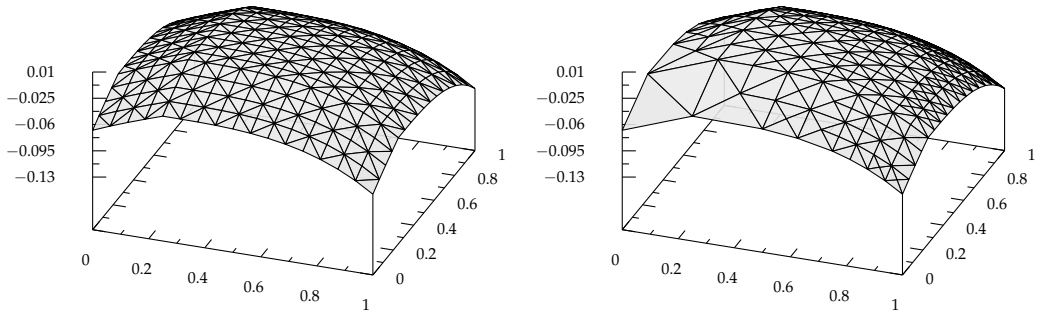

Figure 2.5: Nodal interpolation of the exact solution u_D from (2.18) of the three-well problem (left); numerical solution of the three-well problem (2.19) (right, based on the residual-based refinement indicator (5.5), page 94). Note the kinks along the lines $x_1 = 1/4$ and $x_2 = 1/4$.

is given by

$$W^{\star\star}(y) = \begin{cases} 0 & \text{for } y \in A, \\ W(y) = (y_1 - 1)^2 + y_2^2, & \text{for } y \in B, \\ W(y) = y_1^2 + y_2^2, & \text{for } y \in C, \\ W(y) = y_1^2 + (y_2 - 1)^2 & \text{for } y \in D, \\ y_2^2 & \text{for } y \in E, \\ y_1^2 & \text{for } y \in F, \\ (y_1 + y_2 - 1)^2 / 2 & \text{for } y \in G. \end{cases} \tag{2.17}$$

Figure 2.4 illustrates the sets A, B, C, D, E, F and G. The following lemma proves that the energy density $W^{\star\star}$ complies with the framework of Section 2.2.

(2.4.1) Lemma. *For $p = 2$ the energy density of* (2.17) *satisfies Assumptions (2.2.1) and (2.2.2) with $r = 2$ and $s = 0$.*

Proof. The convexification $W^{\star\star}$ inherits the quadratic growth from W. Bartels (2001, Proof of Example 5.6.4, page 58) proves Assumption (2.2.2). □

Given $\Omega \coloneqq]0,1[^2 \subset \mathbb{R}^2$ set

$$\begin{aligned} u_D(x) &\coloneqq a(x_1 - 1/4) + a(x_2 - 1/4) \quad \text{for } x = (x_1, x_2) \in \Omega \\ \text{with } a(t) &\coloneqq \begin{cases} t^3/6 + t/8 & \text{for } t \leqslant 0, \\ t^5/40 + t^3/8 & \text{for } t \geqslant 0. \end{cases} \end{aligned} \tag{2.18}$$

Similar to the modified two-well problem (2.15) the lower-order term $g = -\operatorname{div}(S(\mathrm{D}u_D))$ prescribes the exact solution $u = u_D$. Thus the three-well problem reads

$$\text{minimise } E^{\star\star}(v) = \int_\Omega (W^{\star\star}(\mathrm{D}v(x)) - g(x)v(x)) \,\mathrm{d}x \quad \text{amongst } v \in \mathcal{A}, \tag{2.19}$$

where $\mathcal{A} = u_D + W_0^{1,2}(\Omega)$. Literal application of (2.16) with $\Gamma \coloneqq \{x \in \mathbb{R}^2 : x_1 = 1/4 \text{ or } x_2 = 1/4\}$ shows that u_D is indeed a solution of the corresponding Euler-Lagrange equation and hence of (2.19). Figure 2.5 displays the exact solution u_D as well as a numerical approximation, computed with the methods of Chapter 5.

In comparison to the two-well problems, the energy density of the three-well problem precludes a result similar to Lemma (2.3.5) and the results of Chapter 4 cannot guarantee uniqueness of the the solutions u of (2.19). However, Theorem (2.2.5) guarantees uniqueness of the stress $\sigma = S(\mathrm{D}u)$ for different solutions u.

2.5 Optimal Design Benchmark

Given two materials a topology optimisation problem seeks a distribution of these materials within the cross section of an infinite bar, such that the amounts of the materials obey a given fixed ratio. The goal is to find a distribution of the materials with maximal torsion stiffness of the bar. After the seminal three-part paper of Kohn and Strang (1986) this topic has gained much attention (Carstensen et al., 2012; Bartels and Carstensen, 2007; Carstensen and Müller, 2002; Kawohl et al., 1991; Goodman et al., 1986).

This section considers a benchmark example from Carstensen et al. (2012, Section 6). For $y \in \mathbb{R}^2$ the degenerate convex energy density reads

$$W^{\star\star}(y) \coloneqq \varphi(|y|) \quad \text{with } \varphi(t) \coloneqq -\lambda/2 + \begin{cases} t^2 & \text{for } 0 \leqslant t \leqslant \sqrt{\lambda}, \\ 2\sqrt{\lambda}(t - \sqrt{\lambda}/2) & \text{for } \sqrt{\lambda} \leqslant t \leqslant 2\sqrt{\lambda}, \\ t^2/2 + \lambda & \text{for } t \geqslant 2\sqrt{\lambda}, \end{cases} \tag{2.20}$$

where $\lambda = 0.0084$. Figure 2.6 illustrates the function φ. The origin of this model and of the parameter λ is described by Bartels and Carstensen (2007, Section 2). The energy density $W^{\star\star}$ enjoys the following properties.

(2.5.1) Lemma. *For $p = 2$ the energy density $W^{\star\star}$ of* (2.20) *satisfies Assumptions (2.2.1) and (2.2.2) with $r = 2$ and $s = 0$.*

Proof. The energy density $W^{\star\star}$ inherits its quadratic growth from φ. Carstensen and Plecháč (1997, Example 3.1) prove Assumption (2.2.2). □

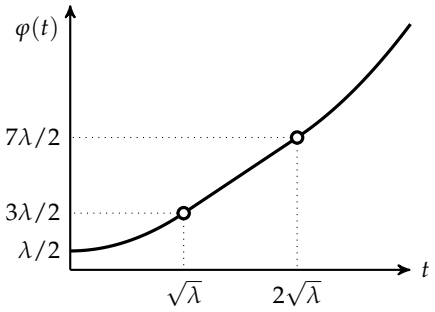

Figure 2.6: Sketch of φ from (2.20). The connecting points of the distinction of cases are highlighted.

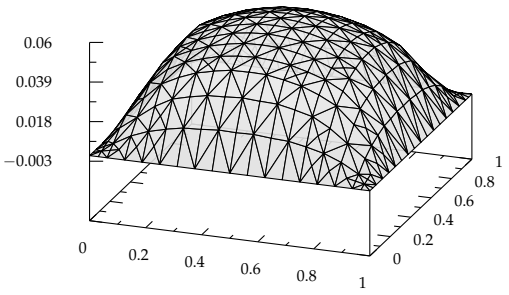

Figure 2.7: Numerical solution of the optimal design problem (2.21) with $g \equiv 1$, based on the residual-based refinement indicator (5.5) (page 94)

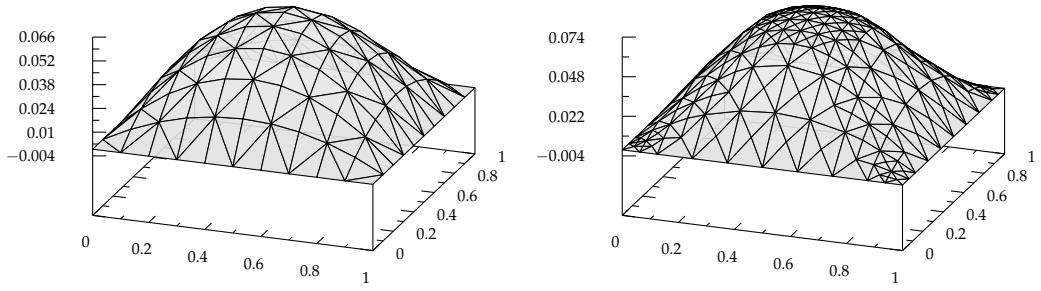

Figure 2.8: Nodal interpolation of the exact solution u from (2.22) of the modified optimal design problem (left); numerical solution of the modified optimal design problem (2.21) (right, based on the residual-based refinement indicator (5.5), page 94)

Given $\Omega \coloneqq]0,1[\subset \mathbb{R}^2$ set $g \equiv 1$ in Ω. Then the optimal design problem reads

$$\text{minimise } E^{\star\star}(v) = \int_\Omega (W^{\star\star}(\mathrm{D}v(x)) - g(x)v(x))\,\mathrm{d}x \;\text{ amongst } v \in \mathcal{A}, \tag{2.21}$$

where $\mathcal{A} = W^{1,2}_0(\Omega)$, i.e., Dirichlet boundary conditions are enforced. In contrast to the benchmark examples of Sections 2.3 and 2.4 no exact solution is known for (2.21). Also, no estimate similar to Lemma (2.3.5) is known for the energy density and uniqueness of the solutions cannot be guaranteed. Yet Theorem (2.2.5) guarantees uniqueness of the stress $\sigma = S(\mathrm{D}u)$ for different solutions u. Figure 2.7 displays an approximate solution, which is based on the methods of Chapter 5.

In order to compare error estimators with the exact error of numerical approximations we also consider an artificially modified lower-order term g which reads (cf. Carstensen et al., 2012, (6.3))

$$g \coloneqq -\operatorname{div}(S(\mathrm{D}u)) \;\text{ with } u(x) \coloneqq x_1x_2(1-x_1)(1-x_2). \tag{2.22}$$

The arguments of (2.16) affirm that u is an exact solution of (2.21) with the function g of (2.22). Figure 2.8 displays the exact solution u as well as a numerical approximation.

3 Finite Element Approximation

This chapter introduces the numerical approximation scheme for the model problem of Section 2.2. The main results of the chapter are threefold: firstly existence and uniqueness results for the discrete model problem are derived, which are similar to the results of Section 2.2. Secondly a multitude of error estimates for discrete solutions are provided, which estimate the difference of the solutions of the discrete and of the continuous model problem. In particular, upper and lower bounds on the error are proved. Finally, difficulties which arise in the solution process of the discrete problem and which are characteristic for degenerate convex problems are analysed. This leads to the introduction of the stabilised discrete problem to counteract these difficulties.

The chapter is structured as follows. Section 3.1 presents the P_1 conforming finite element method in a compact form. It introduces objects like triangulations, finite element function spaces and interpolation operators. Abstract results, such as interpolation error estimates, are also presented. Thereby, Section 3.1 serves as a discrete counterpart of Section 2.1.

Section 3.2, which may be construed as discrete counterpart of Section 2.2, aims at a discrete formulation of the continuous problem (2.2) (page 21). The basic idea is the minimisation of the energy functional amongst a finite-dimensional subspace of the space of admissible functions $\mathcal{A}$. In Section 3.2 the existence and uniqueness of solutions of the discrete minimisation problem is studied.

Sections 3.3 and 3.4 are devoted to the estimation of the error, that is, the difference between continuous and discrete solutions, in some suitable norm. Section 3.3 presents the residual-based error estimator and proves that, up to multiplicative constants, it is a guaranteed upper and lower bound of the error. However, the residual-based error estimator enters these inequalities with *different* exponents, thus giving rise to the reliability-efficiency gap. Section 3.4 presents the averaging error estimator, which is also, up to constant factors, an upper and a lower bound of the error.

Finally, Section 3.5 exposes numerical difficulties which arise from the degenerate convexity of the energy density $W^{\star\star}$. It turns out that degenerate convex problems may even lead to a breakdown of the numerical scheme. Section 3.5 introduces stabilisation techniques as a remedy using the example of an underdetermined linear system with Tikhonov regularisation. It summarises existing stabilisation methods (Bartels et al., 2004b) and presents an improved method, which is the basis of the analysis in Chapter 4.

Note that this chapter assumes $\Omega \subset \mathbb{R}^d$ to be a bounded open set with *polyhedral boundary*, for $d = 2$ or 3. This is necessary such that Ω can be covered properly with triangles or tetrahedra.

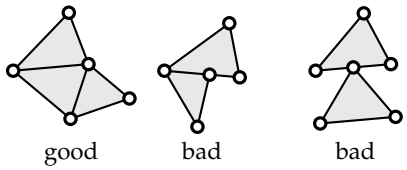

Figure 3.1: Examples of triangulations that satisfy ("good") or violate ("bad") Definition (3.1.1)

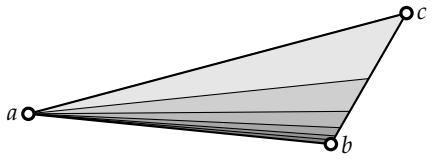

Figure 3.2: Construction of a family of triangulations which is not shape-regular in the sense of Definition (3.1.2). In each step the triangle that touches b is bisected along its edge on $\operatorname{conv}\{b, c\}$.

3.1 Finite Element Spaces and Interpolation Operators

Finite element approximations of partial differential equations rely a partition of the domain Ω and some finite-dimensional function space which is based on this partition. This thesis employs P_1 conforming finite element spaces to obtain approximative solutions of the minimisation problem of Section 2.2. The present section defines conforming P_1 finite element function spaces and studies several interpolation operators. Furthermore, it introduces Raviart-Thomas finite element functions, which are an important tool for the derivation of an error estimator in Section 4.3.

3.1.1 Regular Triangulations

Let $\Omega \subset \mathbb{R}^d$ be a bounded open set with polyhedral boundary. A *triangulation* $\mathcal{T}$ of Ω is a set of closed simplices (i.e., triangles for $d = 2$, tetrahedra for $d = 3$) with positive d-dimensional volume such that $\overline{\Omega} = \bigcup \mathcal{T}$. The vertices of these simplices $T \in \mathcal{T}$ are called *nodes*, the lines between any two nodes of a given simplex T is called an *edge* of T. For $d = 3$ the convex hull of any three nodes of a given T is called a *face* of T. In a dimension-independent fashion, edges (for $d = 2$) or faces (for $d = 3$) are called *sides*. The simplices T are called *elements* of the triangulation $\mathcal{T}$.

(3.1.1) Definition (Triangulation)**.** *A triangulation $\mathcal{T}$ of Ω is* regular *in the sense of Ciarlet (2002) if the intersection of any two distinct elements $T_1, T_2 \in \mathcal{T}$ is*

(a) either empty, $T_1 \cap T_2 = \varnothing$,
(b) or a common node z, that is, $T_1 \cap T_2 = \{z\}$,
(c) or a common edge,
(d) or (if $d = 3$) a common face.

As regular triangulation is called uniform *if all elements are congruent.*

Figure 3.1 illustrates how the regularity of a triangulation might be violated by poorly chosen elements. If a triangulation is not regular, offending nodes are commonly called *hanging nodes*.

For a given triangulation $\mathcal{T}$ the following abbreviations are employed,

$$\mathcal{N} \coloneqq \left\{z \in \overline{\Omega} \,:\, z \text{ node of } \mathcal{T}\right\}, \qquad \mathcal{F}^{\partial\Omega} \coloneqq \left\{F \in \mathcal{F} \,:\, F \subset \partial\Omega\right\},$$
$$\mathcal{F} \coloneqq \left\{F \subset \overline{\Omega} \,:\, F \text{ side of } \mathcal{T}\right\}, \qquad \mathcal{F}^{\Omega} \coloneqq \mathcal{F} \backslash \mathcal{F}^{\partial\Omega}.$$

Furthermore, the following sets (so-called *patches*) are defined,

$$\omega_z \coloneqq \bigcup_{\substack{T\in\mathcal{T}\\ z\in T}} T \text{ for } z\in\mathcal{N}, \qquad \omega_F \coloneqq \bigcup_{\substack{T\in\mathcal{T}\\ F\subset T}} T \text{ for } F\in\mathcal{F}, \qquad \omega_{T_0} \coloneqq \bigcup_{\substack{T\in\mathcal{T}\\ T_0\cap T\neq\emptyset}} T \text{ for } T\in\mathcal{T}.$$

For an element $T\in\mathcal{T}$ and a side $F\in\mathcal{F}$, the following abbreviations are used

$$h_T \coloneqq \operatorname{diam}(T) \text{ and } h_F \coloneqq \operatorname{diam}(F).$$

In order to investigate convergence behaviour of numerical schemes consider families of triangulations of a fixed domain Ω. The individual triangulations of such a family are indexed with a natural number $\ell\in\mathbb{N}_0$, the *level* of the triangulation. Consequently, such a family is denoted with $(\mathcal{T}_\ell)_{\ell\in\mathbb{N}_0}$. This thesis assumes that each member $\mathcal{T}_\ell$ of a given family of triangulations is *finer* than (or equal to) its predecessor $\mathcal{T}_{\ell-1}$ in the sense that

$$\bigcup\mathcal{F}_{\ell-1}\subset\bigcup\mathcal{F}_\ell \text{ for all } \ell\in\mathbb{N}.$$

(3.1.2) Definition (Shape Regularity)**.** *Given an element T denote its inradius (the radius of its insphere) with r_T. A family $(\mathcal{T}_\ell)_{\ell\in\mathbb{N}_0}$ of regular triangulations is called* shape-regular *if*

$$h_T\lesssim r_T \text{ for all } T\in\mathcal{T}_\ell \text{ and } \ell\in\mathbb{N}_0$$

with a generic constant that is independent of T and of ℓ.

Figure 3.2 illustrates the construction of a family of triangulations which is *not* shape-regular. The following lemma presents some elementary facts about shape-regular triangulations.

(3.1.3) Lemma. *Given a shape-regular family of triangulations $(\mathcal{T}_\ell)_{\ell\in\mathbb{N}_0}$ every $T\in\mathcal{T}_\ell$ and $F\in\mathcal{F}_\ell$ with $F\subset T$ satisfy*

(a) $h_T\approx h_F$,
(b) $|T|\approx h_T^d$, *and*
(c) $|F|\approx h_F^{d-1}$.

Furthermore, the number of elements that are covered by a nodal patch ω_z is uniformly bounded in the sense that

(d) $\#\{T\in\mathcal{T}_\ell : T\subset\omega_z\}\approx 1$ *for all $z\in\mathcal{N}_\ell$.*

The generic constants do not depend on the choices of T, F, z or ℓ.

Sketch of the proof. With the notation of Definition (3.1.2) each node $z\in T\in\mathcal{T}_\ell$ satisfies

$$1\lesssim r_T^{d-1}\Big/h_T^{d-1}\leqslant\sphericalangle(z,T)\coloneqq\begin{cases}\text{interior angle of } T \text{ in node } z & \text{for } d=2,\\ \text{interior solid angle of } T \text{ in node } z & \text{for } d=3.\end{cases}$$

This implies (d) because

$$\sum_{\substack{T\in\mathcal{T}_\ell\\ T\subset\omega_z}}\sphericalangle(z,T)\leqslant\begin{cases}2\pi & \text{for } d=2,\\ 4\pi^2 & \text{for } d=3.\end{cases}$$

For $d = 2$ this inequality imposes a lower limit upon all interior angles of all elements $T \in \mathcal{T}_\ell$, independently of ℓ. The law of sines yields $h_T \lesssim h_F$ and therefore (a). For $d = 3$ shape regularity implies $h_F \leqslant h_T \lesssim r_T < r_F$, where r_F is the inradius of the triangle F. Hence the two-dimensional version of (a) applies to all sides F with $F \subset T$ and the observation

$$h_T = \max_{\substack{\widetilde{F}\in\mathcal{F}_\ell \\ \widetilde{F}\subset T}} h_{\widetilde{F}}$$

proves (a) for $d = 3$. (b) and (c) follow from

$$h_T^d \lesssim r_T^d \leqslant |T| \leqslant h_T^d \quad \text{and} \quad h_F^d \lesssim r_F^d \leqslant |F| \leqslant h_F^d. \qquad \square$$

Given a family $(\mathcal{T}_\ell)_{\ell\in\mathbb{N}_0}$ of regular triangulations denote the *mesh size function* of $\mathcal{T}_\ell$ by

$$h_\ell(x) \coloneqq \begin{cases} h_T & \text{for } x \in \operatorname{int} T, T \in \mathcal{T}_\ell, \\ \min\{h_F \,:\, F \in \mathcal{F}_\ell \text{ and } x \in F\} & \text{otherwise.} \end{cases}$$

An important quantity is the *global mesh size* of $\mathcal{T}_\ell$, which is

$$H_\ell \coloneqq \|h_\ell\|_{L^\infty(\Omega)} = \max_{T\in\mathcal{T}_\ell} h_T.$$

The minimal mesh size of a given triangulation $\mathcal{T}_\ell$ is also occasionally referred to, that is $h_{\ell,\min} \coloneqq \min_{T\in\mathcal{T}_\ell} h_T$. A family of triangulations is called *quasi-uniform* if $H_\ell \approx h_{\ell,\min}$. Clearly, a family of uniform triangulations satisfies $H_\ell = h_{\ell,\min}$ and is therefore quasi-uniform.

The previous definitions and observations facilitate the analysis of function spaces that are defined by triangulations. Abbreviate the set of polynomial functions of degree $\leqslant k \in \mathbb{N}_0$ on the domain $\omega \subset \mathbb{R}^d$ with $P_k(\omega)$. Let $\mathcal{T}$ be a triangulation of Ω. Let the notation $u \in P_k(\mathcal{T})$ indicate that u is a function on Ω which is $\mathcal{T}$*-piecewise* polynomial of degree $\leqslant k$. Respective notation applies to the function spaces of Section 2.1. In more formal notation,

$$X(\mathcal{T}) \coloneqq \{u : \Omega \to \mathbb{R} \,:\, u|_{\operatorname{int} T} \in X(\operatorname{int} T) \ \text{ for all } T \in \mathcal{T}\}$$
$$\text{for } X \in \{W^{s,p}, H^s, P_k\}.$$

Note that this definition permits jumps along the sides of the triangulation. The same convention applies to $X(\mathcal{T};\mathbb{R}^n)$ and $X(\mathcal{F})$, as well as to subsets of $\mathcal{T}$ and $\mathcal{F}$.

3.1.2 First-Order Conforming Finite Elements

The numerical analysis of this thesis is based on the space of conforming P_1 finite element functions, which reads

$$\mathcal{S}_1(\mathcal{T}) \coloneqq P_1(\mathcal{T}) \cap \mathcal{C}(\overline{\Omega})$$

for a given triangulation $\mathcal{T}$. A polynomial of degree one on a simplex T in $\mathbb{R}^d$ is uniquely defined by its function values in the vertices of said simplex. Due to the demand of global continuity a function $u \in \mathcal{S}_1(\mathcal{T})$ is uniquely defined by its values on the nodes $z \in \mathcal{N}$. Hence a basis of $\mathcal{S}_1(\mathcal{T})$ is given by the nodal basis functions $(\varphi_z)_{z\in\mathcal{N}}$, which are defined

by

$$\varphi_z(x) \coloneqq \begin{cases} 1 & \text{for } x = z, \\ 0 & \text{for } x \neq z \end{cases} \quad \text{for } x \in \mathcal{N}. \tag{3.1}$$

Figure 3.3 illustrates a nodal basis function on a uniform triangulation of a rectangle.

The *nodal interpolation operator* approximates continuous functions with $\mathcal{S}_1$ finite element function and reads

$$I : \mathcal{C}(\overline{\Omega}) \to \mathcal{S}_1(\mathcal{T}), \quad u \mapsto Iu = \sum_{z \in \mathcal{N}} u(z)\varphi_z.$$

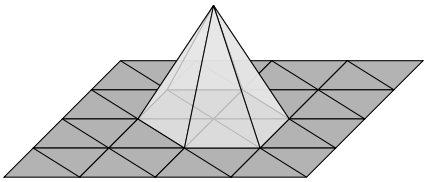

Figure 3.3: Nodal basis function on a uniform grid in $\mathbb{R}^2$

Since the nodal interpolation operator I depends on the triangulation, it is usually indexed with the level ℓ to indicate the specific triangulation it refers to. The following is a collection of interpolation error estimates for I.

(3.1.4) Lemma. *Given a shape-regular family of triangulations $(\mathcal{T}_\ell)_{\ell \in \mathbb{N}_0}$ of Ω, the nodal interpolation operator I_ℓ on $\mathcal{T}_\ell$ satisfies*

$$\begin{aligned} &\|I_\ell u\|_{L^\infty(\Omega)} \leqslant \|u\|_{L^\infty(\Omega)} \quad \text{for } u \in C(\overline{\Omega}), \quad \text{and} \\ &|I_\ell u|_{W^{1,p}(\Omega)} \lesssim |u|_{W^{1,p}(\Omega)} \quad \text{for } u \in W^{1,p}(\Omega), \quad \text{where } d < p \leqslant \infty. \end{aligned}$$

The generic constant depends on p, but not on u or on the level ℓ.

Proof. The first inequality is a consequence of the fact that the $\mathcal{S}_1$ function $I_\ell u$ attains its minimum and maximum in a node of the triangulation, where it coincides with u.

Recall that"1" denotes the identity operator in the context of function operators. Brenner and Scott (2002, Theorem (4.4.4), page 106) prove

$$|(1 - I_\ell)u|_{W^{1,p}(\Omega)} \lesssim |u|_{W^{1,p}(\Omega)} \quad \text{for } u \in W^{1,p}(\Omega)$$

independently of ℓ and u. Note that u is continuous on $\overline{\Omega}$ due to Lemma (2.1.6), hence $I_\ell u$ is well defined. A triangle inequality yields the claim. □

(3.1.5) Lemma (Brenner and Scott, 2002, Theorem (4.4.4), page 106)**.** *Given a d-dimensional simplex T, where any $d \in \mathbb{N}$ is permitted, let $\max\{d/2, 1\} < p \leqslant \infty$. Then it holds that*

$$\|u\|_{L^p(T)} + h_T |u|_{W^{1,p}(T)} \lesssim h_T^2 |u|_{W^{2,p}(T)} \quad \text{for all } u \in W^{2,p}(T) \text{ with } u = 0 \text{ in the nodes of } T.$$

Note that $W^{2,p}(T) \subset \mathcal{C}(T)$ due to Lemma (2.1.6). The generic constant depends on the shape of T, i.e., the ratio of h_T and its inradius, but not on its size.

(3.1.6) Lemma. *Given a shape-regular family of triangulations $(\mathcal{T}_\ell)_{\ell \in \mathbb{N}_0}$ of Ω and $d/2 < p \leqslant \infty$ it holds*

$$\|(1 - I_\ell)u\|_{L^p(\Omega)} + H_\ell |(1 - I_\ell)u|_{W^{1,p}(\Omega)} \lesssim H_\ell^2 \left\|\mathrm{D}_\ell^2 u\right\|_{L^p(\Omega)} \quad \text{for all } u \in W^{2,p}(\mathcal{T}_\ell) \cap \mathcal{C}(\overline{\Omega}).$$

The generic constant is independent of u and of ℓ.

Here and in the following $\mathrm{D}_\ell^2 u$ denotes the $\mathcal{T}_\ell$-piecewise second derivative of u. Likewise, $\Delta_\ell u$ denotes the $\mathcal{T}_\ell$-piecewise Laplacian of u.

Proof. The second derivative $\mathrm{D}^2 I_\ell u$ of $I_\ell u$ vanishes on each element $T \in \mathcal{T}_\ell$, i.e., $\mathrm{D}_\ell^2 I_\ell u \equiv 0$. Given an element $T \in \mathcal{T}_\ell$ Lemma (3.1.5) for $w_\ell := (1 - I_\ell)u$ reads

$$\|w_\ell\|_{L^p(T)} + h_T \, |w_\ell|_{W^{1,p}(T)} \lesssim h_T^2 \, |u|_{W^{2,p}(T)} ,$$

with a generic constant that is independent of ℓ or T due to shape regularity. For $p < \infty$ the assertion follows from the sum over all elements,

$$\begin{aligned} \|w_\ell\|_{L^p(\Omega)}^p &= \sum_{T \in \mathcal{T}_\ell} \|w_\ell\|_{L^p(T)}^p \lesssim \sum_{T \in \mathcal{T}_\ell} h_T^{2p} \, |u|_{W^{2,p}(T)}^p \leqslant H_\ell^{2p} \left\|\mathrm{D}_\ell^2 u\right\|_{L^p(\Omega)}^p , \\ |w_\ell|_{W^{1,p}(\Omega)}^p &= \sum_{T \in \mathcal{T}_\ell} |w_\ell|_{W^{1,p}(T)}^p \lesssim \sum_{T \in \mathcal{T}_\ell} h_T^p \, |u|_{W^{2,p}(T)}^p \leqslant H_\ell^p \left\|\mathrm{D}_\ell^2 u\right\|_{L^p(\Omega)}^p . \end{aligned}$$

For $p = \infty$ the assertion follows from

$$\begin{aligned} \|w_\ell\|_{L^\infty(\Omega)} &= \max_{T \in \mathcal{T}_\ell} \|w_\ell\|_{L^\infty(T)} \lesssim \max_{T \in \mathcal{T}_\ell} h_T^2 \, |u|_{W^{2,\infty}(T)} \leqslant H_\ell^2 \left\|\mathrm{D}_\ell^2 u\right\|_{L^\infty(\Omega)} , \\ |w_\ell|_{W^{1,p}(\Omega)} &= \max_{T \in \mathcal{T}_\ell} |w_\ell|_{W^{1,p}(T)} \lesssim \max_{T \in \mathcal{T}_\ell} h_T \, |u|_{W^{2,\infty}(T)} \leqslant H_\ell \left\|\mathrm{D}_\ell^2 u\right\|_{L^\infty(\Omega)} . \end{aligned}$$ □

For the averaging error estimator of Section 3.4 one requires the definition of the *averaging interpolation operator*, which reads

$$\Sigma : L^1(\Omega) \to \mathcal{S}_1(\mathcal{T}), \quad u \mapsto \Sigma u = \sum_{z \in \mathcal{N}} \left(\fint_{\omega_z} u(x) \mathrm{d}x \right) \varphi_z. \tag{3.2}$$

3.1.3 Piecewise Constant Functions

The space of *piecewise constant* finite element functions is given by $P_0(\mathcal{T})$. E.g., the piecewise gradient of an $\mathcal{S}_1(\mathcal{T})$ function is an $P_0(\mathcal{T}; \mathbb{R}^d)$ function. A corresponding interpolation operator is the L^2 projection Π onto $P_0(\mathcal{T})$,

$$\Pi : L^1(\Omega) \to P_0(\mathcal{T}), \quad u \mapsto \Pi u \ \text{ with } \Pi u(y) := \fint_T u(x) \mathrm{d}x \ \text{ for } y \in \operatorname{int} T, T \in \mathcal{T}.$$

The operator Π enjoys the following stability property.

(3.1.7) Lemma. *Let $\mathcal{T}$ be a regular triangulation of Ω and let $1 \leqslant p \leqslant \infty$. Then*

$$\|\Pi u\|_{L^p(\Omega)} \leqslant \|u\|_{L^p(\Omega)} \ \textit{ for all } u \in L^p(\Omega).$$

Proof. Since $|\Pi u(x)| \leqslant \|u\|_{L^\infty(T)} \leqslant \|u\|_{L^\infty(\Omega)}$ for $x \in T \in \mathcal{T}$ the assertion is true for $p =$

∞. If $p < \infty$ Jensen's inequality (Lemma (2.1.21), page 20) with $f(\zeta) \coloneqq |\zeta|^p$ yields

$$\|\Pi u\|_{L^p(\Omega)}^p = \sum_{T\in\mathcal{T}} |T|\, f\left(\fint u(x)\mathrm{d}x\right) \leqslant \sum_{T\in\mathcal{T}} |T| \fint f(u(x))\mathrm{d}x = \|u\|_{L^p(\Omega)}^p . \qquad \square$$

Given some $1 \leqslant p \leqslant \infty$ and a function $u \in L^p(\Omega)$ the *oscillation* of u with respect to the triangulation $\mathcal{T}$ of Ω is defined by

$$\operatorname{osc}_p(u) \coloneqq \|h_\ell(1-\Pi)u\|_{L^p(\Omega)} . \tag{3.3}$$

The oscillation measures the deviation of a function from its elementwise mean value. Similar to interpolation operators the oscillation operator is indexed with ℓ to indicate the particular triangulation it is based on ("$\operatorname{osc}_{\ell,p}$"). The following lemma is a direct consequence of Poincaré's inequality (Lemma (2.1.16), page 19).

(3.1.8) Lemma. *Let $(\mathcal{T}_\ell)_{\ell\in\mathbb{N}_0}$ be a shape-regular family of triangulations, and let $1 \leqslant p \leqslant \infty$. Then it holds that*

$$\operatorname{osc}_{\ell,p}(u) \lesssim H_\ell^2\, |u|_{W^{1,p}(\Omega)} \quad \text{for } u \in W^{1,p}(\Omega).$$

The generic constant is independent of u and of ℓ.

3.1.4 Raviart-Thomas Functions

Recall the definition of the jump $[\cdot]_F$ from Section 2.1. Raviart and Thomas (1977) introduced the space

$$RT_0(\mathcal{T}) \coloneqq \Big\{ \tau \in P_1(\mathcal{T};\mathbb{R}^d) \,:\, \tau(x) = a(x) + c(x)x \;\text{ with } a \in P_0(\mathcal{T};\mathbb{R}^d), c \in P_0(\mathcal{T};\mathbb{R}), \\ [\tau]_F \cdot n_F = 0 \;\text{ for all } F \in \mathcal{F}^\Omega \Big\} \tag{3.4}$$

in order to approximate $H(\operatorname{div})$ functions with discrete functions. Here and in the following n_F is the unit normal vector of the side $F \in \mathcal{F}$. For an interior side $F \in \mathcal{F}^\Omega$ the direction of n_F is arbitrary, but *fixed* for a given triangulation $\mathcal{T}$. If F is a boundary side, $F \in \mathcal{F}^{\partial\Omega}$, we assume n_F to point *outwards* of Ω. The continuity of the normal components on interior sides implies $RT_0(\mathcal{T}) \subset H(\operatorname{div},\Omega)$ (Braess, 2007, Problem II.5.14, page 74). Also note that the definition of Raviart-Thomas functions implies that the normal component is constant along each side of the triangulation.

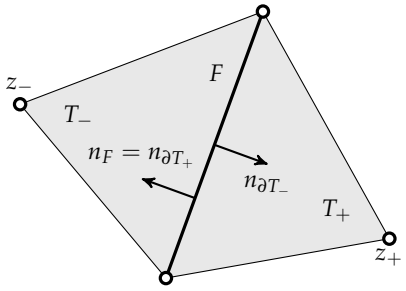

Figure 3.4: Neighbouring elements $T_\pm$ are separated by a side F. The normal vectors of $\mathcal{T}_\pm$ are anti-diagonal along F. By convention, the side's unit normal vector n_F is the *outer-pointing* normal of T_+.

A basis of $RT_0(\mathcal{T})$ can be defined following Carstensen (2009, Definition 3.20, page 179). Given a side $F \in \mathcal{F}$ there are at most two elements $T_\pm \in \mathcal{T}$ with $F \subset T_\pm$. If $F \in \mathcal{F}^{\partial\Omega}$ there is only one element T_+ which contains F, and T_- does not exist. If $F \in \mathcal{F}^\Omega$ the elements

T_+ and T_- are chosen such that the unit normal vector n_F points from T_+ to T_-. Let $z_\pm \in \mathcal{N}$ be the unique nodes of $T_\pm$ with $z_\pm \notin F$, i.e., $T_\pm = \operatorname{conv}(F \cup \{z_\pm\})$. Figure 3.4 illustrates the configuration in the case of an interior side. Define $\varphi_F \in RT_0(\mathcal{T})$ by

$$\varphi_F(x) \coloneqq \begin{cases} \pm \frac{|F|}{2|T_\pm|}(x - z_\pm) & \text{for } x \in T_\pm \\ 0 & \text{otherwise.} \end{cases}$$

Carstensen (2009, Lemma 3.22, page 179) or a simple calculation show that $(\varphi_F)_{F\in\mathcal{F}}$ is a basis of $RT_0(\mathcal{T})$ and

$$\varphi_{F_1}(x) \cdot n_{F_2} = \begin{cases} 1 & \text{for } x \in F_1 = F_2 \in \mathcal{F}, \\ 0 & \text{for } x \in F_2 \in \mathcal{F} \backslash \{F_1\}. \end{cases}$$

With this basis, the *Fortin interpolation operator*, as introduced by Brezzi and Fortin (1991, Section III.3.3, page 125), reads

$$I_{\mathrm{F}} : H(\operatorname{div}, \Omega) \cap L^{2+}(\Omega; \mathbb{R}^d) \to RT_0(\mathcal{T}), \quad \tau \mapsto I_{\mathrm{F}}\tau = \sum_{F\in\mathcal{F}} \left(\fint_F \tau(x) \cdot n_F \mathrm{d}s \right) \varphi_F. \tag{3.5}$$

Carefully note that $\tau \in H(\operatorname{div}, \Omega)$ is *not* enough regularity for the integral. Refer to Brezzi and Fortin (1991, Section III.3.3, page 125) for an explanation on why $\tau \in L^{2+}(\Omega; \mathbb{R}^d)$ is required in addition.

The following lemma is analogous to Lemma (3.1.6).

(3.1.9) Lemma. *Given a shape-regular family of triangulations $(\mathcal{T}_\ell)_{\ell\in\mathbb{N}_0}$ of Ω it holds that*

$$\|(1 - I_{\mathrm{F},\ell})\tau\|_{L^2(\Omega)} \lesssim H_\ell \, |\tau|_{H^1(\Omega)} \quad \textit{for all } \tau \in H(\operatorname{div}, \Omega) \cap L^{2+}(\Omega; \mathbb{R}^d).$$

The generic constant is independent of τ and ℓ.

Proof. For an element $T \in \mathcal{T}_\ell$ Brezzi and Fortin (1991, Proposition 3.6, page 128) show

$$\|(1 - I_{\mathrm{F},\ell})\tau\|^2_{L^2(T)} \lesssim h_T^2 \, |\tau|^2_{H^1(T)}.$$

The sum over all elements concludes the proof. □

The Fortin interpolation operator I_{F} and the L^2 projection Π satisfy the following commuting diagram property.

(3.1.10) Lemma (Commuting Diagram Property (Brezzi and Fortin, 1991, Proposition 3.7, page 129))**.** *Given a triangulation $\mathcal{T}$ of Ω the corresponding interpolation operators I_{F} and Π satisfy*

$$\operatorname{div} \circ I_{\mathrm{F}} = \Pi \circ \operatorname{div} \quad \textit{on the space } H(\operatorname{div}, \Omega) \cap L^{2+}(\Omega; \mathbb{R}^d).$$

3.1.5 Trace Inequality

The section concludes with the following discrete version of the trace theorem (Lemma (2.1.20), page 20).

(3.1.11) Lemma (Trace Inequality)**.** *Let T be a d-dimensional simplex and F one of its sides, and let $1 \leqslant p < \infty$. Then, all $u \in W^{1,p}(T)$ satisfy*

$$\begin{aligned}\|u\|_{L^p(F)}^p &\lesssim h_T^{-1} \|u\|_{L^p(T)}^p + \|u\|_{L^p(T)}^{p-1} \|\mathrm{D}u\|_{L^p(T)} \\ &\lesssim h_T^{-1} \|u\|_{L^p(T)}^p + h_T^{p-1} \|\mathrm{D}u\|_{L^p(T)}^p .\end{aligned}$$

The generic constants depend on the shape of T, i.e., the ratio of h_T and its inradius, but not on its size.

Notes on the proof. The trace inequality is already well-known in the numerical analysis of the finite element method. A rigorous proof of the first assertion can be found in Veeser and Verfürth (2009, Corollary 4.5). Given the Hölder conjugate p' of p, i.e., $1/p + 1/p' = 1$, Young's inequality (Lemma (2.1.22), page 20) conjectures the second assertion by

$$h_T^{-1/p'} \|u\|_{L^p(T)}^{p-1} h_T^{1/p'} \|\mathrm{D}u\|_{L^p(T)} \lesssim h_T^{-1} \|u\|_{L^p(T)}^p + h_T^{p-1} \|\mathrm{D}u\|_{L^p(T)}^p . \qquad \square$$

3.2 Discretisation of the Convex Minimisation Problem

This section establishes and analyses a discretisation of the continuous convex model problem.

Let $d = 2$ or 3 and $\Omega \subset \mathbb{R}^d$ be a bounded Lipschitz domain with polyhedral boundary. Consider the continuous convex model problem (2.2) (page 21) which reads

$$\begin{gathered}\text{minimise } E^{\star\star}(v) = \int_\Omega \Big(W^{\star\star}(\mathrm{D}v(x)) + \alpha \, |v(x) - f(x)|^2 - g(x) \cdot v(x) \Big) \, \mathrm{d}x \\ \text{amongst } v \in \mathcal{A}.\end{gathered} \tag{3.6}$$

Here p' is the Hölder conjugate of some $2 \leqslant p < \infty$, i.e., $1/p + 1/p' = 1$, and $\alpha \geqslant 0$. The convex energy density is given by $W^{\star\star} \in \mathcal{C}^1(\mathbb{R}^{n \times d})$ and the lower-order terms by $f \in L^2(\Omega; \mathbb{R}^n)$ and $g \in L^{p'}(\Omega; \mathbb{R}^n)$. The set of admissible functions reads $\mathcal{A} = u_D + V$ where u_D defines the Dirichlet boundary data and $V = W_0^{1,p}(\Omega; \mathbb{R}^n)$. In contrast to Section 2.2 stricter regularity assumption on u_D are imposed in this and in the subsequent chapters. The precise regularity assumption depends on the initial triangulation $\mathcal{T}_0$ and is therefore stated below in (3.13). Recall the abbreviations of the stress tensor and of the derivative of the energy's lower-order terms

$$\sigma(x) \coloneqq S(\mathrm{D}u(x)) \coloneqq \mathrm{D}W^{\star\star}(\mathrm{D}u(x)) \quad \text{and} \quad \Lambda(x) \coloneqq -2\alpha(u(x) - f(x)) + g(x)$$

for a given solution $u \in \mathcal{A}$ from (2.3) (page 21). With these abbreviations, the continuous Euler-Lagrange equation (2.4) (page 21) reads

$$\int_\Omega (\sigma(x) : \mathrm{D}v(x) - \Lambda(x) \cdot v(x)) \, \mathrm{d}x = 0 \quad \text{for all } v \in V. \tag{3.7}$$

We assume that the energy density $W^{\star\star}$ satisfies the two-sided growth condition (As-

sumption (2.2.1), page 21), which reads

$$|y|^p - 1 \lesssim W^{\star\star}(y) \lesssim |y|^p + 1 \quad \text{for all } y \in \mathbb{R}^{n\times d}, \tag{3.8}$$

as well as convexity control (Assumption (2.2.2), page 22), which reads

$$|S(y_1) - S(y_2)|^r \lesssim \left(1 + |y_1|^s + |y_2|^s\right)(S(y_1) - S(y_2)) : (y_1 - y_2) \tag{3.9}$$

for some fixed r and s with $p' \leqslant r$ and $0 \leqslant s \leqslant rp - r - p$.

3.2.1 Statement of the Discrete Problem

A straight-forward discretisation with conforming P_1 finite element functions is given as follows. Let $(\mathcal{T}_\ell)_{\ell\in\mathbb{N}_0}$ be a family of shape-regular triangulations of the domain Ω, and let the space of discrete admissible functions be $\mathcal{A}_\ell := u_{D,\ell} + V_\ell$ with $V_\ell = \mathcal{S}_1(\mathcal{T}_\ell;\mathbb{R}^n) \cap V$ and the nodal interpolation $u_{D,\ell} = I_\ell u_D$, which is well-defined here since $u_D \in \mathcal{C}(\overline{\Omega};\mathbb{R}^n)$ (cf. (3.13) and Lemma (3.2.1) below). Note that V_ℓ is a finite-dimensional subspace of $W^{1,p}_0(\Omega;\mathbb{R}^n)$. The *discrete (convex) minimisation problem* reads

$$\begin{gathered}\text{minimise } E^{\star\star}(v_\ell) = \int_\Omega \Big(W^{\star\star}(\mathrm{D}v_\ell(x)) + \alpha\,|v_\ell(x) - f(x)|^2 - g(x)\cdot v_\ell(x)\Big)\,\mathrm{d}x \\ \text{amongst } v_\ell \in \mathcal{A}_\ell.\end{gathered} \tag{3.10}$$

Analogously to (2.3) (page 21) abbreviate the discrete stress tensor and the derivative of the energy's lower-order terms with

$$\sigma_\ell(x) := S(\mathrm{D}u_\ell(x)) \quad \text{and} \quad \Lambda_\ell(x) := -2\alpha(u_\ell(x) - f(x)) + g(x) \tag{3.11}$$

for a given fixed $u_\ell \in \mathcal{A}_\ell$. The discrete Euler-Lagrange equation that corresponds to the discrete minimisation problem (3.10) reads

$$\int_\Omega (\sigma_\ell(x) : \mathrm{D}v_\ell(x) - \Lambda_\ell(x) : v_\ell(x))\,\mathrm{d}x = 0 \quad \text{for all } v_\ell \in V. \tag{3.12}$$

Based on the initial triangulation $\mathcal{T}_0$, this and the remaining chapters assume u_D to satisfy

$$u_D \in W^{1,p}(\Omega;\mathbb{R}^n) \cap W^{2,p}(\mathcal{T}_0;\mathbb{R}^n) \cap W^{2,p}(\mathcal{F}_0^{\partial\Omega};\mathbb{R}^n). \tag{3.13}$$

The elementwise and sidewise smoothness conditions of (3.13) permit interpolation estimates for $u_{D,\ell} = I_\ell u_D$, e.g. in the proof of Lemma (3.3.10). In particular, with Lemma (3.2.1) below and Lemma (2.1.6) (page 16), (3.13) ensures $u_D \in \mathcal{C}(\overline{\Omega};\mathbb{R}^n)$. Condition (3.13) is not a severe restriction since u_D matters only on the boundary $\partial\Omega$; its values in the interior of Ω are not significant.

(3.2.1) Lemma. *Given a triangulation $\mathcal{T}$ of the domain $\Omega \subset \mathbb{R}^d$ it holds*

$$W^{1,p}(\Omega) \cap C(\mathcal{T}) \subset C(\overline{\Omega}).$$

Proof. Let $u \in W^{1,p}(\Omega) \cap C(\mathcal{T})$ and $F \in \mathcal{F}^\Omega$. It suffices to show that the jump $[u]_F$ vanishes.

Let $y \in F$, then Evans and Gariepy (1992, Theorem 2, Section 4.9.2, page 164) prove that u is continuous on almost every line $(y + n_F\mathbb{R}) \cap \Omega$ ("almost every" referring to the $(d-1)$-dimensional Hausdorff measure on F). Hence $[u]_F$ vanishes almost everywhere on F. By the continuity of u on both elements which contain F, the jump $[u]_F$ vanishes completely. □

3.2.2 Existence and Uniqueness of Solutions

The following existence and uniqueness results similar to Theorems (2.2.3), (2.2.4) and (2.2.5) hold.

(3.2.2) Theorem (Existence of Solutions)**.** *Given the minimisation problem* (3.10) *let its energy density $W^{\star\star}$ satisfy* (3.8)*. Then there exists a minimiser $u_\ell \in \mathcal{A}_\ell$ of* (3.10)*.*

Proof. Theorem (2.2.3) proves the existence of a minimiser of (3.10) amongst $u_{D,\ell} + V$. Since $u_{D,\ell} + V_\ell$ is a closed subset of $u_{D,\ell} + V$, it also contains a minimiser of (3.10). □

(3.2.3) Theorem. *Given the minimisation problem* (3.10) *let its energy density $W^{\star\star}$ satisfy* (3.8)*. Then every minimiser u_ℓ of* (3.10) *is a solution of the Euler-Lagrange equation* (3.12)*. Conversely, every solution $u_\ell \in \mathcal{A}$ of* (3.12) *is a minimiser of* (3.10)*.*

Notes on the proof. The proof is verbatim to Dacorogna (2004, Proof of Theorem 3.11, page 93) with $W^{1,p}$ and $W_0^{1,p} = V$ replaced by $\mathcal{S}_1(\mathcal{T}_\ell)$ and V_ℓ. See the notes on the proof of Theorem (2.2.4) (page 22) for a necessary modification of the assumptions in Dacorogna (2004). □

(3.2.4) Theorem (Uniqueness)**.** *Assume that the energy density $W^{\star\star}$ of* (3.10) *complies with* (3.8) *and* (3.9)*. Then any two solutions $u_{\ell,1}$ and $u_{\ell,2}$ of* (2.2) *satisfy $S(\mathrm{D}u_{\ell,1}) = S(\mathrm{D}u_{\ell,2})$ almost everywhere in Ω. If furthermore $\alpha > 0$, then also $u_{\ell,1} = u_{\ell,2}$ almost everywhere in Ω.*

Similar to Theorem (2.2.5) the proof of boundedness of discrete solutions is a prerequisite. Note that the bound is not only independent of the actual choice of u_ℓ for a given level ℓ, *but also does not depend on the level ℓ.*

(3.2.5) Lemma. *Given the minimisation problem* (3.10) *let its energy density $W^{\star\star}$ satisfy* (3.8) *and* (3.9)*. Then the set of minimisers is bounded in $W^{1,p}(\Omega;\mathbb{R}^n)$, i.e., $\|u_\ell\|_{W^{1,p}(\Omega)} \lesssim 1$ for all solutions $u_\ell \in \mathcal{A}_\ell$, with a generic constant independent of the choice of ℓ and the choice of u_ℓ.*

Proof. This proof argues along the lines of the proof of Theorem (2.2.5) (page 23). A triangle inequality and Lemmas (2.1.4) (page 16) and (3.1.4) yield

$$\|u_D - u_{D,\ell}\|_{W^{1,p}(\Omega)} \lesssim \|u_D\|_{W^{1,p}(\Omega)} + \|I_\ell u_D\|_{L^\infty(\Omega)} + |I_\ell u_D|_{W^{1,p}(\Omega)} \lesssim 1. \tag{3.14}$$

Given a solution u_ℓ of (3.10), (3.14) and Friedrichs' inequality (Lemma (2.1.17), page 19) for $v_\ell \coloneqq u_\ell - u_{D,\ell}$ show, akin to (2.9) (page 23),

$$\|u_\ell\|_{L^p(\Omega)} \lesssim \|u_{D,\ell}\|_{L^p(\Omega)} + |v_\ell|_{W^{1,p}(\Omega)} \lesssim \|u_{D,\ell}\|_{W^{1,p}(\Omega)} + |u_\ell|_{W^{1,p}(\Omega)} \lesssim 1 + |u_\ell|_{W^{1,p}(\Omega)}\,. \tag{3.15}$$

With u replaced by u_ℓ, the estimate (2.10) (page 23) provides the lower bound

$$E^{\star\star}(u_\ell) \gtrsim |u_\ell|^p_{W^{1,p}(\Omega)} - |u_\ell|_{W^{1,p}(\Omega)} - 1 \tag{3.16}$$

on the energy $E^{\star\star}(u_\ell)$. In contrast to the proof of Theorem (2.2.5) the energy $E^{\star\star}(u_\ell)$ is not constant, but rather depends on ℓ. Hence one requires an upper bound on $E^{\star\star}(u_\ell)$. Similar to (2.10) the two-sided growth condition (3.8), the triangle inequality and (3.14) yield

$$\begin{aligned} E^{\star\star}(u_\ell) &\leqslant E^{\star\star}(u_{D,\ell}) \\ &\lesssim |u_{D,\ell}|^p_{W^{1,p}(\Omega)} + |\Omega| + \|u_{D,\ell}\|^2_{L^2(\Omega)} + \|f\|^2_{L^2(\Omega)} + \|g\|_{L^{p'}(\Omega)} \|u_{D,\ell}\|_{L^p(\Omega)} \\ &\lesssim |u_D|^p_{W^{1,p}(\Omega)} + \|u_D\|^2_{L^2(\Omega)} + \|g\|_{L^{p'}(\Omega)} \|u_D\|_{L^p(\Omega)} + 1 \lesssim 1. \end{aligned} \tag{3.17}$$

Akin to (2.11), the combination of (3.16) and (3.17) proves the existence of a constant $C > 0$ which is independent of ℓ and u_ℓ, and which satisfies

$$|u_\ell|^p_{W^{1,p}(\Omega)} - |u_\ell|_{W^{1,p}(\Omega)} - 1 < C.$$

Therefore $|u_\ell|_{W^{1,p}(\Omega)}$ is bounded by the positive root of $X^p - X - 1 - C = 0$, and (3.15) yields a bound on $\|u_\ell\|_{L^p(\Omega)}$. □

Proof of Theorem (3.2.4). Lemma (3.2.5) ensures the existence of $W^{1,p}$-bounds on $u_{\ell,1}$ and $u_{\ell,2}$, hence Lemma (2.2.7) (page 23) applies. The very same arguments of the proof of Theorem (2.2.5), applied to the discrete Euler-Lagrange equation (3.12), prove the assertions of Theorem (3.2.4). □

3.3 Residual-Based Error Estimation

This section is devoted to error estimations of the discrete problem of Section 3.2. The following results are mostly due to Carstensen and Plecháč (1997). Some of the arguments therein support the understanding of Chapter 4, therefore the full proofs are recited here.

Recall the continuous model problem (3.6) and its discrete counterpart (3.10) from the introduction of Section 3.2 (page 39). Assume the energy density $W^{\star\star}$ satisfies the two-sided growth condition (3.8) and convexity control (3.9), and that the family of triangulations $(\mathcal{T}_\ell)_{\ell\in\mathbb{N}_0}$ is shape-regular. Hence the generic constants in the following results do not depend on the level ℓ.

A few words on terminology are in order. An error estimator is called *a priori* if its bound on the error does not depend on the discrete solution (e.g. the estimate of Theorem (3.3.1) below), otherwise it is called *a posteriori* (e.g. the estimate of Theorem (3.3.2) below). An error estimator is called *reliable* if it provides an upper bound on the error (e.g. Theorem (3.3.2)), it is called *efficient* if it provides a lower bound on the error. Refer to Carstensen and Jensen (2006, Section 1) for a more elaborate examination.

3.3.1 Main Results

The main results of this section are the a priori error estimate in Theorem (3.3.1) and the a posteriori error estimate in Theorem (3.3.2). The latter theorem defines the residual-based error estimator $\eta_{\mathrm{R},q,\ell}$ in (3.20). The relevant proofs are presented at the end of the section.

(3.3.1) Theorem. *Let $u \in \mathcal{A}$ be a solution of the continuous problem* (3.6) *and σ its stress tensor. Let $u_\ell \in \mathcal{A}_\ell$ be a solution of the discrete problem* (3.10) *and σ_ℓ its stress tensor. Then the errors $e_\ell := u - u_\ell$ and $\delta_\ell := \sigma - \sigma_\ell$ satisfy, for all $v_\ell \in V_\ell$,*

$$\int_\Omega \delta_\ell(x) : \mathrm{D}e_\ell(x)\mathrm{d}x + \|\delta_\ell\|_{L^{p'}(\Omega)}^r + \alpha \|e_\ell\|_{L^2(\Omega)}^2 \lesssim |e_\ell - v_\ell|_{W^{1,p}(\Omega)}^{r'} + \alpha \|e_\ell - v_\ell\|_{L^2(\Omega)}^2,$$

where r' is the Hölder conjugate of r. The integral on the left-hand side is nonnegative. If additionally $u \in W^{2,p}(\mathcal{T}_0;\mathbb{R}^n)$ we have

$$\int_\Omega \delta_\ell(x) : \mathrm{D}e_\ell(x)\mathrm{d}x + \|\delta_\ell\|_{L^{p'}(\Omega)}^r + \alpha \|e_\ell\|_{L^2(\Omega)}^2 \lesssim H_\ell^{r'} + \alpha H_\ell^4. \tag{3.18}$$

In particular, the summands on the left-hand side converge to zero as $H_\ell \to 0$. The generic constants do not depend on ℓ and u_ℓ.

The proof below shows that the generic constant in (3.18) contains the $\mathcal{T}_\ell$-piecewise second derivative of u. Since u does not depend on ℓ, such constants may be hidden in the notation of "$\lesssim$". However, note that the errors vanish obviously if $u \equiv 0$. In the following theorem, and for the rest of the thesis, $\mathrm{D}^2_{\ell,\partial\Omega} u_D$ denotes the $\mathcal{F}_\ell^{\partial\Omega}$-piecewise $(d-1)$-dimensional second derivative of u_D on $\partial\Omega$. Although this term is independent of ℓ as well, it is not hidden in "$\lesssim$": problems with homogeneous boundary conditions are not uncommon (see e.g. the optimal design benchmark of Section 2.5) and in such cases one has $u_D \equiv 0$ and the corresponding terms in (3.19) vanish.

(3.3.2) Theorem. *Let $u \in \mathcal{A}$ be a solution of the continuous problem* (3.6) *and σ its stress tensor. Let $u_\ell \in \mathcal{A}_\ell$ be a solution of the discrete problem* (3.10) *and σ_ℓ its stress tensor. Assume $g \in L^{q'}(\Omega;\mathbb{R}^n)$, where q' is the Hölder conjugate of some $2 \leqslant q \leqslant p$. Furthermore, r' denotes the Hölder conjugate of r. Then the errors $e_\ell := u - u_\ell$ and $\delta_\ell := \sigma - \sigma_\ell$ satisfy*

$$\begin{aligned}\int_\Omega \delta_\ell(x) : \mathrm{D}e_\ell(x)\mathrm{d}x + \|\delta_\ell\|_{L^{p'}(\Omega)}^r + \alpha \|e_\ell\|_{L^2(\Omega)}^2 \\ \lesssim\ & H_\ell^{(1+1/p)r'} \left\|\mathrm{D}^2_{\ell,\partial\Omega} u_D\right\|_{L^p(\partial\Omega)}^{r'} + \alpha H_\ell^5 \left\|\mathrm{D}^2_{\ell,\partial\Omega} u_D\right\|_{L^2(\partial\Omega)}^2 \\ & + \left(|e_\ell|_{W^{1,q}(\Omega)} + H_\ell^{1+1/q} \left\|\mathrm{D}^2_{\ell,\partial\Omega} u_D\right\|_{L^q(\partial\Omega)}\right) \eta_{\mathrm{R},q,\ell}\end{aligned} \tag{3.19}$$

with the residual-based error estimator

$$\eta_{\mathrm{R},q,\ell} := \left(\sum_{T\in\mathcal{T}_\ell} h_T^{q'} \|\Lambda_\ell\|_{L^{q'}(T)}^{q'}\right)^{1/q'} + \left(\sum_{F\in\mathcal{F}_\ell^\Omega} h_F \|[\sigma_\ell]_F\, n_F\|_{L^{q'}(F)}^{q'}\right)^{1/q'}. \tag{3.20}$$

The integral on the left-hand side of (3.19) *is nonnegative. The sum in parentheses on the right-hand side of* (3.19) *is bounded. The generic constant does not depend on ℓ and u_ℓ.*

In general, there is no improved estimate for the sum in parentheses on the right-hand side of (3.19) beyond boundedness. Carstensen and Plecháč (1997, Remark 7.1) also observe this and conclude that (3.19) could be sharpened in the presence of sufficient control of $|e_\ell|_{W^{1,q}(\Omega)}$. The failure to control this term accounts for the reliability-efficiency gap; see also the discussion following Theorem (3.3.6) for an explanation of the reliability-efficiency gap.

Theorems (3.3.1) and (3.3.2) estimate not only the error of the stress σ_ℓ and, if $\alpha = 0$, the error of u_ℓ, but also the integral $\int_\Omega \delta_\ell(x) : \mathrm{D}e_\ell(x)\mathrm{d}x$. The following lemma yields control of the error $u - u_\ell$ even in the case $\alpha = 0$, if condition (3.21) is satisfied. This condition is not of purely artificial nature — it is for example satisfied by the two-well benchmark (see Lemma (2.3.5), page 27).

(3.3.3) Lemma (Bartels et al., 2004b, Lemma 9.1)**.** *Given arbitrary $u \in \mathcal{A}$ and $u_\ell \in \mathcal{A}_\ell$ for $\ell \in \mathbb{N}_0$, denote their stress tensors with σ and σ_ℓ, and let $e_\ell := u - u_\ell$ and $\delta_\ell := \sigma - \sigma_\ell$. The generic constants in the following inequalities may not depend on ℓ and u_ℓ. If the energy density $W^{\star\star}$ permits*

$$\|\mathrm{D}e_\ell\, z\|^2_{L^2(\Omega)} \lesssim \int_\Omega \delta_\ell(x) : \mathrm{D}e_\ell(x)\mathrm{d}x \quad \text{for some fixed } z \in \mathbb{R}^d \setminus \{0\}\,, \tag{3.21}$$

then e_ℓ and δ_ℓ satisfy

$$\|e_\ell\|^2_{L^2(\Omega)} \lesssim H_\ell^3 \left\|\mathrm{D}^2_{\ell,\partial\Omega} u_D\right\|^2_{L^2(\Omega)} + \int_\Omega \delta_\ell(x) : \mathrm{D}e_\ell(x)\mathrm{d}x.$$

Theorems (3.3.1) and (3.3.2) together with Lemma (3.3.3) immediately conjecture the following corollaries.

(3.3.4) Corollary. *Given the situation of Theorem (3.3.1) assume that the energy density $W^{\star\star}$ complies with* (3.21)*. Then the error e_ℓ satisfies*

$$\|e_\ell\|^2_{L^2(\Omega)} \lesssim H_\ell^{r'} + \alpha H_\ell^4 + H_\ell^3 \left\|\mathrm{D}^2_{\ell,\partial\Omega} u_D\right\|^2_{L^2(\partial\Omega)}.$$

The generic constant does not depend on ℓ and u_ℓ. In particular, $u_\ell \to u$ in $L^2(\Omega;\mathbb{R}^n)$ as $H_\ell \to 0$.

(3.3.5) Corollary. *Given the situation of Theorem (3.3.2) assume that the energy density $W^{\star\star}$ complies with* (3.21)*. Then the error e_ℓ satisfies*

$$\begin{aligned}\|e_\ell\|^2_{L^2(\Omega)} \lesssim H_\ell^{(1+1/p)r'} \left\|\mathrm{D}^2_{\ell,\partial\Omega} u_D\right\|^{r'}_{L^p(\partial\Omega)} + H_\ell^3 \left\|\mathrm{D}^2_{\ell,\partial\Omega} u_D\right\|^2_{L^2(\partial\Omega)} \\ + \left(|e_\ell|_{W^{1,q}(\Omega)} + H_\ell^{1+1/q} \left\|\mathrm{D}^2_{\ell,\partial\Omega} u_D\right\|_{L^q(\partial\Omega)}\right) \eta_{\mathrm{R},q,\ell}.\end{aligned}$$

The sum in parentheses on the right-hand side is bounded. The generic constant does not depend on ℓ and u_ℓ.

A particular consequence of Corollary (3.3.4) is uniqueness of the continuous solution u for problems which satisfy (3.21). However, due to the regularity restrictions of Theorem

(3.3.1) uniqueness is valid only within the set $\mathcal{A} \cap W^{2,p}(\mathcal{T}_0;\mathbb{R}^n)$. Theorem (4.2.3) (page 75) provides uniqueness amongst all $u \in \mathcal{A}$ (cf. Remark (4.2.4), page 76).

(3.3.6) Theorem (Efficiency)**.** *Let $u \in \mathcal{A}$ be a solution of the continuous problem* (3.6) *and σ its stress tensor. Let $(u_\ell)_{\ell\in\mathbb{N}_0}$ be a sequence of discrete functions $u_\ell \in \mathcal{A}_\ell$ with stress tensors σ_ℓ. Assume $g \in L^{q'}(\Omega;\mathbb{R}^n)$ and $\sigma \in L^{q'}(\Omega;\mathbb{R}^{n\times d})$, where q' is the Hölder conjugate of some $2 \leqslant q \leqslant p$, i.e., $1/q + 1/q' = 1$. Then the errors $e_\ell := u - u_\ell$ and $\delta_\ell := \sigma - \sigma_\ell$ and the residual-based error estimator $\eta_{\mathrm{R},q,\ell}$ of* (3.20) *satisfy*

$$\eta_{\mathrm{R},q,\ell} \lesssim \|\delta_\ell\|_{L^{q'}(\Omega)} + \alpha H_\ell \|e_\ell\|_{L^{q'}(\Omega)} + \mathrm{osc}_{\ell,q'}(\Lambda_\ell).$$

The generic constant does not depend on ℓ and u_ℓ.

The proof of the preceding theorem is postponed to page 53.

Observe that the exponents of the errors in Theorem (3.3.6) are *lower* than those in Theorem (3.3.2). Therefore $\eta_{\mathrm{R},q,\ell}$ constitutes an upper and a lower bound on the errors of u_ℓ (if $\alpha > 0$) and σ_ℓ, however, with different exponents. The gap between the upper and lower bound is called *reliability-efficiency gap*. Refer to the analysis following Theorem (4.3.1) (on page 80) for a discussion of the reliability-efficiency gap in the context of stabilisation, and to Section 4.4 for an approach to the reduction of the reliability-efficiency gap.

(3.3.7) Remark. *One may expect the oscillation in Theorem (3.3.6) to be of higher order: the discrete solutions u_ℓ are bounded in $W^{1,p}(\Omega;\mathbb{R}^n)$ by Lemma (3.2.5), therefore Lemma (3.1.8) ensures* $\mathrm{osc}_{\ell,q'}(\Lambda_\ell) \lesssim H_\ell^2$ *if $\Lambda \in W^{1,p}(\Omega;\mathbb{R}^n)$.*

3.3.2 The Residual

The proofs of Theorems (3.3.1) and (3.3.2) are based on the *residual* Res_ℓ which, for a given solution u_ℓ on the level ℓ with σ_ℓ and Λ_ℓ from (3.11), reads

$$\mathrm{Res}_\ell(v) := -\int_\Omega (\sigma_\ell(x) : \mathrm{D}v(x) - \Lambda_\ell(x)\cdot v(x))\,\mathrm{d}x \quad \text{for } v \in W^{1,p}(\Omega;\mathbb{R}^n). \tag{3.22}$$

Note that by the discrete Euler-Lagrange equation (3.12)

$$\mathrm{Res}_\ell(v_\ell) = 0 \quad \text{for } v_\ell \in V_\ell. \tag{3.23}$$

This property is called *Galerkin orthogonality*.

The following result is an important prerequisite for the proofs of Theorems (3.3.1) and (3.3.2). Note that it does *not* require u_ℓ to be a solution of the discrete problem (3.10).

(3.3.8) Lemma. *Let $u \in \mathcal{A}$ be a solution of the continuous problem* (3.6) *and σ its stress tensor. Let $(u_\ell)_{\ell\in\mathbb{N}_0}$ be a sequence of discrete functions $u_\ell \in \mathcal{A}_\ell$ with $|u_\ell|_{W^{1,p}(\Omega)} \lesssim 1$ and stress tensors σ_ℓ. Then the errors $e_\ell := u - u_\ell$ and $\delta_\ell := \sigma - \sigma_\ell$ satisfy, for all $v \in V$,*

$$\int_\Omega \delta_\ell(x) : \mathrm{D}e_\ell(x)\mathrm{d}x + \|\delta_\ell\|_{L^{p'}(\Omega)}^r + \alpha\|e_\ell\|_{L^2(\Omega)}^2 \lesssim |e_\ell - v|_{W^{1,p}(\Omega)}^{r'} + \alpha\|e_\ell - v\|_{L^2(\Omega)}^2 + \mathrm{Res}_\ell(v),$$

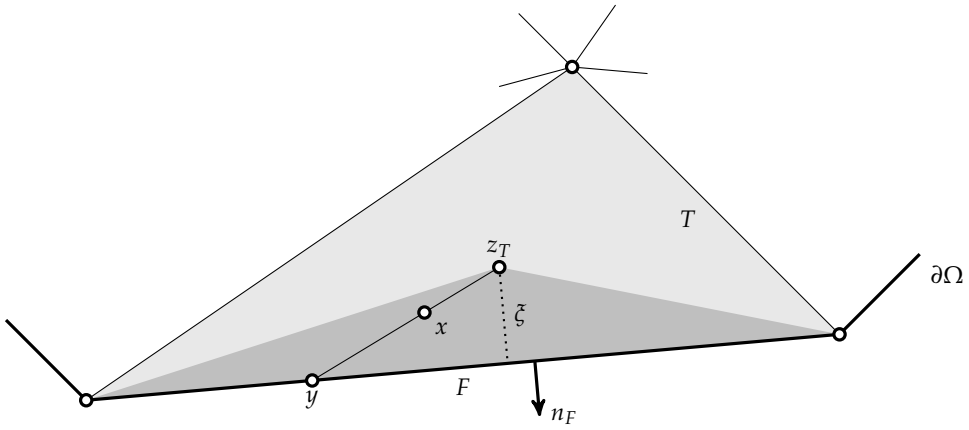

Figure 3.5: Construction principle of the operator B_ℓ on a triangle T with a boundary side $F \subset T \cap \partial\Omega$. The value in x is given by the linear interpolation between z_T and y as defined in (3.24). The height ξ of the sub-triangle $\mathrm{conv}(\{z_T\} \cup F)$ is an important quantity in the proof of Lemma (3.3.10).

where r' is the Hölder conjugate of r, i.e., $1/r + 1/r' = 1$. The integral on the left-hand side is nonnegative. The generic constant does not depend on ℓ and u_ℓ.

3.3.3 Treatment of Inhomogeneous Boundary Conditions

In order to derive Theorem (3.3.2), one needs to control the norms of $e_\ell - v$ as well as the residual $\mathrm{Res}_\ell(v)$ in Lemma (3.3.8). In the case of homogeneous boundary conditions, i.e. $u_D \equiv 0$, this control is accomplished with $v = e_\ell$. In the general case, however, additional difficulties arise from the fact that e_ℓ does no longer vanish along the boundary. As a remedy Bartels et al. (2004a, Proof of Proposition 4.1) introduce the following extension operator B_ℓ.

(3.3.9) Definition. *Given a triangulation $\mathcal{T}_\ell$ of Ω and $w \in \mathcal{C}(\partial\Omega)$, an extension $B_\ell w$ of w on Ω is given as follows.*

- *On each interior node $z \in \mathcal{N}_\ell \backslash \partial\Omega$ set $B_\ell w(z) = 0$.*
- *$B_\ell w$ is affine on each interior side $F \in \mathcal{F}_\ell^\Omega$.*
- *For an element $T \in \mathcal{T}_\ell$ denote its center of gravity with z_T. For each point $x \in T$ there are $y \in \partial T$ and $\beta \in [0,1]$ such that*

$$x = \beta y + (1-\beta) z_T. \tag{3.24}$$

β is unique, y is unique for $\beta > 0$. With these set $B_\ell w(x) = \beta B_\ell w(y)$.

This defines an operator $B_\ell : \mathcal{C}(\partial\Omega) \to \mathcal{C}(\Omega)$.

Figure 3.5 illustrates the construction of B_ℓ on a triangle that has a common side with the boundary $\partial\Omega$. The construction method of Definition (3.3.9) sets $B_\ell w = 0$ in all interior nodes and in the centers of all elements, then uses affine interpolation between these points and the boundary $\partial\Omega$. It is obvious that $B_\ell w$ inherits the continuity of w.

Furthermore, it is clear that B_ℓ is a linear operator. The following lemma provides an estimate on B_ℓ.

(3.3.10) Lemma. *Let $(\mathcal{T}_\ell)_{\ell\in\mathbb{N}_0}$ be a shape-regular family of triangulations of Ω and $1 < q < \infty$. Then B_ℓ satisfies for all $w \in W^{2,q}(\mathcal{F}_0^{\partial\Omega}) \cap W^{1,q}(\Omega) \cap \mathcal{C}(\overline{\Omega})$*

$$\|B_\ell(1-I_\ell)w\|_{L^q(\Omega)} + H_\ell\,|B_\ell(1-I_\ell)w|_{W^{1,q}(\Omega)} \lesssim H_\ell^{2+1/q}\,\left\|\mathrm{D}^2_{\ell,\partial\Omega}w\right\|_{L^q(\partial\Omega)}.$$

The generic constant does not depend on ℓ and w.

Lemma (3.3.10) yields an estimate on the right-hand side of Lemma (3.3.8). This estimate is formulated as another lemma because it is required again in Section 3.4 and Chapter 4.

(3.3.11) Lemma. *Let $u \in \mathcal{A}$ be a solution of the continuous problem* (3.6) *and σ its stress tensor. Let $(u_\ell)_{\ell\in\mathbb{N}_0}$ be a sequence of discrete functions $u_\ell \in \mathcal{A}_\ell$ with $|u_\ell|_{W^{1,p}(\Omega)} \lesssim 1$ and stress tensors σ_ℓ. Then the errors $e_\ell := u - u_\ell$ and $\delta_\ell := \sigma - \sigma_\ell$ satisfy*

$$\begin{aligned}\int_\Omega \delta_\ell(x) : \mathrm{D}e_\ell(x)\mathrm{d}x + \|\delta_\ell\|^r_{L^{p'}(\Omega)} + \alpha\,\|e_\ell\|^2_{L^2(\Omega)}&\\ \lesssim H_\ell^{(1+1/p)r'}\,\left\|\mathrm{D}^2_{\ell,\partial\Omega}u_D\right\|^{r'}_{L^p(\partial\Omega)} + \alpha H_\ell^5\,\left\|\mathrm{D}^2_{\ell,\partial\Omega}u_D\right\|^2_{L^2(\partial\Omega)} + \mathrm{Res}_\ell((1-B_\ell)e_\ell),&\end{aligned}$$

where r' is the Hölder conjugate of r, i.e., $1/r + 1/r' = 1$. The integral on the left-hand side is nonnegative. The generic constant does not depend on ℓ and u_ℓ.

3.3.4 Proofs

Proof of Lemma (3.3.8). The continuous Euler-Lagrange equation (3.7) shows

$$\mathrm{Res}_\ell(v) = \int_\Omega \delta_\ell(x) : \mathrm{D}v(x)\mathrm{d}x - \int_\Omega e_\ell(x)\cdot v(x)\mathrm{d}x. \tag{3.25}$$

Set $w_\ell := e_\ell - v$. Lemma (3.2.5) asserts an upper bound on $\|u_\ell\|_{W^{1,p}(\Omega)}$, therefore Lemma (2.2.7) (page 23) applies to u and u_ℓ. This and (3.25) yield

$$\begin{aligned}\int_\Omega \delta_\ell(x) : \mathrm{D}e_\ell(x)\mathrm{d}x + \|\delta_\ell\|^r_{L^{p'}(\Omega)} + \alpha\,\|e_\ell\|^2_{L^2(\Omega)}&\\ \lesssim \int_\Omega \delta_\ell(x) : \mathrm{D}e_\ell(x)\mathrm{d}x + 2\alpha\int_\Omega e_\ell(x)\cdot e_\ell(x)\mathrm{d}x&\\ = \int_\Omega \delta_\ell(x) : \mathrm{D}w_\ell(x)\mathrm{d}x + 2\alpha\int_\Omega e_\ell(x)\cdot w_\ell(x)\mathrm{d}x + \mathrm{Res}_\ell(v)&\\ \leqslant \|\delta_\ell\|_{L^{p'}(\Omega)}\,|w_\ell|_{W^{1,p}(\Omega)} + 2\alpha\,\|e_\ell\|_{L^2(\Omega)}\,\|w_\ell\|_{L^2(\Omega)} + \mathrm{Res}_\ell(v).&\end{aligned}$$

Absorption of $\|\delta_\ell\|_{L^{p'}(\Omega)}$ and $\|e_\ell\|_{L^2(\Omega)}$ (see Lemma (2.1.23), page 20, for the absorption technique) concludes the proof. □

Proof of Theorem (3.3.1). The first inequality is a direct consequence of Lemma (3.3.8) and (3.23). Lemma (2.2.7) proves the nonnegativity of the integral. The second inequality

follows from Lemma (3.1.6) with $v_\ell \coloneqq I_\ell e_\ell = I_\ell u - u_\ell \in V_\ell$. Note that Lemmas (2.1.6) (page 16) and (3.2.1) ensure $u \in \mathcal{C}(\overline{\Omega}; \mathbb{R}^n)$, hence $I_\ell u$ is well-defined. □

Proof of Lemma (3.3.10). Denote $w_\ell \coloneqq (1 - I_\ell)w$. The proof consists of three steps.

Claim A. On each $T \in \mathcal{T}_\ell$ it holds that

$$\|B_\ell w_\ell\|^q_{L^q(T)} \approx h_T \, \|w_\ell\|^q_{L^q(\partial T \cap \partial\Omega)} \,. \tag{3.26}$$

Proof of Claim A. By Definition (3.3.9) $B_\ell w_\ell = 0$ on elements that do not contain any boundary side. Hence (3.26) is obviously true for such elements, and the remainder of the proof considers elements which contain at least one boundary side.

Definition (3.3.9) splits each element $T \in \mathcal{T}_\ell$ into $d+1$ subelements, each one associated to a side F of T. It suffices to prove (3.26) for each of those subelements. The claimed estimate then follows from the sum over all subelements.

Assume $T \in \mathcal{T}_\ell$ to be an element with at least one boundary side $F \subset T \cap \partial\Omega$. By translation invariance we assume that the center of gravity of T is $z_T = 0$. The subelement that corresponds to F is given by $\widehat{T} = \operatorname{conv}(\{0\} \cup F) \subset T$. The height of $\widehat{T}$ with respect to z is $\xi = n_F \cdot x$, where n_F denotes the outer-pointing unit normal vector of F (see Figure 3.5 for an illustration). For a point $x \in \widehat{T}$, (3.24) reads $x = \beta y$ with $y \in F$. Apply Cavalieri's principle to split the integral over $x \in \widehat{T}$ into an integral over $\beta \in]0,1[$ and an integral over $y \in F$,

$$\begin{aligned}
\|B_\ell w_\ell\|^q_{L^q(\widehat{T})} &= \int_{x\in\widehat{T}} |B_\ell w_\ell(x)|^q \,\mathrm{d}x = \int_{x\in\widehat{T}} \beta^q \, |w_\ell(x/\beta)|^q \,\mathrm{d}x \\
&= \int_{\beta\in]0,1[} \beta^q \int_{x\in\beta F} |w_\ell(x/\beta)|^q \,\mathrm{d}s_x \xi \mathrm{d}\beta \\
&= \int_{\beta\in]0,1[} \beta^q \int_{y\in F} |w_\ell(y)|^q \, \beta^{d-1} \mathrm{d}s_y \xi \mathrm{d}\beta \\
&= \frac{\xi}{q+d} \, \|w_\ell\|^q_{L^q(F)} \,.
\end{aligned} \tag{3.27}$$

The integration variable is written below the integral sign for improved clarity here. Shape regularity justifies $\xi \approx h_T$, hence (3.26) is valid for $\widehat{T}$ and thus for T.

Claim B. On each $T \in \mathcal{T}_\ell$ it holds that

$$|B_\ell w_\ell|^q_{W^{1,q}(T)} \lesssim h_T^{1-q} \, \|w_\ell\|^q_{L^q(\partial T \cap \partial\Omega)} + h_T \, |w_\ell|^q_{W^{1,q}(\partial T \cap \partial\Omega)} \,. \tag{3.28}$$

Proof of Claim B. The following arguments are an adaption of Bartels et al. (2004a, Proposition 4.1), which proves (3.28) for $q = 2$.

In the following arguments the derivative with respect to x is denoted by ∂_x, e.g., in general $\partial_x B_\ell w_\ell(y)$ and $\mathrm{D}B_\ell w_\ell(y)$ are different. Also, derivatives of scalar functions, like $\partial_x B_\ell w_\ell(y)$ and $\mathrm{D}B_\ell w_\ell(y)$, are treated as *row vectors*. This allows for a compact notation of scalar products and dyadic products, like $ab^{\mathrm{T}} = a \otimes b$ for equal sized column vectors a and b. Recall that the symbol "1" denotes the identity, irrespective of the mathematical

structure at hand. With this notational convention a product rule for $x = \beta y$ gives

$$1 = \partial_x(\beta y) = y\partial_x\beta + \beta\partial_x y = \frac{1}{\xi} y n_F^{\mathrm{T}} + \beta\partial_x y \in \mathbb{R}^{d\times d}.$$

The chain-rule proves

$$\begin{aligned}
\mathrm{D}B_\ell w_\ell(x) &= \partial_x(\beta w_\ell(y)) = w_\ell(y)\partial_x\beta + \beta\partial_x w_\ell(y) \\
&= \frac{1}{\xi} w_\ell(y) n_F^{\mathrm{T}} + \beta\partial_y w_\ell(y)\partial_x y \\
&= \frac{1}{\xi} w_\ell(y) n_F^{\mathrm{T}} + \beta\partial_y w_\ell(y)\left(1 - \frac{1}{\xi} y n_F^{\mathrm{T}}\right).
\end{aligned}$$

Be aware that $\partial_y w_\ell(y)$ is in fact the $(d-1)$-dimensional derivative of w_ℓ on the surface F, also written as $\mathrm{D}_F w_\ell(y)$. Naturally, this derivative is orthogonal to n_F. Shape regularity and the assumption $z = 0$ justify $|y| \lesssim h_T \approx \xi$. We apply the orthogonal projection mappings $n_F n_F^{\mathrm{T}}$ and $(1 - n_F n_F^{\mathrm{T}})$ to decompose $\mathrm{D}B_\ell w_\ell(x)$ into its tangential and its normal component, with respect to the side F. The normal component satisfies

$$\begin{aligned}
\left|\mathrm{D}B_\ell w_\ell(x) n_F n_F^{\mathrm{T}}\right|^2 &= \frac{1}{\xi^2} \left|w_\ell(y) - \mathrm{D}_F w_\ell(y) y\right|^2 \\
&\leqslant \frac{1}{\xi^2} \left|w_\ell(y)\right|^2 + \left|y/\xi\right|^2 \left|\mathrm{D}_F w_\ell(y)\right|^2 \\
&\lesssim h_T^{-2} \left|w_\ell(y)\right|^2 + \left|\mathrm{D}_F w_\ell(y)\right|^2.
\end{aligned}$$

The decomposition of $\left|\mathrm{D}B_\ell w_\ell(x)\right|^2$ thus fulfils

$$\begin{aligned}
\left|\mathrm{D}B_\ell w_\ell(x)\right|^2 &= \left|\mathrm{D}B_\ell w_\ell(x)(1 - n_F n_F^{\mathrm{T}})\right|^2 + \left|\mathrm{D}B_\ell w_\ell(x) n_F n_F^{\mathrm{T}}\right|^2 \\
&\lesssim h_T^{-2} \left|w_\ell(y)\right|^2 + \left|\mathrm{D}_F w_\ell(y)\right|^2.
\end{aligned}$$

For the integration of $\left|\mathrm{D}B_\ell w_\ell(x)\right|^q$ over $\widehat{T}$ Cavalieri's principle shows, in the same fashion as in (3.27),

$$\begin{aligned}
\left\|\mathrm{D}B_\ell w_\ell\right\|_{L^q(\widehat{T})}^q &= \int_{x\in\widehat{T}} \left|\mathrm{D}B_\ell w_\ell(x)\right|^q \mathrm{d}x \\
&\lesssim \int_{\beta\in]0,1[} \int_{x\in\beta F} \left(h_T^{-q} \left|w_\ell(y)\right|^q + \left|\mathrm{D}_F w_\ell(y)\right|^q\right) \mathrm{d}s_x \xi \mathrm{d}\beta \\
&= \int_{\beta\in]0,1[} \int_{y\in F} \left(h_T^{-q} \left|w_\ell(y)\right|^q + \left|\mathrm{D}_F w_\ell(y)\right|^q\right) \beta^{d-1} \mathrm{d}s_y \xi \mathrm{d}\beta \\
&\approx h_T \left\|\mathrm{D}_F w_\ell\right\|_{L^q(F)}^q + h_T^{1-q} \left\|w_\ell\right\|_{L^q(F)}^q.
\end{aligned}$$

Proof of the lemma. The sum over all elements $T \in \mathcal{T}_\ell$ of (3.26) and Lemma (3.1.5) yield

$$\left\|B_\ell w_\ell\right\|_{L^q(\Omega)}^q \approx \sum_{T\in\mathcal{T}_\ell} h_T \left\|w_\ell\right\|_{L^q(\partial T\cap\partial\Omega)}^q \approx \sum_{F\in\mathcal{F}_\ell^{\partial\Omega}} h_F \left\|w_\ell\right\|_{L^q(F)}^q$$

$$\lesssim \sum_{F\in\mathcal{F}_\ell^{\partial\Omega}} h_F^{1+2q}\,|w|^q_{W^{2,q}(F)} \leqslant H_\ell^{1+2q}\left\|\mathrm{D}^2_{\ell,\partial\Omega} w\right\|^q_{L^q(\partial\Omega)}.$$

Likewise, (3.28) and Lemma (3.1.5) yield

$$\begin{aligned}|B_\ell w_\ell|^q_{W^{1,q}(\Omega)} &\approx \sum_{F\in\mathcal{F}_\ell^{\partial\Omega}} \left(h_F^{1-q}\,\|w_\ell\|^q_{L^q(F)} + h_F\,|w_\ell|^q_{W^{1,q}(F)}\right)\\ &\lesssim \sum_{F\in\mathcal{F}_\ell^{\partial\Omega}} h_F^{1+q}\,|w|^q_{W^{2,q}(F)} \leqslant H_\ell^{1+q}\left\|\mathrm{D}^2_{\ell,\partial\Omega} w\right\|^q_{L^q(\partial\Omega)}.\end{aligned}$$ □

Proof of Lemma (3.3.11). Note that $e_\ell = (1-I_\ell)u_D$ on the boundary $\partial\Omega$. With $v \coloneqq (1-B_\ell)e_\ell \in V$ Lemma (3.3.10) yields

$$\begin{aligned}\|e_\ell - v\|^2_{L^2(\Omega)} &= \|B_\ell e_\ell\|^2_{L^2(\Omega)} \lesssim H_\ell^5\left\|\mathrm{D}^2_{\ell,\partial\Omega} u_D\right\|^2_{L^2(\partial\Omega)}, \text{ and}\\ |e_\ell - v|^{r'}_{W^{1,p}(\Omega)} &= |B_\ell e_\ell|^{r'}_{W^{1,p}(\Omega)} \lesssim H_\ell^{(1+1/p)r'}\left\|\mathrm{D}^2_{\ell,\partial\Omega} u_D\right\|^{r'}_{L^p(\partial\Omega)}.\end{aligned}$$

Lemma (3.3.8) and the choice of v directly prove the lemma. □

Proof of Theorem (3.3.2). Lemma (3.3.10) and a triangle inequality show for $v \coloneqq (1-B_\ell)e_\ell \in V$

$$|v|_{W^{1,q}(\Omega)} \leqslant |e_\ell|_{W^{1,q}(\Omega)} + |B_\ell e_\ell|_{W^{1,q}(\Omega)} \lesssim |e_\ell|_{W^{1,q}(\Omega)} + H_\ell^{1+1/q}\left\|\mathrm{D}^2_{\ell,\partial\Omega} u_D\right\|_{L^q(\partial\Omega)}. \tag{3.29}$$

The boundedness of the right-hand side is a consequence of Lemma (3.2.5). With Lemma (3.3.11) it remains to prove

$$\mathrm{Res}_\ell(v) \lesssim \eta_{\mathrm{R},q,\ell}\,|v|_{W^{1,q}(\Omega)}. \tag{3.30}$$

Recall the definition of the nodal basis functions φ_z from (3.1), and define a function $v_\ell \in V_\ell$ by

$$v_\ell = \sum_{z\in\mathcal{N}_\ell\cap\Omega}\left(⨍_{\omega_z} v(x)\mathrm{d}x\right)\varphi_z.$$

This function equals the averaging interpolation $\Sigma_\ell v$ (cf. (3.2)) of v in interior nodes $z \in \mathcal{N}_\ell \cap \Omega$, but it vanishes on boundary nodes $z \in \mathcal{N}_\ell \cap \partial\Omega$. Hence $v = v_\ell = 0$ on $\partial\Omega$. The subsequent claims follow the arguments of Braess (2007, II.6.9 "Clément's Interpolation", page 84).

Claim A.

$$\|v - v_\ell\|_{L^q(T)} \lesssim h_T\,|v|_{W^{1,q}(\omega_T)} \quad \text{for all } T \in \mathcal{T}_\ell. \tag{3.31}$$

Proof of Claim A. Let $T = \mathrm{conv}\{z_0, \ldots, z_d\} \in \mathcal{T}_\ell$. For an interior node $z_j \in \mathcal{N}_\ell \cap \Omega$ Poincaré's inequality (Lemma (2.1.16), page 19) yields on ω_{z_j}

$$\left\|v - v_\ell(z_j)\right\|_{L^q\left(\omega_{z_j}\right)} \lesssim h_T\,|v|_{W^{1,q}\left(\omega_{z_j}\right)}.$$

For a boundary node $z_j \in \mathcal{N}_\ell \cap \partial\Omega$ Friedrichs' inequality (Lemma (2.1.17), page 19) yields

on ω_{z_j}

$$\|v\|_{L^q(\omega_{z_j})} \lesssim h_T \, |v|_{W^{1,q}(\omega_{z_j})} .$$

Altogether the preceding observations yield Claim A because $\left\|\varphi_{z_j}\right\|_{L^\infty(T)} \leqslant 1$ and

$$\|v - v_\ell\|_{L^q(T)}^q = \left\| \sum_{j=0}^{d} (v - v_\ell(z_j))\varphi_{z_j} \right\|_{L^q(T)}^q \lesssim \sum_{j=0}^{d} \left\|v - v_\ell(z_j)\right\|_{L^q(T)}^q \lesssim h_T^q \sum_{j=0}^{d} |v|_{W^{1,q}(\omega_T)}^q .$$

Claim B. Given a side $F \in \mathcal{F}_\ell$ which is part of the elements T_+ and T_- (with $T_+ \neq T_-$ if $F \in \mathcal{F}_\ell^\Omega$, as illustrated in Figure 3.4), it holds that

$$\|v - v_\ell\|_{L^q(F)} \lesssim h_F^{1-1/q} \, |v|_{W^{1,q}(\omega_{T_+} \cap \omega_{T_-})} . \tag{3.32}$$

Proof of Claim B. Let $F = \operatorname{conv}\{z_1, \ldots, z_d\} \in \mathcal{F}_\ell$. Note that $\omega_F \subset \omega_{z_j}$ for all $j = 1, \ldots, d$. The trace inequality (Lemma (3.1.11)) and (3.31) lead to

$$\left\|v - v_\ell(z_j)\right\|_{L^q(F)}^q \lesssim h_F^{-1} \left\|v - v_\ell(z_j)\right\|_{L^q(\omega_F)}^q + h_F^{q-1} \, |v|_{W^{1,q}(\omega_F)}^q \lesssim h_F^{q-1} \, |v|_{W^{1,q}(\omega_F)}^q .$$

Similar to the proof of Claim A, this and the observation $\left\|\varphi_{z_j}\right\|_{L^\infty(T)} \leqslant 1$ prove (3.32) because

$$\|v - v_\ell\|_{L^q(F)}^q = \left\| \sum_{j=1}^{d} (v - v_\ell(z_j))\varphi_{z_j} \right\|_{L^q(F)}^q \lesssim \sum_{j=1}^{d} \left\|v - v_\ell(z_j)\right\|_{L^q(F)}^q \lesssim h_F^{q-1} \sum_{j=1}^{d} |v|_{W^{1,q}(\omega_{z_j})}^q .$$

Proof of (3.30). The Galerkin orthogonality allows to inject v_ℓ into the argument of the residual. An integration by parts on each element shows

$$\begin{aligned}
\operatorname{Res}_\ell(v) = \operatorname{Res}_\ell(v - v_\ell) &= \sum_{T \in \mathcal{T}_\ell} \int_T (\Lambda_\ell(x) \cdot (v - v_\ell)(x) - \sigma_\ell(x) : \mathrm{D}(v - v_\ell)(x)) \, \mathrm{d}x \\
&= \sum_{T \in \mathcal{T}_\ell} \int_T \Lambda_\ell(x) \cdot (v - v_\ell)(x) \mathrm{d}x && (3.33) \\
&\quad - \sum_{T \in \mathcal{T}_\ell} \int_{\partial T} (\sigma_\ell(x) n_{\partial T}(x)) \cdot (v - v_\ell)(x) \mathrm{d}s && (3.34) \\
&\quad + \sum_{T \in \mathcal{T}_\ell} \int_T \operatorname{div} \sigma_\ell \cdot (v - v_\ell)(x) \mathrm{d}x. && (3.35)
\end{aligned}$$

The discrete stress σ_ℓ is $\mathcal{T}_\ell$-piecewise constant, hence the summand (3.35) vanishes. Since $v = v_\ell = 0$ on $\partial\Omega$, the integrand in (3.34) vanishes on boundary sides $F = \partial T \cap \partial\Omega \in \mathcal{F}_\ell^{\partial\Omega}$. Consider two neighbouring elements $T_\pm \in \mathcal{T}_\ell$ and their common side $F = T_+ \cap T_- \in \mathcal{F}_\ell^\Omega$. Figure 3.4 illustrates the arrangement of the normal vectors of two neighbouring elements. The outer-pointing unit normal vectors $n_{\partial T_\pm}$ are anti-diagonal on F. Hence, on

F, the sum of the integrands of (3.34), which stem from the two elements $T_\pm$, reads

$$\sigma_\ell|_{T_+} n_{\partial T_+} + \sigma_\ell|_{T_-} n_{\partial T_-} = \left(\sigma_\ell|_{T_+} - \sigma_\ell|_{T_-}\right) n_F =: [\sigma_\ell]_F \, n_F, \tag{3.36}$$

where $[\sigma_\ell]_F$ denotes the jump of σ_ℓ along F (cf. Definition (2.1.13), page 18). With (3.36), the sum of (3.34) recombines to

$$\begin{aligned}
&\sum_{T\in\mathcal{T}_\ell} \int_{\partial T} (\sigma_\ell(x) n_{\partial T}(x)) \cdot (v - v_\ell)(x) \mathrm{d}s \\
&\qquad = \sum_{\substack{F\in\mathcal{F}_\ell^\Omega \\ F = T_+ \cap T_-}} \int_F \left(\sigma_\ell|_{T_+} n_{\partial T_+} + \sigma_\ell|_{T_-} n_{\partial T_-}\right) \cdot (v - v_\ell)(x) \mathrm{d}s \\
&\qquad = \sum_{F\in\mathcal{F}_\ell^\Omega} \int_F [\sigma_\ell]_F \, n_F \cdot (v - v_\ell)(x) \mathrm{d}s.
\end{aligned} \tag{3.37}$$

Lemma (3.1.3) (d) ensures that the number of elements that are covered by the patch ω_T is bounded independently of ℓ. Therefore

$$\begin{aligned}
\sum_{T\in\mathcal{T}_\ell} |\omega_T| \approx |\Omega| \approx \sum_{F = T_+\cap T_- \in \mathcal{F}_\ell^\Omega} \left|\omega_{T_+} \cap \omega_{T_-}\right| \quad \text{and in particular} \\
\sum_{T\in\mathcal{T}_\ell} |v|^q_{W^{1,q}(\omega_T)} \approx |v|^q_{W^{1,q}(\Omega)} \approx \sum_{F = T_+\cap T_- \in \mathcal{F}_\ell^\Omega} |v|^q_{W^{1,q}\left(\omega_{T_+}\cap\omega_{T_-}\right)}.
\end{aligned}$$

With (3.31), (3.32) and Hölder's inequality (for functions and for vectors) we obtain (3.30) via

$$\begin{aligned}
\mathrm{Res}_\ell(v) &= \sum_{T\in\mathcal{T}_\ell} \int_T \Lambda_\ell(x) \cdot (v - v_\ell)(x) \mathrm{d}x - \sum_{F\in\mathcal{F}_\ell^\Omega} \int_F [\sigma_\ell]_F \, n_F \cdot (v - v_\ell)(x) \mathrm{d}s \\
&\leqslant \sum_{T\in\mathcal{T}_\ell} \|\Lambda_\ell\|_{L^{q'}(T)} \|v - v_\ell\|_{L^q(T)} + \sum_{F\in\mathcal{F}_\ell^\Omega} \|[\sigma_\ell]_F \, n_F\|_{L^{q'}(F)} \|v - v_\ell\|_{L^q(F)} \\
&\lesssim \sum_{T\in\mathcal{T}_\ell} h_T \|\Lambda_\ell\|_{L^{q'}(T)} |v|_{W^{1,q}(\omega_T)} \\
&\quad + \sum_{F = T_+\cap T_- \in \mathcal{F}_\ell^\Omega} h_F^{1-1/q} \|[\sigma_\ell]_F \, n_F\|_{L^{q'}(F)} |v|_{W^{1,q}\left(\omega_{T_+}\cap\omega_{T_-}\right)} \\
&\lesssim \eta_{\mathrm{R},q,\ell} \, |v|_{W^{1,q}(\Omega)}.
\end{aligned}$$

□

Proof of Lemma (3.3.3) . The principal part of the proof is the derivation of

$$\|e_\ell\|^2_{L^2(\Omega)} \lesssim \|e_\ell - v\|^2_{H^1(\Omega)} + \int_\Omega \delta_\ell(x) : \mathrm{D}e_\ell(x) \mathrm{d}x \tag{3.38}$$

for all $v \in \mathcal{D}(\Omega;\mathbb{R}^n)$. A density argument then leads to the claim of Lemma (3.3.3).

Recall that Ω is bounded with a polyhedral boundary. For $y \in \mathbb{R}^d$ the line $S_y = y + z\mathbb{R}$

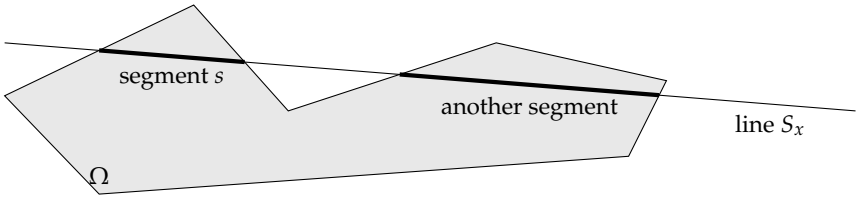

Figure 3.6: The one-dimensional affine space $S_y = y + z\mathbb{R}$ of the proof of Lemma (3.3.3) intersects the two-dimensional domain Ω with polygonal boundary. In this illustration the intersection consists of two separate segments.

has zero or more intersection segments s with Ω; see Figure 3.6 for a two-dimensional illustration. Any $v \in \mathcal{D}(\Omega;\mathbb{R}^n)$ vanishes on the two endpoints of each segment s. Friedrichs' inequality (Lemma (2.1.17), page 19, see also Remark (2.1.18)) shows for each segment s

$$\int_s |v(x)|^2 \,\mathrm{d}s \lesssim |s|^2 \int_s |\mathrm{D}v(x)z|^2 \,\mathrm{d}s.$$

This and $\left|S_y \cap \Omega\right| \leqslant \operatorname{diam}(\Omega)$ yield

$$\int_{S_y} |v(x)|^2 \,\mathrm{d}s \lesssim \operatorname{diam}(\Omega)^2 \int_{S_y} |\mathrm{D}v(x)z|^2 \,\mathrm{d}s \lesssim \int_{S_y} |\mathrm{D}v(x)z|^2 \,\mathrm{d}s.$$

Integration over the domain $z^\perp = \left\{y \in \mathbb{R}^d \,:\, y \cdot z = 0\right\}$ and Fubini's theorem lead to

$$\|v\|^2_{L^2(\Omega)} \lesssim \|\mathrm{D}v\, z\|^2_{L^2(\Omega)}.$$

Note that $w_\ell = e_\ell - v$ satisfies $\|\mathrm{D}w_\ell\, z\|_{L^2(\Omega)} \lesssim |w_\ell|_{H^1(\Omega)}$. Two triangle inequalities and condition (3.21) finally show

$$\begin{aligned}
\|e_\ell\|^2_{L^2(\Omega)} &\lesssim \|w_\ell\|^2_{L^2(\Omega)} + \|v\|^2_{L^2(\Omega)} \\
&\lesssim \|w_\ell\|^2_{L^2(\Omega)} + \|\mathrm{D}v\, z\|^2_{L^2(\Omega)} \\
&\lesssim \|w_\ell\|^2_{L^2(\Omega)} + \|\mathrm{D}w_\ell\, z\|^2_{L^2(\Omega)} + \|\mathrm{D}e_\ell\, z\|^2_{L^2(\Omega)} \\
&\lesssim \|w_\ell\|^2_{H^1(\Omega)} + \int_\Omega \delta_\ell(x) : \mathrm{D}e_\ell(x)\mathrm{d}x.
\end{aligned}$$

Hence (3.38) is valid for all $v \in \mathcal{D}(\Omega;\mathbb{R}^n)$ and, by density of $\mathcal{D}(\Omega)$ in $H^1_0(\Omega)$, also for all $v \in H^1_0(\Omega;\mathbb{R}^n)$. Lemma (3.3.10) shows for the particular choice $v := (1 - B_\ell)e_\ell \in H^1_0(\Omega;\mathbb{R}^n)$

$$\|e_\ell - v\|^2_{H^1(\Omega)} = \|B_\ell(1 - I_\ell)u_D\|^2_{H^1(\Omega)} \lesssim H_\ell^3 \left\|\mathrm{D}^2_{\ell,\partial\Omega} u_D\right\|^2_{L^2(\Omega)}. \qquad \square$$

The following proof of efficiency uses the bubble function technique by Verfürth (1996, 1994).

Proof of Theorem (3.3.6). Recall the nodal basis function φ_z of the node $z \in \mathcal{N}$ from (3.1). For a given element $T \in \mathcal{T}_\ell$ and a given interior side $F \in \mathcal{F}_\ell^\Omega$ we denote their *bubble*

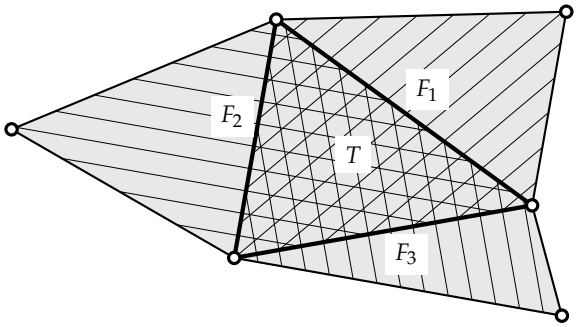

Figure 3.7: A triangle $T \in \mathcal{T}_\ell$ is a subset of the patch ω_{F_j} of each of its three edges F_j. Hence, $\left|\bigcup_{F\in\mathcal{F}_\ell} \omega_F\right| \leqslant 3\,|\Omega|$. Each patch is distinctly hatched here.

functions b_T and b_F by

$$b_T \coloneqq \prod_{z\in\mathcal{N}_\ell\cap T} \varphi_z \in P_{d+1}(T) \cap W_0^{1,q}(T) \;\text{ and }\; b_F \coloneqq \prod_{z\in\mathcal{N}_\ell\cap F} \varphi_z \in P_d(\omega_F) \cap W_0^{1,q}(\omega_F).$$

Verfürth (1994, Lemma 5.1) or a scaling argument prove

$$h_T\,|b_T|_{W^{1,q}(T)}\,\|1\|_{L^{q'}(T)} \lesssim \int_T b_T(x)\mathrm{d}x \;\text{ for all } T\in\mathcal{T}_\ell, \tag{3.39}$$

$$h_F^{1/q'}\,|b_F|_{W^{1,q}(\omega_F)}\,\|1\|_{L^{q'}(F)} \lesssim \int_F b_F(x)\mathrm{d}s \;\text{ for all } F\in\mathcal{F}_\ell^\Omega, \tag{3.40}$$

where the generic constants depend only on the shape of the elements, not on their size.

Since the discrete stress σ_ℓ is $\mathcal{T}_\ell$-piecewise constant integration by parts yields for all $T \in \mathcal{T}_\ell$ and $F \in \mathcal{F}_\ell^\Omega$

$$\int_T \sigma_\ell(x)\mathrm{D}b_T(x)\mathrm{d}x = 0 \;\text{ and }\; \int_{\omega_F} \sigma_\ell(x)\mathrm{D}b_F(x)\mathrm{d}x = \int_F [\sigma_\ell]_F\, n_F b_F(x)\mathrm{d}s.$$

The continuous Euler-Lagrange equation (3.7) with $v = b_T$ or $v = b_T$ leads to

$$\int_T \Lambda_\ell(x)b_T(x)\mathrm{d}x = \int_T \left(2\alpha e_\ell(x)b_T(x) + \delta_\ell(x)\mathrm{D}b_T(x)\right)\mathrm{d}x, \tag{3.41}$$

$$\int_F [\sigma_\ell]_F\, n_F b_F(x)\mathrm{d}s = -\int_{\omega_F} \left(2\alpha e_\ell(x)b_F(x) + \delta_\ell(x)\mathrm{D}b_F(x) - \Lambda_\ell(x)b_F(x)\right)\mathrm{d}x. \tag{3.42}$$

With (3.39), (3.41), and Friedrichs' inequality (Lemma (2.1.17), page 19) for b_T we obtain

$$\begin{aligned} h_T\,|b_T|_{W^{1,q}(T)}\,\|\Pi_\ell\Lambda_\ell\|_{L^{q'}(T)} &\lesssim \int_T \Lambda_\ell(x)b_T(x)\mathrm{d}x - \int_T (1-\Pi_\ell)\Lambda_\ell(x)b_T(x)\mathrm{d}x \\ &\lesssim \left(\|\delta_\ell\|_{L^{q'}(T)} + \alpha h_T\,\|e_\ell\|_{L^{q'}(T)} + h_T\,\|(1-\Pi_\ell)\Lambda_\ell\|_{L^{q'}(T)}\right)|b_T|_{W^{1,q}(T)} \end{aligned}$$

and therefore

$$h_T \|\Lambda_\ell\|_{L^{q'}(T)} \lesssim h_T \|\Pi_\ell \Lambda_\ell\|_{L^{q'}(T)} + h_T \|(1-\Pi_\ell)\Lambda_\ell\|_{L^{q'}(T)} \\ \lesssim \|\delta_\ell\|_{L^{q'}(T)} + \alpha h_T \|e_\ell\|_{L^{q'}(T)} + h_T \|(1-\Pi_\ell)\Lambda_\ell\|_{L^{q'}(T)} \quad (3.43)$$

Let $T_\pm \in \mathcal{T}_\ell$ denote the two elements which compose the patch ω_F. Shape regularity ensures $h_{T_\pm} \approx h_F$. Therefore (3.43) yields

$$h_F \|\Lambda_\ell\|_{L^{q'}(\omega_F)} \lesssim \|\delta_\ell\|_{L^{q'}(\omega_F)} + \alpha h_F \|e_\ell\|_{L^{q'}(\omega_F)} + h_F \|(1-\Pi_\ell)\Lambda_\ell\|_{L^{q'}(\omega_F)}.$$

Akin to the estimates above (3.39), (3.41), Friedrichs' inequality for b_F and the preceding estimate yield

$$\begin{aligned} h_F^{1/q'} |b_F|_{W^{1,q}(\omega_F)} \|[\sigma_\ell]_F n_F\|_{L^{q'}(F)} &\lesssim \int_F [\sigma_\ell]_F n_F b_F(x) \mathrm{d}s \\ &\lesssim \left(\|\delta_\ell\|_{L^{q'}(\omega_F)} + \alpha h_F \|e_\ell\|_{L^{q'}(\omega_F)} + h_F \|\Lambda_\ell\|_{L^{q'}(\omega_F)} \right) |b_F|_{W^{1,q}(\omega_F)} \\ &\lesssim \left(\|\delta_\ell\|_{L^{q'}(\omega_F)} + \alpha h_F \|e_\ell\|_{L^{q'}(\omega_F)} + h_F \|(1-\Pi_\ell)\Lambda_\ell\|_{L^{q'}(T)} \right) |b_F|_{W^{1,q}(\omega_F)} \end{aligned}$$

and consequently

$$h_F^{1/q'} \|[\sigma_\ell]_F n_F\|_{L^{q'}(F)} \lesssim \|\delta_\ell\|_{L^{q'}(\omega_F)} + \alpha h_F \|e_\ell\|_{L^{q'}(\omega_F)} + h_F \|(1-\Pi_\ell)\Lambda_\ell\|_{L^{q'}(\omega_F)}.$$

This eventually leads to

$$\begin{aligned} \sum_{F \in \mathcal{F}_\ell^\Omega} h_F \|[\sigma_\ell]_F n_F\|_{L^{q'}(F)}^{q'} &\lesssim \sum_{F \in \mathcal{F}_\ell^\Omega} \left(\|\delta_\ell\|_{L^{q'}(\omega_F)}^{q'} + \alpha^{q'} h_F^{q'} \|e_\ell\|_{L^{q'}(\omega_F)}^{q'} + \|h_F(1-\Pi_\ell)\Lambda_\ell\|_{L^{q'}(\omega_F)}^{q'} \right) \\ &\leqslant (d+1) \left(\|\delta_\ell\|_{L^{q'}(\Omega)}^{q'} + \alpha^{q'} H_\ell^{q'} \|e_\ell\|_{L^{q'}(\Omega)}^{q'} + \mathrm{osc}_{\ell,q'}(\Lambda_\ell)^{q'} \right). \end{aligned}$$

The factor $d+1$ stems from the fact that each element $T \in \mathcal{T}_\ell$ contains $d+1$ sides $F \in \mathcal{F}_\ell$. Hence T is a subset of the patches ω_F of at most $d+1$ interior sides $F \in \mathcal{F}_\ell^\Omega$. See Figure 3.7 for an illustration of a triangle and the patches of its three edges in $\mathbb{R}^2$. Likewise, (3.43) leads to

$$\sum_{T \in \mathcal{T}_\ell} h_T^{q'} \|\Lambda_\ell\|_{L^{q'}(T)}^{q'} \lesssim \|\delta_\ell\|_{L^{q'}(\Omega)}^{q'} + \alpha^{q'} H_\ell^{q'} \|e_\ell\|_{L^{q'}(\Omega)}^{q'} + \mathrm{osc}_{\ell,q'}(\Lambda_\ell)^{q'}.$$

The substitution of the preceding estimates into the definition of the residual-based error estimator (3.20) concludes the proof. □

3.4 Averaging Error Estimator

This section briefly presents the averaging error estimator (Carstensen and Jochimsen, 2003, Equation (1.11)) and gives a reliability and an efficiency result. The numerical experiments of Chapter 5 employ the averaging error estimator and compare it with the residual-based error estimator of Section 3.3 as well as with the flux error estimator, which is introduced in Section 4.3 (page 78). The arguments which lead to the reliability and

efficiency results are not significant for the remaining sections of the thesis. For this reason merely a sketch of the proofs is provided below.

The general assumptions of Section 3.3 are still in effect. In particular, the energy density $W^{\star\star}$ satisfies the two-sided growth condition (3.8) and convexity control (3.9), and the family of triangulations $(\mathcal{T}_\ell)_{\ell\in\mathbb{N}_0}$ is assumed to be shape-regular. Further recall the terminology of the introduction of Section 3.3 with regards to error estimators.

The following theorem provides a definition of the averaging error estimator and states its reliability with respect to the error of the discrete stress. The theorem employs a modified (node-patch-wise) oscillation operator which is defined by Carstensen (1999, Theorem 3.1) and reads, for $1 \leqslant q < \infty$ and $w \in L^q(\Omega)$,

$$\widetilde{\operatorname{osc}}_{\ell,q}(w)^q \coloneqq \sum_{z\in\mathcal{N}_\ell\cap\Omega} \left\| h_\ell \psi_z \left(w - \fint_{\omega_z} w(x)\mathrm{d}x \right) \right\|^q_{L^q(\omega_z)} .$$

The functions $\{\psi_z : z \in \mathcal{N}_\ell \cap \Omega\} \subset \mathcal{S}_1(\mathcal{T}_\ell)$ are also defined by Carstensen (1999, Theorem 3.1) and constitute a partition of unity on Ω with respect to the interior nodes.

3.4.1 Reliability and Efficiency

(3.4.1) Theorem. *Let $u \in \mathcal{A}$ be a solution of the continuous problem* (3.6) *and σ its stress tensor. Let $u_\ell \in \mathcal{A}_\ell$ be a solution of the discrete problem* (3.10) *with stress tensor σ_ℓ. Assume $g \in L^{q'}(\Omega;\mathbb{R}^n)$, where q' is the Hölder conjugate of some $2 \leqslant q \leqslant p$. Furthermore, r' denotes the Hölder conjugate of r. Then the errors $e_\ell \coloneqq u - u_\ell$ and $\delta_\ell \coloneqq \sigma - \sigma_\ell$ satisfy*

$$\begin{aligned} \int_\Omega \delta_\ell(x) : \mathrm{D}e_\ell(x)\mathrm{d}x + \|\delta_\ell\|^r_{L^{p'}(\Omega)} + \alpha \|e_\ell\|^2_{L^2(\Omega)} \\ \lesssim \quad & H_\ell^{(1+1/p)r'} \left\|\mathrm{D}^2_{\ell,\partial\Omega} u_D\right\|^{r'}_{L^p(\partial\Omega)} + \alpha H_\ell^5 \left\|\mathrm{D}^2_{\ell,\partial\Omega} u_D\right\|^2_{L^2(\partial\Omega)} \\ & + \left(|e_\ell|_{W^{1,q}(\Omega)} + H_\ell^{1+1/q} \left\|\mathrm{D}^2_{\ell,\partial\Omega} u_D\right\|_{L^q(\partial\Omega)} \right) \left(\widetilde{\operatorname{osc}}_{\ell,q'}(\Lambda_\ell) + \eta_{\mathrm{A},q,\ell} \right) \end{aligned} \tag{3.44}$$

with the averaging error estimator

$$\eta_{\mathrm{A},q,\ell} \coloneqq \|(1-\Sigma_\ell)\sigma_\ell\|_{L^{q'}(\Omega)} . \tag{3.45}$$

The integral on the left-hand side of (3.44) *is nonnegative. The first sum in parentheses on the right-hand side is bounded.*

If furthermore the energy density $W^{\star\star}$ complies with (3.21) *then the error e_ℓ satisfies*

$$\begin{aligned} \|e_\ell\|^2_{L^2(\Omega)} \lesssim H_\ell^{(1+1/p)r'} \left\|\mathrm{D}^2_{\ell,\partial\Omega} u_D\right\|^{r'}_{L^p(\partial\Omega)} + H_\ell^3 \left\|\mathrm{D}^2_{\ell,\partial\Omega} u_D\right\|^2_{L^2(\partial\Omega)} \\ + \left(|e_\ell|_{W^{1,q}(\Omega)} + H_\ell^{1+1/q} \left\|\mathrm{D}^2_{\ell,\partial\Omega} u_D\right\|_{L^q(\partial\Omega)} \right) \left(\widetilde{\operatorname{osc}}_{\ell,q'}(\Lambda_\ell) + \eta_{\mathrm{A},q,\ell} \right) . \end{aligned}$$

The generic constants do not depend on ℓ and u_ℓ.

Note that Remark (3.3.7) applies to the node-patch-wise oscillations $\widetilde{\operatorname{osc}}_{\ell,q'}$ as well. Therefore we may expect these oscillations to be of higher order, at least in the case of smooth lower-order terms.

(3.4.2) Theorem (Efficiency). *Let $u \in \mathcal{A}$ be a solution of the continuous problem* (3.6) *and σ its stress tensor. Let $(u_\ell)_{\ell\in\mathbb{N}_0}$ be a sequence of discrete functions $u_\ell \in \mathcal{A}_\ell$ with stress tensors σ_ℓ. Assume $\sigma \in L^{q'}(\Omega;\mathbb{R}^{n\times d})$, where q' is the Hölder conjugate of some $2 \leqslant q \leqslant p$, i.e., $1/q + 1/q' = 1$. Then the error $\delta_\ell \coloneqq \sigma - \sigma_\ell$ and the averaging error estimator $\eta_{\mathrm{A},q,\ell}$ of* (3.45) *satisfy for any $\tau_\ell \in \mathcal{S}_1(\mathcal{T}_\ell;\mathbb{R}^{n\times d})$*

$$\eta_{\mathrm{A},q,\ell} \lesssim \|\delta_\ell\|_{L^{q'}(\Omega)} + \|\sigma - \tau_\ell\|_{L^{q'}(\Omega)}.$$

If furthermore $\sigma \in W^{1,q'}(\Omega;\mathbb{R}^{n\times d})$ then

$$\eta_{\mathrm{A},q,\ell} \lesssim \|\delta_\ell\|_{L^{q'}(\Omega)} + H_\ell\, |\sigma|_{W^{1,q'}(\Omega)}.$$

The generic constants do not depend on ℓ, τ_ℓ and u_ℓ.

3.4.2 Sketches of the Proof

Carstensen (1999, Definition 2.2) introduces an interpolation operator which is required for the proof of Theorem (3.4.1). The definition of this operator is not significant for the thesis and hence skipped. However, the following lemma on approximation and stability properties is required.

(3.4.3) Lemma (Carstensen, 1999, Theorem 3.1). *Let $(\mathcal{T}_\ell)_{\ell\in\mathbb{N}_0}$ be a shape-regular family of triangulations, and let $1 < q, q' < \infty$ with $1/q + 1/q' = 1$. Then there exists an interpolation operator*

$$J_\ell : L^1(\Omega) \to \mathcal{S}_1(\mathcal{T}_\ell) \cap W^{1,q}_0(\Omega)$$

on each triangulation $\mathcal{T}_\ell$ which satisfies for all $v \in W^{1,q}_0(\Omega)$ and $w \in L^{q'}(\Omega)$

$$\left\|h_\ell^{-1}(1 - J_\ell)v\right\|_{L^q(\Omega)} + |(1 - J_\ell)v|_{W^{1,q}(\Omega)} \lesssim |v|_{W^{1,q}(\Omega)},$$
$$\int_\Omega w(x)(1 - J_\ell)v(x)\mathrm{d}x \lesssim |v|_{W^{1,q}(\Omega)}\, \widetilde{\mathrm{osc}}_{\ell,q'}(w),$$

where the generic constant is independent of v, w and ℓ.

Sketch of the proof of Theorem (3.4.1). Akin to (3.29) $v \coloneqq (1 - B_\ell)e_\ell \in V$ satisfies

$$|v|_{W^{1,q}(\Omega)} \lesssim |e_\ell|_{W^{1,q}(\Omega)} + H_\ell^{1+1/q} \left\|\mathrm{D}^2_{\ell,\partial\Omega} u_D\right\|_{L^q(\partial\Omega)},$$

where the right-hand side is bounded by Lemma (3.2.5). With Lemma (3.3.11) it remains to prove

$$\mathrm{Res}_\ell(v) \lesssim \left(\eta_{\mathrm{A},q,\ell} + \widetilde{\mathrm{osc}}_{\ell,q'}(\Lambda_\ell)\right) |v|_{W^{1,q}(\Omega)}.$$

We follow the arguments of Carstensen and Jochimsen (2003, Proof of Theorem 4.2). Let $w_\ell \coloneqq (1 - J_\ell)v$ with the interpolation operator J_ℓ of Lemma (3.4.3). The Galerkin

orthogonality (3.23), an integration by parts and Lemma (3.4.3) yield

$$\begin{aligned}\mathrm{Res}_\ell(v) &= \mathrm{Res}_\ell(w_\ell)\\ &= \int_\Omega (\Lambda_\ell(x)\cdot w_\ell(x) - \Sigma_\ell\sigma_\ell(x) : \mathrm{D}w_\ell(x) + (1-\Sigma_\ell)\sigma_\ell(x) : \mathrm{D}w_\ell(x))\,\mathrm{d}x\\ &= \int_\Omega \Big(\Lambda_\ell(x)\cdot w_\ell(x) + h_\ell \operatorname{div}\Sigma_\ell\sigma_\ell(x)\cdot h_\ell^{-1} w_\ell(x) + (1-\Sigma_\ell)\sigma_\ell(x) : \mathrm{D}w_\ell(x)\Big)\,\mathrm{d}x\\ &\lesssim \Big(\widetilde{\mathrm{osc}}_{\ell,q'}(\Lambda_\ell) + \|h_\ell \operatorname{div}\Sigma_\ell\sigma_\ell\|_{L^{q'}(\Omega)} + \|(1-\Sigma_\ell)\sigma_\ell\|_{L^{q'}(\Omega)}\Big)\,|w_\ell|_{W^{1,q}(\Omega)}\,.\end{aligned}$$

Lemma (3.4.3) proves $|w_\ell|_{W^{1,q}(\Omega)} \lesssim |v|_{W^{1,q}(\Omega)}$. Since $\Sigma_\ell\sigma_\ell$ is an affine function and $\operatorname{div}\sigma_\ell = 0$ on each element $T \in \mathcal{T}_\ell$, an inverse estimate (cf. Brenner and Scott, 2002, Lemma (4.5.3)) proves

$$\begin{aligned}\|h_\ell \operatorname{div}\Sigma_\ell\sigma_\ell\|_{L^{q'}(\Omega)}^{q'} &= \sum_{T\in\mathcal{T}_\ell} h_T^{q'}\,\|\operatorname{div}(1-\Sigma_\ell)\sigma_\ell\|_{L^{q'}(T)}^{q'} \lesssim \sum_{T\in\mathcal{T}_\ell} h_T^{q'}\,|(1-\Sigma_\ell)\sigma_\ell|_{W^{1,q'}(T)}^{q'}\\ &\lesssim \sum_{T\in\mathcal{T}_\ell} \|(1-\Sigma_\ell)\sigma_\ell\|_{L^{q'}(T)}^{q'} = \|(1-\Sigma_\ell)\sigma_\ell\|_{L^{q'}(\Omega)}^{q'}\,.\end{aligned}$$

□

Carstensen (2004a, Theorem 4.1) proves efficiency in the case $q = 2$. In the following the equivalence of norms in finite-dimensional vector spaces is employed to argue that the proof of Carstensen (2004a) also applies for $q \neq 2$.

(3.4.4) Lemma. *Let $\mathcal{T}$ be a regular triangulation and let $p, q \in [1, \infty[$.*

(a) Given an element $T \in \mathcal{T}$ it holds

$$\|u\|_{L^p(T)} \approx |T|^{(q-p)/(qp)}\,\|u\|_{L^q(T)} \quad \text{for } u \in P_1(T).$$

(b) Given a node $z \in \mathcal{N}$ denote its nodal basis function (cf. (3.1)) with φ_z and let $\widetilde{\mathcal{T}} := \{T \in \mathcal{T} : T \subset \omega_z\}$. Then

$$\|u\|_{L^2(\omega_z)} \approx \left\|\varphi_z^{1/2} u\right\|_{L^2(\omega_z)} \quad \text{for } u \in P_1(\widetilde{\mathcal{T}}).$$

The generic constants depends on p, q, and on the shape of the elements, but not on their size.

Proof. Note that the vector spaces $P_1(T)$ and $P_1(\widetilde{\mathcal{T}})$ are finite dimensional. Up to the factor $|T|^{(q-p)/(qp)}$, the claim of (a) follows from the equivalence of the norms of finite-dimensional vector spaces. The factor $|T|^{(q-p)/(qp)}$ then is justified by Lemma (2.1.4) (page 16).

In the situation of (b) $\varphi_z^{1/2}$ is positive on ω_z up to a set of zero measure. Therefore the expression on the right-hand side of the claimed equality is a norm on $P_1(\widetilde{\mathcal{T}})$ and the equivalence of norms proves the claim. Direct calculation shows that both sides scale equally with the size of ω_z. □

Sketch of the proof of Theorem (3.4.2). Lemma (3.4.4) (a) shows

$$\|(1-\Sigma_\ell)\sigma_\ell\|_{L^{q'}(\Omega)}^{q'} = \sum_{T\in\mathcal{T}_\ell} \|(1-\Sigma_\ell)\sigma_\ell\|_{L^{q'}(T)}^{q'} \approx \sum_{T\in\mathcal{T}_\ell} |T|^{(2-q')/2} \|(1-\Sigma_\ell)\sigma_\ell\|_{L^2(T)}^{q'}.$$

The proof of Theorem 4.1 by Carstensen (2004a), with p_h, q_h and r_h replaced by σ_ℓ, $\Sigma_\ell\sigma_\ell$ and τ_ℓ, respectively, yields

$$\|(1-\Sigma_\ell)\sigma_\ell\|_{L^2(T)}^2 \lesssim \sum_{z\in T\cap\mathcal{N}_\ell} \left\|\varphi_z^{1/2}(\sigma_\ell-\tau_\ell)\right\|_{L^2(\omega_z)}^2.$$

Most notably, the generic constants of this inequality *do not even depend on the shape* of the participating elements. The shape regularity ensures that the number of elements within a node patch ω_z is bounded uniformly (cf. Lemma (3.1.3) (d)). This and Lemma (3.4.4) finally prove

$$\|(1-\Sigma_\ell)\sigma_\ell\|_{L^{q'}(\Omega)}^{q'} \lesssim \|\sigma_\ell-\tau_\ell\|_{L^{q'}(\Omega)}^{q'}.$$

A triangle inequality concludes the proof of the first claim. The second claim is a consequence of the same arguments which led to (3.31). □

3.5 Stabilisation

So far a discretisation (3.10) of the convex continuous problem has been established in Section 3.2, based on conforming P_1 finite element functions. An a priori and an a posteriori error estimate have also been provided in Section 3.3. Commonly the energy density $W^{\star\star}$ is the convex hull of a nonconvex energy density W and thus it is not strictly convex. An iterative Newton-Raphson solver which determines an approximate solution u_ℓ of (3.10) utilises the Hessian of the discrete energy $E^{\star\star}$. Note that the set of admissible functions $\mathcal{A}_\ell$ is an affine space of dimension $\#(\mathcal{N}_\ell\cap\Omega)$, hence the Hessian of $E^{\star\star}|_{\mathcal{A}_\ell}$ is a matrix in $\mathbb{R}^{\#(\mathcal{N}_\ell\cap\Omega)\times\#(\mathcal{N}_\ell\cap\Omega)}$. If $W^{\star\star}$ is not strictly convex, said Hessian matrix is possibly ill-conditioned. This poses a serious difficulty to the algorithm which solves a linear system with the Hessian in each iteration step.

The spectral condition number $\kappa(H)$ of a symmetric matrix H is given by the absolute value of the ratio of its largest and its smallest eigenvalue,

$$\kappa(H) := |\lambda_{\max}(H)/\lambda_{\min}(H)|. \tag{3.46}$$

Figure 3.8 depicts the spectral condition numbers $\kappa(\mathrm{D}^2E^{\star\star})$ of the Hessians of $E^{\star\star}$ in the discrete solutions u_ℓ for the benchmark examples of Chapter 2 for different numbers of degrees of freedom. The numerical experiments which led to Figure 3.8 are based on the residual-based refinement indicator of (5.6) (page 95, cf. Chapter 5 for details on the algorithms). The figure indicates that the condition number of the Hessian increases with the number of degrees of freedom. For the three-well benchmark of Section 2.4, in particular, the condition number (as computed by MATLAB) becomes ∞ beyond 574 degrees of freedom. MATLAB's minimisation algorithm can cope with this condition until 33 169 degrees of freedom are reached, then aborts the solution process with the

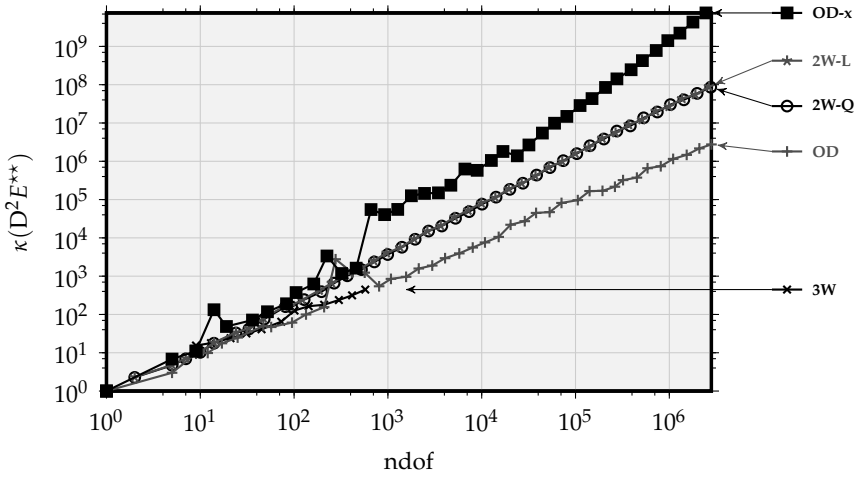

Figure 3.8: Spectral condition number of the Hessian matrix $\mathrm{D}^2E^{\star\star}$ (on $\mathcal{A}_\ell$) as function of the number of degrees of freedom (ndof). The computations are based on adaptive mesh refinements, controlled by the residual-based refinement indicator of (5.6) (page 95). See Table 5.1 (page 92) for the abbreviations of the benchmark examples.

message "Input to EIG must not contain NaN or Inf". The error message is a consequence of an ill-conditioned Hessian.

This section motivates stabilisation schemes as a remedy for the difficulties caused by the lack of strict convexity. To this end the stabilised discrete problem is introduced in (3.49). Chapter 4 is dedicated to the error analysis of the stabilised discrete problem.

3.5.1 Tikhonov Regularisation

Stabilisation methods are inspired by Tikhonov regularisation (Tikhonov et al., 1995). The following gives a short layout of the basic idea before stabilisation methods for the discrete problem (3.10) are introduced.

Given a singular matrix $A \in \mathbb{R}^{n\times n}$ and a vector $b \in \mathbb{R}^n$ the linear system

$$Ax = b$$

admits multiple solutions or none at all. A standard approach is to minimise the ℓ^2 norm of the residual,

$$\min_{x\in\mathbb{R}^n} |Ax - b|^2 , \tag{3.47}$$

which ensures the existence of a solution, but not its uniqueness. Tikhonov regularisation adds a positive definite term $|Tx|^2$ to (3.47), which yields the regularised problem

$$\min_{x\in\mathbb{R}^n} \left(|Ax - b|^2 + |Tx|^2 \right) . \tag{3.48}$$

For each nonsingular matrix $T \in \mathbb{R}^{n\times n}$ the problem (3.48) admits a unique minimiser x. The minimiser depend on the choice of the matrix T. In this sense, Tikhonov regularisation is also a selection process.

3.5.2 Stabilisation and Strong Convergence

In the spirit of (3.48) consider a modified version of the discrete problem (3.10), which reads

$$\begin{aligned}\text{minimise } E_\ell^{\star\star}(v_\ell) &\coloneqq E^{\star\star}(v_\ell) + \frac{1}{2}a_\ell(v_\ell, v_\ell)\\ &= \int_\Omega \Big(W^{\star\star}(\mathrm{D}v_\ell(x)) + \alpha\,|v_\ell(x) - f(x)|^2 - g(x)\cdot v_\ell(x)\Big)\,\mathrm{d}x + \frac{1}{2}a_\ell(v_\ell, v_\ell)\\ &\qquad\qquad \text{amongst } v_\ell \in \mathcal{A}_\ell. \quad (3.49)\end{aligned}$$

The additional term $a_\ell(\cdot,\cdot)$, the *stabilisation function*, is supposed to be positive definite on V and therefore ensures strict convexity of the stabilised energy $E_\ell^{\star\star}$. The index ℓ of a_ℓ emphasises that the stabilisation may depend on the mesh.

Bartels et al. (2004b) propose three different choices for a_ℓ, namely, for $\gamma > -1$,

$$a_\ell^{(\mathrm{a})}(v,w) \coloneqq \sum_{F\in\mathcal{F}_\ell^\Omega} h_F^\gamma \int_F [\mathrm{D}v]_F : [\mathrm{D}w]_F\,\mathrm{d}s \quad \text{for } v,w \in H^{3/2+}(\mathcal{T}_\ell;\mathbb{R}^n), \tag{3.50}$$

$$a_\ell^{(\mathrm{b})}(v,w) \coloneqq \sum_{T\in\mathcal{T}_\ell} h_T^{\gamma-1} \int_T (1-\Sigma_\ell)\mathrm{D}v(x) : (1-\Sigma_\ell)\mathrm{D}w(x)\mathrm{d}x \quad \text{for } v,w \in H^1(\mathcal{T}_\ell;\mathbb{R}^n), \tag{3.51}$$

$$a_\ell^{(\mathrm{c})}(v,w) \coloneqq \sum_{T\in\mathcal{T}_\ell} h_T^{\gamma} \int_T \mathrm{D}v(x) : \mathrm{D}w(x)\mathrm{d}x \quad \text{for } v,w \in H^1(\mathcal{T}_\ell;\mathbb{R}^n). \tag{3.52}$$

Note that Lemma (2.1.11) ensures that the integral of $a_\ell^{(\mathrm{a})}$ is well-defined. The observations of Bartels et al. (2004b, Section 1) are quite remarkable:

> We prove for relevant examples that proper stabilisation maintains the convergence rates of the discrete problem, and, which came much to a surprise, yields even strong convergence of the strain variables in certain circumstances.

However, their result has two severe drawbacks: strong convergence requires an exact solution $u \in H^{3/2+}(\Omega;\mathbb{R}^n)$ and can only be guaranteed on quasi-uniform triangulations, i.e., if $H_\ell \approx h_{\ell,\min}$. If these conditions are satisfied, $a_\ell^{(\mathrm{a})}$ and $a_\ell^{(\mathrm{b})}$ yield strong convergence for $-1 < \gamma < 3$, while $a_\ell^{(\mathrm{c})}$ does so for a γ which depends on the smoothness of the exact solution u (Bartels et al., 2004b, Theorems 6.1, 7.1, and 8.1). This rules out many practical examples like the microstructure benchmark of Section 2.3 (page 25) and also forbids adaptive algorithms where local mesh refinement usually violates quasi-uniformity.

This thesis considers a modified version of the stabilisation function $a_\ell^{(\mathrm{a})}$ of (3.50) that reads

$$a_\ell(v,w) \coloneqq H_\ell^{\gamma+1} \sum_{F\in\mathcal{F}_\ell^\Omega} h_F^{-1} \int_F [\mathrm{D}v]_F : [\mathrm{D}w]_F\,\mathrm{d}s \quad \text{for } v,w \in H^{3/2+}(\mathcal{T}_\ell;\mathbb{R}^n), \tag{3.53}$$

and its associated norm $|||\cdot|||_\ell \coloneqq a_\ell(\cdot,\cdot)$ (formally a semi-norm on $H^{3/2+}(\mathcal{T}_\ell;\mathbb{R}^n)$, but a norm on $H^{3/2+}(\mathcal{T}_\ell;\mathbb{R}^n) \cap H_0^1(\Omega;\mathbb{R}^n)$). The stabilisation of (3.53) is proposed by Boiger

and Carstensen (2010, Equation (2.3)) to restore strong convergence on triangulations that are not quasi-uniform. Chapter 4 provides a detailed error analysis of the stabilisation a_ℓ of (3.53). To support this analysis Theorem (4.1.3) (page 68) of Section 4.1 repeats the convergence result of Bartels et al. (2004b) for the stabilisation $a_\ell^{(\mathrm{a})}$ of (3.50). In the remaining part of the thesis "a_ℓ" refers to the stabilisation (3.53) unless noted otherwise.

Notably, strong convergence of discrete approximations has already been observed by Nicolaides and Walkington (1995). They considered a one-dimensional variational problem similar to the two-well benchmark of Section 2.3 and proved strong $W^{1,4}$-convergence of a continuous and piecewise linear approximation (Nicolaides and Walkington, 1995, Theorem 2.6).

3.5.3 Existence and Euler-Lagrange Equation

To conclude the section, the following are existence and equivalence results similar to Section 3.2, but for the *stabilised problem* (3.49).

(3.5.1) Theorem (Existence of Solutions)**.** *Given the minimisation problem* (3.49) *let its energy density* $W^{\star\star}$ *satisfy* (3.8)*. Then there exists a minimiser* $u_\ell \in \mathcal{A}_\ell$ *of* (3.49)*. This also holds if* a_ℓ *in* (3.49) *is replaced by one of the stabilisations* $a_\ell^{(\mathrm{a})}$, $a_\ell^{(\mathrm{b})}$ *or* $a_\ell^{(\mathrm{c})}$ *of* (3.50)–(3.52)*.*

Proof. Theorem (3.2.2) ensures $\inf_{u_\ell \in \mathcal{A}_\ell} E^{\star\star}(u_\ell) > -\infty$ for the unstabilised discrete problem (3.10). Since each of the stabilisation terms is positive definite, we have $E_\ell^{\star\star}(u_\ell) \geqslant E^{\star\star}(u_\ell)$ for all $u_\ell \in \mathcal{A}_\ell$ and therefore $\inf_{u_\ell \in \mathcal{A}_\ell} E_\ell^{\star\star}(u_\ell) > -\infty$. As in the proof of Theorem (3.2.2) the closeness of $\mathcal{A}_\ell$ ensures the existence of a minimiser. □

With the abbreviations of (3.11) the discrete Euler-Lagrange equation that corresponds to the stabilised discrete problem (3.49) reads

$$\int_\Omega (\sigma_\ell(x) : \mathrm{D}v_\ell(x) - \Lambda_\ell(x) : v_\ell(x)) \,\mathrm{d}x + a_\ell(u_\ell, v_\ell) = 0 \quad \text{for all } v_\ell \in V_\ell. \tag{3.54}$$

(3.5.2) Theorem. *Given the minimisation problem* (3.49) *let its energy density* $W^{\star\star}$ *satisfy* (3.8)*. Then every minimiser* u_ℓ *of* (3.49) *is a solution of the Euler-Lagrange equation* (3.54)*. Conversely, every solution* $u_\ell \in \mathcal{A}_\ell$ *of* (3.54) *is a minimiser of* (3.49)*. This equivalency also holds if, in* (3.49) *and* (3.54)*,* a_ℓ *is replaced by one of the stabilisations* $a_\ell^{(\mathrm{a})}$, $a_\ell^{(\mathrm{b})}$ *or* $a_\ell^{(\mathrm{c})}$ *of* (3.50)–(3.52)*.*

Proof. Akin to Theorem (3.2.3) the proof is similar to the proof of Theorem 3.11 by Dacorogna (2004, page 93). Therefore we concentrate on the alterations of the proof that are caused by the additional stabilisation term. Also, recall the notes on the proof of Theorem (2.2.4) (page 22), which state a necessary modification of the assumptions of Dacorogna (2004).

The second step in the proof of Dacorogna (2004) computes the derivative of the energy. For the discrete problem (3.10) without stabilisation, the derivative reads, for all $u_\ell, v_\ell \in \mathcal{S}_1(\mathcal{T}_\ell; \mathbb{R}^n)$,

$$\lim_{\varepsilon \to 0} \frac{1}{\varepsilon} \left(E^{\star\star}(u_\ell + \varepsilon v_\ell) - E^{\star\star}(u_\ell)\right) = \int_\Omega (\sigma_\ell(x) : \mathrm{D}v_\ell(x) + \Lambda_\ell(x) \cdot v_\ell(x)) \,\mathrm{d}x. \tag{3.55}$$

The stabilisation a_ℓ of (3.53) is symmetric and positive semi-definite on the finite-dimensional space $\mathcal{S}_1(\mathcal{T}_\ell; \mathbb{R}^n)$, therefore

$$\lim_{\varepsilon \to 0} \frac{1}{\varepsilon} \left(|||u_\ell + \varepsilon v_\ell|||_\ell^2 - |||u_\ell|||_\ell^2 \right) = 2a_\ell(u_\ell, v_\ell) \quad \text{for all } u_\ell, v_\ell \in \mathcal{S}_1(\mathcal{T}_\ell; \mathbb{R}^n).$$

The stabilisations of (3.50)–(3.52) and their respective norms enjoy the same property. The limits (3.55) and (3.5.3) yield a derivative of the stabilised energy that reads for all $u_\ell, v_\ell \in \mathcal{S}_1(\mathcal{T}_\ell; \mathbb{R}^n)$

$$\lim_{\varepsilon \to 0} \frac{1}{\varepsilon} \left(E_\ell^{\star\star}(u_\ell + \varepsilon v_\ell) - E_\ell^{\star\star}(u_\ell) \right) = \int_\Omega \left(\sigma_\ell(x) : \mathrm{D} v_\ell(x) + \Lambda_\ell(x) \cdot v_\ell(x) \right) \mathrm{d}x + a_\ell(u_\ell, v_\ell).$$

These investigations, together with steps 3 and 4 of the proof of Theorem 3.11 by Dacorogna (2004) show the claimed equivalence. □

4 Stabilised Error Estimation

This chapter investigates error estimates of the stabilised discrete problem (3.49) (page 61). Based on the results of Bartels et al. (2004b) it develops the a priori error estimators of Boiger and Carstensen (2010, 2012+) for unstructured triangulations. Furthermore, it derives the a posteriori results of Boiger and Carstensen (2012+) with a special focus on interface problems.

Recall the convex model problem (2.2) from Section 2.2 (page 21). Given a bounded Lipschitz domain $\Omega \subset \mathbb{R}^d$ with polyhedral boundary for $d = 2$ or 3, the continuous model problem reads

$$\text{minimise } E^{\star\star}(v) = \int_\Omega \Big(W^{\star\star}(\mathrm{D}v(x)) + \alpha \, |v(x) - f(x)|^2 - g(x) \cdot v(x) \Big) \, \mathrm{d}x \qquad \text{amongst } v \in \mathcal{A}. \tag{4.1}$$

The functions that form the integrand of (4.1) satisfy $f \in L^2(\Omega;\mathbb{R}^n)$, $g \in L^{p'}(\Omega;\mathbb{R}^n)$ and $W^{\star\star} \in \mathcal{C}^1(\mathbb{R}^{n\times d};\mathbb{R})$ with $n \in \mathbb{N}$, $\alpha \geqslant 0$, and the Hölder conjugate p' of $p \geqslant 2$, i.e., $1/p + 1/p' = 1$. The set of admissible functions reads $\mathcal{A} = u_D + V$ where u_D defines the Dirichlet boundary data and $V = W^{1,p}_0(\Omega;\mathbb{R}^n)$. See (3.13) (page 40) or below for smoothness conditions on u_D.

This chapter assumes that the terms of (4.1) comply with the regularity assumptions stated in Section 2.2 (page 21) as follows. The energy density satisfies the *two-sided growth condition* from Assumption (2.2.1) (page 21), which reads

$$|y|^p - 1 \lesssim W^{\star\star}(y) \lesssim |y|^p + 1 \quad \text{for all } y \in \mathbb{R}^{n\times d}, \tag{4.2}$$

and the *convexity control* Assumption (2.2.2) (page 22), i.e., there are parameters r and s with $p' \leqslant r$ and $0 \leqslant s \leqslant rp - r - p$ such that $S \coloneqq \mathrm{D}W^{\star\star}$ satisfies for all $y_1, y_2 \in \mathbb{R}^{n\times d}$

$$|S(y_1) - S(y_2)|^r \lesssim \big(1 + |y_1|^s + |y_2|^s\big) \, (S(y_1) - S(y_2)) : (y_1 - y_2) \, .$$

In the following, r' denotes the Hölder conjugate of r, i.e., $1/r + 1/r' = 1$. Recall the abbreviations (2.3) of Section 2.2 (page 21) for a given solution $u \in \mathcal{A}$, which read

$$\sigma(x) \coloneqq S(\mathrm{D}u(x)) \coloneqq \mathrm{D}W^{\star\star}(\mathrm{D}u(x)) \quad \text{and} \quad \Lambda(x) \coloneqq -2\alpha(u(x) - f(x)) + g(x).$$

Theorem (2.2.4) (page 22) concludes that the set of solutions $u \in \mathcal{A}$ of (4.1) is identical to the set of solutions of the corresponding Euler-Lagrange equation (2.4) (page 21), which reads

$$\int_\Omega (\sigma(x) : \mathrm{D}v(x) - \Lambda(x) \cdot v(x)) \, \mathrm{d}x = 0 \quad \text{for all } v \in V. \tag{4.3}$$

Let $(\mathcal{T}_\ell)_{\ell\in\mathbb{N}_0}$ be a family of shape-regular triangulations of the domain Ω, and assume

that u_D satisfies (3.13) (page 40), i.e.,

$$u_D \in W^{1,p}(\Omega;\mathbb{R}^n) \cap W^{2,p}(\mathcal{T}_0;\mathbb{R}^n) \cap W^{2,p}(\mathcal{F}_0^{\partial\Omega};\mathbb{R}^n).$$

Note that this implies $u_D \in \mathcal{C}(\overline{\Omega};\mathbb{R}^n)$ (cf. Lemma (3.2.1), page 40). The set of discrete admissible functions on $\mathcal{T}_\ell$ reads $\mathcal{A}_\ell := u_{D,\ell} + V_\ell$ with $V_\ell = \mathcal{S}_1(\mathcal{T}_\ell;\mathbb{R}^n) \cap V$ and the nodal interpolant $u_{D,\ell} = I_\ell u_D$. Recall the stabilisation (3.53) (page 61) and its associated norm, which read for $\gamma > -1$

$$\begin{aligned} a_\ell(v,w) &:= H_\ell^{1+\gamma} \sum_{F\in\mathcal{F}_\ell^\Omega} h_F^{-1} \int_F [\mathrm{D}v]_F : [\mathrm{D}w]_F \,\mathrm{d}s \\ \text{and} \quad |||v|||_\ell^2 &:= a_\ell(v,v) \quad \text{for } v,w \in H^{3/2+}(\mathcal{T}_\ell;\mathbb{R}^n). \end{aligned} \tag{4.4}$$

The stabilised discrete problem is given by

$$\text{minimise } E_\ell^{\star\star}(v_\ell) := E^{\star\star}(v_\ell) + \frac{1}{2}\,|||v_\ell|||_\ell^2 \quad \text{amongst } v_\ell \in \mathcal{A}_\ell. \tag{4.5}$$

By Theorem (3.5.2) (page 62), (4.5) is equivalent to the discrete Euler-Lagrange equation (3.54) (page 62), which reads

$$\int_\Omega (\sigma_\ell(x) : \mathrm{D}v_\ell(x) - \Lambda_\ell(x)\cdot v_\ell(x))\,\mathrm{d}x + a_\ell(u_\ell, v_\ell) = 0 \quad \text{for all } v_\ell \in V_\ell, \tag{4.6}$$

with the abbreviations of (3.11) (page 40), i.e., for a given $u_\ell \in \mathcal{A}_\ell$,

$$\sigma_\ell(x) := S(\mathrm{D}u_\ell(x)) \quad \text{and} \quad \Lambda_\ell(x) := -2\alpha(u_\ell(x) - f(x)) + g(x).$$

The remaining content of this chapter is as follows. Section 4.1 investigates the stabilisation function $a_\ell^{(\mathrm{a})}$ of (3.50) (page 61). Theorem (4.1.3) recites the a priori error estimate

$$\|u - u_\ell\|_{H^1(\Omega)} \lesssim H_\ell^{1/2} \quad \text{for } \gamma = 1, r = 2 \tag{4.7}$$

by Bartels et al. (2004b, Theorem 6.1). Note that (4.7) is particularly important for the reconstruction of Young measure-valued solutions of nonconvex problems from $\mathrm{D}u_\ell$ since it ensures *strong* H^1 convergence $u_\ell \to u$; see Remark (2.3.4) (page 27) and the references therein for more information about the solution of the nonconvex minimisation problem. The proof of Theorem (4.1.3) shows that (4.7) is confined to quasi-uniform triangulations and requires severe regularity assumptions on u. Similar to Bartels et al. (2004b, Lemma 9.1) and to the results of Section 3.3, Lemma (3.3.3) (page 44) permits the extension of the scope of (4.7) if condition (3.21) (page 44) is satisfied, which reads for any $u \in \mathcal{A}$ and $u_\ell \in \mathcal{A}_\ell$ with stress tensors σ and σ_ℓ

$$\|\mathrm{D}e_\ell\, z\|_{L^2(\Omega)}^2 \lesssim \int_\Omega \delta_\ell(x) : \mathrm{D}e_\ell(x)\mathrm{d}x \quad \text{for some fixed } z \in \mathbb{R}^d\setminus\{0\}\,, \tag{4.8}$$

where $e_\ell := u - u_\ell$ and $\delta_\ell := \sigma - \sigma_\ell$, and the generic constant does not depend on ℓ and u_ℓ.

The proof of Theorem (4.1.3) in Section 4.1 is also a preliminary of Theorem (4.2.1)

in Section 4.2, which proves that the discrete problem with the stabilisation a_ℓ of (4.4) permits the same a priori error estimate (4.7) even on families of triangulations which lack quasi-uniformity. This result is a first step towards the application of adaptive algorithms, which, in general, do not ensure quasi-uniformity of the generated grids. Theorem (4.2.3) derives an a priori error estimate which reads

$$\|\sigma - \sigma_\ell\|_{L^{p'}(\Omega)} + \alpha \|u - u_\ell\|_{L^2(\Omega)} + |||u_\ell|||_\ell \to 0 \quad \text{for } H_\ell \to 0.$$

In contrast to (4.7), Theorem (4.2.3) does not require any further regularity assumptions on the exact solution besides $u \in W^{1,p}(\Omega;\mathbb{R}^n)$.

Section 4.3 presents an a posteriori error estimator. The stabilisation term in the discrete problem (4.6) poses a difficulty in that the residual does not obey the Galerkin orthogonality. This prevents the application of the residual-based error estimator of Theorem (3.3.2) (page 43). Instead Theorem (4.3.1) derives the error estimator

$$m_q(\tau) \coloneqq \|\sigma_\ell - \tau\|_{L^{q'}(\Omega)} + \|\Pi_\ell \Lambda_\ell + \operatorname{div} \tau\|_{L^{q'}(\Omega)} + \operatorname{osc}_{\ell,q'}(\Lambda_\ell),$$

for any $\tau \in H(\operatorname{div},\Omega;\mathbb{R}^{n\times d})$ and $2 \leqslant q \leqslant p$ with Hölder conjugate q', and proves that $m_q(\tau)$ is reliable, irrespective of any assumptions on the discrete solution u_ℓ. Theorem (4.3.2) states efficiency of $m_q(\tau)$ for a particular choice of τ. However, different exponents of the norms of the error terms in the reliability and efficiency estimates for $p \neq 2$ highlight the reliability-efficiency gap.

Chapter 4 concludes with a refined analysis for interface problems with an exact solution u that is smooth up to a $(d-1)$-dimensional subset $\Gamma \subset \overline{\Omega}$. Section 4.4 proves strong convergence of gradients for unique solutions $u \in W^{1,\infty}(\Omega;\mathbb{R}^n) \cap W^{2,p}(\Omega\backslash\Gamma;\mathbb{R}^n)$, which leads to an improvement of the a posteriori error estimator of Section 4.3, and furthermore to an a posteriori error estimator for the error $|u - u_\ell|_{H^1(\Omega)}$.

4.1 Convergence of Gradients on Uniform Grids

This section investigates the convergence behaviour of the stabilisation function of (3.50), which reads

$$a_\ell^{(\mathrm{a})}(v,w) \coloneqq \sum_{F\in\mathcal{F}_\ell^\Omega} h_F^\gamma \int_F [\mathrm{D}v]_F : [\mathrm{D}w]_F \,\mathrm{d}s \quad \text{for } v,w \in H^{3/2+}(\mathcal{T}_\ell;\mathbb{R}^n). \tag{4.9}$$

The following principal convergence theorems originate from Bartels et al. (2004b).

4.1.1 Convergence Theorems

The following general error estimate is an extension of Theorem 2.1 by Bartels et al. (2004b). In the course of the proof some lemmas are given along the way which are required in the remaining sections of this chapter.

(4.1.1) Theorem. *Let $u \in \mathcal{A}$ be a solution of the continuous problem* (4.1) *and σ its stress tensor. Let $u_\ell \in \mathcal{A}_\ell$ be a solution of the discrete problem* (4.5) *and σ_ℓ its discrete stress tensor, where the*

stabilisation in (4.5) *is given either by* (4.4) *or by* (4.9)*, and let* $|||\cdot|||_\ell$ *denote the respective norm. If* $u \in W^{2,p}(\mathcal{T}_0;\mathbb{R}^n) \cap H^{3/2+}(\Omega;\mathbb{R}^n)$ *the errors* $e_\ell := u - u_\ell$ *and* $\delta_\ell := \sigma - \sigma_\ell$ *satisfy for all* $v_\ell \in V_\ell$

$$\int_\Omega \delta_\ell(x) : \mathrm{D}e_\ell(x)\mathrm{d}x + \|\delta_\ell\|_{L^{p'}(\Omega)}^r + \alpha \|e_\ell\|_{L^2(\Omega)}^2 + |||e_\ell|||_\ell^2 \lesssim |e_\ell - v_\ell|_{W^{1,p}(\Omega)}^{r'} + \alpha \|e_\ell - v_\ell\|_{L^2(\Omega)}^2 + |||e_\ell - v_\ell|||_\ell^2,$$

where r' *is the Hölder conjugate of* r*, i.e.,* $1/r + 1/r' = 1$*. The integral on the left-hand side is nonnegative. The generic constant does not depend on* ℓ *and* u_ℓ*.*

A consequence of Theorem (4.1.1) is convergence of the discrete stress $\sigma_\ell \to \sigma$ and, under certain circumstances, also $u_\ell \to u$. This observation is stated as another theorem.

(4.1.2) Theorem (L^2 Convergence)**.** *In the situation of Theorem (4.1.1) the errors* e_ℓ *and* δ_ℓ *satisfy*

$$\int_\Omega \delta_\ell(x) : \mathrm{D}e_\ell(x)\mathrm{d}x + \|\delta_\ell\|_{L^{p'}(\Omega)}^r + \alpha \|e_\ell\|_{L^2(\Omega)}^2 + |||e_\ell|||_\ell^2 \lesssim H_\ell^{\min\{r',1+\gamma\}} + \alpha H_\ell^4.$$

In particular, the summands on the left-hand side converge to zero as $H_\ell \to 0$*.*

If furthermore condition (4.8) *is satisfied the error* e_ℓ *satisfies*

$$\|e_\ell\|_{L^2(\Omega)}^2 \lesssim H_\ell^{\min\{r',1+\gamma\}} + \alpha H_\ell^4 + H_\ell^3 \left\|\mathrm{D}_{\ell,\partial\Omega}^2 u_D\right\|_{L^2(\partial\Omega)}^2$$

and $u_\ell \to u$ *in* $L^2(\Omega;\mathbb{R}^n)$ *as* $H_\ell \to 0$*. The generic constants do not depend on* ℓ *and* u_ℓ*.*

The section concludes with the proof of the following convergence theorem, which is an extension of Theorem 6.1 by Bartels et al. (2004b), see also Remark (4.1.4). Recall the definition of $h_{\ell,\min} := \min_{T\in\mathcal{T}_\ell} h_T$ from page 34.

(4.1.3) Theorem (Convergence of Gradients)**.** *Let* $u \in \mathcal{A}$ *be a solution of the continuous problem* (4.1) *and* $u_\ell \in \mathcal{A}_\ell$ *be a solution of the discrete problem* (4.5)*, where the stabilisation is given by* (4.9)*. Assume* $u \in W^{2,p}(\mathcal{T}_0;\mathbb{R}^n) \cap H^{3/2+}(\Omega;\mathbb{R}^n)$*. Assume further that the family of triangulations* $(\mathcal{T}_\ell)_{\ell\in\mathbb{N}_0}$ *is quasi-uniform in the sense that* $H_\ell \approx h_{\ell,\min}$*. If* $\alpha > 0$*, or if* (4.8) *is satisfied,* $e_\ell := u - u_\ell$ *fulfils*

$$\|e_\ell\|_{H^1(\Omega)} \lesssim H_\ell^{\zeta/4} \quad \text{with } \zeta = \min\left\{2r' + 2 - 2\gamma,\ 2r' - 1 - \gamma,\ 1 + \gamma,\ \xi\right\} \quad \text{and}$$
$$\xi = \begin{cases} 10 - 2\gamma & \text{for } \alpha > 0, \\ 4 & \text{for } \alpha = 0 \equiv u_D, \\ \min\{r' + 2 - \gamma,\ 3\} & \text{for } \alpha = 0 \not\equiv u_D, \end{cases} \tag{4.10}$$

where r' *is the Hölder conjugate of* r*, i.e.,* $1/r + 1/r' = 1$*. The generic constant does not depend on* ℓ *and* u_ℓ*. In particular,* $u_\ell \to u$ *in* $H^1(\Omega;\mathbb{R}^n)$ *if* $H_\ell \to 0$ *and* $\zeta > 0$*.*

(4.1.4) Remark. *For* $\alpha > 0$*,* $r \leqslant 2$*, and* $\gamma < 3$*, the estimate* (4.10) *of Theorem (4.1.3) simplifies to*

$$\|e_\ell\|_{H^1(\Omega)} \lesssim H_\ell^{\zeta/4} \quad \text{with } \zeta = \min\left\{1 + \gamma,\ 2r' - 1 - \gamma\right\}$$

and $\zeta = 2$ for $\gamma = 1$. This is consistent with Theorem 6.1 by Bartels et al. (2004b) and indicates that $\gamma = 1$ is an optimal choice to ensure fast convergence. See also Remark (4.2.2) for an analogous simplification of Theorem (4.2.1).

4.1.2 Preliminary Lemmas

Recall that the symbol "1" denotes the identity operator within the ring of function operators. The following results apply to each of the stabilisations of (4.4) and (4.9). In any case the notation "$|||\cdot|||_\ell$" refers to the respective stabilisation at hand.

(4.1.5) Lemma. *The stabilisations* (4.4) *and* (4.9) *satisfy*

$$|||(1 - I_\ell)v|||_\ell^2 \lesssim H_\ell^{1+\gamma} \left\|\mathrm{D}_\ell^2 v\right\|_{L^2(\Omega)}^2 \quad \textit{for all } v \in H^2(\mathcal{T}_\ell; \mathbb{R}^n),$$

where the generic constant is independent of ℓ and v.

Proof. Abbreviate $w_\ell := (1 - I_\ell)v$. Consider an interior side $F \in \mathcal{F}_\ell^\Omega$ which is shared by the two elements $T_+, T_- \in \mathcal{T}_\ell$, cf. Figure 3.4 (page 37) for an illustration in $\mathbb{R}^2$. A simple triangle inequality splits the jump terms of the stabilisation into both elements' contributions,

$$|[\mathrm{D}w_\ell]_F| = \left|\mathrm{D}w_\ell|_{T_+} - \mathrm{D}w_\ell|_{T_-}\right| \leqslant \left|\mathrm{D}w_\ell|_{T_+}\right| + \left|\mathrm{D}w_\ell|_{T_-}\right|.$$

The trace inequality (Lemma (3.1.11), page 39) for T_+ and T_- yields

$$\left\|\mathrm{D}w_\ell|_{T_\pm}\right\|_{L^2(F)}^2 \lesssim h_{T_\pm}^{-1} |w_\ell|_{H^1(T_\pm)}^2 + h_{T_\pm} |w_\ell|_{H^2(T_\pm)}^2.$$

Shape regularity of the triangulations $(\mathcal{T}_\ell)_{\ell\in\mathbb{N}_0}$ accounts for $h_{T_\pm} \approx h_F$. Lemma (3.1.5) (page 35) proves $|w_\ell|_{H^1(T_\pm)} \lesssim h_F |w_\ell|_{H^2(T_\pm)}$. Recall the notation $\omega_F := T_+ \cup T_-$. The preceding observations lead to

$$\|[\mathrm{D}w_\ell]_F\|_{L^2(F)}^2 \lesssim \left\|\mathrm{D}w_\ell|_{T_+}\right\|_{L^2(F)}^2 + \left\|\mathrm{D}w_\ell|_{T_-}\right\|_{L^2(F)}^2 \lesssim h_F \left\|\mathrm{D}_\ell^2 w_\ell\right\|_{L^2(\omega_F)}^2. \tag{4.11}$$

Note that $\mathrm{D}_\ell^2 w_\ell = \mathrm{D}_\ell^2 v$. The claim for the norm $|||\cdot|||_\ell$ of the stabilisation a_ℓ of (4.4) then follows from the sum over all interior sides $F \in \mathcal{F}_\ell^\Omega$,

$$\begin{aligned} |||w_\ell|||_\ell^2 &= H_\ell^{1+\gamma} \sum_{F\in\mathcal{F}_\ell^\Omega} h_F^{-1} \|[\mathrm{D}w_\ell]_F\|_{L^2(F)}^2 \\ &\lesssim H_\ell^{1+\gamma} \sum_{F\in\mathcal{F}_\ell^\Omega} \left\|\mathrm{D}_\ell^2 w_\ell\right\|_{L^2(\omega_F)}^2 \leqslant (d+1) H_\ell^{1+\gamma} \left\|\mathrm{D}_\ell^2 v\right\|_{L^2(\Omega)}^2. \end{aligned}$$

We already observed the factor $d + 1$ in the proof of Theorem (3.3.6) (on page 53). The factor stems from the fact that each element $T \in \mathcal{T}_\ell$ contains $d + 1$ sides $F \in \mathcal{F}_\ell$. See Figure 3.7 (page 54) for an illustration. Since

$$a_\ell^{(\mathrm{a})}(w_\ell, w_\ell) \leqslant a_\ell(w_\ell, w_\ell),$$

the claim also holds for the norm of the stabilisation $a_\ell^{(\mathrm{a})}$ of (4.9). □

(4.1.6) Lemma. *The discrete solutions $u_\ell \in \mathcal{A}_\ell$ of* (4.5) *are bounded in $W^{1,p}$, i.e., $\|u_\ell\|_{W^{1,p}(\Omega)} \lesssim 1$. This also holds with a_ℓ replaced by $a_\ell^{(\mathrm{a})}$ in* (4.5).

Lemma (4.1.6) is the stabilised counterpart of Lemma (3.2.5) (page 41) and the proof is very similar. Therefore, the following proof merely stresses the differences to the proof of Lemma (3.2.5).

Proof. Observe that the inequalities (3.14), (3.15) and (3.16) (page 41) are also valid if u_ℓ is a discrete minimiser of the stabilised problem (4.5). Similar to (3.17) the two-sided growth condition (4.2) shows

$$\begin{aligned} &E^{\star\star}(u_\ell) \leqslant E_\ell^{\star\star}(u_\ell) \leqslant E_\ell^{\star\star}(u_{D,\ell}) \\ &\lesssim |u_{D,\ell}|^p_{W^{1,p}(\Omega)} + |\Omega| + \|u_{D,\ell}\|^2_{L^2(\Omega)} + \|f\|^2_{L^2(\Omega)} + \|g\|_{L^{p'}(\Omega)} \|u_{D,\ell}\|_{L^p(\Omega)} + |||u_{D,\ell}|||^2_\ell . \end{aligned} \tag{4.12}$$

In contrast to (3.17), however, the preceding inequality contains the stabilisation norm of $u_{D,\ell}$. A triangle inequality and Lemma (4.1.5) prove

$$|||u_{D,\ell}|||_\ell \leqslant |||u_D|||_\ell + |||(1 - I_\ell)u_D|||_\ell \lesssim 1.$$

The norm $\|u_{D,\ell}\|_{W^{1,p}(\Omega)}$ is bounded due to (3.14), therefore (4.12) yields an upper bound on $E^{\star\star}(u_\ell)$. Akin to (2.11) (page 23) the estimate (3.16) conjectures

$$|u_\ell|^p_{W^{1,p}(\Omega)} - |u_\ell|_{W^{1,p}(\Omega)} - 1 < C$$

for a fixed constant $C > 0$ which is independent of ℓ and u_ℓ. Hence $|u_\ell|_{W^{1,p}(\Omega)}$ is bounded by the positive root of $X^p - X - 1 - C = 0$, and (3.15) yields a bound on $\|u_\ell\|_{L^p(\Omega)}$. □

(4.1.7) Lemma. *Given solutions $u \in \mathcal{A}$ of* (4.1) *and $u_\ell \in \mathcal{A}_\ell$ of* (4.5) *with stress tensors σ and σ_ℓ, the errors $e_\ell := u - u_\ell$ and $\delta_\ell := \sigma - \sigma_\ell$ satisfy for all $v_\ell \in V_\ell$*

$$\begin{aligned} \int_\Omega \delta_\ell(x) : \mathrm{D}e_\ell(x)\mathrm{d}x + \|\delta_\ell\|^r_{L^{p'}(\Omega)} + \alpha \|e_\ell\|^2_{L^2(\Omega)} \\ \lesssim |e_\ell - v_\ell|^{r'}_{W^{1,p}(\Omega)} + \alpha \|e_\ell - v_\ell\|^2_{L^2(\Omega)} + a_\ell(u_\ell, v_\ell), \end{aligned} \tag{4.13}$$

where r' is the Hölder conjugate of r, i.e., $1/r + 1/r' = 1$. This inequality also holds with a_ℓ replaced by $a_\ell^{(\mathrm{a})}$ in (4.5) *and* (4.13). *The generic constant does not depend on ℓ and u_ℓ. The integral on the left-hand side is nonnegative.*

The following proof combines the ideas of Bartels et al. (2004b, Lemmas 4.2–4.3).

Proof. The difference of the Euler-Lagrange equations (4.3) and (4.6) with $v = v_\ell \in V_\ell$ reads

$$\int_\Omega (\delta_\ell(x) : \mathrm{D}v_\ell(x) + 2\alpha e_\ell(x) \cdot v_\ell(x))\, \mathrm{d}x = a_\ell(u_\ell, v_\ell).$$

With a Hölder inequality, a Cauchy inequality, and Lemma (2.2.7) (page 23, with $u_1 = u$

and $u_2 = u_\ell$), the preceding equation transforms into

$$\begin{aligned}\int_\Omega \delta_\ell(x) : \mathrm{D}e_\ell(x)\mathrm{d}x &+ 2\alpha \left\|e_\ell\right\|^2_{L^2(\Omega)} - a_\ell(u_\ell, v_\ell)\\ &= \int_\Omega \left(\delta_\ell(x) : \mathrm{D}(e_\ell - v_\ell)(x) + 2\alpha e_\ell(x) : (e_\ell - v_\ell)(x)\right)\mathrm{d}x\\ &\leqslant \left\|\delta_\ell\right\|_{L^{p'}(\Omega)} \left|e_\ell - v_\ell\right|_{W^{1,p}(\Omega)} + 2\alpha \left\|e_\ell\right\|_{L^2(\Omega)} \left\|e_\ell - v_\ell\right\|_{L^2(\Omega)}\\ &\lesssim \left(\int_\Omega \delta_\ell(x) : \mathrm{D}e_\ell(x)\mathrm{d}x\right)^{1/r} \left|e_\ell - v_\ell\right|_{W^{1,p}(\Omega)} + \alpha \left\|e_\ell\right\|_{L^2(\Omega)} \left\|e_\ell - v_\ell\right\|_{L^2(\Omega)}.\end{aligned}$$

Lemma (2.2.7) applies because the discrete solutions are bounded due to Lemma (4.1.6). Since $r > 1$, the absorption of $\int_\Omega \delta_\ell(x) : \mathrm{D}e_\ell(x)\mathrm{d}x$ and $\left\|e_\ell\right\|_{L^2(\Omega)}$ (see Lemma (2.1.23), page 20, for the absorption technique) leads to

$$\int_\Omega \delta_\ell(x) : \mathrm{D}e_\ell(x)\mathrm{d}x + \alpha \left\|e_\ell\right\|^2_{L^2(\Omega)} \lesssim \left|e_\ell - v_\ell\right|^{r'}_{W^{1,p}(\Omega)} + \alpha \left\|e_\ell - v_\ell\right\|^2_{L^2(\Omega)} + a_\ell(u_\ell, v_\ell).$$

Note that this inequality also holds in the case $\alpha = 0$. Finally Lemma (2.2.7) proves the assertions. □

The following lemma arranges an estimate of the error on the boundary of Ω.

(4.1.8) Lemma. *Given a solution $u \in \mathcal{A} \cap H^2(\mathcal{T}_\ell; \mathbb{R}^n)$ of the continuous problem* (4.1) *and an arbitrary discrete function $u_\ell \in \mathcal{A}_\ell$, the error $e_\ell \coloneqq u - u_\ell$ satisfies*

$$\left|\int_{\partial\Omega} (\mathrm{D}e_\ell(x) n_{\partial\Omega}(x)) \cdot e_\ell(x)\mathrm{d}s\right|^2 \lesssim H_\ell^3 \left|e_\ell\right|_{H^1(\Omega)} \left\|\mathrm{D}^2_{\ell,\partial\Omega} u_D\right\|^2_{L^2(\partial\Omega)} \left(\left|e_\ell\right|_{H^1(\Omega)} + H_\ell\right).$$

The generic constant does not depend on ℓ and u_ℓ.

Proof. Since $u_\ell \in \mathcal{A}_\ell$ we have $e_\ell|_{\partial\Omega} = (1 - I_\ell)u_D|_{\partial\Omega}$. Let $F \in \mathcal{F}_\ell^{\partial\Omega}$ be a side of the boundary and $T = \omega_F \in \mathcal{T}_\ell$ the unique element with $F \subset T$. Then a $(d-1)$-dimensional version of Lemma (3.1.5) (page 35) shows

$$\left\|e_\ell\right\|_{L^2(F)} \lesssim h_F^2 \left\|\mathrm{D}_F^2 e_\ell\right\|_{L^2(F)}.$$

Here D_F^2 denotes the projection of the second derivative onto the hyperplane with normal n_F in the sense that

$$\mathrm{D}_F^2 e_\ell = (1 - n_F n_F^{\mathrm{T}})\, \mathrm{D}^2 v\, (1 - n_F n_F^{\mathrm{T}})$$

for some extension $v \in H^2(\mathbb{R}^d)$ of $e_\ell|_F$. Lemma (2.1.11) (page 18) ensures the existence of such an extension v. The trace inequality (Lemma (3.1.11), page 39) for $\mathrm{D}e_\ell$ reads

$$\left\|\mathrm{D}e_\ell\right\|^2_{L^2(F)} \lesssim h_F^{-1} \left\|\mathrm{D}e_\ell\right\|^2_{L^2(T)} + \left\|\mathrm{D}e_\ell\right\|_{L^2(T)} \left\|\mathrm{D}^2 e_\ell\right\|_{L^2(T)}.$$

Note that $\mathrm{D}^2 e_\ell = \mathrm{D}^2 u$ $\mathcal{T}_\ell$- and $\mathcal{F}_\ell$-elementwise. Finally, Cauchy's inequality yields

$$\begin{aligned}
&\left| \sum_{F\in\mathcal{F}_\ell^{\partial\Omega}} \int_F (\mathrm{D}e_\ell(x) n_F)\cdot e_\ell(x)\mathrm{d}s \right| \\
&\qquad \leqslant \sum_{F\in\mathcal{F}_\ell^{\partial\Omega}} \|\mathrm{D}e_\ell\|_{L^2(F)} \|e_\ell\|_{L^2(F)} \\
&\qquad \lesssim \sum_{F\in\mathcal{F}_\ell^{\partial\Omega}} \left(h_F^{3/2} \|\mathrm{D}e_\ell\|_{L^2(\omega_F)} + h_F^2 \|\mathrm{D}e_\ell\|_{L^2(\omega_F)}^{1/2} \left\|\mathrm{D}^2 u\right\|_{L^2(\omega_F)}^{1/2} \right) \left\|\mathrm{D}_F^2 u_D\right\|_{L^2(F)} \\
&\qquad \lesssim \left(H_\ell^{3/2} \|\mathrm{D}e_\ell\|_{L^2(\Omega)} + H_\ell^2 \|\mathrm{D}e_\ell\|_{L^2(\Omega)}^{1/2} \left\|\mathrm{D}_\ell^2 u\right\|_{L^2(\Omega)}^{1/2} \right) \left\|\mathrm{D}_{\ell,\partial\Omega}^2 u_D\right\|_{L^2(\partial\Omega)} . \quad \square
\end{aligned}$$

4.1.3 Proofs of the Convergence Theorems

Proof of Theorem (4.1.1). The presumed smoothness of the exact solution $u \in H^{3/2+}(\Omega;\mathbb{R}^n)$ guarantees that the gradient $\mathrm{D}u$ is continuous along sides $F \in \mathcal{F}_\ell^\Omega$ of the triangulations (cf. Lemma (2.1.14), page 18), hence $a_\ell(u, v_\ell) = 0$. This holds for the stabilisations of (4.4) and (4.9) likewise. A Cauchy inequality of the stabilisation and a Young inequality (Lemma (2.1.22), page 20) yield

$$a_\ell(u_\ell, v_\ell) = -a_\ell(e_\ell, v_\ell) = a_\ell(e_\ell, e_\ell - v_\ell) - |||e_\ell|||_\ell^2 \leqslant \frac{1}{2} |||e_\ell - v_\ell|||_\ell^2 - \frac{1}{2} |||e_\ell|||_\ell^2 . \tag{4.14}$$

The substitution of (4.14) in Lemma (4.1.7) yields the claim. Lemma (2.2.7) (page 23) proves that the integral term is nonnegative, as already mentioned in the proof of Lemma (4.1.7). $\square$

Proof of Theorem (4.1.2). Set $v_\ell = I_\ell e_\ell$ in Theorem (4.1.1). Note that $\mathrm{D}_\ell^2(e_\ell - v_\ell) = \mathrm{D}_\ell^2 e_\ell = \mathrm{D}_\ell^2 u$. Lemmas (3.1.6) (page 35) and (4.1.5) hence yield

$$\begin{aligned}
&\int_\Omega \delta_\ell(x) : \mathrm{D}e_\ell(x)\mathrm{d}x + \|\delta_\ell\|_{L^{p'}(\Omega)}^r + \alpha \|e_\ell\|_{L^2(\Omega)}^2 + |||e_\ell|||_\ell^2 \\
&\qquad\qquad \lesssim H_\ell^{r'} |u|_{W^{1,p}(\Omega)}^{r'} + \alpha H_\ell^4 \left\|\mathrm{D}_\ell^2 u\right\|_{L^2(\Omega)}^2 + H_\ell^{1+\gamma} \left\|\mathrm{D}_\ell^2 u\right\|_{L^2(\Omega)}^2 .
\end{aligned}$$

Mind that $H_\ell^{r'} + H_\ell^{1+\gamma} \approx H_\ell^{\min\{r',1+\gamma\}}$. The second claim of Theorem (4.1.2) is an immediate consequence of the first one and of Lemma (3.3.3) (page 44). $\square$

Proof of Theorem (4.1.3). The following proof adheres to the arguments of Bartels et al. (2004b, Proof of Theorem 6.1).

Since u_ℓ is piecewise affine it holds $\mathrm{D}_\ell^2 e_\ell = \mathrm{D}_\ell^2 u$. Integration by parts on each element T

$\in \mathcal{T}_\ell$ shows

$$\begin{aligned}|e_\ell|^2_{H^1(\Omega)} &= \sum_{T\in\mathcal{T}_\ell} \int_T \mathrm{D}e_\ell(x) : \mathrm{D}e_\ell(x)\mathrm{d}x \\ &= \sum_{T\in\mathcal{T}_\ell} \left(\int_{\partial T} (\mathrm{D}e_\ell(x) n_{\partial T}(x)) \cdot e_\ell(x)\mathrm{d}s - \int_T \Delta_\ell u(x) \cdot e_\ell(x)\mathrm{d}x \right),\end{aligned}$$

where Δ_ℓ denotes the $\mathcal{T}_\ell$-piecewise Laplacian. The boundary integrals split into integrals over sides $F \in \mathcal{F}_\ell$. The same arguments that led to (3.36) (in the proof of Theorem (3.3.2), page 52) yield

$$\mathrm{D}e_\ell|_{T_+} n_{\partial T_+} + \mathrm{D}e_\ell|_{T_-} n_{\partial T_-} = \left(\mathrm{D}e_\ell|_{T_+} - \mathrm{D}e_\ell|_{T_-}\right) n_F =: [\mathrm{D}e_\ell]_F \, n_F \quad \text{on } F.$$

In contrast to the proof of Theorem (3.3.2), however, the integrand does not vanish on boundary sides in general. Similar to (3.37) we obtain

$$\begin{aligned}|e_\ell|^2_{H^1(\Omega)} = \sum_{F\in\mathcal{F}_\ell^{\partial\Omega}} \int_F (\mathrm{D}e_\ell(x) n_F) \cdot e_\ell(x)\mathrm{d}s \\ + \sum_{F\in\mathcal{F}_\ell^{\Omega}} \int_F ([\mathrm{D}e_\ell]_F \, n_F) \cdot e_\ell(x)\mathrm{d}s - \int_\Omega \Delta_\ell u(x) \cdot e_\ell(x)\mathrm{d}x. \quad (4.15)\end{aligned}$$

Lemma (4.1.8) estimates the first term on the right-hand side. A simple Cauchy inequality shows

$$\int_\Omega \Delta_\ell u(x) \cdot e_\ell(x)\mathrm{d}x \leqslant \|\Delta_\ell u\|_{L^2(\Omega)} \, \|e_\ell\|_{L^2(\Omega)} \lesssim \|e_\ell\|_{L^2(\Omega)}. \quad (4.16)$$

It remains to estimate the second term on the right-hand side of (4.15). The injection of $h_F^{\pm\gamma/2}$ and the application of two Cauchy inequalities, to isolate the stabilisation $a_\ell^{(\mathrm{a})}$, yield

$$\begin{aligned}\sum_{F\in\mathcal{F}_\ell^{\Omega}} \int_F ([\mathrm{D}e_\ell]_F \, n_F) \cdot e_\ell(x)\mathrm{d}s &\leqslant \sum_{F\in\mathcal{F}_\ell^{\Omega}} h_F^{\gamma/2} \, \|[\mathrm{D}e_\ell]_F\|_{L^2(F)} \, h_F^{-\gamma/2} \, \|e_\ell\|_{L^2(F)} \\ &\leqslant a_\ell^{(\mathrm{a})}(e_\ell, e_\ell)^{1/2} \left(\sum_{F\in\mathcal{F}_\ell^{\Omega}} h_F^{-\gamma} \, \|e_\ell\|^2_{L^2(F)} \right)^{1/2}. \quad (4.17)\end{aligned}$$

The quasi-uniformity of the sets of triangulations allows for

$$\max_{F\in\mathcal{F}_\ell^{\Omega}} h_F^{-1} \approx (\max_{F\in\mathcal{F}_\ell^{\Omega}} h_F)^{-1}.$$

The trace inequality (Lemma (3.1.11), page 39) estimates the remaining factor

$$\begin{aligned}\sum_{F\in\mathcal{F}_\ell^{\Omega}} h_F^{-\gamma} \, \|e_\ell\|^2_{L^2(F)} &\lesssim \sum_{F\in\mathcal{F}_\ell^{\Omega}} \left(h_F^{-(\gamma+1)} \, \|e_\ell\|^2_{L^2(\omega_F)} + h_F^{1-\gamma} \, \|\mathrm{D}e_\ell\|^2_{L^2(\omega_F)} \right) \\ &\lesssim H_\ell^{-(\gamma+1)} \, \|e_\ell\|^2_{L^2(\Omega)} + H_\ell^{1-\gamma} \, |e_\ell|^2_{H^1(\Omega)}. \quad (4.18)\end{aligned}$$

The preceding estimates combine to

$$|e_\ell|^2_{H^1(\Omega)} \lesssim \|e_\ell\|_{L^2(\Omega)} + H_\ell^{3/2} |e_\ell|^{1/2}_{H^1(\Omega)} \left\|\mathrm{D}^2_{\ell,\partial\Omega} u_D\right\|_{L^2(\partial\Omega)} \left(|e_\ell|_{H^1(\Omega)} + H_\ell\right)^{1/2} + a_\ell^{(\mathrm{a})}(e_\ell, e_\ell)^{1/2} \left(H_\ell^{-(\gamma+1)/2} \|e_\ell\|_{L^2(\Omega)} + H_\ell^{(1-\gamma)/2} |e_\ell|_{H^1(\Omega)}\right). \quad (4.19)$$

Lemmas (2.1.4) (page 16) and (4.1.6) ensure that $\|u_\ell\|_{L^2(\Omega)}$ is bounded, therefore $\|e_\ell\|^2_{L^2(\Omega)} \lesssim \|e_\ell\|_{L^2(\Omega)}$. This observation and the absorptions of $|e_\ell|^{1/2}_{H^2(\Omega)}$ and $|e_\ell|_{H^2(\Omega)}$ (cf. Lemma (2.1.23), page 20) prove

$$\|e_\ell\|^2_{H^1(\Omega)} \lesssim \|e_\ell\|_{L^2(\Omega)} + H_\ell^{-(\gamma+1)/2} a_\ell^{(\mathrm{a})}(e_\ell, e_\ell)^{1/2} \|e_\ell\|_{L^2(\Omega)} + H_\ell^{8/3} \left\|\mathrm{D}^2_{\ell,\partial\Omega} u_D\right\|_{L^2(\partial\Omega)} + H_\ell^{1-\gamma} a_\ell^{(\mathrm{a})}(e_\ell, e_\ell). \quad (4.20)$$

We consider the square of (4.20) to reduce the number of fractions in the following estimates. Theorem (4.1.2) provides the estimate $a_\ell^{(\mathrm{a})}(e_\ell, e_\ell) \lesssim H_\ell^{\min\{r',1+\gamma\}} + \alpha H_\ell^4$, thus

$$\begin{aligned}\|e_\ell\|^4_{H^1(\Omega)} \lesssim\ & \|e_\ell\|^2_{L^2(\Omega)} \left(1 + H_\ell^{\min\{r'-1-\gamma,0\}} + \alpha H_\ell^{3-\gamma}\right) \\ & + H_\ell^{16/3} \left\|\mathrm{D}^2_{\ell,\partial\Omega} u_D\right\|^2_{L^2(\partial\Omega)} + H_\ell^{\min\{2r'+2-2\gamma,4\}} + \alpha H_\ell^{10-2\gamma} \\ \lesssim\ & \|e_\ell\|^2_{L^2(\Omega)} \left(H_\ell^{\min\{0,r'-1-\gamma\}} + \alpha H_\ell^{3-\gamma}\right) + H_\ell^{\min\{4,2r'+2-2\gamma\}} + \alpha H_\ell^{10-2\gamma}. \quad (4.21)\end{aligned}$$

In the remaining part of this proof, the right-hand side of (4.21) is studied for each of the three cases of (4.10).

- For $\alpha > 0$ Theorem (4.1.2) also provides the estimate $\|e_\ell\|^2_{L^2(\Omega)} \lesssim H_\ell^{\min\{r',1+\gamma,4\}}$, which yields

$$\begin{aligned}\|e_\ell\|^4_{H^1(\Omega)} &\lesssim H_\ell^{\min\{4,1+\gamma,r'\}} H_\ell^{\min\{0,3-\gamma,r'-1-\gamma\}} + H_\ell^{\min\{4,10-2\gamma,2r'+2-2\gamma\}} \\ &\lesssim H_\ell^{\min\{4,\ 1+\gamma,\ r',\ 7-\gamma,\ r'+3-\gamma,\ 2r'-1-\gamma,\ 10-2\gamma,\ 2r'+2-2\gamma\}}.\end{aligned}$$

- For $\alpha = 0 \equiv u_D$ Theorem (4.1.2) states $\|e_\ell\|^2_{L^2(\Omega)} \lesssim H_\ell^{\min\{1+\gamma,r'\}}$ and therefore

$$\|e_\ell\|^4_{H^1(\Omega)} \lesssim H_\ell^{\min\{1+\gamma,\ r',\ 2r'-1-\gamma,\ 4,\ 2r'+2-2\gamma\}}.$$

- For $\alpha = 0 \not\equiv u_D$ one obtains $\|e_\ell\|^2_{L^2(\Omega)} \lesssim H_\ell^{\min\{3,1+\gamma,r'\}}$ and hence

$$\|e_\ell\|^4_{H^1(\Omega)} \lesssim H_\ell^{\min\{3,\ 1+\gamma,\ r',\ r'+2-\gamma,\ 2r'-1-\gamma,\ 2r'+2-2\gamma\}}.$$

In all three cases the convex combinations

$$\begin{aligned} r' &= \tfrac{1}{2}(1+\gamma) + \tfrac{1}{2}(2r'-1-\gamma), & 4 &= \tfrac{1}{2}(1+\gamma) + \tfrac{1}{2}(7-\gamma), \\ r'+3-\gamma &= \tfrac{1}{2}(2r'-1-\gamma) + \tfrac{1}{2}(7-\gamma), \text{ and} & 7-\gamma &= \tfrac{2}{3}(10-2\gamma) + \tfrac{1}{3}(1+\gamma) \end{aligned}$$

permit to drop some of the terms in the minima. The remaining terms are precisely those given in (4.10). □

4.2 Convergence Results on Unstructured Grids

Theorems (4.1.2) and (4.1.3) provide a priori estimates for the error $u - u_\ell$ with explicit convergence rates, yet they rely on the rather heavy-handed smoothness assumption $u \in H^{3/2+}(\Omega;\mathbb{R}^n)$. This smoothness assumption is required to ensure $a_\ell(u,\cdot) \equiv 0$, however, it is violated by applications, e.g., the two-well and the three-well benchmarks of Sections 2.3 and 2.4 (pages 25 and 27). Furthermore, in general the restriction to quasi-uniform triangulations in Theorem (4.1.3) is incompatible with adaptive algorithms: adaptive mesh refinements tend to concentrate on areas where the data or the solution are nonsmooth or oscillating and yield a high ratio $H_\ell/h_{\ell,\min}$.

This section investigates the convergence behaviour of the discrete problem (4.5) with the stabilisation a_ℓ of (4.4). Theorem (4.2.1) demonstrates that the stabilisation of (4.4) in fact improves Theorem (4.1.3) in that it does not require quasi-uniformity. A less general version of Theorem (4.2.1) has been published by Boiger and Carstensen (2010, Theorem 4.4), see also Remark (4.2.2). Note that Theorem (4.2.1) applies to the stabilisation (4.4) only. Theorem (4.2.3) provides a more general convergence result. It proves convergence of the discrete stress $\sigma_\ell \to \sigma$ in $L^{p'}(\Omega;\mathbb{R}^{n\times d})$ and, if $\alpha > 0$ or if (4.8) is satisfied, $u_\ell \to u$ in $L^2(\Omega;\mathbb{R}^n)$. In contrast to Theorems (3.3.1) (page 43) and (4.1.2), Theorem (4.2.3) does not demand any higher regularity of the solution $u \in \mathcal{A}$. This result will be published by Boiger and Carstensen (2012+, Theorem 3.1).

4.2.1 Convergence Theorems

(4.2.1) Theorem (Convergence of Gradients)**.** *Let $u \in \mathcal{A}$ be a solution of the continuous problem* (4.1) *and $u_\ell \in \mathcal{A}_\ell$ be a solution of the discrete problem* (4.5)*, where the stabilisation is given by* (4.4)*. Assume $u \in W^{2,p}(\mathcal{T}_0;\mathbb{R}^n) \cap H^{3/2+}(\Omega;\mathbb{R}^n)$. If $\alpha > 0$, or if* (4.8) *is satisfied, $e_\ell := u - u_\ell$ fulfils*

$$\|e_\ell\|_{H^1(\Omega)} \lesssim H_\ell^{\zeta/4}$$

with ζ as in (4.10)*. The generic constant does not depend on ℓ and u_ℓ. In particular, $u_\ell \to u$ in $H^1(\Omega;\mathbb{R}^n)$ if $H_\ell \to 0$ and $\zeta > 0$.*

(4.2.2) Remark. *For $r \leqslant 2$ and $\gamma < 3$ the estimate* (4.10) *in the context of Theorem (4.2.1) simplifies to*

$$\|e_\ell\|_{H^1(\Omega)} \lesssim H_\ell^{\zeta/4} \text{ with } \zeta = \begin{cases} \min\{1+\gamma,\ 2r'-1-\gamma\} & \text{for } \alpha > 0, \\ \min\{1+\gamma,\ 3-\gamma\} & \text{for } \alpha = 0, \end{cases}$$

and $\zeta = 2$ for $\gamma = 1$. This is consistent with Theorem 4.4 by Boiger and Carstensen (2010) and, akin to Remark (4.1.4), supports $\gamma = 1$ as optimal choice for fast convergence.

(4.2.3) Theorem (L^2 Convergence)**.** *Let $u \in \mathcal{A}$ be a solution of the continuous problem* (4.1) *and σ its stress tensor. Let $u_\ell \in \mathcal{A}_\ell$ be a solution of the discrete problem* (4.5) *and σ_ℓ its discrete*

stress tensor, where the stabilisation in (4.5) *is given either by* (4.4) *or by* (4.9)*, and let* $|||\cdot|||_\ell$ *denote the respective norm. Then the errors* $e_\ell := u - u_\ell$ *and* $\delta_\ell := \sigma - \sigma_\ell$ *satisfy*

$$\int_\Omega \delta_\ell(x) : \mathrm{D}e_\ell(x)\mathrm{d}x + \|\delta_\ell\|_{L^{p'}(\Omega)} + \alpha \|e_\ell\|_{L^2(\Omega)} + |||u_\ell|||_\ell \to 0 \ \text{ as } H_\ell \to 0. \tag{4.22}$$

The integral on the left-hand side is nonnegative.

If (4.8) *is satisfied we also have* $u_\ell \to u$ *in* $L^2(\Omega;\mathbb{R}^n)$ *as* $H_\ell \to 0$*, independently of* α*.*

(4.2.4) Remark (Convergence Implies Uniqueness)**.** *Theorem (2.2.5) (page 23) already establishes uniqueness of the continuous solution* σ *and, if* $\alpha > 0$*, of* u*. Theorem (4.2.3) proves*

$$u_\ell \to u \ \text{ in } L^2(\Omega;\mathbb{R}^n) \ \text{ (for } \alpha > 0) \ \text{ and } \ \sigma_\ell \to \sigma \ \text{ in } L^{p'}(\Omega;\mathbb{R}^n)$$

and therefore confirms Theorem (2.2.5) since limits are unique. Moreover, for problems which satisfy (3.21)*, Theorem (2.2.5) ensures convergence and therefore uniqueness even for* $\alpha = 0$*.*

4.2.2 Proof of Theorem (4.2.1)

The proof of Theorem (4.2.1) is similar to the proof of Theorem (4.1.3), but the following lemma is required to replace the estimates (4.17) and (4.18). This lemma is consistent with the "Estimate on C" in the proof of Theorem 4.4 by Boiger and Carstensen (2010).

(4.2.5) Lemma. *Every* $v \in H^1(\Omega;\mathbb{R}^n)$ *and* $w \in H^{3/2+}(\mathcal{T}_\ell;\mathbb{R}^n)$ *satisfy*

$$\sum_{F\in\mathcal{F}_\ell^\Omega} \int_F ([\mathrm{D}w]_F\, n_F)\cdot v(x)\mathrm{d}s \lesssim |||w|||_\ell \left(H_\ell^{-(1+\gamma)/2} \|v\|_{L^2(\Omega)} + H_\ell^{(1-\gamma)/2} |v|_{H^1(\Omega)} \right). \tag{4.23}$$

The generic constant is independent of v*,* w *and* ℓ*.*

Proof. We inject $h_F^{\mp 1/2}$ into the integral on the left-hand side of (4.23) in order to recover the stabilisation (4.4). Two Cauchy inequalities reveal

$$\begin{aligned}\sum_{F\in\mathcal{F}_\ell^\Omega} \int_F ([\mathrm{D}w]_F\, n_F)\cdot v(x)\mathrm{d}s &\leqslant \sum_{F\in\mathcal{F}_\ell^\Omega} h_F^{-1/2} \|[\mathrm{D}w]_F\|_{L^2(F)}\, h_F^{1/2} \|v\|_{L^2(F)} \\ &\leqslant H_\ell^{-(1+\gamma)/2} |||w|||_\ell \left(\sum_{F\in\mathcal{F}_\ell^\Omega} h_F \|v\|_{L^2(F)}^2 \right)^{1/2}.\end{aligned}$$

The trace inequality (Lemma (3.1.11), page 39) estimates the sum on the right-hand side

$$\sum_{F\in\mathcal{F}_\ell^\Omega} h_F \|v\|_{L^2(F)}^2 \lesssim \sum_{F\in\mathcal{F}_\ell^\Omega} \left(\|v\|_{L^2(\omega_F)}^2 + h_F^2 |v|_{H^1(\omega_F)}^2 \right) \lesssim \|v\|_{L^2(\Omega)}^2 + H_\ell^2 |v|_{H^1(\Omega)}^2.$$

The combination of these inequalities proves (4.23). □

Proof of Theorem (4.2.1). This proof follows the strategy of the proof of Theorem (4.1.3).

Integration by parts on each element and a rearrangement of the integrals of the elements' boundaries lead to (4.15). Lemma (4.1.8) and (4.16) yield

$$|e_\ell|^2_{H^1(\Omega)} \lesssim \|e_\ell\|_{L^2(\Omega)} + H_\ell^{3/2} |e_\ell|^{1/2}_{H^1(\Omega)} \left\|\mathrm{D}^2_{\ell,\partial\Omega} u_D\right\|_{L^2(\partial\Omega)} \left(|e_\ell|_{H^1(\Omega)} + H_\ell\right)^{1/2} + \sum_{F\in\mathcal{F}_\ell^\Omega} \int_F ([\mathrm{D}e_\ell]_F\, n_F)\cdot e_\ell(x)\mathrm{d}s.$$

See the beginning of the proof of Theorem (4.1.3) for details on the estimates and Figure 3.4 (page 37) for an explanation of the rearrangement of the boundary terms.

The estimation of the last summand differs from Theorem (4.1.3) as we do not assume quasi-uniformity of the triangulations anymore. Lemma (4.2.5) yields (4.23) with v and w replaced by e_ℓ, and hence

$$|e_\ell|^2_{H^1(\Omega)} \lesssim \|e_\ell\|_{L^2(\Omega)} + H_\ell^{3/2} |e_\ell|^{1/2}_{H^1(\Omega)} \left\|\mathrm{D}^2_{\ell,\partial\Omega} u_D\right\|_{L^2(\partial\Omega)} \left(|e_\ell|_{H^1(\Omega)} + H_\ell\right)^{1/2} + |||e_\ell|||_\ell \left(H_\ell^{-(\gamma+1)/2} \|e_\ell\|_{L^2(\Omega)} + H_\ell^{(1-\gamma)/2} |e_\ell|_{H^1(\Omega)}\right).$$

This is (4.19) from the proof of Theorem (4.1.3) with a_ℓ in the place of $a_\ell^{(\mathrm{a})}$. Following the proof of Theorem (4.1.3) again, the absorption of $|e_\ell|_{H^1(\Omega)}$ (cf. Lemma (2.1.23), page 20) leads to (4.20). Theorem (4.1.2) shows (4.21) and yields the convergence rate of (4.10). □

4.2.3 Proof of Theorem (4.2.3)

The arguments of the following proof match those of Boiger and Carstensen (2012+, Section 3).

Proof of Theorem (4.2.3). The basic idea of the following proof is to replace the exact solution u with a smooth approximation, then to proceed as in Theorem (4.1.2).

Given $0 < \varepsilon < 1$ Definition (2.1.1) of $W_0^{1,p}$ (page 14) guarantees the existence of an approximation $w_\varepsilon \in \mathcal{D}(\Omega;\mathbb{R}^n)$ of $u - u_D \in W_0^{1,p}(\Omega;\mathbb{R}^n)$ with

$$\|u - u_D - w_\varepsilon\|_{W^{1,p}(\Omega)} \leqslant \varepsilon.$$

Claim: A level $\ell_\varepsilon \in \mathbb{N}$ exists such that for all levels $\ell \geqslant \ell_\varepsilon$ the left-hand side of (4.22) is bounded by ε up to a generic constant, i.e.,

$$\int_\Omega \delta_\ell(x) : \mathrm{D}e_\ell(x)\mathrm{d}x + \|\delta_\ell\|_{L^{p'}(\Omega)} + \alpha \|e_\ell\|_{L^2(\Omega)} + |||u_\ell|||_\ell \lesssim \varepsilon \quad \text{for all } \ell \geqslant \ell_\varepsilon. \tag{4.24}$$

The generic constant is independent of ℓ and ε. Lemmas (4.1.6) and (2.2.7) (page 23) show that the integral on the left-hand side is nonnegative. Hence (4.24) is equivalent to (4.22).

Proof of the claim. Define $v_\ell := I_\ell w_\varepsilon + u_{D,\ell} - u_\ell = I_\ell(w_\varepsilon + u_D) - u_\ell \in V_\ell$. Akin to (4.14) in the proof of Theorem (4.1.1), a Cauchy inequality of the stabilisation shows

$$a_\ell(u_\ell, v_\ell) = a_\ell(u_\ell, I_\ell(w_\varepsilon + u_D)) - a_\ell(u_\ell, u_\ell) \leqslant \frac{1}{2} |||I_\ell(w_\varepsilon + u_D)|||^2_\ell - \frac{1}{2} |||u_\ell|||^2_\ell. \tag{4.25}$$

Simple algebraic transformations demonstrate that $e_\ell - v_\ell$ is represented by

$$e_\ell - v_\ell = (u - u_D - w_\varepsilon) + (1 - I_\ell)\,(w_\varepsilon + u_D)\,. \tag{4.26}$$

We substitute (4.25) and (4.26) in Lemma (4.1.7), add $\frac{1}{2}\,|||u_\ell|||_\ell$ on both sides and apply a triangle inequality to split up the norms. This approach leads to

$$\begin{aligned}
&\int_\Omega \delta_\ell(x) : \mathrm{D}e_\ell(x)\mathrm{d}x + \|\delta_\ell\|_{L^{p'}(\Omega)}^r + \alpha\,\|e_\ell\|_{L^2(\Omega)}^2 + \frac{1}{2}\,|||u_\ell|||_\ell^2 \\
&\quad\lesssim |e_\ell - v_\ell|_{W^{1,p}(\Omega)}^{r'} + \alpha\,\|e_\ell - v_\ell\|_{L^2(\Omega)}^2 + \frac{1}{2}\,|||I_\ell(w_\varepsilon + u_D)|||_\ell^2 \\
&\quad\lesssim |u - u_D - w_\varepsilon|_{W^{1,p}(\Omega)}^{r'} + \alpha\,\|u - u_D - w_\varepsilon\|_{L^2(\Omega)}^2 \\
&\qquad + |(1 - I_\ell)(w_\varepsilon + u_D)|_{W^{1,p}(\Omega)}^{r'} + \alpha\,\|(1 - I_\ell)(w_\varepsilon + u_D)\|_{L^2(\Omega)}^2 + |||I_\ell(w_\varepsilon + u_D)|||_\ell^2\,.
\end{aligned} \tag{4.27}$$

With $p \geqslant 2$ Lemma (2.1.4) (page 16) shows $\|\cdot\|_{L^2(\Omega)} \lesssim \|\cdot\|_{W^{1,p}(\Omega)}$. Since $r' > 1$ and $\varepsilon < 1$ the first two summands of the right-hand side on (4.27) satisfy

$$|u - u_D - w_\varepsilon|_{W^{1,p}(\Omega)}^{r'} + \alpha\,\|u - u_D - w_\varepsilon\|_{L^2(\Omega)}^2 \lesssim \varepsilon.$$

The smoothness of $w_\varepsilon + u_D$ ensures $|||w_\varepsilon + u_D|||_\ell = 0$. Lemmas (3.1.6) (page 35) and (4.1.5) yield

$$\begin{aligned}
|(1 - I_\ell)(w_\varepsilon + u_D)|_{W^{1,p}(\Omega)}^{r'} + \alpha\,\|(1 - I_\ell)(w_\varepsilon + u_D)\|_{L^2(\Omega)}^2 &\lesssim H_\ell^{r'} + H_\ell^4 \to 0, \\
|||I_\ell(w_\varepsilon + u_D)|||_\ell^2 = |||(1 - I_\ell)(w_\varepsilon + u_D)|||_\ell^2 &\lesssim H_\ell^{\gamma+1} \to 0.
\end{aligned}$$

This and (4.27) prove the existence of an $\ell_\varepsilon \in \mathbb{N}$ such that

$$\int_\Omega \delta_\ell(x) : \mathrm{D}e_\ell(x)\mathrm{d}x + \|\delta_\ell\|_{L^{p'}(\Omega)}^r + \alpha\,\|e_\ell\|_{L^2(\Omega)}^2 + |||u_\ell|||_\ell \lesssim \varepsilon \quad \text{for } \ell \geqslant \ell_\varepsilon.$$

This is equivalent to (4.24) and therefore proves (4.22). If (4.8) is satisfied, (4.22) and Lemma (3.3.3) (page 44) prove $u_\ell \to u$ in $L^2(\Omega;\mathbb{R}^n)$. □

4.3 A Posteriori Error Estimation

Theorem (3.3.2) (page 43) presents the residual-based a posteriori error estimator $\eta_{\mathrm{R},q,\ell}$ and proves its reliability with respect to the unstabilised discrete problem (3.10) (page 40). Recall the definition of the residual (3.22) (page 45), which reads

$$\mathrm{Res}_\ell(v) \coloneqq -\int_\Omega (\sigma_\ell(x) : \mathrm{D}v(x) - \Lambda_\ell(x)\cdot v(x))\,\mathrm{d}x \quad \text{for } v \in W^{1,p}(\Omega;\mathbb{R}^n). \tag{4.28}$$

The proof of reliability relies on the Galerkin orthogonality (3.23) (page 45). However, due to the added stabilisation term, solutions of the stabilised problem (4.5) do *not* satisfy

the Galerkin orthogonality,

$$\mathrm{Res}_\ell(v_\ell) = a_\ell(u_\ell, v_\ell) \neq 0 \text{ in general for } v_\ell \in V_\ell.$$

Therefore the proof of Theorem (3.3.2) does not apply to the stabilised problem. It would stand to reason to simply incorporate the stabilisation term into a "stabilised residual" $\widetilde{\mathrm{Res}_\ell}(v) \coloneqq \mathrm{Res}_\ell(v) - a_\ell(u_\ell, v)$. With the modified residual, however, the stabilisation yields an additional term in the final estimates of the proof of Theorem (3.3.2) (on page 52), which the author failed to control.

This section pursues a different strategy to derive a guaranteed upper bound on the error of a discrete solution u_ℓ, which is inspired by equilibration error estimator techniques (Repin et al., 2003; Carstensen and Merdon, 2012, Section 5.2). The following Theorem (4.3.1) does *not* assume Galerkin orthogonality. In fact, it does not require u_ℓ to be a solution at all, any $|\cdot|_{W^{1,p}(\Omega)}$-bounded sequence $(u_\ell)_{\ell\in\mathbb{N}_0}$ of discrete functions is allowed. Hence, for the actual computation of u_ℓ, iterative solvers are permitted and termination criteria are not a sensitive issue. Preliminary versions of the following theorems can be found in Boiger and Carstensen (2012+, Section 4).

4.3.1 The Flux Error Estimator

The following theorem employs the oscillation operator, which reads (cf. (3.3), page 37)

$$\mathrm{osc}_{\ell,p}(v) \coloneqq \|h_\ell(1-\Pi_\ell)v\|_{L^p(\Omega)} \quad \text{for } v \in L^p(\Omega).$$

(4.3.1) Theorem (Flux Error Estimator)**.** *Let $u \in \mathcal{A}$ be a solution of the continuous problem* (4.1) *and σ its stress tensor. Let $(u_\ell)_{\ell\in\mathbb{N}_0}$ be a sequence of discrete functions $u_\ell \in \mathcal{A}_\ell$ with $|u_\ell|_{W^{1,p}(\Omega)} \lesssim 1$ and stress tensors σ_ℓ. Assume $g \in L^{q'}(\Omega;\mathbb{R}^n)$, where q' is the Hölder conjugate of some $2 \leqslant q \leqslant p$. Furthermore, r' denotes the Hölder conjugate of r. Then the errors $e_\ell \coloneqq u - u_\ell$ and $\delta_\ell \coloneqq \sigma - \sigma_\ell$ satisfy*

$$\begin{aligned}\int_\Omega \delta_\ell(x) : \mathrm{D}e_\ell(x)\mathrm{d}x + \|\delta_\ell\|^r_{L^{p'}(\Omega)} + \alpha\,\|e_\ell\|^2_{L^2(\Omega)} \\ \lesssim H_\ell^{(1+1/p)r'} \left\|\mathrm{D}^2_{\ell,\partial\Omega} u_D\right\|^{r'}_{L^p(\partial\Omega)} + \alpha H_\ell^5 \left\|\mathrm{D}^2_{\ell,\partial\Omega} u_D\right\|^2_{L^2(\partial\Omega)} \\ + \left(|e_\ell|_{W^{1,q}(\Omega)} + H_\ell^{1+1/q}\left\|\mathrm{D}^2_{\ell,\partial\Omega} u_D\right\|_{L^q(\partial\Omega)}\right) m_q(\tau)\end{aligned} \tag{4.29}$$

for any $\tau \in H(\mathrm{div},\Omega;\mathbb{R}^{n\times d})$, where

$$m_q(\tau) \coloneqq \|\sigma_\ell - \tau\|_{L^{q'}(\Omega)} + \|\Pi_\ell\Lambda_\ell + \mathrm{div}\,\tau\|_{L^{q'}(\Omega)} + \mathrm{osc}_{\ell,q'}(\Lambda_\ell). \tag{4.30}$$

The integral on the left-hand side of (4.29) *is nonnegative.*

If furthermore (4.8) *is satisfied then*

$$\begin{aligned}\|e_\ell\|^2_{L^2(\Omega)} \lesssim H_\ell^{(1+1/p)r'} \left\|\mathrm{D}^2_{\ell,\partial\Omega} u_D\right\|^{r'}_{L^p(\partial\Omega)} + H_\ell^3 \left\|\mathrm{D}^2_{\ell,\partial\Omega} u_D\right\|^2_{L^2(\partial\Omega)} \\ + \left(|e_\ell|_{W^{1,q}(\Omega)} + H_\ell^{1+1/q}\left\|\mathrm{D}^2_{\ell,\partial\Omega} u_D\right\|_{L^q(\partial\Omega)}\right) m_q(\tau).\end{aligned} \tag{4.31}$$

The generic constants do not depend on ℓ and u_ℓ.

We discuss a suggestion for the choice of the function τ. Recall the space of Raviart-Thomas functions (3.4) (page 37), which reads

$$RT_0(\mathcal{T}_\ell) = \Big\{ \tau \in P_1(\mathcal{T}_\ell;\mathbb{R}^d) \,:\, \tau(x) = a(x) + c(x)x \;\text{ with } a \in P_0(\mathcal{T};\mathbb{R}^d), c \in P_0(\mathcal{T};\mathbb{R}), \\ [\tau]_F \cdot n_F = 0 \;\text{ for all } F \in \mathcal{F}_\ell^\Omega \Big\} \subset H(\mathrm{div},\Omega).$$

To obtain an optimal upper bound of the error, Boiger and Carstensen (2012+, Section 4) propose the computation of an approximate minimiser $\tau_\ell \in RT_0(\mathcal{T}_\ell)^n$ of

$$\|\sigma_\ell - \tau_\ell\|_{L^{q'}(\Omega)} + \|\Pi_\ell \Lambda_\ell + \mathrm{div}\,\tau_\ell\|_{L^{q'}(\Omega)}\,. \tag{4.32}$$

With the minimiser τ_ℓ the *flux error estimator* reads

$$\eta_{\mathrm{F},q,\ell} \coloneqq m_q(\tau_\ell) \coloneqq \|\sigma_\ell - \tau_\ell\|_{L^{q'}(\Omega)} + \|\Pi_\ell \Lambda_\ell + \mathrm{div}\,\tau_\ell\|_{L^{q'}(\Omega)} + \mathrm{osc}_{\ell,q'}(\Lambda_\ell) \tag{4.33}$$

and satisfies (4.29) and (4.31) in Theorem (4.3.1) (with $m_q(\tau)$ replaced by $\eta_{\mathrm{F},q,\ell}$). Section 5.5 (page 101) presents an algorithm for the computation of an approximate minimiser τ_ℓ, along with a refinement indicator which is based on $\eta_{\mathrm{F},q,\ell}$.

Lemma (4.1.6) demonstrates the boundedness of the discrete solutions u_ℓ of (4.5) in $W^{1,p}(\Omega)$, and therefore also in $W^{1,q}(\Omega)$. Hence the sum in parentheses on the right-hand side of (4.29) is bounded. For $q = 2$ and under certain assumptions on the regularity of u, even better estimates of $|e_\ell|_{H^1(\Omega)}$ are possible, e.g., in Theorems (4.2.1) and (4.4.2). The failure to provide an improved estimate of $|e_\ell|_{W^{1,q}(\Omega)}$ for $q > 2$ accounts for the reliability-efficiency gap. See also Carstensen and Plecháč (1997, Remark 7.1) and the discussion below Theorem (3.3.2) (page 43) for an analogue observation in the context of residual-based error estimation. The following theorem proves that $\eta_{\mathrm{F},q,\ell}$ is also a lower bound for the error. Similar to Theorem (3.3.6) (page 45) the reliability-efficiency gap becomes apparent here in that the exponents of the error are *lower* than in Theorem (4.3.1).

(4.3.2) Theorem (Efficiency (Boiger and Carstensen, 2012+, Theorem 4.2))**.** *In the situation of Theorem (4.3.1) assume additionally that the continuous stress is $\sigma \in H(\mathrm{div},\Omega;\mathbb{R}^{n\times d}) \cap L^{2+}(\Omega;\mathbb{R}^{n\times d})$. Then the Fortin interpolant $\tau_\ell \coloneqq I_{\mathrm{F},\ell}\sigma \in RT_0(\mathcal{T}_\ell)^n$, as defined in* (3.5) *(page 38), satisfies*

$$\|\sigma_\ell - \tau_\ell\|_{L^{q'}(\Omega)} + \|\Pi_\ell \Lambda_\ell + \mathrm{div}\,\tau_\ell\|_{L^{q'}(\Omega)} \leqslant \|\delta_\ell\|_{L^{q'}(\Omega)} + 2\alpha\,\|e_\ell\|_{L^{q'}(\Omega)} + \|\sigma - \tau_\ell\|_{L^{q'}(\Omega)}\,.$$

In particular, if $\sigma \in H^1(\Omega;\mathbb{R}^{n\times d})$,

$$\|\sigma_\ell - \tau_\ell\|_{L^{q'}(\Omega)} + \|\Pi_\ell \Lambda_\ell + \mathrm{div}\,\tau_\ell\|_{L^{q'}(\Omega)} \lesssim \|\delta_\ell\|_{L^{q'}(\Omega)} + 2\alpha\,\|e_\ell\|_{L^{q'}(\Omega)} + H_\ell,$$

where the generic constant is independent of ℓ and u_ℓ.

4.3.2 Proof of Efficiency and Reliability

Proof of Theorem (4.3.1). Recall the extension operator B_ℓ of Definition (3.3.9) (page 46). Similar to (3.29) in the proof of Theorem (3.3.2) (on page 50), Lemma (3.3.10) (page 47) shows for $v \coloneqq (1 - B_\ell)e_\ell \in V$

$$|v|_{W^{1,q}(\Omega)} \lesssim |e_\ell|_{W^{1,q}(\Omega)} + H_\ell^{1+1/q} \left\| \mathrm{D}^2_{\ell,\partial\Omega} u_D \right\|_{L^q(\partial\Omega)}.$$

Note that Lemma (3.3.11) (page 47) does *not* require u_ℓ to be a solution of the (unstabilised) discrete problem. Therefore it applies to the present situation as well and it remains to prove

$$\mathrm{Res}_\ell(v) \lesssim m_q(\tau)\, |v|_{W^{1,q}(\Omega)}. \tag{4.34}$$

Since $v = 0$ on the boundary $\partial\Omega$, an integration by parts confirms

$$\int_\Omega \tau(x) : \mathrm{D}v(x)\mathrm{d}x = -\int_\Omega \operatorname{div} \tau(x) \cdot v(x)\mathrm{d}x.$$

Poincaré's inequality (Lemma (2.1.16), page 19), on each element $T \in \mathcal{T}_\ell$, yields

$$\left\| h_\ell^{-1}(1 - \Pi_\ell)v \right\|^q_{L^q(\Omega)} = \sum_{T\in\mathcal{T}_\ell} h_T^{-q} \|v - \Pi_\ell v\|^q_{L^q(T)} \lesssim \sum_{T\in\mathcal{T}_\ell} \|\mathrm{D}v\|^q_{L^q(T)} = |v|^q_{W^{1,q}(\Omega)}.$$

The operator Π_ℓ is an orthogonal projection, hence a Hölder inequality leads to

$$\begin{aligned}\int_\Omega (1 - \Pi_\ell)\Lambda_\ell(x) \cdot v(x)\mathrm{d}x &= \int_\Omega h_\ell(x)(1 - \Pi_\ell)\Lambda_\ell(x) \cdot h_\ell(x)^{-1}(1 - \Pi_\ell)v(x)\mathrm{d}x \\ &\lesssim \mathrm{osc}_{\ell,q'}(\Lambda_\ell)\, |v|_{W^{1,q}(\Omega)}.\end{aligned}$$

The injection of $\pm\tau : \mathrm{D}v$ and $\pm\Pi_\ell\Lambda_\ell$ into the definition of the residual (4.28), two Hölder inequalities and the preceding observations verify

$$\begin{aligned}\mathrm{Res}_\ell(v) &= -\int_\Omega (\sigma_\ell(x) - \tau_\ell(x)) : \mathrm{D}v(x)\mathrm{d}x \\ &\quad + \int_\Omega (\operatorname{div} \tau_\ell(x) + \Pi_\ell\Lambda_\ell(x)) \cdot v(x)\mathrm{d}x + \int_\Omega (1 - \Pi_\ell)\Lambda_\ell(x) \cdot v(x)\mathrm{d}x \\ &\lesssim \|\sigma_\ell - \tau_\ell\|_{L^{q'}(\Omega)}\, |v|_{W^{1,q}(\Omega)} \\ &\quad + \|\operatorname{div} \tau_\ell + \Pi_\ell\Lambda_\ell\|_{L^{q'}(\Omega)}\, \|v\|_{L^q(\Omega)} + \mathrm{osc}_{\ell,q'}(\Lambda_\ell)\, |v|_{W^{1,q}(\Omega)}.\end{aligned}$$

Friedrichs' inequality (Lemma (2.1.17), page 19) shows $\|v\|_{L^q(\Omega)} \lesssim |v|_{W^{1,q}(\Omega)}$ and concludes the proof of (4.34).

If (4.8) is satisfied, Lemma (3.3.3) (page 44) implies (4.31). □

Proof of Theorem (4.3.2). Since $\sigma \in H(\operatorname{div}, \Omega; \mathbb{R}^{n\times d})$, an integration by parts transforms the continuous Euler-Lagrange equation (4.3) into

$$\int_\Omega (\operatorname{div} \sigma(x) + \Lambda(x)) \cdot v(x)\mathrm{d}x = 0 \quad \text{for all } v \in V.$$

The fundamental lemma of the calculus of variations (Lemma (2.1.15), page 19) conjectures $\operatorname{div}\sigma + \Lambda = 0$ almost everywhere in Ω. The commutative property of $I_{\mathrm{F},\ell}$ and Π_ℓ (Lemma (3.1.10), page 38) and Lemma (3.1.7) (page 36) yield

$$\|\Pi_\ell \Lambda_\ell + \operatorname{div}\tau_\ell\|_{L^{q'}(\Omega)} = \|\Pi_\ell(\Lambda_\ell - \Lambda)\|_{L^{q'}(\Omega)} = 2\alpha \|\Pi_\ell e_\ell\|_{L^{q'}(\Omega)} \leqslant 2\alpha \|e_\ell\|_{L^{q'}(\Omega)}.$$

Finally, a triangle inequality shows

$$\|\sigma_\ell - \tau_\ell\|_{L^{q'}(\Omega)} \leqslant \|\sigma - \tau_\ell\|_{L^{q'}(\Omega)} + \|\delta_\ell\|_{L^{q'}(\Omega)}.$$

For $\sigma \in H^1(\Omega;\mathbb{R}^{n\times d})$ the Fortin interpolation error estimate of Lemma (3.1.9) (page 38) and $q' \leqslant 2$ conclude the proof. □

4.4 Improved Analysis for Interface Problems

The preceding sections deal with problems that are either assumed to be unrealistically smooth (such as $u \in H^{3/2+}(\Omega;\mathbb{R}^n)$ in Theorem (4.1.3)) or that do not carry any smoothness assumptions besides $W^{1,p}$ (e.g. in Theorem (4.2.3)). This section investigates problems with an exact solution u that is smooth up to a $(d-1)$-dimensional interface $\Gamma \subset \Omega$. The motivation for this scenario are interface model problems like the two-well and the three-well examples of Sections 2.3 and 2.4 (pages 25 and 27). The goal is to reduce the reliability-efficiency gap between Theorem (4.3.1) and Theorem (4.3.2). This section will be published in some preliminary version by Boiger and Carstensen (2012+, Section 5).

Let $u \in \mathcal{A}$ be a minimiser of the continuous problem (4.1). Given a finite union $\Gamma \subset \overline{\Omega}$ of $(d-1)$-dimensional Lipschitz surfaces in $\overline{\Omega}$, assume the solution u complies with

$$u \in W^{1,\infty}(\Omega;\mathbb{R}^n) \cap W^{2,p}(\Omega\backslash\Gamma;\mathbb{R}^n). \tag{4.35}$$

Recall from Lemma (2.1.7) (page 16) that $u \in W^{1,\infty}(\Omega;\mathbb{R}^n)$ is tantamount to Lipschitz continuity of u and therefore implies that the nodal interpolant $I_\ell u$ is well-defined. Chipot and Evans (1986) provide sufficient conditions for Lipschitz continuity of the solution u in the context of convex minimisation problems. This section permits $\Gamma = \varnothing$, hence the following results also hold if u is a highly regular minimiser, $u \in W^{2,p}(\Omega;\mathbb{R}^n)$.

4.4.1 Convergence Results

The following Theorem (4.4.1) provides a result similar to (4.20) in the proof of Theorem (4.1.3) in the sense that it derives an upper bound of the error $|u - u_\ell|_{H^1(\Omega)}$ which depends on the error $\|u - u_\ell\|_{L^2(\Omega)}$. Note that Theorem (4.4.1) is key for the narrowing of the reliability-efficiency gap: while the general case of Section 4.3 permits the pessimistic estimate $|u - u_\ell|_{H^1(\Omega)} \lesssim 1$ only, the following result provides an improved estimate, which leads to a sharper version of Theorem (4.3.1).

(4.4.1) Theorem. *Let $u \in \mathcal{A}$ be a solution of the continuous problem* (4.1) *which complies with* (4.35). *Let $(u_\ell)_{\ell\in\mathbb{N}_0}$ be a sequence of discrete functions $u_\ell \in \mathcal{A}_\ell$ with $\|u_\ell\|_{L^2(\Omega)} \lesssim 1$. Then the*

error $e_\ell \coloneqq u - u_\ell$ *satisfies*

$$|e_\ell|^2_{H^1(\Omega)} \lesssim H_\ell^{5/3} \left\|\mathrm{D}^2_{\ell,\partial\Omega} u_D\right\|^{2/3}_{L^2(\partial\Omega)} + \|e_\ell\|^{2/3}_{L^2(\Omega)} + H_\ell^{1-\gamma} \left|\!\left|\!\left| u_\ell \right|\!\right|\!\right|^2_\ell + H_\ell^{-(1+\gamma)/2} \left|\!\left|\!\left| u_\ell \right|\!\right|\!\right|_\ell \left(H_\ell^{5/2} \left\|\mathrm{D}^2_{\ell,\partial\Omega} u_D\right\|_{L^2(\partial\Omega)} + \|e_\ell\|_{L^2(\Omega)} \right).$$

The generic constants do not depend on ℓ *and* u_ℓ.

Recall that Lemma (4.1.6) implies the boundedness of $\|u_\ell\|_{L^2(\Omega)}$ for the solutions u_ℓ of the discrete problem (4.5). The following theorem derives improved a posteriori error estimators which are based on the estimate of Theorem (4.4.1).

(4.4.2) Theorem. *Let* $u \in \mathcal{A}$ *be a solution of the continuous problem* (4.1) *and* σ *its stress tensor. Let* $(u_\ell)_{\ell\in\mathbb{N}_0}$ *be a sequence of discrete functions* $u_\ell \in \mathcal{A}_\ell$ *with* $|u_\ell|_{W^{1,p}(\Omega)} \lesssim 1$ *and stress tensors* σ_ℓ. *Adopting the notation of* (4.30) *with* $q = q' = 2$, *we abbreviate for* $\tau \in H(\mathrm{div}, \Omega; \mathbb{R}^{n\times d})$

$$m_2(\tau) \coloneqq \|\sigma_\ell - \tau\|_{L^2(\Omega)} + \|\Pi_\ell \Lambda_\ell + \mathrm{div}\,\tau\|_{L^2(\Omega)} + \mathrm{osc}_{\ell,2}(\Lambda_\ell), \quad \textit{and}$$
$$M(\tau) \coloneqq m_2(\tau) \left(H_\ell^{(1-\gamma)/2} \left|\!\left|\!\left| u_\ell \right|\!\right|\!\right|_\ell + H_\ell^{1-\gamma/4} \left|\!\left|\!\left| u_\ell \right|\!\right|\!\right|^{1/2}_\ell \right).$$

Provided that the solution u *complies with* (4.35) *and* $\alpha > 0$, *the errors* $e_\ell \coloneqq u - u_\ell$ *and* $\delta_\ell \coloneqq \sigma - \sigma_\ell$ *satisfy for any* $\tau \in H(\mathrm{div}, \Omega; \mathbb{R}^{n\times d})$

$$\|\delta_\ell\|^r_{L^{p'}(\Omega)} + \|e_\ell\|^2_{L^2(\Omega)} \lesssim H_\ell^{\min\{5,(1+1/p)r'\}} + m_2(\tau)^{6/5} + H_\ell^{-(1+\gamma)/3} m_2(\tau)^{4/3} \left|\!\left|\!\left| u_\ell \right|\!\right|\!\right|^{2/3}_\ell + M(\tau) \quad (4.36)$$

and

$$\begin{aligned} &|e_\ell|^2_{H^1(\Omega)} \lesssim \\ &\quad H_\ell^{\min\{5,(1+1/p)r'\}/3} + m_2(\tau)^{2/5} + H_\ell^{-(1+\gamma)/9} m_2(\tau)^{4/9} \left|\!\left|\!\left| u_\ell \right|\!\right|\!\right|^{2/9}_\ell \\ &+ M(\tau)^{1/3} + H_\ell^{1-\gamma} \left|\!\left|\!\left| u_\ell \right|\!\right|\!\right|^2_\ell + H_\ell^{-(1+\gamma)/2} \left|\!\left|\!\left| u_\ell \right|\!\right|\!\right|_\ell M(\tau)^{1/2} \\ &+ H_\ell^{-(1+\gamma)/2} \left|\!\left|\!\left| u_\ell \right|\!\right|\!\right|_\ell \left(H_\ell^{\min\{5,(1+1/p)r'\}} + m_2(\tau)^{6/5} + H_\ell^{-(1+\gamma)/3} m_2(\tau)^{4/3} \left|\!\left|\!\left| u_\ell \right|\!\right|\!\right|^{2/3}_\ell \right)^{1/2}, \end{aligned} \quad (4.37)$$

where r' *is the Hölder conjugate of* r, *i.e.*, $1/r + 1/r' = 1$. *The generic constants do not depend on* ℓ *and* u_ℓ.

Given an approximate minimiser $\tau_\ell \in RT_0(\mathcal{T}_\ell)^n$ of (4.32) with $q = 2$, i.e., of

$$\|\sigma_\ell - \tau_\ell\|_{L^2(\Omega)} + \|\Pi_\ell \Lambda_\ell + \mathrm{div}\,\tau_\ell\|_{L^2(\Omega)},$$

the flux error estimator of (4.33) reads

$$\eta_{\mathrm{F},2,\ell} = \|\sigma_\ell - \tau_\ell\|_{L^2(\Omega)} + \|\Pi_\ell \Lambda_\ell + \mathrm{div}\,\tau_\ell\|_{L^2(\Omega)} + \mathrm{osc}_{\ell,2}(\Lambda_\ell).$$

Theorem (4.4.2) with $\tau = \tau_\ell$ gives rise to the improved a posteriori error estimators

$$\begin{aligned}\eta_{\mathrm{L},\ell} \coloneqq\ & H_\ell^{\min\{5,(1+1/p)r'\}} + \eta_{\mathrm{F},2,\ell}^{6/5} + H_\ell^{-(1+\gamma)/3}\eta_{\mathrm{F},2,\ell}^{4/3}\left|\!\left|\!\left|u_\ell\right|\!\right|\!\right|_\ell^{2/3} \\ & + \eta_{\mathrm{F},2,\ell}\left(H_\ell^{(1-\gamma)/2}\left|\!\left|\!\left|u_\ell\right|\!\right|\!\right|_\ell + H_\ell^{1-\gamma/4}\left|\!\left|\!\left|u_\ell\right|\!\right|\!\right|_\ell^{1/2}\right)\end{aligned} \tag{4.38}$$

and

$$\begin{aligned}\eta_{\mathrm{H},\ell} \coloneqq\ & H_\ell^{\min\{5,(1+1/p)r'\}/3} + \eta_{\mathrm{F},2,\ell}^{2/5} + H_\ell^{-(1+\gamma)/9}\eta_{\mathrm{F},2,\ell}^{4/9}\left|\!\left|\!\left|u_\ell\right|\!\right|\!\right|_\ell^{2/9} \\ & + \eta_{\mathrm{F},2,\ell}^{1/3}\left(H_\ell^{(1-\gamma)/2}\left|\!\left|\!\left|u_\ell\right|\!\right|\!\right|_\ell + H_\ell^{1-\gamma/4}\left|\!\left|\!\left|u_\ell\right|\!\right|\!\right|_\ell^{1/2}\right)^{1/3} + H_\ell^{1-\gamma}\left|\!\left|\!\left|u_\ell\right|\!\right|\!\right|_\ell^2 \\ & + H_\ell^{-(1+\gamma)/2}\left|\!\left|\!\left|u_\ell\right|\!\right|\!\right|_\ell \eta_{\mathrm{F},2,\ell}^{1/2}\left(H_\ell^{(1-\gamma)/2}\left|\!\left|\!\left|u_\ell\right|\!\right|\!\right|_\ell + H_\ell^{1-\gamma/4}\left|\!\left|\!\left|u_\ell\right|\!\right|\!\right|_\ell^{1/2}\right)^{1/2} \\ & + H_\ell^{-(1+\gamma)/2}\left|\!\left|\!\left|u_\ell\right|\!\right|\!\right|_\ell \left(H_\ell^{\min\{5,(1+1/p)r'\}} + \eta_{\mathrm{F},2,\ell}^{6/5} + H_\ell^{-(1+\gamma)/3}\eta_{\mathrm{F},2,\ell}^{4/3}\left|\!\left|\!\left|u_\ell\right|\!\right|\!\right|_\ell^{2/3}\right)^{1/2}.\end{aligned} \tag{4.39}$$

Theorem (4.4.2) implies

$$\left\|\delta_\ell\right\|_{L^{p'}(\Omega)}^r + \left\|e_\ell\right\|_{L^2(\Omega)}^2 \lesssim \eta_{\mathrm{L},\ell} \quad \text{and} \quad \left|e_\ell\right|_{H^1(\Omega)}^2 \lesssim \eta_{\mathrm{H},\ell}.$$

(4.4.3) Remark. *Similar to the distinction of cases in* (4.10) *it is possible to derive modified error estimates if $u_D \equiv 0$ and even for $\alpha = 0$ if* (4.8) *is satisfied. This leads to additional powers of H_ℓ in the expressions of $\eta_{\mathrm{L},\ell}$ and $\eta_{\mathrm{H},\ell}$. However, we may expect these terms to be of higher order, at least in the numerical examples of Chapter 5. Furthermore, such modifications increase the complexity of the error estimators beyond proportionality. Therefore the thesis does not pursue this approach.*

Before this section concludes with the proofs of the preceding theorems it states the following a priori estimate, which is similar to Theorem (4.1.2), but applies to interface problems.

(4.4.4) Theorem. *Let $u \in \mathcal{A}$ be a solution of the continuous problem* (4.1) *and σ its stress tensor. Let $u_\ell \in \mathcal{A}_\ell$ be a solution of the discrete problem* (4.5) *and σ_ℓ its stress tensor. Abbreviate the sets*

$$\begin{aligned}\mathcal{T}_\ell(\Gamma) &\coloneqq \left\{T \in \mathcal{T}_\ell \,:\, T \cap \Gamma \neq \varnothing\right\}, \\ \Omega_{\Gamma,\ell} \coloneqq \operatorname{int}\left(\bigcup \mathcal{T}_\ell(\Gamma)\right) \ &\text{and}\ \ \Omega_{\Gamma,\ell}^{\mathrm{C}} \coloneqq \Omega\backslash\Omega_{\Gamma,\ell}.\end{aligned}$$

If the solution u complies with (4.35) *the errors $e_\ell \coloneqq u - u_\ell$ and $\delta_\ell \coloneqq \sigma - \sigma_\ell$ satisfy*

$$\begin{aligned}\int_\Omega \delta_\ell(x) : \mathrm{D}e_\ell(x)\mathrm{d}x + \left\|\delta_\ell\right\|_{L^{p'}(\Omega)}^r + \alpha\left\|e_\ell\right\|_{L^2(\Omega)}^2 + \left|\!\left|\!\left|u_\ell\right|\!\right|\!\right|_\ell^2 & \\ \lesssim H_\ell^{\min\{r',1+\gamma\}} + \alpha H_\ell^2 + \left|\Omega_{\Gamma,\ell}\right|^{r'/p} + H_\ell^{d+\gamma-1}\#\mathcal{T}_\ell(\Gamma),&\end{aligned} \tag{4.40}$$

where r' is the Hölder conjugate of r, i.e., $1/r + 1/r' = 1$.

If furthermore (4.8) *is satisfied then*

$$\left\|e_\ell\right\|_{L^2(\Omega)}^2 \lesssim H_\ell^{\min\{r',1+\gamma\}} + \alpha H_\ell^2 + H_\ell^3\left\|\mathrm{D}_{\ell,\partial\Omega}^2 u_D\right\|_{L^2(\partial\Omega)}^2 + \left|\Omega_{\Gamma,\ell}\right|^{r'/p} + H_\ell^{d+\gamma-1}\#\mathcal{T}_\ell(\Gamma).$$

The generic constants do not depend on ℓ and u_ℓ.

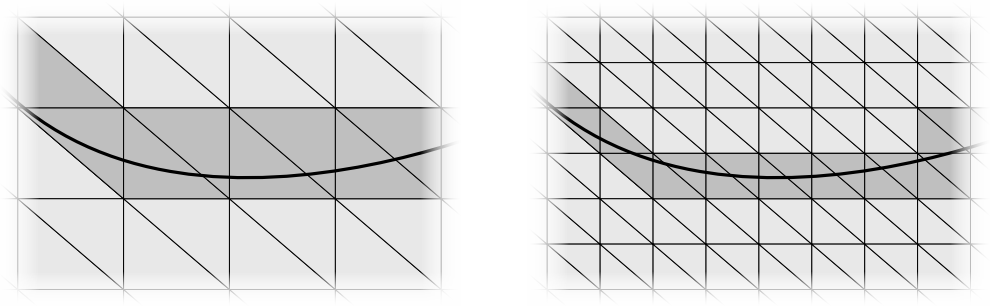

Figure 4.1: Illustration of $\Omega_{\Gamma,\ell}$ of Theorem (4.4.4) for uniform triangulations, before (left) and after (right) a "red" refinement (cf. Section 5.3, page 97)

The a priori error estimate of (4.40) depends heavily on the triangulations and the localisation of the interface Γ, which obviates the derivation of more explicit error bounds in the case of adaptive mesh refinements. However, an investigation of the simple case of uniform meshes leads to some heuristics for the quantities $|\Omega_{\Gamma,\ell}|$ and $\#\mathcal{T}_\ell(\Gamma)$. On a sufficiently fine uniform triangulation the $(d-1)$-dimensional area of Γ that is covered by an element $T \in \mathcal{T}_\ell(\Gamma)$ can be expected to be proportional to H_ℓ^{d-1}, i.e., $|T \cap \Gamma| \approx H_\ell^{d-1}$. This observation indicates $\#\mathcal{T}_\ell(\Gamma) \approx |\Gamma| / H_\ell^{d-1}$. Figure 4.1 depicts an interface line Γ and the set $\Omega_{\Gamma,\ell}$ for two consecutive levels of a family of uniform triangulations. The uniformity also implies $|T| \approx H_\ell^d$ for all elements $T \in \mathcal{T}_\ell$, hence $|\Omega_{\Gamma,\ell}| \approx H_\ell^d / H_\ell^{d-1} = H_\ell$. With this heuristics (4.40) simplifies to

$$\int_\Omega \delta_\ell(x) : \mathrm{D}e_\ell(x)\mathrm{d}x + \|\delta_\ell\|_{L^{p'}(\Omega)}^r + \alpha \|e_\ell\|_{L^2(\Omega)}^2 + |||u_\ell|||_\ell^2 \lesssim H_\ell^{\min\{r'/p,\gamma\}} + \alpha H_\ell^2. \tag{4.41}$$

The estimate (4.41) suggests that $\gamma > 0$ is a precondition for convergence. Yet, (4.41) is purely heuristic, and an adaptive algorithm which concentrates its mesh refinements near the interface might display a different convergence behaviour.

4.4.2 Proofs

Proof of Theorem (4.4.1). With the extension operator B_ℓ from Definition (3.3.9) (page 46) let $w_\ell \coloneqq B_\ell e_\ell$ and $v \coloneqq e_\ell - w_\ell \in V$. We intend to apply integration by parts to

$$\int_\Omega \mathrm{D}e_\ell(x) : \mathrm{D}v(x)\mathrm{d}x. \tag{4.42}$$

Since $v(x) = 0$ on the boundary $\partial\Omega$ the only boundary terms that appear stem from discontinuities in the interior of Ω. Such boundary terms are twofold: on the one hand $\mathrm{D}u_\ell$ is possibly discontinuous along interior sides $F \in \mathcal{F}_\ell^\Omega$. Note that the elementwise second derivative of u_ℓ vanishes. Analogous to (3.36) (in the proof of Theorem (3.3.2), on

page 52) and (4.15) these discontinuities yield jumps along the edges, i.e.,

$$\int_\Omega \mathrm{D}u_\ell(x) : \mathrm{D}v(x)\mathrm{d}x = \sum_{T\in\mathcal{T}_\ell} \int_{\partial T} \mathrm{D}u_\ell(x) n_{\partial T}(x) \cdot v(x)\mathrm{d}s = \sum_{F\in\mathcal{F}_\ell^\Omega} \int_F [\mathrm{D}u_\ell]_F \, n_F \cdot v(x)\mathrm{d}s. \tag{4.43}$$

On the other hand $\mathrm{D}u$ is possibly discontinuous along the interface Γ. Up to a set of zero measure, Γ is a $(d-1)$-dimensional Lipschitz surface which divides a local neighbourhood of a point $x \in \Gamma$ into two sets $\omega_\pm$. See Figure 2.1 (page 18) for a two-dimensional illustration of the sets $\omega_\pm$. The outer-pointing unit normal vectors of $\omega_\pm$ in x are anti-diagonal. The same arguments that led to (4.43) also support

$$\int_\Omega \mathrm{D}u(x) : \mathrm{D}v(x)\mathrm{d}x = \int_\Gamma [\mathrm{D}u]_\Gamma \, n_\Gamma(x) \cdot v(x)\mathrm{d}s - \int_{\Omega\setminus\Gamma} \Delta u(x) \cdot v(x)\mathrm{d}x.$$

Altogether an integration by parts of (4.42) yields

$$\begin{aligned}\int_\Omega \mathrm{D}(u-u_\ell)(x) : \mathrm{D}v(x)\mathrm{d}x = \int_\Gamma [\mathrm{D}u]_\Gamma \; n_\Gamma(x) \cdot v(x)\mathrm{d}s \\ - \sum_{F\in\mathcal{F}_\ell^\Omega} \int_F [\mathrm{D}u_\ell]_F \; n_F \cdot v(x)\mathrm{d}s - \int_{\Omega\setminus\Gamma} \Delta u(x) \cdot v(x)\mathrm{d}x.\end{aligned}$$

A Hölder inequality estimates the first integral on the right-hand side. Recall that u is assumed to be Lipschitz continuous. Lemma (2.1.4) (page 16) and the trace theorem on $\Omega \setminus \Gamma$ (Lemma (2.1.20), page 20) then lead to

$$\begin{aligned}\int_\Gamma [\mathrm{D}u]_\Gamma \; n_\Gamma(x) \cdot v(x)\mathrm{d}s &\leqslant \|[\mathrm{D}u]_\Gamma\|_{L^\infty(\Gamma)} \, \|v\|_{L^1(\Gamma)} \\ &\lesssim |u|_{W^{1,\infty}(\Omega)} \, \|v\|_{L^2(\Gamma)} \\ &\lesssim \|v\|_{L^2(\Omega)} + \|v\|_{L^2(\Omega)}^{1/2} \, |v|_{H^1(\Omega)}^{1/2}.\end{aligned}$$

Lemma (4.2.5) with u_ℓ in place of w shows

$$\sum_{F\in\mathcal{F}_\ell^\Omega} \int_F [\mathrm{D}u_\ell]_F \, n_F \cdot v(x)\mathrm{d}s \lesssim |||u_\ell|||_\ell \left(H_\ell^{-(1+\gamma)/2} \, \|v\|_{L^2(\Omega)} + H_\ell^{(1-\gamma)/2} \, |v|_{H^1(\Omega)} \right).$$

Since the Laplacian of u is independent of ℓ, a Cauchy inequality proves

$$\int_{\Omega\setminus\Gamma} \Delta u(x) \cdot v(x)\mathrm{d}x \leqslant \|\Delta u\|_{L^2(\Omega\setminus\Gamma)} \, \|v\|_{L^2(\Omega\setminus\Gamma)} \lesssim \|v\|_{L^2(\Omega)}.$$

The combination of the preceding inequalities demonstrates

$$\begin{aligned}|e_\ell|_{H^1(\Omega)}^2 &= \int_\Omega \mathrm{D}e_\ell(x) : \mathrm{D}w_\ell(x)\mathrm{d}x + \int_\Omega \mathrm{D}(u-u_\ell)(x) : \mathrm{D}v(x)\mathrm{d}x \\ &\lesssim |e_\ell|_{H^1(\Omega)} \, |w_\ell|_{H^1(\Omega)} + \|v\|_{L^2(\Omega)} + \|v\|_{L^2(\Omega)}^{1/2} \, |v|_{H^1(\Omega)}^{1/2}\end{aligned}$$

$$+ \left|\!\left|\!\left| u_\ell \right|\!\right|\!\right|_\ell \left(H_\ell^{-(1+\gamma)/2} \left\| v \right\|_{L^2(\Omega)} + H_\ell^{(1-\gamma)/2} \left| v \right|_{H^1(\Omega)} \right).$$

The absorption of $|e_\ell|_{H^1(\Omega)}$ (cf. Lemma (2.1.23), page 20) and a triangle inequality for $v = e_\ell - w_\ell$ yield

$$\begin{aligned} |v|_{H^1(\Omega)}^2 &\lesssim |w_\ell|_{H^1(\Omega)}^2 + |e_\ell|_{H^1(\Omega)}^2 \\ &\lesssim |w_\ell|_{H^1(\Omega)}^2 + \|v\|_{L^2(\Omega)} + \|v\|_{L^2(\Omega)}^{1/2} |v|_{H^1(\Omega)}^{1/2} \\ &\quad + \left|\!\left|\!\left| u_\ell \right|\!\right|\!\right|_\ell \left(H_\ell^{-(1+\gamma)/2} \left\| v \right\|_{L^2(\Omega)} + H_\ell^{(1-\gamma)/2} \left| v \right|_{H^1(\Omega)} \right). \end{aligned}$$

We further absorb $|v|_{H^1(\Omega)}$ and $|v|_{H^1(\Omega)}^{1/2}$. The latter one leaves behind the summand $\|v\|_{L^2(\Omega)}^{2/3}$ on the right-hand side. Lemma (3.3.10) (page 47) shows for $w_\ell = B_\ell e_\ell = B_\ell(1 - I_\ell)u_D$

$$\|w_\ell\|_{L^2(\Omega)}^2 \lesssim H_\ell^5 \left\| \mathrm{D}_{\ell,\partial\Omega}^2 u_D \right\|_{L^2(\partial\Omega)}^2 \quad \text{and} \quad |w_\ell|_{H^1(\Omega)}^2 \lesssim H_\ell^3 \left\| \mathrm{D}_{\ell,\partial\Omega}^2 u_D \right\|_{L^2(\partial\Omega)}^2. \tag{4.44}$$

The boundedness of $\|u_\ell\|_{L^2(\Omega)}$ and (4.44) imply $\|v\|_{L^2(\Omega)} \lesssim \|v\|_{L^2(\Omega)}^{2/3} \lesssim 1$. Thus

$$|v|_{H^1(\Omega)}^2 \lesssim |w_\ell|_{H^1(\Omega)}^2 + \|v\|_{L^2(\Omega)}^{2/3} + H_\ell^{1-\gamma} \left|\!\left|\!\left| u_\ell \right|\!\right|\!\right|_\ell^2 + H_\ell^{-(1+\gamma)/2} \left|\!\left|\!\left| u_\ell \right|\!\right|\!\right|_\ell \|v\|_{L^2(\Omega)}.$$

The substitution of $v = e_\ell - w_\ell$ and another triangle inequality prove

$$\begin{aligned} |e_\ell|_{H^1(\Omega)}^2 &\lesssim |w_\ell|_{H^1(\Omega)}^2 + |v|_{H^1(\Omega)}^2 \\ &\lesssim |w_\ell|_{H^1(\Omega)}^2 + \|w_\ell\|_{L^2(\Omega)}^{2/3} + \|e_\ell\|_{L^2(\Omega)}^{2/3} + \left|\!\left|\!\left| u_\ell \right|\!\right|\!\right|_\ell^2 H_\ell^{1-\gamma} \\ &\quad + H_\ell^{-(1+\gamma)/2} \left|\!\left|\!\left| u_\ell \right|\!\right|\!\right|_\ell \left(\|w_\ell\|_{L^2(\Omega)} + \|e_\ell\|_{L^2(\Omega)} \right). \end{aligned}$$

This estimate, (4.44) and the removal of higher-order terms of H_ℓ lead to the claim. □

Proof of Theorem (4.4.2). Theorem (4.3.1) with $q = 2$ states

$$\|\delta_\ell\|_{L^{p'}(\Omega)}^r + \|e_\ell\|_{L^2(\Omega)}^2 \lesssim H_\ell^{\min\{5,(1+1/p)r'\}} + m_2(\tau) \left(|e_\ell|_{H^1(\Omega)} + H_\ell^{3/2} \right).$$

Note that $\|u_\ell\|_{L^2(\Omega)} \lesssim 1$ because of (3.15) (page 41) and Lemma (2.1.4) (page 16). Substitute $|e_\ell|_{H^1(\Omega)}$ from Theorem (4.4.1) to obtain

$$\begin{aligned} &\|\delta_\ell\|_{L^{p'}(\Omega)}^r + \|e_\ell\|_{L^2(\Omega)}^2 \lesssim H_\ell^{\min\{5,(1+1/p)r'\}} \\ &+ m_2(\tau) \left(H_\ell^{5/6} + \|e_\ell\|_{L^2(\Omega)}^{1/3} + H_\ell^{(1-\gamma)/2} \left|\!\left|\!\left| u_\ell \right|\!\right|\!\right|_\ell + H_\ell^{-(1+\gamma)/4} \left|\!\left|\!\left| u_\ell \right|\!\right|\!\right|_\ell^{1/2} \left(H_\ell^{5/4} + \|e_\ell\|_{L^2(\Omega)}^{1/2} \right) \right). \end{aligned}$$

A Young inequality (Lemma (2.1.22), page 20) shows $H_\ell^{5/6} m_2(\tau) \lesssim H_\ell^5 + m_2(\tau)^{6/5}$. Then the absorption of $\|e_\ell\|_{L^2(\Omega)}$ (cf. Lemma (2.1.23), page 20) directly leads to (4.36). The

substitution of $\|e_\ell\|_{L^2(\Omega)}$ from (4.36) into Theorem (4.4.1) expands to

$$\begin{aligned}|e_\ell|^2_{H^1(\Omega)} \lesssim\ & H_\ell^{5/3} + H_\ell^{\min\{5,(1+1/p)r'\}/3} + m_2(\tau)^{2/5} + H_\ell^{-(1+\gamma)/9} m_2(\tau)^{4/9} \|\!|u_\ell|\!\|_\ell^{2/9} \\ & + M(\tau)^{1/3} + H_\ell^{1-\gamma} \|\!|u_\ell|\!\|_\ell^2 + H_\ell^{2-\gamma/2} \|\!|u_\ell|\!\|_\ell \\ & + H_\ell^{-(1+\gamma)/2} \|\!|u_\ell|\!\|_\ell \left(H_\ell^{\min\{5,(1+1/p)r'\}/2} + m_2(\tau)^{3/5} \right) \\ & + H_\ell^{-(1+\gamma)/2} \|\!|u_\ell|\!\|_\ell \left(H_\ell^{-(1+\gamma)/6} m_2(\tau)^{2/3} \|\!|u_\ell|\!\|_\ell^{1/3} + M(\tau)^{1/2} \right).\end{aligned}$$

Another Young inequality shows

$$H_\ell^{2-\gamma/2} \|\!|u_\ell|\!\|_\ell = H_\ell^{3/2} H_\ell^{(1-\gamma)/2} \|\!|u_\ell|\!\|_\ell \lesssim H_\ell^3 + H_\ell^{1-\gamma} \|\!|u_\ell|\!\|_\ell^2,$$

which finally proves (4.37). □

Proof of Theorem (4.4.4). Let $v_\ell := I_\ell e_\ell = I_\ell u - u_\ell$. A Cauchy inequality for the stabilisation a_ℓ yields

$$a_\ell(u_\ell, v_\ell) = a_\ell(u_\ell, I_\ell u) - \|\!|u_\ell|\!\|_\ell^2 \leqslant \|\!|u_\ell|\!\|_\ell \|\!|I_\ell u|\!\|_\ell - \|\!|u_\ell|\!\|_\ell^2 \leqslant \frac{1}{2} \|\!|I_\ell u|\!\|_\ell^2 - \frac{1}{2} \|\!|u_\ell|\!\|_\ell^2.$$

With this estimate for $a_\ell(u_\ell, v_\ell)$ and $w_\ell := e_\ell - v_\ell = (1 - I_\ell)u$, Lemma (4.1.7) states

$$\begin{aligned}\int_\Omega \delta_\ell(x) : \mathrm{D}e_\ell(x)\mathrm{d}x + \|\delta_\ell\|^r_{L^{p'}(\Omega)} + \alpha \|e_\ell\|^2_{L^2(\Omega)} & \\ \lesssim |w_\ell|^{r'}_{W^{1,p}(\Omega)} + \alpha \|w_\ell\|^2_{L^2(\Omega)} + \|\!|I_\ell u|\!\|_\ell^2 - \|\!|u_\ell|\!\|_\ell^2.&\end{aligned}$$

This proves an upper bound on the left-hand side of (4.40) which reads

$$\begin{aligned}\int_\Omega \delta_\ell(x) : \mathrm{D}e_\ell(x)\mathrm{d}x + \|\delta_\ell\|^r_{L^{p'}(\Omega)} + \alpha \|e_\ell\|^2_{L^2(\Omega)} + \|\!|u_\ell|\!\|_\ell^2 & \\ \lesssim |w_\ell|^{r'}_{W^{1,p}(\Omega)} + \alpha \|w_\ell\|^2_{L^2(\Omega)} + \|\!|I_\ell u|\!\|_\ell^2.&\end{aligned} \tag{4.45}$$

The following proves (4.40) by providing estimates for each of the summands on the left-hand side of (4.45).

Note that w_ℓ is Lipschitz continuous by Lemma (3.1.4) (page 35) and $w_\ell(z) = 0$ on each node $z \in \mathcal{N}_\ell$. The very definition of Lipschitz continuity shows for each $T \in \mathcal{T}_\ell$

$$w_\ell(x) \leqslant |w_\ell|_{W^{1,\infty}(T)} \operatorname{diam}(T) \leqslant H_\ell |w_\ell|_{W^{1,\infty}(\Omega)} \quad \text{for all } x \in T.$$

Lemmas (3.1.4) and (2.1.4) (pages 35 and 16) and a triangle inequality lead to

$$\|w_\ell\|_{L^2(\Omega)} \lesssim \|w_\ell\|_{L^\infty(\Omega)} \leqslant H_\ell |w_\ell|_{W^{1,\infty}(\Omega)} \lesssim H_\ell |u|_{W^{1,\infty}(\Omega)}.$$

The same arguments plus Lemma (3.1.6) (page 35) on $\Omega^{\mathrm{C}}_{\Gamma,\ell}$ yield

$$|w_\ell|^p_{W^{1,p}(\Omega)} = |w_\ell|^p_{W^{1,p}(\Omega_{\Gamma,\ell})} + |w_\ell|^p_{W^{1,p}(\Omega^{\mathrm{C}}_{\Gamma,\ell})}$$

$$\begin{aligned}
&\lesssim |\Omega_{\Gamma,\ell}|\, |w_\ell|^p_{W^{1,\infty}(\Omega_{\Gamma,\ell})} + H_\ell^p\, |u|^p_{W^{2,p}(\Omega^{\mathrm{C}}_{\Gamma,\ell})} \\
&\lesssim |\Omega_{\Gamma,\ell}|\, |u|^p_{W^{1,\infty}(\Omega)} + H_\ell^p\, |u|^p_{W^{2,p}(\Omega\setminus\Gamma)}\,.
\end{aligned}$$

Denote the set of all interior sides $F \in \mathcal{F}_\ell^\Omega$ whose patches ω_F do and do not touch the interface Γ with

$$\mathcal{F}_\ell(\Gamma) \coloneqq \left\{ F \in \mathcal{F}_\ell^\Omega \,:\, \omega_F \cap \Gamma \neq \varnothing \right\} \quad \text{and} \quad \mathcal{F}_\ell^{\mathrm{C}}(\Gamma) \coloneqq \mathcal{F}_\ell^\Omega \backslash \mathcal{F}_\ell(\Gamma) \quad \text{respectively.}$$

Let $F \in \mathcal{F}_\ell^{\mathrm{C}}(\Gamma)$, then $u \in H^2(\omega_F)$. This implies $[\mathrm{D}u]_F = [\mathrm{D}w_\ell]_F$ and ensures that w_ℓ complies with (4.11) from the proof of Lemma (4.1.5). Conversely, let $F \in \mathcal{F}_\ell(\Gamma)$. Shape regularity of the triangulations shows $|F| \approx h_F^{d-1}$, hence Lemma (2.1.4) (page 16) on F yields

$$\|[\mathrm{D}I_\ell u]_F\|^2_{L^2(F)} \leqslant |F|\, \|[\mathrm{D}I_\ell u]_F\|^2_{L^\infty(F)} \lesssim h_F^{d-1}\, |I_\ell u|^2_{W^{1,\infty}(\omega_F)} \leqslant h_F^{d-1}\, |u|^2_{W^{1,\infty}(\omega_F)}\,.$$

Recall that $\mathrm{D}^2_\ell I_\ell u \equiv 0$. Since each element's boundary is covered by exactly $d+1$ sides it holds $\#\mathcal{F}_\ell(\Gamma) \leqslant (d+1)\#\mathcal{T}_\ell(\Gamma)$. This leads to

$$\begin{aligned}
|||I_\ell u|||^2_\ell &= H_\ell^{1+\gamma} \left(\sum_{F\in\mathcal{F}_\ell^{\mathrm{C}}(\Gamma)} h_F^{-1}\, \|[\mathrm{D}w_\ell]_F\|^2_{L^2(F)} + \sum_{F\in\mathcal{F}_\ell(\Gamma)} h_F^{-1}\, \|[\mathrm{D}I_\ell u]_F\|^2_{L^2(F)} \right) \\
&\lesssim H_\ell^{1+\gamma} \left(\sum_{F\in\mathcal{F}_\ell^{\mathrm{C}}(\Gamma)} \left\|\mathrm{D}^2_\ell w_\ell\right\|^2_{L^2(\omega_F)} + \sum_{F\in\mathcal{F}_\ell(\Gamma)} h_F^{d-2}\, |u|^2_{W^{1,\infty}(\omega_F)} \right) \\
&\lesssim H_\ell^{1+\gamma}\, |u|^2_{H^2(\Omega\setminus\Gamma)} + H_\ell^{d+\gamma-1}\, |u|^2_{W^{1,\infty}(\Omega)}\, \#\mathcal{T}_\ell(\Gamma).
\end{aligned}$$

The preceding inequalities prove (4.40). The second assertion is a consequence of Lemma (3.3.3) (page 44). □

5 Numerical Simulations

This chapter presents and discusses numerical methods for the solution of the discrete minimisation problems and the impact of the stabilisation term.

While the analysis of Chapter 4 concerns the general case $u : \Omega \subset \mathbb{R}^d \to \mathbb{R}^n$, the algorithms and benchmark examples of this chapter are restricted to the two-dimensional scalar-valued case, that is, $d = 2$ and $n = 1$. Recall the convex model problem (2.2) from Section 2.2 (page 21). Given a bounded Lipschitz domain $\Omega \subset \mathbb{R}^2$ with polygonal boundary the continuous problem reads

$$\begin{aligned} \text{minimise } E^{\star\star}(v) = \int_\Omega \Big(W^{\star\star}(\mathrm{D}v(x)) + \alpha \left| v(x) - f(x) \right|^2 - g(x)v(x) \Big) \,\mathrm{d}x \\ \text{amongst } v \in \mathcal{A}, \end{aligned} \tag{5.1}$$

where $W^{\star\star} \in \mathcal{C}^1(\mathbb{R}^2)$, $f \in L^2(\Omega)$, $g \in L^{p'}(\Omega)$ and $\alpha \geqslant 0$, and p' is the Hölder conjugate of some $p \geqslant 2$, i.e., $1/p + 1/p' = 1$.

Given a family of shape-regular triangulations $(\mathcal{T}_\ell)_{\ell \in \mathbb{N}_0}$ of the domain Ω, the set of admissible functions reads $\mathcal{A} = u_D + V$, where (cf. (3.13), page 40)

$$u_D \in W^{1,p}(\Omega) \cap W^{2,p}(\mathcal{T}_0) \cap W^{2,p}(\mathcal{F}_0^{\partial\Omega}). \tag{5.2}$$

Recall the stabilisation (3.53) (page 61) and its associated norm, which read

$$\begin{aligned} a_\ell(v, w) &\coloneqq H_\ell^{1+\gamma} \sum_{F \in \mathcal{F}_\ell^\Omega} h_F^{-1} \int_F [\mathrm{D}v]_F \cdot [\mathrm{D}w]_F \,\mathrm{d}s \\ \text{and} \quad |||v|||_\ell^2 &\coloneqq a_\ell(v, v) \quad \text{for } v, w \in H^{3/2+}(\mathcal{T}_\ell). \end{aligned} \tag{5.3}$$

With a_ℓ and the set of discrete admissible functions $\mathcal{A}_\ell \coloneqq u_{D,\ell} + V_\ell$ on $\mathcal{T}_\ell$, the stabilised discrete problem reads

$$\text{minimise } E_\ell^{\star\star}(v_\ell) \coloneqq E^{\star\star}(v_\ell) + \frac{1}{2} C \, |||v_\ell|||_\ell^2 \quad \text{amongst } v_\ell \in \mathcal{A}_\ell. \tag{5.4}$$

The coefficient C is introduced in (5.4) to study the effects of strong ($C \gg 1$) and weak ($C \ll 1$) stabilisation in Section 5.4. Apart from that section $C = 1 = \gamma$ is used for all numerical experiments with the stabilised discrete problem. Naturally, the unstabilised discrete problem (3.10) (page 40) is equivalent to (5.4) with $C = 0$. Recall the abbreviations of (3.11) (page 40), which, for a given discrete solution $u_\ell \in \mathcal{A}_\ell$, read

$$\sigma_\ell(x) \coloneqq S(\mathrm{D}u_\ell(x)) \quad \text{and} \quad \Lambda_\ell(x) \coloneqq -2\alpha(u_\ell(x) - f(x)) + g(x).$$

The structure of this chapter is as follows. Section 5.1 explains the generic loop which

Type	Indicator	Abbr.
residual-based	$\eta_{\mathrm{R},p,\ell}(T)$	**R**
averaging	$\eta_{\mathrm{A},p,\ell}(T)$	**A**
flux	$\eta_{\mathrm{F},p,\ell}(T)$	**F**
uniform		**U**

Name	Section	Variation	Abbr.
two-well	2.3	$g \equiv 0 < \alpha$	**2W-Q**
two-well	2.3	$g \not\equiv 0 = \alpha$	**2W-L**
three-well	2.4		**3W**
optimal design	2.5	$g \equiv 1$	**OD**
optimal design	2.5	$g \not\equiv 1$	**OD-x**

Table 5.1: Abbreviations of mesh refinement indicators (left, from Section 5.2) and of numerical benchmark examples (right, from Section 5.6). These abbreviations are commonly used in convergence plots and in the Table 5.2 of convergence rates.

consists of the four steps SOLVE, ESTIMATE, MARK, and REFINE. Since all experiments are based on MATLAB, the actual minimisation of (5.4) (the step SOLVE) is performed by the nonlinear minimisation function `fminunc`, which is part of MATLAB's optimisation toolbox. Section 5.1 provides a brief description of the algorithm in this MATLAB function.

The step ESTIMATE is responsible for the estimation of the error of the discrete solution u_ℓ. Section 5.2 recalls the error estimators of the previous chapters and derives refinement indicators, which estimate the *local* error. The flux refinement indicator $\eta_{\mathrm{F},q,\ell}$ requires a nonlinear minimisation on its own. Section 5.5 presents an efficient algorithm for the minimisation. Based on these refinement indicators the step MARK marks triangles in $\mathcal{T}_\ell$ for refinement. Section 5.2 employs Dörfler marking to determine a set $\mathcal{T}_{\mathrm{M},\ell}$ of triangles which require refinement.

The step REFINE is the focus of Section 5.3 and derives a new triangulation $\mathcal{T}_{\ell+1}$ by splitting up the triangles in $\mathcal{T}_{\mathrm{M},\ell}$ into smaller ones. To this end the so-called red-green-blue refinements are used that ensure that the triangulations obtained preserve their shape regularity.

Section 5.4 demonstrates the effects of the stabilisation a_ℓ. In particular, it provides an investigation of the impact of the parameters γ and C on the condition number of the Hessian of $E_\ell^{\star\star}$ as well as on the error of the discrete solution. The conclusion is that the choice $\gamma = 1 = C$ appears to be optimal, at least for the benchmark examples in this thesis.

Section 5.6 describes the specific setup for the numerical experiments with the benchmark examples of Sections 2.3, 2.4 and 2.5. The experiments consist of the application of the AFEM loop to respective problems. Each problem is solved numerically, with and without stabilisation, with uniform mesh refinements as well as with adaptive mesh refinements controlled by refinement indicators of Section 5.2. The computation leads to a sequence of discrete solutions $(u_\ell)_{\ell\in\mathbb{N}_0}$ as well as sequences of stresses and error estimators. Appendix A presents the graphs which show the convergence of the errors and their estimators. Table 5.2 collects the observed convergence rates of the experiments. To distinguish the benchmark examples and the refinement types, the convergence plots and Table 5.2 use the abbreviations of Table 5.1.

Finally, Section 5.7 presents an analysis of the observations from the numerical examples. It turns out that stabilisation improves the condition number of the Hessian matrix. Furthermore, the refined error estimators of Section 4.4 (page 82) for interface problems reduce the reliability-efficiency gap. However, it also becomes apparent that, with stabilisation, convergence of adaptive algorithms is in general not superior to convergence of uniform algorithms. We shall conclude that the choice of the stabilisation is

not optimal and future research on adaptive stabilised algorithms is in order.

The numerical experiments of this chapter have been conducted on a cluster with eight CPUs per node (Intel®Xeon®CPU X5550 @ 2.67GHz, with SUSE Linux Enterprise Server 11). The software which has been used is MATLAB (Version 7.11.0.584, R2010b), and the code package AFEM (Carstensen and Numerical Analysis Group, HU Berlin, 2009), which provides a general framework for adaptive finite element methods. Note that this chapter intends to present numerical methods, not code. However, Appendix B presents the code which implements the algorithms of this chapter.

5.1 The AFEM Loop

The basic building block of the adaptive finite element method is the state-of-the-art AFEM loop. After the preparation of an initial triangulation $\mathcal{T}_0$ and an initial guess $u_{-1} \in \mathcal{S}_1(\mathcal{T}_0)$, the AFEM loop (cf. Verfürth, 1996, Introduction, page 1, Alberty et al., 1999) repeats the four steps

$$\text{SOLVE}, \quad \text{ESTIMATE}, \quad \text{MARK}, \quad \text{REFINE},$$

until some termination criterion is satisfied.

SOLVE computes an approximate minimiser u_ℓ of the discrete problem (5.4) on a given triangulation $\mathcal{T}_\ell$. The space of discrete admissible functions $\mathcal{A}_\ell$ is an affine space and its dimension coincides with the number of inner nodes $N_\ell := \#\{z \in \mathcal{N}_\ell : z \in \Omega\}$, which is also the number of degrees of freedom, because nodes on the boundary $\partial\Omega$ assume fixed values. Hence (5.4) is an N_ℓ-dimensional minimisation problem. The following experiments employ the MATLAB function `fminunc`, which implements a general purpose minimisation method. In the current implementation its algorithm is a trust-region method which is based on the work of Coleman and Li (1994, 1996). `fminunc` requires an initial guess for the solution to start the iterative solver, and tolerance values, which serve as stopping criteria. The experiments of this chapter use the solution of the previous AFEM iteration, $u_{\ell-1}$, as initial guess; $u_{-1}(z)$ is initialised to 0 on all interior nodes $z \in \mathcal{N}_0 \cap \Omega$ on the initial level $\ell = 0$.

The default tolerances for changes of the function value and of the the solution vector are 10^{-6}. The a posteriori error estimators of Sections 4.3 and 4.4 (pages 78 and 82) do not require u_ℓ to be an exact solution of the discrete problem. Therefore the termination criteria which are used inside `fminunc` are not a critical issue here and just the default settings of MATLAB are used.

Section 5.4 presents an investigation of the effects of the parameters γ in (5.4) and C in (5.3) for the stabilisation function. However, the numerical experiments of Section 5.6 are all performed with $\gamma = 1 = C$.

ESTIMATE computes one or more a posteriori error estimators η_ℓ which estimate the error of the solution u_ℓ. MARK computes a refinement indicator $\eta_\ell(T)$ for each triangle $T \in \mathcal{T}_\ell$ which estimates the *local* error of u_ℓ on that triangle. Based on the refinement indicators the step MARK then determines ("marks") a subset $\mathcal{T}_{\mathrm{M},\ell} \subset \mathcal{T}_\ell$ which contains all triangles deserving refinement. The details of these two steps are laid out in Section 5.2.

Input: $\mathcal{T}_0$, u_{-1}
for $\ell = 0, 1, 2, \ldots$ **do**
  SOLVE: Compute discrete minimiser u_ℓ of (5.4) from initial guess $u_{\ell-1}$;
  ESTIMATE: Compute error estimator η_ℓ from u_ℓ;
  MARK
    Compute refinement indicators $(\eta_\ell(T))_{T\in\mathcal{T}_\ell}$ (local error of u_ℓ);
    Determine subset $\mathcal{T}_{\mathrm{M},\ell} \subset \mathcal{T}_\ell$ of triangles to be refined
  REFINE: Generate refinement $\mathcal{T}_{\ell+1}$ of $\mathcal{T}_\ell$ such that $\mathcal{T}_{\mathrm{M},\ell} \cap \mathcal{T}_{\ell+1} = \varnothing$;
  if $N_\ell > N_{\max}$ **then return**

Algorithm 5.1: General layout of the AFEM loop. The loop terminates if the number of degrees of freedom N_ℓ exceeds a predefined limit $N_{\max}$.

REFINE generates a refined triangulation $\mathcal{T}_{\ell+1}$ out of $\mathcal{T}_\ell$. The refinement algorithm has to ensure regularity of $\mathcal{T}_{\ell+1}$ in the sense of Definition (3.1.1) (page 32) and shape regularity of $(\mathcal{T}_\ell)_{\ell\in\mathbb{N}_0}$ in the sense of Definition (3.1.2) (page 33). Section 5.3 describes the details of the algorithm.

Possible termination criteria for the AFEM loop may be elapsed time, or a limit on the number of degrees of freedom N_ℓ or on the level ℓ, or a tolerance for the error estimator of the step ESTIMATE. The following experiments use a limit on N_ℓ as termination criterion: the computation stops if $N_\ell > N_{\max} \coloneqq 3\,000\,000$. The result of the preceding setup is Algorithm 5.1.

5.2 Error Estimation and Marking

The step ESTIMATE computes a *global* error estimator η_ℓ for the solution u_ℓ of the discrete problem (5.4). The step MARK computes a *local* refinement indicator $\eta_\ell(T)$ that estimates the contribution of a triangle T towards the global error. This section derives three refinement indicators $\eta_{\mathrm{R},q,\ell}(T)$, $\eta_{\mathrm{A},q,\ell}(T)$ and $\eta_{\mathrm{F},q,\ell}(T)$ that are based on the respective error estimators $\eta_{\mathrm{R},q,\ell}$, $\eta_{\mathrm{A},q,\ell}$ and $\eta_{\mathrm{F},q,\ell}$ from previous chapters. The details of the marking process that marks triangles for later refinement are also discussed in this section. Note that convergence plots in upcoming sections use the abbreviations of Table 5.1 to distinguish the refinement indicators.

5.2.1 Residual-Based Refinement Indicator

Recall the residual-based error estimator of (3.20) (page 43), which reads for $2 \leqslant q \leqslant p$

$$\eta_{\mathrm{R},q,\ell} \coloneqq \left(\sum_{T\in\mathcal{T}_\ell} h_T^{q'} \, \|\Lambda_\ell\|_{L^{q'}(T)}^{q'} \right)^{1/q'} + \left(\sum_{F\in\mathcal{F}_\ell^\Omega} h_F \, \|[\sigma_\ell]_F \, n_F\|_{L^{q'}(F)}^{q'} \right)^{1/q'}, \tag{5.5}$$

where q' is the Hölder conjugate of q, i.e., $1/q + 1/q' = 1$. Theorems (3.3.2) and (3.3.6) show that $\eta_{\mathrm{R},q,\ell}$ is an upper and a lower bound of the error of the unstabilised discrete problem (5.4) (with $C = 0$), up to boundary terms and oscillations. For a given triangle T

$\in \mathcal{T}_\ell$ define the residual-based refinement indicator

$$\eta_{\mathrm{R},q,\ell}(T)^{q'} \coloneqq |T|^{q'/2} \|\Lambda_\ell\|^{q'}_{L^{q'}(T)} + |T|^{1/2} \sum_{\substack{F \in \mathcal{F}_\ell^\Omega \\ F \subset T}} \|[\sigma_\ell]_F \cdot n_F\|^{q'}_{L^{q'}(F)}. \tag{5.6}$$

For historical reasons the definition of $\eta_{\mathrm{R},q,\ell}(T)$ uses $|T|$ as measure of the local mesh size. Shape regularity ensures $\sum_{T\in\mathcal{T}_\ell} \eta_{\mathrm{R},q,\ell}(T)^{q'} \approx \eta^{q'}_{\mathrm{R},q,\ell}$, which justifies the interpretation of $\eta_{\mathrm{R},q,\ell}(T)$ as local error estimator.

5.2.2 Averaging Refinement Indicator

For some $2 \leqslant q \leqslant p$ the averaging error estimator $\eta_{\mathrm{A},q,\ell}$ of (3.45) (page 56) and the corresponding refinement indicator on a triangle $T \in \mathcal{T}_\ell$ read

$$\eta_{\mathrm{A},q,\ell} \coloneqq \|(1-\Sigma_\ell)\sigma_\ell\|_{L^{q'}(\Omega)} \quad \text{and} \quad \eta_{\mathrm{A},q,\ell}(T) \coloneqq \|(1-\Sigma_\ell)\sigma_\ell\|_{L^{q'}(T)},$$

where q' is the Hölder conjugate of q, and Σ_ℓ denotes the averaging interpolation operator (cf. (3.2), page 36). The averaging error estimator is reliable and efficient due to Theorems (3.4.1) and (3.4.2) (pages 56 and 57) with respect to the unstabilised discrete problem (5.4) (with $C = 0$), up to boundary terms and oscillations. Clearly it holds $\sum_{T\in\mathcal{T}_\ell} \eta_{\mathrm{A},q,\ell}(T)^{q'} = \eta^{q'}_{\mathrm{A},q,\ell}$. Therefore Section 5.6 employs $\eta_{\mathrm{A},q,\ell}(T)$ as refinement indicator.

5.2.3 Flux Refinement Indicator

Recall the definition of the oscillation $\mathrm{osc}_{\ell,q}$ from (3.3) (page 37). For some $2 \leqslant q \leqslant p$ and its Hölder conjugate q' the flux error estimator of (4.33) (page 80) is given by

$$\eta_{\mathrm{F},q,\ell} \coloneqq \|\sigma_\ell - \tau_\ell\|_{L^{q'}(\Omega)} + \|\Pi_\ell\Lambda_\ell + \operatorname{div}\tau_\ell\|_{L^{q'}(\Omega)} + \mathrm{osc}_{\ell,q'}(\Lambda_\ell),$$

where $\tau_\ell \in RT_0(\mathcal{T}_\ell)^n$ is an (approximate) minimiser of

$$\|\sigma_\ell - \tau_\ell\|_{L^{q'}(\Omega)} + \|\Pi_\ell\Lambda_\ell + \operatorname{div}\tau_\ell\|_{L^{q'}(\Omega)}. \tag{5.7}$$

Theorem (4.3.1) (page 79) guarantees that $\eta_{\mathrm{F},q,\ell}$ is an upper bound of the error for any choice of τ_ℓ, up to a multiplicative constant and boundary terms. The computation of τ_ℓ is a nontrivial task since the objective function (5.7) is *not a quadratic form* even for $q = 2$. Therefore Section 5.5 derives a computationally feasible algorithm for the minimisation of (5.7).

With an approximate minimiser τ_ℓ at hand the flux refinement indicator on the triangle $T \in \mathcal{T}_\ell$ reads

$$\eta_{\mathrm{F},q,\ell}(T)^{q'} \coloneqq \|\sigma_\ell - \tau_\ell\|^{q'}_{L^{q'}(T)} + \|\Pi_\ell\Lambda_\ell + \operatorname{div}\tau_\ell\|^{q'}_{L^{q'}(T)} + h_T^{q'} \|(1-\Pi_\ell)\Lambda_\ell\|^{q'}_{L^{q'}(T)}. \tag{5.8}$$

This term satisfies $\sum_{T\in\mathcal{T}_\ell} \eta_{\mathrm{F},q,\ell}(T)^{q'} \approx \eta^{q'}_{\mathrm{F},q,\ell}$ and is therefore a suitable estimator of the local error.

5.2.4 Error Estimation for Interface Problems

The a posteriori error estimators of (4.38) and (4.39) read

$$\begin{aligned}\eta_{\mathrm{L},\ell} \coloneqq\ & H_\ell^{\min\{5,(1+1/p)r'\}} + \eta_{\mathrm{F},2,\ell}^{6/5} + H_\ell^{-(1+\gamma)/3}\eta_{\mathrm{F},2,\ell}^{4/3}\,|||u_\ell|||_\ell^{2/3} \\ & + \eta_{\mathrm{F},2,\ell}\left(H_\ell^{(1-\gamma)/2}\,|||u_\ell|||_\ell + H_\ell^{1-\gamma/4}\,|||u_\ell|||_\ell^{1/2}\right)\end{aligned}$$

and

$$\begin{aligned}\eta_{\mathrm{H},\ell} \coloneqq\ & H_\ell^{\min\{5,(1+1/p)r'\}/3} + \eta_{\mathrm{F},2,\ell}^{2/5} + H_\ell^{-(1+\gamma)/9}\eta_{\mathrm{F},2,\ell}^{4/9}\,|||u_\ell|||_\ell^{2/9} \\ & + \eta_{\mathrm{F},2,\ell}^{1/3}\left(H_\ell^{(1-\gamma)/2}\,|||u_\ell|||_\ell + H_\ell^{1-\gamma/4}\,|||u_\ell|||_\ell^{1/2}\right)^{1/3} + H_\ell^{1-\gamma}\,|||u_\ell|||_\ell^2 \\ & + H_\ell^{-(1+\gamma)/2}\,|||u_\ell|||_\ell\,\eta_{\mathrm{F},2,\ell}^{1/2}\left(H_\ell^{(1-\gamma)/2}\,|||u_\ell|||_\ell + H_\ell^{1-\gamma/4}\,|||u_\ell|||_\ell^{1/2}\right)^{1/2} \\ & + H_\ell^{-(1+\gamma)/2}\,|||u_\ell|||_\ell\left(H_\ell^{\min\{5,(1+1/p)r'\}} + \eta_{\mathrm{F},2,\ell}^{6/5} + H_\ell^{-(1+\gamma)/3}\eta_{\mathrm{F},2,\ell}^{4/3}\,|||u_\ell|||_\ell^{2/3}\right)^{1/2}.\end{aligned}$$

Assume $\alpha > 0$ and that the exact solution u complies with the smoothness condition (4.35) (page 82). Then Theorem (4.4.2) (page 83) ensures that $\eta_{\mathrm{L},\ell}$ and $\eta_{\mathrm{H},\ell}$ are reliable error estimators in the sense that

$$\|\delta_\ell\|_{L^{p'}(\Omega)}^r + \|e_\ell\|_{L^2(\Omega)}^2 \lesssim \eta_{\mathrm{L},\ell} \quad\text{and}\quad |e_\ell|_{H^2(\Omega)}^2 \lesssim \eta_{\mathrm{H},\ell}.$$

The benchmark examples in Section 5.6 consider these error estimators, even for $\alpha = 0$. However, due to their complexity and nonlocal nature (via the global mesh size H_ℓ), we refrain from deriving a local error estimator from $\eta_{\mathrm{L},\ell}$ or $\eta_{\mathrm{H},\ell}$.

5.2.5 Dörfler Marking

Dörfler (1996) introduces the following strategy to derive a set $\mathcal{T}_{\mathrm{M},\ell} \subset \mathcal{T}_\ell$ of triangles which are marked for refinement. Given a fixed constant $0 < \theta < 1$ and refinement indicators $(\eta_\ell(T))_{T\in\mathcal{T}_\ell}$, find a set $\mathcal{T}_{\mathrm{M},\ell} \subset \mathcal{T}_\ell$ of minimal cardinality such that the local errors of the elements in $\mathcal{T}_{\mathrm{M},\ell}$ cover at least θ times the total estimated error η_ℓ ("bulk criterion"), in the sense that

$$\sum_{T\in\mathcal{T}_{\mathrm{M},\ell}} \eta_\ell(T)^{q'} \geqslant \theta \sum_{T\in\mathcal{T}_\ell} \eta_\ell(T)^{q'} \approx \theta\eta_\ell^{q'} \tag{5.9}$$

with some q which is consistent with the indicator $\eta_\ell(T)$, and the Hölder conjugate q' of q, i.e., $1/q + 1/q' = 1$. The condition (5.9) ensures $\#\mathcal{T}_{\mathrm{M},\ell} \leqslant \lceil\theta\#\mathcal{T}_\ell\rceil$. Cascón et al. (2008, Theorem 4.1, for details see also Kreuzer and Siebert, 2011, Corollary 3.7) prove that (5.9) implies the *contraction property*

$$\|\delta_{\ell+k}\|_{L^2(\Omega)}^2 + \eta_{\mathrm{R},2,\ell+k}^2 \lesssim \rho^k\left(\|\delta_\ell\|_{L^2(\Omega)}^2 + \eta_{\mathrm{R},2,\ell}^2\right) \quad\text{for } \ell, k \in \mathbb{N}_0 \tag{5.10}$$

for a fixed $0 < \rho < 1$ and a certain class of problems, which is included in the class of Section 2.2 (page 21).

The numerical experiments of this chapter follow the strategy of Dörfler (1996) and

Input: $\mathcal{T}_\ell$, set of marked triangles $\mathcal{T}_{\mathrm{M},\ell}$
$\mathcal{F}_{\mathrm{M},\ell}^{(0)} \coloneqq \{\mathrm{ref}(T) \,:\, T \in \mathcal{T}_{\mathrm{M},\ell}\}$;
for $j = 1, 2, \ldots$ **do**
  $\mathcal{F}_{\mathrm{M},\ell}^{(j)} \coloneqq \mathcal{F}_{\mathrm{M},\ell}^{(j-1)} \cup \Big\{\mathrm{ref}(T) \,:\, T \in \mathcal{T}_\ell \text{ with } \{F \in \mathcal{F}_\ell \,:\, F \subset T\} \cap \mathcal{F}_{\mathrm{M},\ell}^{(j-1)} \neq \varnothing\Big\}$;
  if $\mathcal{F}_{\mathrm{M},\ell}^{(j-1)} = \mathcal{F}_{\mathrm{M},\ell}^{(j)}$ **then return**
Output: set of marked edges $\mathcal{F}_{\mathrm{M},\ell} \coloneqq \mathcal{F}_{\mathrm{M},\ell}^{(j)}$

Algorithm 5.2: The *closure algorithm*. It ensures that the set of marked edges $\mathcal{F}_{\mathrm{M},\ell}$ complies with (5.11), i.e., if a triangle T contains a marked edge its reference edge $\mathrm{ref}(T)$ is marked as well.

choose a set $\mathcal{T}_{\mathrm{M},\ell} \subset \mathcal{T}_\ell$ of minimal cardinality which satisfies (5.9) with $\theta = 1/2$ for one of the refinement indicators $\eta_{\mathrm{R},q,\ell}$, $\eta_{\mathrm{A},q,\ell}$ or $\eta_{\mathrm{F},q,\ell}$. The set $\mathcal{T}_{\mathrm{M},\ell}$ then is handed over to the REFINE step.

5.3 Mesh Refinement

Based on the set $\mathcal{T}_{\mathrm{M},\ell} \subset \mathcal{T}_\ell$ the step REFINE derives a finer triangulation $\mathcal{T}_{\ell+1}$. In doing so, it has to ensure that the new triangulation is indeed regular in the sense of Definition (3.1.1) (page 32) and that each triangle in $\mathcal{T}_{\mathrm{M},\ell}$ is refined, meaning that it is divided into two or more sub-triangles. Furthermore, the resulting family of triangulations must comply with the Definition (3.1.2) of shape regularity (page 33), i.e., the ratio of the diameter and the inradius of every triangle must be uniformly bounded. This section describes the *red-green-blue refinement strategy*, which ensures shape regularity. For further reading refer to Karkulik et al. (2012), Carstensen (2004b) and Verfürth (1996, Section 4.1, page 108).

The red-green-blue refinement strategy requires the concept of the reference edge of a triangle: for each $T \in \mathcal{T}_\ell$ let $\mathrm{ref}(T) \in \mathcal{F}_\ell$ denote one of the three edges of T. The edge $\mathrm{ref}(T)$ is called *reference edge* of T. The set $\mathcal{F}_{\mathrm{M},\ell} \subset \mathcal{F}_\ell$ of *marked edges* is the set of smallest cardinality that contains the reference edges of all marked triangles plus the reference edges of all triangles that contain at least one marked edge. In formal notation, this is equivalent to

$$\begin{aligned} &\{\mathrm{ref}(T) \,:\, T \in \mathcal{T}_{\mathrm{M},\ell}\} \subset \mathcal{F}_{\mathrm{M},\ell}, \text{ and} \\ &\mathrm{ref}(T) \in \mathcal{F}_{\mathrm{M},\ell} \text{ for all } T \in \mathcal{T}_\ell \text{ with } \{F \in \mathcal{F}_\ell \,:\, F \subset T\} \cap \mathcal{F}_{\mathrm{M},\ell} \neq \varnothing. \end{aligned} \tag{5.11}$$

A closure algorithm (Algorithm 5.2) determines the set $\mathcal{F}_{\mathrm{M},\ell}$. The relation (5.11) ensures that the resulting triangulation $\mathcal{T}_{\ell+1}$ is regular in the sense of Definition (3.1.1) (page 32, cf. Carstensen, 2004b, Remark 2.2).

Based on the thus derived set $\mathcal{F}_{\mathrm{M},\ell}$ the red-green-blue refinement strategy divides each triangle into a maximum of four sub-triangles, which form the new triangulation $\mathcal{T}_{\ell+1}$. Triangles of $\mathcal{T}_\ell$ that do not contain a marked edge are left unchanged. Triangles with one, two, or three marked edges are divided into two, three, or four sub-triangles, with new reference edges as depicted in Figure 5.1. These refinements of a triangle are commonly called "red" (three marked edges), "green" (one marked edge) and "blue" (two marked

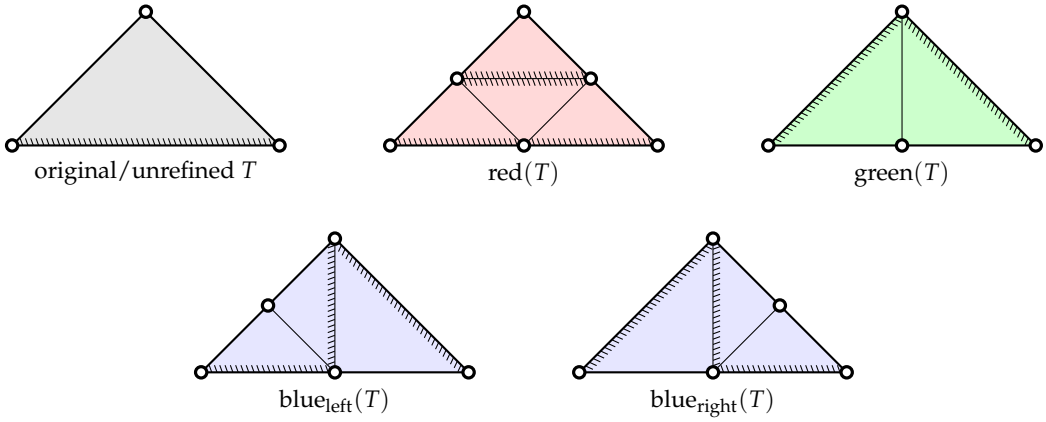

Figure 5.1: Divisions of the "original" triangle into four ("red"), two ("green") and three ("blue") sub-triangles, as described in Section 5.3. Each marked edge is divided into two edges. The new reference edges are hatched here. Note that there are two possible arrangements with two marked edges (the "blue" case); both are depicted.

edges) refinement. See also Carstensen (2004b, Figures 1–3) for another illustration. This refinement strategy ensures that, after a finite number of initial refinements, all newly generated triangles in $\mathcal{T}_{\ell+1}$ are similar to triangles of previous triangulations. This guarantees shape regularity of the resulting family of triangulations (cf. Verfürth, 1996, Section 4.1, page 108 and Carstensen, 2004b). Karkulik et al. (2012, Theorem 5) furthermore prove that the number of refined triangles is limited through

$$\#\mathcal{T}_\ell - \#\mathcal{T}_0 \lesssim \sum_{k=0}^{\ell-1} \#\mathcal{T}_{\mathrm{M},k} \leqslant \#\mathcal{T}_\ell - \#\mathcal{T}_0,$$

where the generic constant depends on the initial mesh $\mathcal{T}_0$, but not on ℓ or on the sets of marked triangles $\mathcal{T}_{\mathrm{M},k}$.

We also employ *uniform* mesh refinements to compare the results with those of adaptive mesh refinements. Uniform refinements are accomplished with $\mathcal{F}_{\mathrm{M},\ell} \coloneqq \mathcal{F}_\ell$, i.e., "red" refinements are applied to all triangles. The resulting family of triangulations is quasi-uniform, i.e. $H_\ell \approx h_{\ell,\min}$. Obviously, uniform "red" mesh refinements imply $\#\mathcal{T}_{\ell+1} = 4\#\mathcal{T}_\ell$. In accordance with Table 5.1, uniform refinements are abbreviated with "U" in Table 5.2 and in the convergence plots of Appendix A.

Note that the step REFINE is also responsible for the prolongation of the discrete solution u_ℓ to the new level $\ell + 1$. The prolongation is required because u_ℓ serves as initial guess for the iterative solver that computes $u_{\ell+1}$. Since $\mathcal{S}_1(\mathcal{T}_{\ell+1}) \subset \mathcal{S}_1(\mathcal{T}_\ell)$, u_ℓ can be represented exactly on the new grid.

For the benchmark examples in Section 5.6 the longest edge of each triangle $T \in \mathcal{T}_0$ is chosen as its reference edge in the initial triangulation $\mathcal{T}_0$. Note, however, that Carstensen (2004b, Algorithm 2.1) suggests a different strategy for the choice of the initial reference edges. With the initial meshes in the benchmark examples of Section 5.6 (see Figures 5.6, 5.7 and 5.8) the strategy of Carstensen (2004b) leads to the same reference edges.

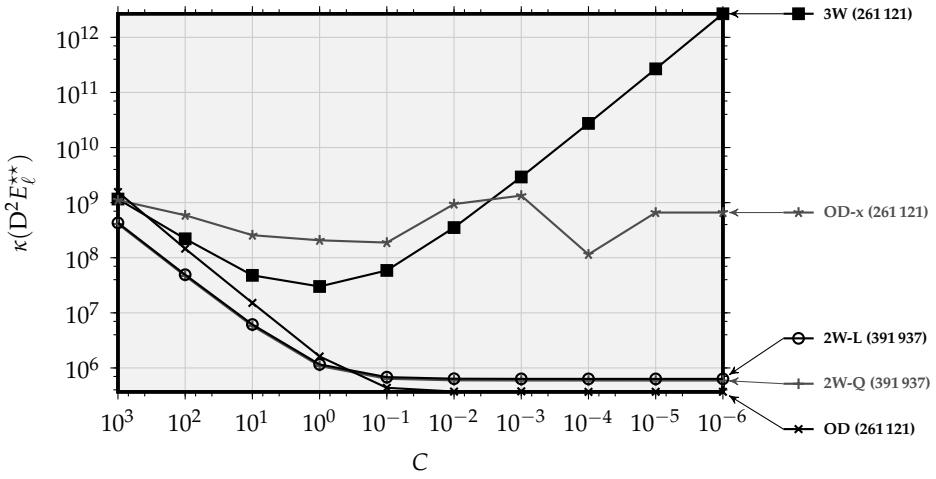

Figure 5.2: Condition number of the Hessian matrix $\mathrm{D}^2 E_\ell^{\star\star}$ as function of the coefficient C in (5.4). The number in parentheses states the number of degrees of freedom of the underlying mesh.

5.4 Effects of the Parameters γ and C

This section presents an investigation of the implications of different choices of the parameters γ in (5.4) and C in (5.3). Section 3.5 (page 59) introduced the concept of stabilisation as a remedy for ill-conditioned Hessian matrices. Recall the spectral condition number of (3.46) (page 59). The condition number $\kappa(\mathrm{D}^2 E_\ell^{\star\star}(u_\ell))$ of the Hessian matrix of the stabilised discrete energy hence acts as an indicator for the impact of the stabilisation. Figure 5.2 displays the spectral condition numbers of the Hessian matrix of problem (5.4) for $\gamma = 1$ and different values of C. The Hessian is evaluated in the discrete solution u_ℓ on a uniform grid with approximately 300 000 degrees of freedom. The figure indicates that the two-well problem and the unmodified optimal design problem are already well-conditioned. The three-well problem, however, suffers from its degeneracy and its condition numbers are greatly improved by the stabilisation. The hyperbolic nature of the corresponding graph in Figure 5.2 suggests that the condition number of the Hessian behaves like

$$\log \kappa \sim \log C + 1/\log C.$$

We conclude from Figure 5.2 that $C = 1$ is an optimal choice for the three-well problem and an acceptable choice for the other benchmark problems as well. However, since the results of Chapter 4 concern asymptotic behaviour only and are devoid of multiplicative constants, this conclusion is purely empirical and not backed by any theory.

Figure 5.3 shows the error of the discrete stress tensors of problem (5.4), a result of the same computations that led to Figure 5.2. It confirms that $C = 1$ is a good tradeoff: while the error does not improve (much) for $C < 1$, values of $C > 1$ lead to much stronger errors caused by the high distortions that are a result of the stabilisation. Note that the numerical experiments described in the previous paragraphs of this section are all based on fixed triangulations. Since $H_\ell^{\gamma+1}$ is a factor in the stabilisation (5.3) modifications of C are equivalent to modifications of γ on fixed meshes; different values of γ would merely

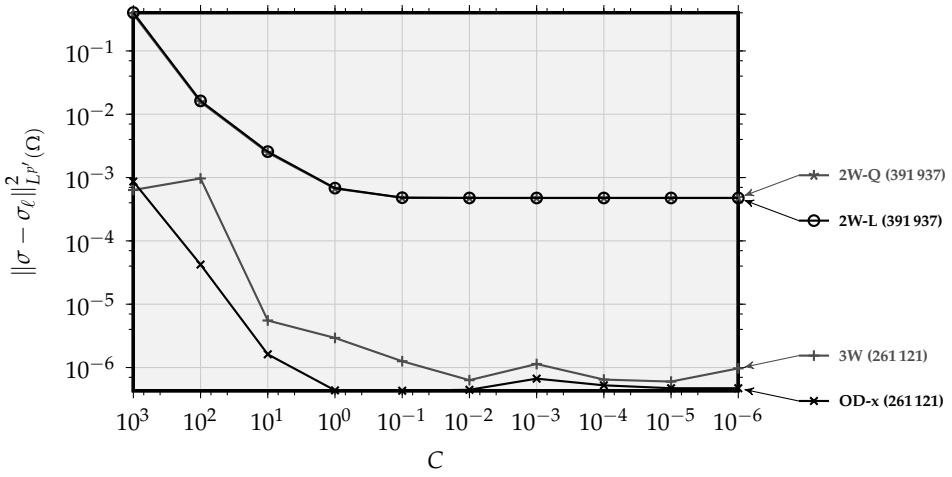

Figure 5.3: Error $\|\sigma - \sigma_\ell\|^2_{L^{p'}(\Omega)}$ of the discrete stress tensor as function of the coefficient C in (5.4). The number in parentheses states the number of degrees of freedom of the underlying mesh.

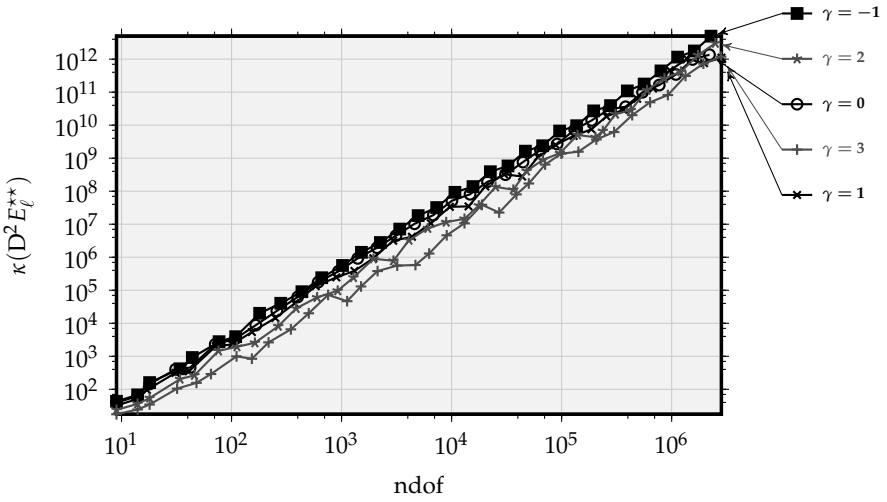

Figure 5.4: Condition number of the Hessian matrix $\mathrm{D}^2 E^{\star\star}_\ell$ of the three-well example (cf. Section 5.6) as function of the number of degrees of freedom (ndof), computed for several values of γ with the flux refinement indicator $\eta_{\mathrm{F},2,\ell}(T)$.

shift the graphs of Figures 5.2 and 5.3 horizontally.

To study the impact of different values of γ consider the three-well problem, which suffers the most from its ill-conditioned Hessians. Figures 5.4 and 5.5 show the condition numbers of the Hessians and the errors of the stress tensors σ_ℓ of the discrete solution of the three-well problem for different values of γ. The solutions are based on adaptive mesh refinements, controlled with the flux refinement indicator $\eta_{\mathrm{F},2,\ell}(T)$ of (5.8), with the coefficient $C = 1$. Figure 5.4 shows that the condition numbers increase with the number of degrees of freedom. A closer look reveals that the condition numbers for $\gamma = -1$ and $\gamma = 3$ differ by an order of magnitude. The observed convergence rate of the error of the

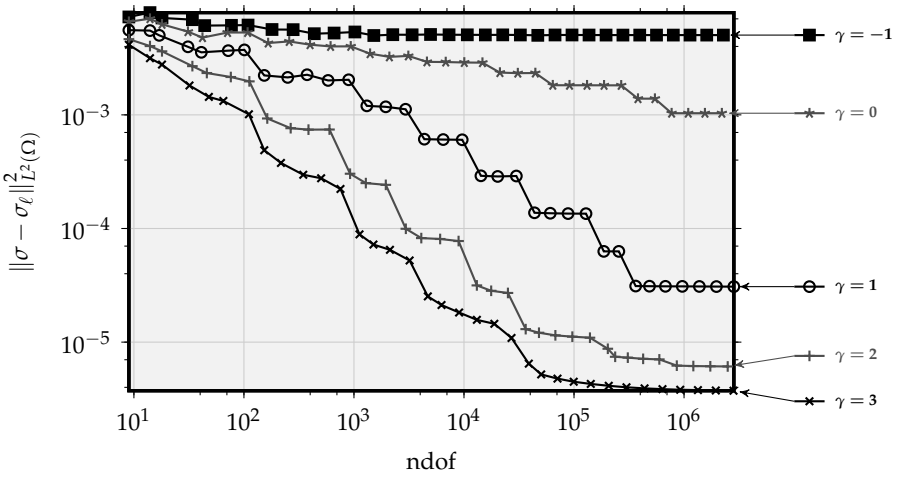

Figure 5.5: Error $\|\sigma - \sigma_\ell\|^2_{L^2(\Omega)}$ of the discrete stress of the three-well example (cf. Section 5.6) as function of the number of degrees of freedom (ndof), computed for several values of γ with the flux refinement indicator $\eta_{\mathrm{F},2,\ell}(T)$.

stress for $\gamma = 1$ is 1. For $\gamma = 2$ and 3 the rate improves to 1.2. The convergence rates are given as powers of $1/\sqrt{\mathrm{ndof}}$, which is approximately proportional to H_ℓ on uniform grids; see also the caption of Table 5.2.

Theorems (4.1.3) and (4.2.1) (pages 68 and 75, see also Remarks (4.1.4) and (4.2.2) on pages 68 and 75) suggest $\gamma = 1$ as the optimal choice. In consideration of the aforementioned observations the following experiments adhere to this suggestion.

5.5 Computation of the Flux Error Estimator

This section discusses the minimisation of (5.7) with respect to $\tau_\ell \in RT_0(\mathcal{T}_\ell)$, which is necessary to compute the flux error estimator $\eta_{\mathrm{F},q,\ell}$ and its refinement indicator. Recall that a Raviart-Thomas function τ_ℓ is uniquely defined by its normal components on each edge of the triangulation $\mathcal{T}_\ell$ at hand. Hence the vector space $RT_0(\mathcal{T}_\ell)$ is equivalent to $\mathbb{R}^{\#\mathcal{F}_\ell}$ and the computation of the minimiser τ_ℓ of (5.7) is a $\#\mathcal{F}_\ell$-dimensional minimisation problem. Note that (5.7) is *not* a quadratic form even for $q = 2$ and the minimisation is therefore a nontrivial problem. However, a high-quality minimiser is not required since Theorem (4.3.1) proves reliability even for arbitrary $\tau_\ell \in RT_0(\mathcal{T}_\ell)$.

Aiming at minimal computational efforts we resort to the following iterative scheme to obtain an approximate minimiser τ_ℓ for $q = 2$. The scheme is inspired by Valdman (2009) and Carstensen and Merdon (2012, Algorithm 5.1). Elementary analysis confirms that

$$(a+b)^2 = a^2 + 2ab + b^2 = \min_{s>0} \left((1+s)a^2 + (1+1/s)b^2\right) \quad \text{for } a, b > 0$$

with unique minimiser $s = b/a$. For some fixed $s > 0$ the minimisation of the quadratic form

$$(1+s)\,\|\sigma_\ell - \tau_\ell\|^2_{L^2(\Omega)} + (1+1/s)\,\|\Pi_\ell \Lambda_\ell + \operatorname{div} \tau_\ell\|^2_{L^2(\Omega)} \tag{5.12}$$

with respect to $\tau_\ell \in RT_0(\mathcal{T}_\ell)$ is a computationally trivial task: after the computation of the

Input: σ_ℓ, $\Pi_\ell \Lambda_\ell$
$s^{(1)} = 1$;
for $k = 1, 2, 3$ **do**
  Compute minimiser $\tau_\ell^{(k)}$ of the quadratic functional
  $M(s^{(k)}, \tau_\ell) \coloneqq (1 + s^{(k)}) \, \|\sigma_\ell - \tau_\ell\|^2_{L^2(\Omega)} + (1 + \frac{1}{s^{(k)}}) \, \|\Pi_\ell \Lambda_\ell + \operatorname{div} \tau_\ell\|^2_{L^2(\Omega)}$;
  if $D^2_{\tau_\ell} M(s^{(k)}, \tau_\ell^{(k)})$ *nearly singular (MATLAB "warning")* **then return** $\tau_\ell^{(k)}$;
  $s^{(k+1)} \coloneqq \left\| \Pi_\ell \Lambda + \operatorname{div} \tau_\ell^{(k)} \right\|_{L^2(\Omega)} \Big/ \left\| \sigma_\ell - \tau_\ell^{(k)} \right\|_{L^2(\Omega)}$;
  if $\max \left\{ s^{(k+1)}, 1/s^{(k+1)}, \frac{|s^{(k+1)} - s^{(k)}|}{s^{(k+1)} + s^{(k)}} \right\} < \varepsilon_{\mathrm{M}}^{0.8}$ **then return** $\tau_\ell^{(k)}$;
Output: approximate minimiser τ_ℓ of (5.7)

Algorithm 5.3: Iterative computation of an approximate minimiser $\tau_\ell \in RT_0(\mathcal{T}_\ell)$ of (5.7). A single Newton step performs the minimisation of $M(s^{(k)}, \cdot)$. The result τ_ℓ of the iteration is required for the flux error estimator $\eta_{\mathrm{F},q,\ell}$.

(sparse) Hessian matrix a single Newton step leads to the minimiser. These considerations lead to Algorithm 5.3, which alternately minimises (5.12) with respect to τ_ℓ and with respect to s. Undisplayed experiments have shown that the Hessian of (5.12) with respect to τ_ℓ tends to become singular, particularly on highly refined meshes. This leads to a breakdown of the minimisation algorithm and degenerate results, i.e., "NaN", which is the computational symbol of the result of the division $0/0$. To counter this effect, Algorithm 5.3 honours MATLAB's warning concerning the singularity of the Hessian and terminates the iteration. To avoid degenerate values of s, we also terminate the iteration if s or $1/s$ or the relative change of s drop below the tolerance of $\varepsilon_{\mathrm{M}}^{0.8}$, where ε_{M} denotes the machine precision. Finally, further undisplayed experiments have shown that no significant improvements of the minimum value occur after three iterations, therefore the iteration is unconditionally stopped beyond that.

For $q > 2$ it is not possible to rewrite the minimisation into an iteration of Newton steps with sparse Hessians. Yet, since an approximate minimiser is sufficient the solution τ_ℓ of Algorithm 5.3, computed for $q = 2$, is used even for the evaluation of $\eta_{\mathrm{F},q,\ell}$ with $q > 2$.

5.6 Benchmark Examples

Sections 2.3, 2.4 and 2.5 describe a total of five benchmark examples. This section introduces the actual discrete setting for each of those examples as well as the numerical results. The general algorithm of Section 5.1 derives different sequences $(u_\ell)_{\ell \in \mathbb{N}_0}$ of solutions, depending on the use of the stabilisation ($C = 1$ or $C = 0$) and the choice of the refinement strategy (uniform refinements, or refinements controlled by one of the refinement indicators of Section 5.2). Appendix A contains the numerous convergence graphs of the errors, error estimators, and of H_ℓ, for each of the choices of the parameters mentioned above. Table 5.2 summarises the convergence rates as powers of $1/\sqrt{\mathrm{ndof}}$. Boiger and Carstensen (2012+, Section 6) present a preliminary version of the results and observations of this section.

Note that the rates in Table 5.2 have been generated automatically by linear regression. Convergence rates with high oscillations (Pearson's coefficient less than 0.98) are put in parentheses, inconclusive rates (Pearson's coefficient less than 0.90) are marked by "—" in Table 5.2.

5.6.1 Two-Well Benchmark

The two-well benchmark of (2.14) (page 26 in Section 2.3) with quadratic lower-order terms is given by (5.1) with $p = 4$, $\alpha = 1$, $g \equiv 0$ and the energy density $W^{\star\star}$ of Lemma (2.3.1). The lower-order terms are provided by

$$f(x) \coloneqq -3t^5/128 - t^3/3 \quad \text{with } t \coloneqq (3(x_1 - 1) + 2x_2)/\sqrt{13}.$$

The domain is the open rectangle $\Omega \coloneqq]0,1[\times]0, \frac{3}{2}[$. According to Lemma (2.3.3) (page 26) the unique exact minimiser of the two-well problem with boundary conditions prescribed by u_D of (2.13) (page 25) reads

$$u(x) = \begin{cases} f(x) & \text{for } t \leqslant 0, \\ t^3/24 + t & \text{for } t \geqslant 0 \end{cases} \tag{5.13}$$

and exhibits an interface along the line $t = 0$; see Figure 5.6 for the position of the interface in Ω, and Figure 2.3 (page 26) for an illustration of the solution u. Due to the interface line, the function u_D of (2.13), which is identical to (5.13), does not comply with the strict smoothness conditions of (5.2). This is not fatal, however, because the values of u_D matter on the boundary only. The interface meets the boundary $\partial\Omega$ in two corners of the rectangular domain Ω. Since $u|_{\partial\Omega}$ is $\mathcal{F}_0^{\partial\Omega}$-edgewise polynomial and globally continuous, there exists an extension $u_D \in C^\infty(\Omega)$ that complies with (5.2) and satisfies $u - u_D \in V \coloneqq W_0^{1,4}(\Omega)$. This extension u_D yields the same discrete set of admissible functions $\mathcal{A}_\ell = I_\ell u_D + \mathcal{S}_1(\mathcal{T}_\ell)$. The numerical experiments with the two-well problem with quadratic lower-order terms lead to the convergence graphs of Figures A.1 and A.2 and the empirical convergence rates in the "2W-Q" rows of Table 5.2.

The modified two-well problem of (2.15) (page 26 in Section 2.3) with linear lower-order terms differs from its counterpart with quadratic lower-order terms in that $\alpha = 0$ and $g \coloneqq -\operatorname{div}(\mathrm{D}W^{\star\star}(\mathrm{D}u))$ is defined such that (5.13) is an exact solution here as well. Note that Lemma (2.3.5) (page 27) proves that the two-well problem of (2.15) complies with the condition (3.21) (page 44). Hence, most of the results of Chapter 4 which apply to the two-well problem with quadratic lower-order terms also apply to its counterpart with linear lower-order terms. In particular, uniqueness of the exact solution u is guaranteed by Theorem (4.2.3) (page 75, see also Remark (4.2.4)). The numerical experiments with the two-well problem with linear lower-order terms lead to the convergence graphs of Figures A.3 and A.4 and the empirical convergence rates in the "2W-L" rows of Table 5.2.

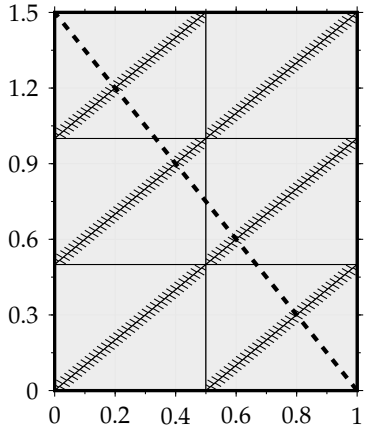

Figure 5.6: The initial triangulation $\mathcal{T}_0$ for the two-well benchmark ensures that adaptive mesh refinements *cannot* resolve the discontinuity Γ exactly (indicated by the thick dashed line). Reference edges are hatched (as in Figure 5.1).

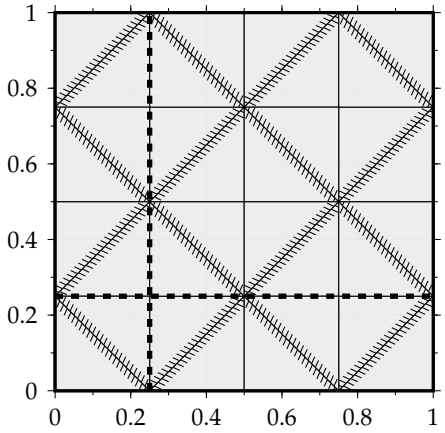

Figure 5.7: The initial triangulation $\mathcal{T}_0$ for the three-well benchmark resolves the discontinuities of the lower-order term f exactly (indicated by thick dashed lines). Reference edges are hatched (as in Figure 5.1).

5.6.2 Three-Well Problem

The energy density $W^{\star\star}$ of the three-well benchmark is the convex hull of

$$W : \mathbb{R}^2 \to \mathbb{R}, \quad y \mapsto \min\left\{|y|^2, |y-(1,0)|^2, |y-(0,1)|^2\right\},$$

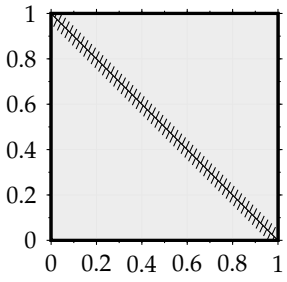

Figure 5.8: Initial triangulation $\mathcal{T}_0$ for the optimal design benchmark. Reference edges are hatched (as in Figure 5.1).

which is given explicitely by (2.17) (page 28). The three-well benchmark of (2.19) (page 29 in Section 2.4) consists of the minimisation problem (5.1) on the domain $\Omega :=]0,1[^2$ with $p = 2$, $\alpha = 0$ and the lower-order function $g := -\operatorname{div}(\mathrm{D}W^{\star\star}(\mathrm{D}u_D))$, where u_D is given by (2.18). The choice of g ensures that $u = u_D$ is a solution of the continuous problem. Recall that the function u_D of (2.18) exhibits discontinuities of its derivative along the lines $\{x : x_1 = \frac{1}{4}\}$ and $\{x : x_2 = \frac{1}{4}\}$. Therefore the initial triangulation $\mathcal{T}_0$ of Figure 5.7 covers these lines with edges. Note that due to $\alpha = 0$ uniqueness of the solution u of the continuous problem is not guaranteed. However, Theorem (2.2.5) (page 23) ensures uniqueness of the stress σ. The same holds for the discrete solution u_ℓ and σ_ℓ due to Theorem (3.2.4) (page 41). The numerical experiments with the three-well problem lead to the convergence graphs of Figures A.5 and A.6 and the empirical convergence rates in the "3W" rows of Table 5.2. Note that the three-well benchmark suffers severely from the effects of ill-conditioned Hessians. Using "R"-, "A"- and "F"-adaptive mesh refinements the MATLAB solver fails without stabilisation beyond 33 169, 24 573 and 687 324 degrees of freedom, respectively. The error message "Input to EIG

must not contain NaN or Inf" indicates that the solution of a linear system with singular matrix led to nonfinite numbers.

5.6.3 Optimal Design

The optimal design benchmark of Section 2.5 (page 29) is given by (5.1) on the domain $\Omega :=]0,1[$ with $p = 2$, $\alpha = 0$, $g \equiv 1$ and the energy density of (2.20). See Figure 2.6 (page 30) for an illustration of φ. No exact solution of the continuous problem is known, therefore Figures A.7 and A.8 only show the convergence graphs of the error estimators, and of H_ℓ. Figure 5.8 depicts the initial triangulation $\mathcal{T}_0$. The empirical convergence rates are denoted in the "OD" rows of Table 5.2.

To compare the numerical solution with an exact solution, the modified optimal design benchmark is also considered. It differs from the problem described above in the choice of the lower-order term g. The choice of (2.22),

$$g := -\operatorname{div}(\mathrm{D}W^{\star\star}(\mathrm{D}u)) \quad \text{with } u(x) := x_1 x_2 (1-x_1)(1-x_2), \tag{5.14}$$

ensures that u is a solution of the continuous problem. The numerical experiments with the modified optimal design benchmark, i.e., with g as in (5.14), lead to the convergence graphs of Figures A.9 and A.10 and the empirical convergence rates in the "OD-x" rows of Table 5.2.

5.6.4 Empirical Convergence Behaviour

Theorem (4.2.3) (page 75) states that $\|\sigma - \sigma_\ell\|_{L^{p'}(\Omega)}$ and $|||u_\ell|||_\ell$ converge to zero as $H_\ell \to 0$. The relation $H_{\ell+1} = H_\ell/2$ ensures convergence of H_ℓ for uniform mesh refinements. For adaptive mesh refinements, however, convergence of H_ℓ is not clear a priori. The empirical rates of Table 5.2 confirm the convergence of σ_ℓ and of $|||u_\ell|||_\ell$ in all benchmark examples but the "R"- and "A"-adaptive versions of the three-well problem. A close look at Figure A.6 reveals that H_ℓ does not drop below 0.2, let alone converge to zero. This accounts for the lack of convergence of σ_ℓ and of $|||u_\ell|||_\ell$ in the cases of "R"- and "A"-adaptive mesh refinements. Theorem (4.2.3) also asserts convergence of $u_\ell \to u$ in L^2 for both two-well benchmarks ("2W-Q" and "2W-L"), which is confirmed by Table 5.2.

For interface problems Theorem (4.4.4) (page 84) and (4.41) even promise

$$\|\sigma - \sigma_\ell\|^2_{L^{4/3}(\Omega)} + \alpha \|u - u_\ell\|^2_{L^2(\Omega)} + |||u_\ell|||^2_\ell \lesssim H_\ell^{2/p}$$

on uniform grids, and $\|u - u_\ell\|^2_{L^2(\Omega)} \lesssim H_\ell^{1/2}$ for the two-well benchmark with linear lower-order terms. This estimate does not apply to the unmodified optimal design benchmark as the smoothness of the exact solution is unknown. For the other benchmark examples, the observed rates excel the a priori expectation of Theorem (4.4.4), even with adaptive mesh refinements where the estimate of (4.41) cannot be guaranteed.

Up to boundary values Theorem (4.4.1) (page 82) claims

$$|u - u_\ell|^2_{H^1(\Omega)} \lesssim \|u - u_\ell\|^{2/3}_{L^2(\Omega)} + |||u_\ell|||^2_\ell + H_\ell^{-1} |||u_\ell|||_\ell \, \|u - u_\ell\|_{L^2(\Omega)}. \tag{5.15}$$

Err./Est.:		$\|\delta_\ell\|^2_{L^{p'}(\Omega)}$		$\|e_\ell\|^2_{L^2(\Omega)}$		$\|\|\|u_\ell\|\|\|^2_\ell$	$\eta_{\mathrm{R},p,\ell}$	$\eta_{\mathrm{A},p,\ell}$		$\eta_{\mathrm{F},p,\ell}$		$\eta_{\mathrm{L},\ell}$	$\|e_\ell\|^2_{H^1(\Omega)}$		$\eta_{\mathrm{H},\ell}$	H_ℓ	
Stabilised:		□	☒	□	☒	☒	□	□	☒	□	☒	☒	□	☒	☒	□	☒
2W-Q	**U**	1.7	1.7	1.5	1.4	1.4	0.8	0.8	0.8	0.9	0.9	1.0	0.6	0.5	0.3	0.9	0.9
	R	2.1	1.4	(1.7)	1.2	1.2	1.1	1.1	1.0	1.1	1.0	1.1	(0.7)	0.4	0.4	0.6	0.7
	A	2.1	1.3	(1.7)	1.1	1.1	1.0	1.1	1.0	1.1	0.9	1.0	(0.7)	0.4	0.4	0.7	0.7
	F	2.1	1.3	(1.7)	1.1	1.1	1.1	1.1	1.0	1.1	0.9	1.0	(0.7)	0.4	0.4	0.7	0.7
2W-L	**U**	1.7	1.7	1.5	1.4	1.4	0.8	0.8	0.8	0.9	0.9	1.0	0.6	0.5	0.3	0.9	0.9
	R	2.1	1.4	(1.7)	1.1	1.1	1.1	1.1	1.0	1.1	1.0	1.1	(0.7)	0.4	0.4	0.6	0.7
	A	2.1	1.3	(1.7)	1.1	1.1	1.0	1.1	1.0	1.1	0.9	1.1	(0.7)	0.4	0.4	0.7	0.7
	F	2.1	1.4	(1.7)	1.1	1.1	1.1	1.1	1.0	1.1	0.9	1.1	(0.7)	0.4	0.4	0.7	0.7
3W	**U**	(1.0)	1.5	—	1.4	1.6	0.9	0.9	0.9	(0.6)	0.9	1.1	—	0.5	0.4	1.0	1.0
	R	1.9	(0.3)	—	(0.3)	—	1.0	1.0	1.0	1.1	—	(0.3)	(0.9)	(0.1)	—	(0.2)	(0.1)
	A	1.9	(0.3)	—	(0.2)	—	0.9	1.0	1.0	1.1	—	—	(0.9)	(0.1)	—	(0.2)	(0.1)
	F	1.8	1.0	—	0.9	(0.8)	1.0	1.0	0.8	1.0	0.6	0.8	—	0.3	0.3	(0.2)	0.5
OD	**U**					(1.0)	0.9	0.8	(0.7)	0.8	0.9	1.1			0.4	0.9	0.9
	R					(1.1)	0.9	0.9	0.8	0.9	0.9	1.2			0.4	0.9	0.9
	A					(0.9)	0.9	0.9	(0.8)	0.9	0.8	1.1			0.4	0.9	0.8
	F					—	0.9	0.9	(0.7)	0.9	0.8	1.1			0.4	0.9	0.8
OD-x	**U**	1.8	1.9	—	(1.3)	(1.2)	0.9	0.9	(0.7)	1.1	1.1	1.4	—	(1.1)	0.5	0.9	0.9
	R	1.8	1.7	—	(1.3)	(1.1)	1.0	1.0	0.8	1.1	1.0	1.3	—	(1.2)	0.5	0.8	0.8
	A	1.7	1.7	—	(1.2)	(1.1)	1.0	1.0	0.8	1.1	1.1	1.3	—	(1.1)	0.5	0.8	0.8
	F	1.8	1.6	—	(1.1)	(1.0)	0.9	1.0	0.8	1.1	1.0	1.2	(0.9)	(1.1)	0.5	0.8	0.7

Table 5.2: Convergence rates of the errors $\delta_\ell \coloneqq \sigma - \sigma_\ell$, $e_\ell \coloneqq u - u_\ell$ and $\mathrm{D}e_\ell$, of their various error estimators, and of H_ℓ. Each row represents a benchmark example and a specific choice of refinement (see Table 5.1). The second column heading indicates if stabilisation is used ("☒", $C = 1$) or not ("□", $C = 0$). Errors of the optimal design benchmark ("OD") are not available and therefore left blank. The rates are given as powers of the representative mesh size $1/\sqrt{\mathrm{ndof}}$, which is proportional to H_ℓ for uniform mesh refinements up to boundary nodes. Convergence behaviour which is affected by significant oscillations is put into parentheses, or marked by "—" if it is inconclusive. See Section 5.7 for conclusions.

Akin to Theorem (4.4.4), (5.15) applies to all benchmark problems but the unmodified optimal design problem. Table 5.2 shows that the product $H_\ell^{-1} \|\!|u_\ell|\!\|_\ell \, \|u - u_\ell\|_{L^2(\Omega)}$ dominates the right-hand side in all examples and confirms (5.15). Moreover, (5.15) even holds with equality of the convergence rates for the two- and three-well examples. This demonstrates the efficiency of Theorem (4.4.4) for interface problems.

5.6.5 Error Estimator Reliability and Efficiency

Theorem (4.3.1) (page 79) claims

$$\|\sigma - \sigma_\ell\|^2_{L^{p'}(\Omega)} + \alpha \, \|u - u_\ell\|^2_{L^2(\Omega)} \lesssim \eta_{\mathrm{F},p,\ell} \, |u - u_\ell|_{W^{1,p}(\Omega)} \tag{5.16}$$

up to perturbations on the boundary, where the right-hand side is an upper bound of the L^2 error of u_ℓ also for the two-well benchmark with linear lower-order terms. Table 5.2 verify (5.16) with the pessimistic estimate $|u - u_\ell|_{W^{1,p}(\Omega)} \lesssim 1$. Moreover, in the examples with $p = 2$, Table 5.2 suggests that the estimate of Theorem (4.3.1) accurately predicts the errors of u_ℓ and σ_ℓ. In the case of the two-well benchmarks (with $p = 4$) the convergence rates of Table 5.2 also support (5.16), with $|u - u_\ell|_{W^{1,p}(\Omega)}$ replaced by $|u - u_\ell|_{H^1(\Omega)}$.

For the two-well benchmarks the improved analysis of Theorem (4.4.2) and Remark (4.4.3) in Section 4.4 (page 82) suggests furthermore

$$\|\sigma - \sigma_\ell\|^r_{L^{p'}(\Omega)} + \|u - u_\ell\|^2_{L^2(\Omega)} \lesssim \eta_{\mathrm{L},\ell} \quad \text{and} \quad |u - u_\ell|^2_{H^2(\Omega)} \lesssim \eta_{\mathrm{H},\ell},$$

which is confirmed by Table 5.2. In the case of adaptive mesh refinements the error estimators $\eta_{\mathrm{L},\ell}$ and $\eta_{\mathrm{H},\ell}$ indeed accurately predict the errors of the two-well and three-well examples.

Recall $\|u - u_\ell\|_{L^{p'}(\Omega)} \lesssim \|u - u_\ell\|_{L^2(\Omega)}$. With this relation, the efficiency estimate of Theorem (4.3.2) (page 80) states, up to oscillations of the lower-order terms and a Fortin interpolation error of σ,

$$\eta_{\mathrm{F},p,\ell} \lesssim \|\sigma - \sigma_\ell\|_{L^{p'}(\Omega)} + \alpha \, \|u - u_\ell\|_{L^2(\Omega)} .$$

The convergence rates of Table 5.2 support the estimate, however, with significant differences of the rates.

5.7 Summary and Concluding Remarks

The exhaustive numerical experiments of Section 5.6 culminate in Table 5.2 and permit us to compare the performance of the error estimators and to study the impact of the stabilisation a_ℓ. This section presents an analysis of the observations and points to open questions and possible further research. Boiger and Carstensen (2012+, Section 6) give a preliminary version of the following conclusions.

5.7.1 Impact of Stabilisation

For uniform mesh refinements the convergence rates of the error $\|\sigma - \sigma_\ell\|^2_{L^{p'}(\Omega)}$ with and without stabilisation coincide. This is also true for the error estimators $\eta_{\mathrm{A},p,\ell}$ and $\eta_{\mathrm{F},p,\ell}$ and, in the case of the two-well examples, for the errors $\|u - u_\ell\|^2_{L^2(\Omega)}$ and $|u - u_\ell|^2_{H^1(\Omega)}$. Stabilisation even improves the convergence rate of the stress σ_ℓ in the three-well example with uniform mesh refinements, which affirms that the stabilisation a_ℓ with $\gamma = 1$ preserves the convergence rate of the errors. The adaptive mesh refinements of Section 5.2, however, exhibit suboptimal convergence rates of the errors with added stabilisation, which attests to the perturbation that accompanies the stabilisation term. In particular, the convergence rates of the stress σ_ℓ of the two- and three-well benchmarks are significantly lower with stabilisation. This suggests that the adaptive mesh refinements are not well-suited for stabilised problems and an improved adaptive algorithm beyond the scope of the thesis is required which balances local refinements with global stabilisation. As an exception, the stabilisation actually facilitates the convergence of the error $\|u - u_\ell\|^2_{L^2(\Omega)}$, and even of $|u - u_\ell|^2_{H^1(\Omega)}$, in the case of the modified optimal design benchmark with "R"- and "A"-adaptive mesh refinements.

Figure 5.2 shows that the use of stabilisation can indeed lead to improved condition numbers of the Hessian of the discrete energy. In particular, the adaptive algorithms fails in the three-well example without stabilisation due to the ill-conditioned Hessian (cf. Subsection 5.6.2).

5.7.2 Impact of Adaptive Mesh Refinements

In the case of the two-well and the three-well problems without stabilisation, the observed convergence rates of the errors $\|\sigma - \sigma_\ell\|^2_{L^{p'}(\Omega)}$ and $\|u - u_\ell\|^2_{L^2(\Omega)}$ and, to a lesser extent, their estimators $\eta_{\mathrm{R},p,\ell}$, $\eta_{\mathrm{A},p,\ell}$ and $\eta_{\mathrm{F},p,\ell}$ are approximately higher for adaptive mesh refinements in comparison to uniform refinements. Figures A.2 and A.4 also suggest that adaptivity improves the convergence of the gradient error $|u - u_\ell|^2_{H^1(\Omega)}$ without stabilisation. Yet, with stabilisation the errors of u_ℓ and σ_ℓ converge faster for uniform meshes than for adaptive meshes.

From (5.10) we expect that adaptive mesh refinements improve the convergence rates of the error estimators (cf. Cascón et al., 2008; Kreuzer and Siebert, 2011). In the case of the two-well benchmark Table 5.2 confirms this expectation for all error estimators of Section 5.2. For the stabilised three-well example, however, Table 5.2 shows that adaptivity severely reduces the convergence speed of $\eta_{\mathrm{F},2,\ell}$ (for "F"-adaptive mesh refinements) or even leads to no convergence at all (for "R"- and "A"-adaptive mesh refinements).

For the optimal design example, the convergence of the global mesh size H_ℓ in Table 5.2 indicates that adaptivity yields almost uniform mesh refinements. This accounts for the fact that, in contrast to the preceding observations, the convergence rates of the error $\|\sigma - \sigma_\ell\|^2_{L^{p'}(\Omega)}$ and its estimators $\eta_{\mathrm{R},p,\ell}$, $\eta_{\mathrm{A},p,\ell}$ and $\eta_{\mathrm{F},p,\ell}$ are mostly unaffected by the use of adaptive mesh refinements.

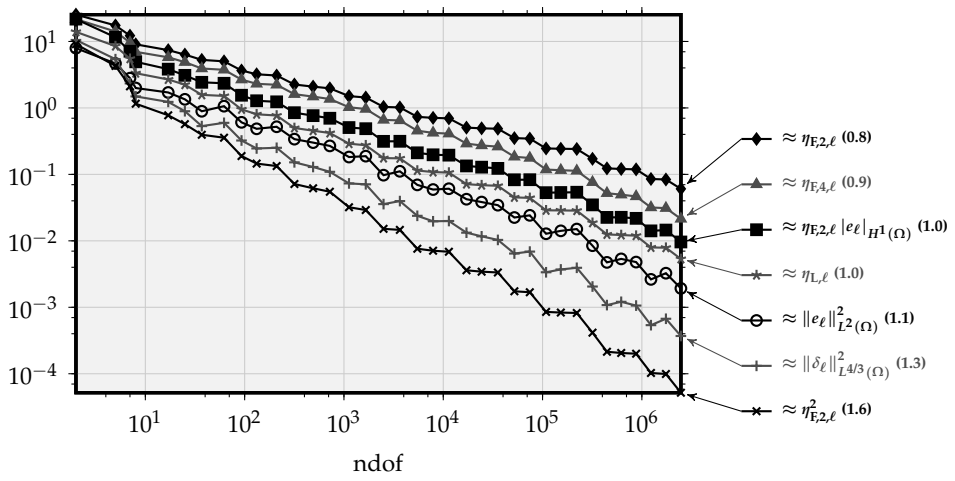

Figure 5.9: Reliability and efficiency of the flux error estimator $\eta_{\mathrm{F},\cdot,\ell}$ and the improved interface error estimator $\eta_{\mathrm{L},\ell}$ using the two-well example ("2W-Q") with "F"-adaptive mesh refinements. The numbers in parentheses are the actual convergence rates, as powers of the representative mesh size $1/\sqrt{\mathrm{ndof}}$ akin to Table 5.2. Recall $e_\ell \coloneqq u - u_\ell$ and $\delta_\ell \coloneqq \sigma - \sigma_\ell$, and note that, in order to emphasize the difference of the slopes, the graphs of this figure are rescaled, i.e., shifted vertically, such that no intersections occur.

5.7.3 Strong Convergence of Gradients

Up to smoothness conditions and the values of α, the a priori convergence result of Theorem (4.2.1) (page 75, see also Remark (4.2.2), page 75) reads $\|u - u_\ell\|^2_{H^1(\Omega)} \lesssim H_\ell$ for all benchmark examples. Table 5.2 shows that the two- and three-well interface problems clearly fall short of Theorem (4.2.1), whereas the modified optimal design benchmark exceeds the predicted convergence rate. Figure A.10 demonstrates that, surprisingly, stabilisation in fact *improves* the error $\|u - u_\ell\|^2_{H^1(\Omega)}$ in the optimal design example, with the exception of "F"-adaptive mesh refinements.

The error estimator $\eta_{\mathrm{H},\ell}$ for interface problems with $\alpha > 0$ accurately predicts the error $|u - u_\ell|^2_{H^1(\Omega)}$ of the gradient, even in the case of the three-well example. This holds for uniform and (with high precision) adaptive mesh refinements and indicates that $\eta_{\mathrm{H},\ell}$ is a reliable and efficient error estimator for stabilised interface problems.

5.7.4 Reliability-Efficiency Gap

The experiments verify the estimate (5.16) of Theorem (4.3.1) (page 79). In fact, the error $\|\sigma - \sigma_\ell\|^2_{L^{p'}(\Omega)}$ converges considerably faster than the estimator $\eta_{\mathrm{F},p,\ell}$. This illustrates that the estimate $|u - u_\ell|_{W^{1,p}(\Omega)} \lesssim 1$ does not reflect the true convergence $u_\ell \to u$ in $W^{1,p}(\Omega)$ and is too pessimistic (see also the discussion on page 80, following Theorem (4.3.1)). Table 5.2 confirms that the product $\eta_{\mathrm{F},p,\ell}\,|u - u_\ell|_{H^1(\Omega)}$ predicts the error $\|\sigma - \sigma_\ell\|^2_{L^{p'}(\Omega)}$ more accurately than $\eta_{\mathrm{F},p,\ell}$ alone, in fact precisely in the case of the modified optimal design benchmark.

Figure 5.9 illustrates the reliability-efficiency gap as the literal gap which is visible between the convergence graphs of the (reliable) error estimators $\eta_{\mathrm{F},2,\ell}$ and $\eta_{\mathrm{F},4,\ell}$ and the

(efficient) error estimator $\eta^2_{\mathrm{F},2,\ell}$. The figure also demonstrates that the improved error estimator $\eta_{\mathrm{L},\ell}$ converges faster than the general estimator $\eta_{\mathrm{F},2,\ell}$. Table 5.2 shows that the improvement is significant and that the error estimators $\eta_{\mathrm{L},\ell}$ and $\eta_{\mathrm{H},\ell}$ for interface problems accurately predict the errors in the case of adaptive mesh refinements with stabilisation. Therefore the results of Section 4.4 (page 82) actually narrow the reliability-efficiency gap.

A Benchmark Convergence Graphs

This appendix chapter collects the convergence graphs of the benchmark examples of Section 5.6 (page 102). The following figures depict the graphs of the errors of u_ℓ and σ_ℓ and the error estimators of Section 5.2 (page 94). For adaptive mesh refinements the figures also depict H_ℓ.

Each benchmark example has been computed with and without stabilisation, with uniform and with adaptive mesh refinements. The letters in parentheses in the labels of each graph distinguish between stabilised and nonstabilised computations (stabilisation is marked with an "S"), and between uniform and adaptive mesh refinements (see Table 5.1, page 92, for the abbreviations).

Note that each benchmark is represented by two figures in this appendix chapter: one figure depicts the errors $\|u - u_\ell\|^2_{L^2(\Omega)}$ and $\|\sigma - \sigma_\ell\|^2_{L^{p'}(\Omega)}$ and their estimators $\eta_{\mathrm{F},p,\ell}$, $\eta_{\mathrm{R},p,\ell}$, $\eta_{\mathrm{A},p,\ell}$ and $\eta_{\mathrm{L},\ell}$, another figure depicts the error $|u - u_\ell|^2_{H^1(\Omega)}$ and its estimator $\eta_{\mathrm{H},\ell}$. Since the former figures are already saturated with convergence graphs, the extra graphs of H_ℓ are also part of the latter figures. In order to keep the amount of graphs per figure moderate, some graphs — like "R"- and "A"-adaptive computations with stabilisation, or interface error estimators without stabilisation — are not shown.

Refer to Chapter 5 for a description of the numerical experiments which lead to the following graphs, and to Section 5.6 (page 102) for a summary of the individual benchmark examples, in particular to Table 5.2 (page 106) for an assembly of the convergence rates.

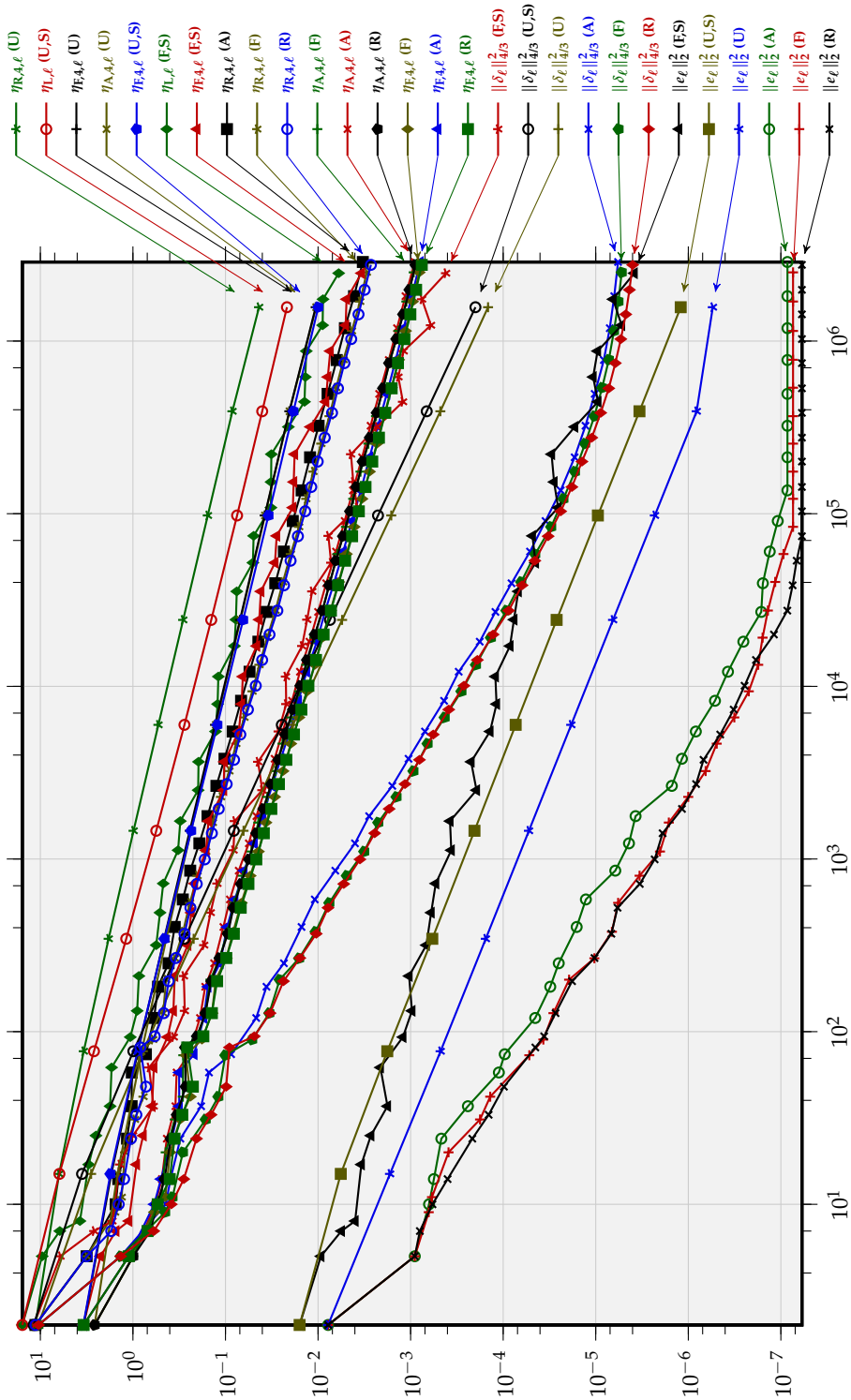

Figure A.1: Convergence graphs of the errors $e_\ell := u - u_\ell$ and $\delta_\ell := \sigma - \sigma_\ell$, and of their estimators for the two-well benchmark with quadratic lower-order terms ("2W-Q"), plotted against the number of degrees of freedom. The letters in parentheses denote the refinement indicator (see Table 5.1, page 92) and the use of stabilisation ("S").

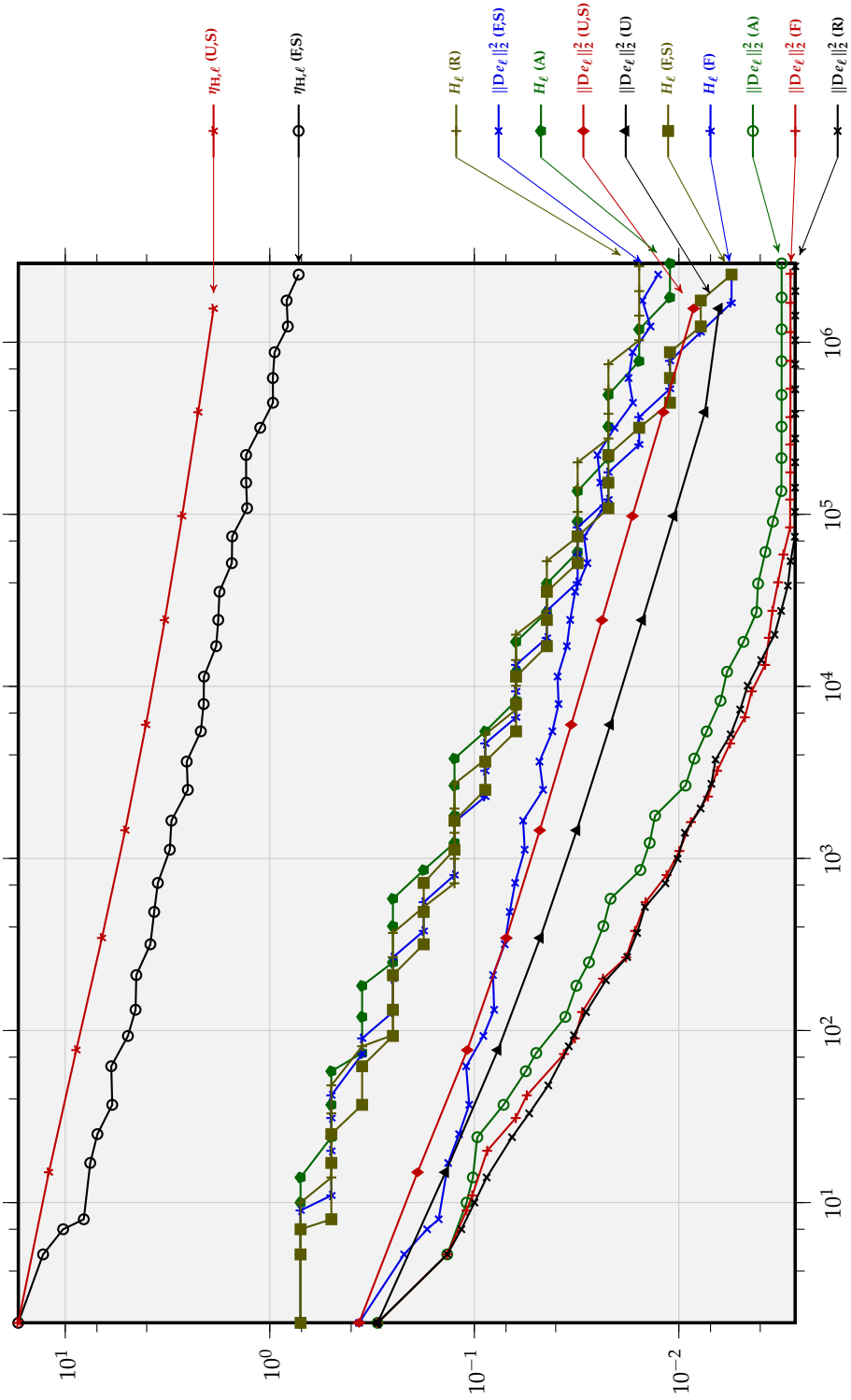

Figure A.2: Convergence graphs of the error $De_\ell := D(u - u_\ell)$, the error estimator $\eta_{H,\ell}$, and of H_ℓ, for the two-well benchmark with quadratic lower-order terms ("2W-Q"), plotted against the number of degrees of freedom. The letters in parentheses denote the refinement indicator (see Table 5.1, page 92) and the use of stabilisation ("S").

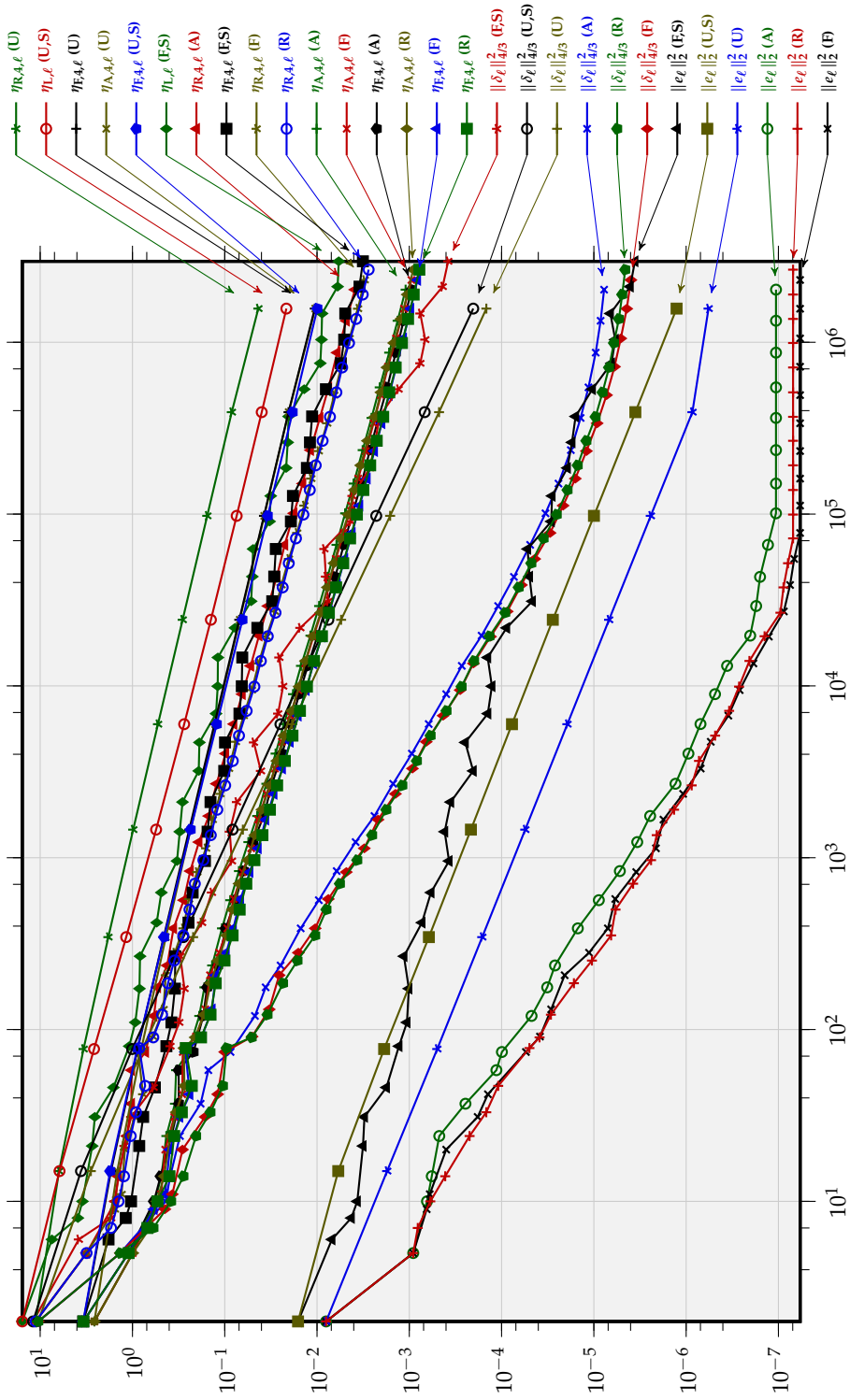

Figure A.3: Convergence graphs of the errors $e_\ell := u - u_\ell$ and $\delta_\ell := \sigma - \sigma_\ell$, and of their estimators for the two-well benchmark with linear lower-order terms ("2W-L"), plotted against the number of degrees of freedom. The letters in parentheses denote the refinement indicator (see Table 5.1, page 92) and the use of stabilisation ("S").

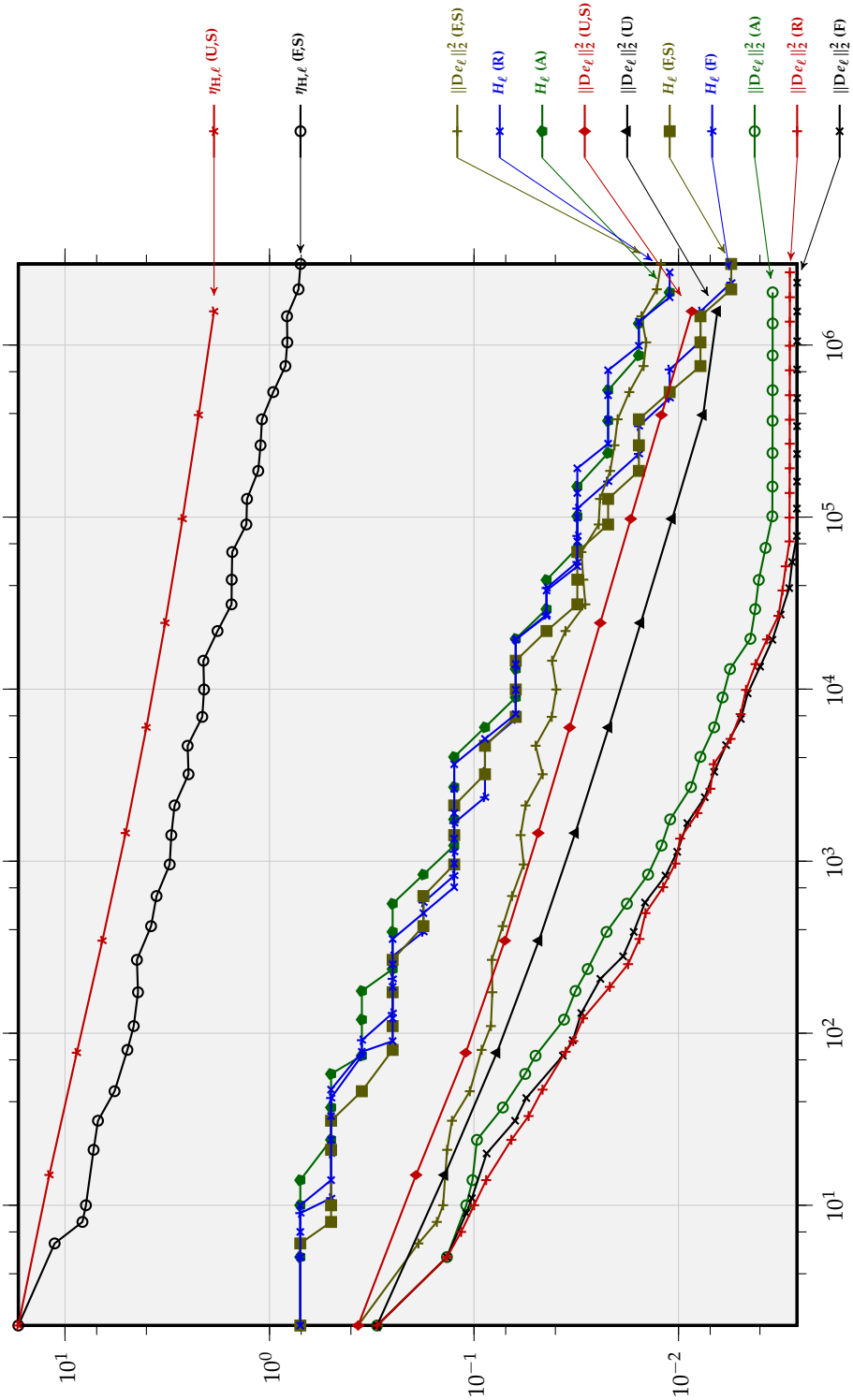

Figure A.4: Convergence graphs of the error $De_\ell := D(u - u_\ell)$, the error estimator $\eta_{H,\ell}$, and of H_ℓ, for the two-well benchmark with linear lower-order terms ("2W-L"), plotted against the number of degrees of freedom. The letters in parentheses denote the refinement indicator (see Table 5.1, page 92) and the use of stabilisation ("S").

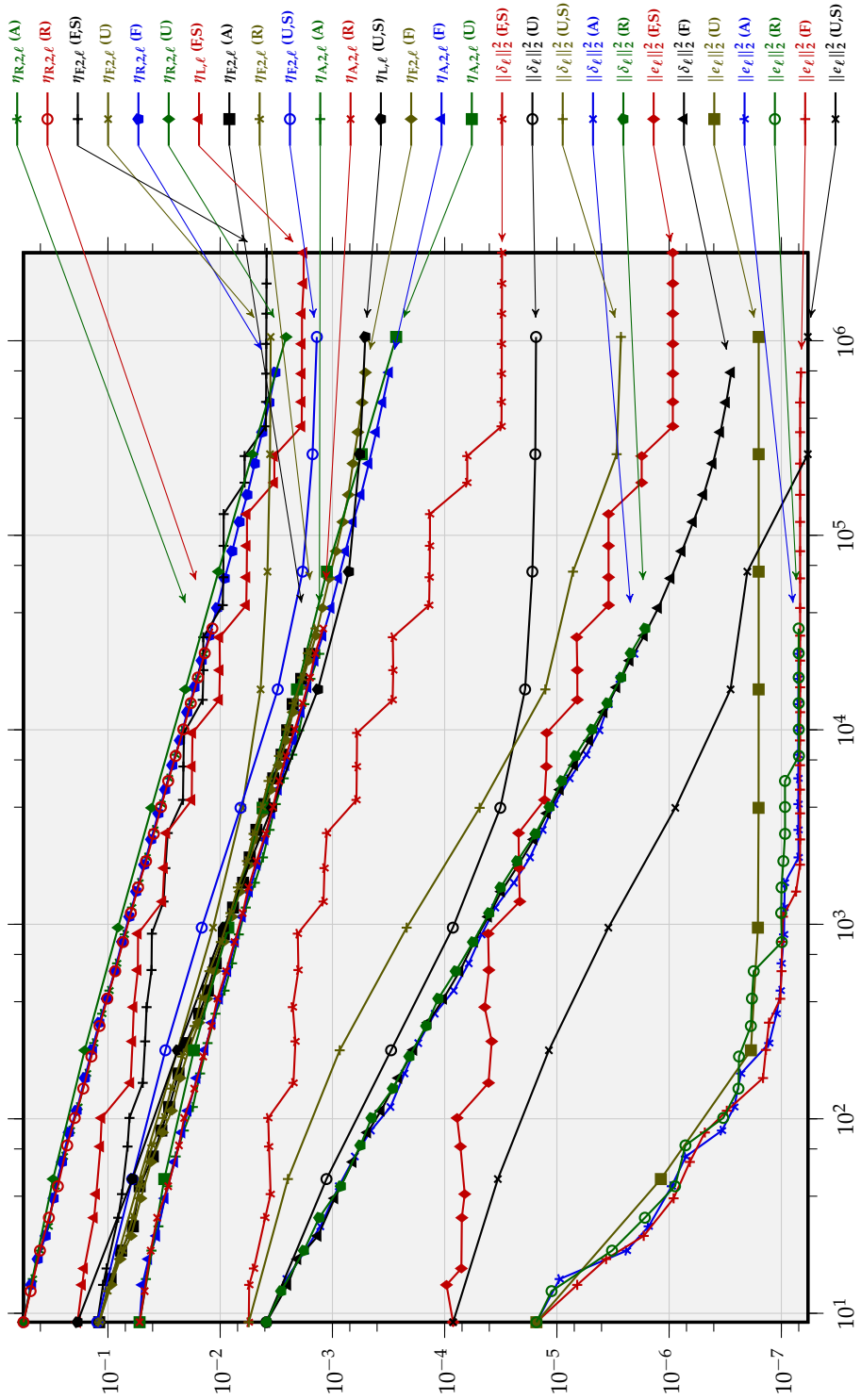

Figure A.5: Convergence graphs of the errors $e_\ell := u - u_\ell$ and $\delta_\ell := \sigma - \sigma_\ell$, and of their estimators for the three-well benchmark ("3W"), plotted against the number of degrees of freedom. The letters in parentheses denote the refinement indicator (see Table 5.1, page 92) and the use of stabilisation ("S").

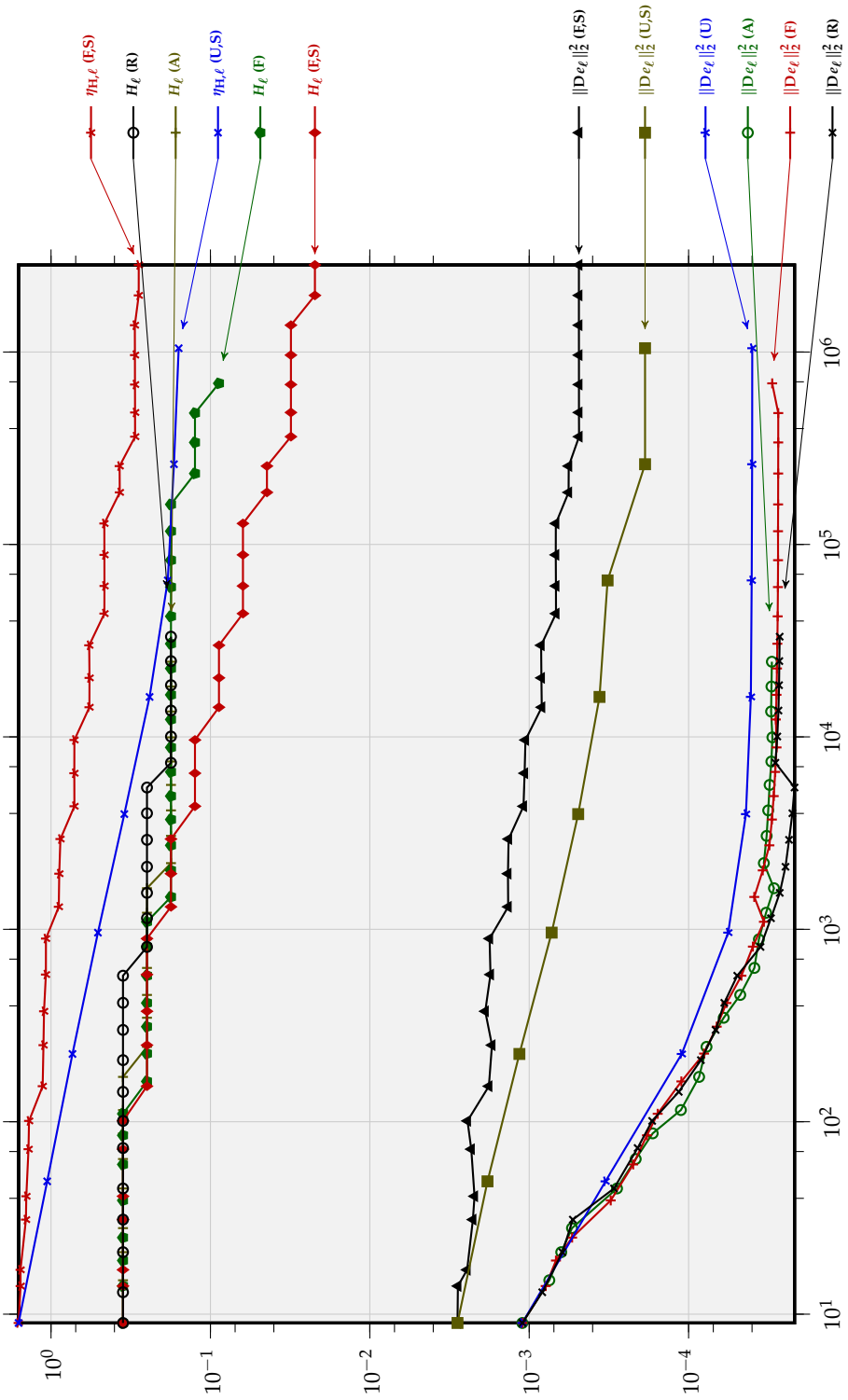

Figure A.6: Convergence graphs of the error $De_\ell := D(u - u_\ell)$, the error estimator $\eta_{H,\ell}$, and of H_ℓ, for the three-well benchmark ("3W"), plotted against the number of degrees of freedom. The letters in parentheses denote the refinement indicator (see Table 5.1, page 92) and the use of stabilisation ("S").

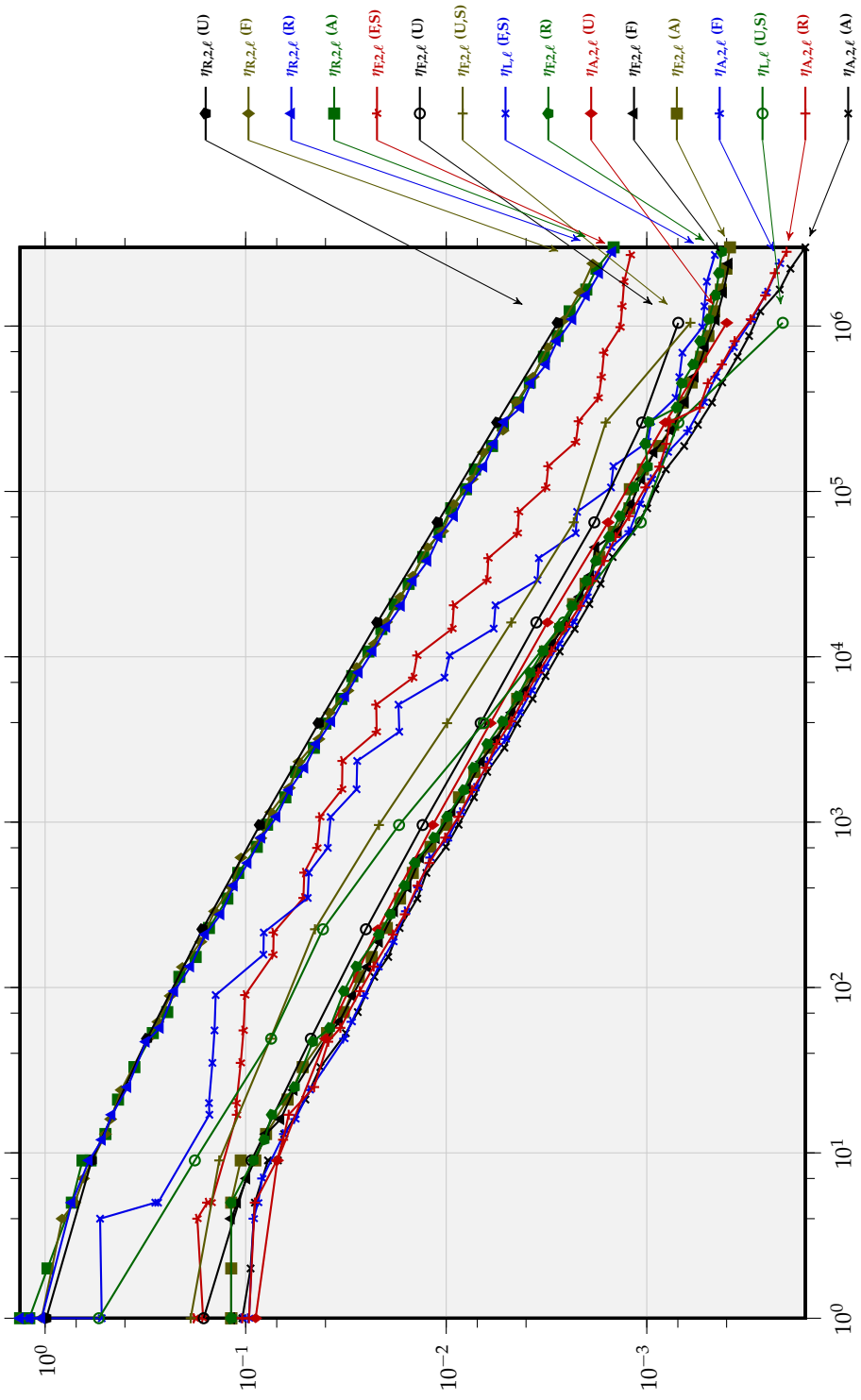

Figure A.7: Convergence graphs of the error estimators $\eta_{F,2,\ell}$, $\eta_{R,2,\ell}$, $\eta_{A,2,\ell}$, and $\eta_{L,\ell}$ for the optimal design benchmark ("OD"), plotted against the number of degrees of freedom. The letters in parentheses denote the refinement indicator (see Table 5.1, page 92) and the use of stabilisation ("S").

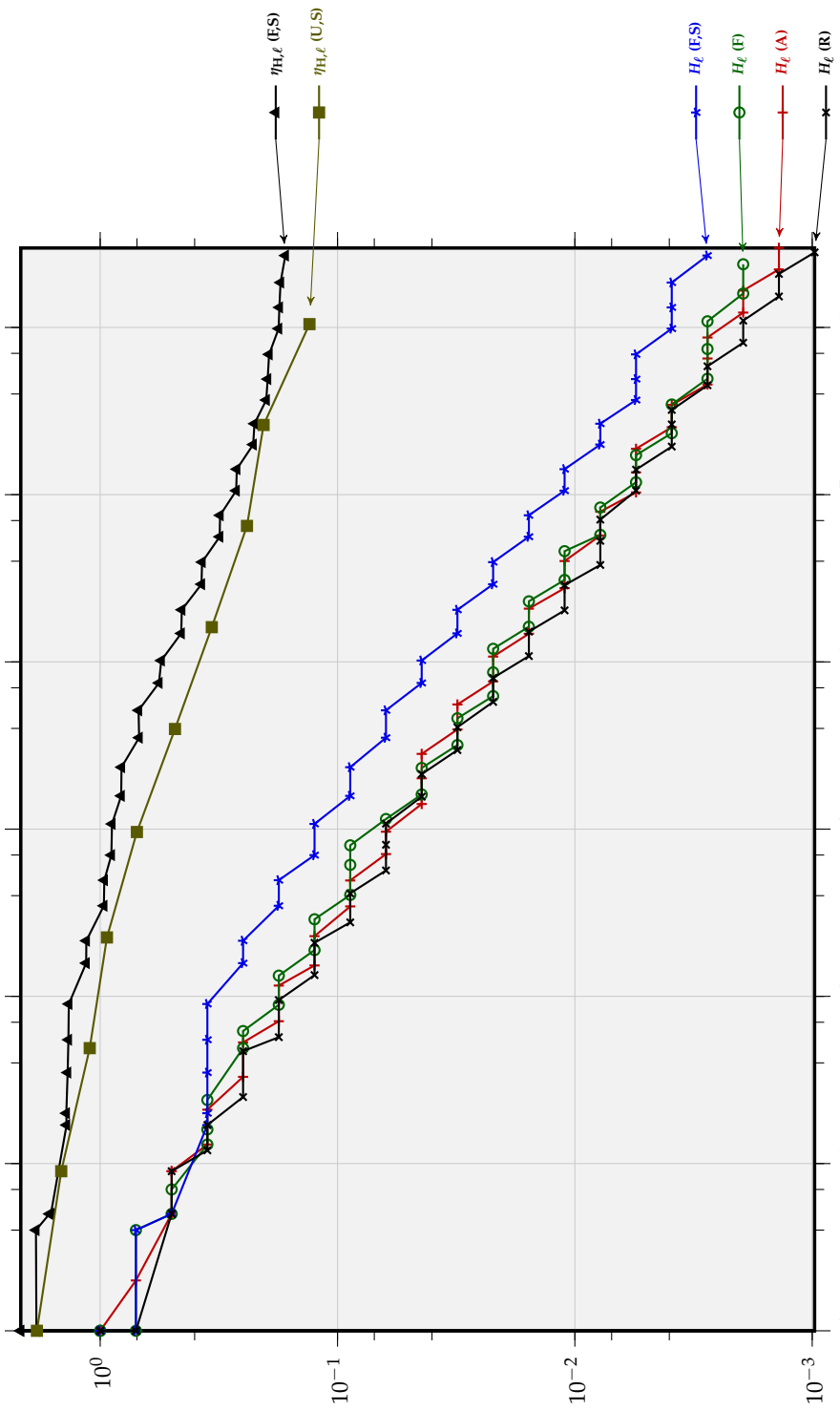

Figure A.8: Convergence graphs of the error estimator $\eta_{H,\ell}$ and of H_ℓ for the optimal design benchmark ("OD"), plotted against the number of degrees of freedom. The letters in parentheses denote the refinement indicator (see Table 5.1, page 92) and the use of stabilisation ("S").

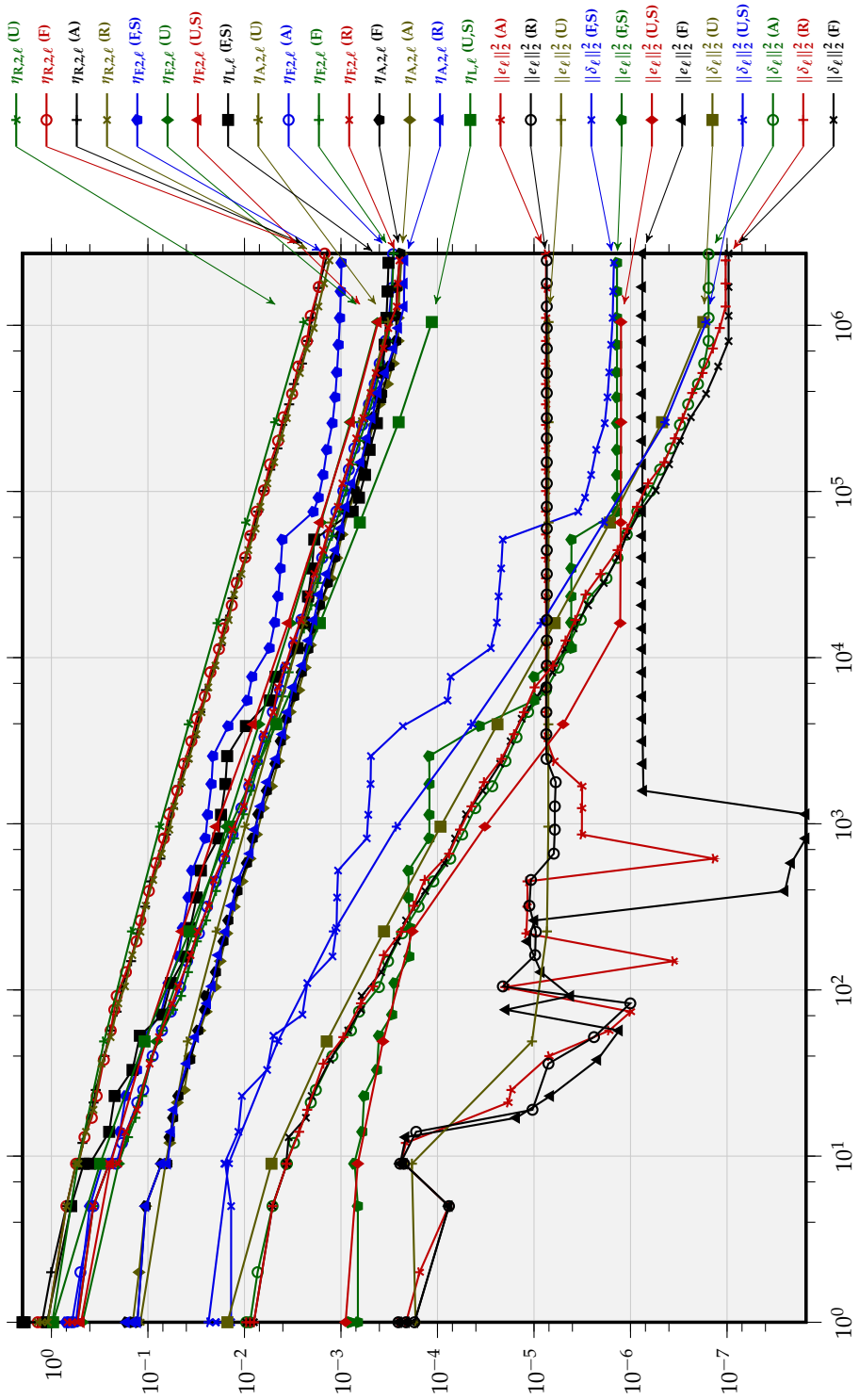

Figure A.9: Convergence graphs of the errors $e_\ell := u - u_\ell$ and $\delta_\ell := \sigma - \sigma_\ell$, and of their estimators for the modified optimal design benchmark ("OD-x"), plotted against the number of degrees of freedom. The letters in parentheses denote the refinement indicator (see Table 5.1, page 92) and the use of stabilisation ("S").

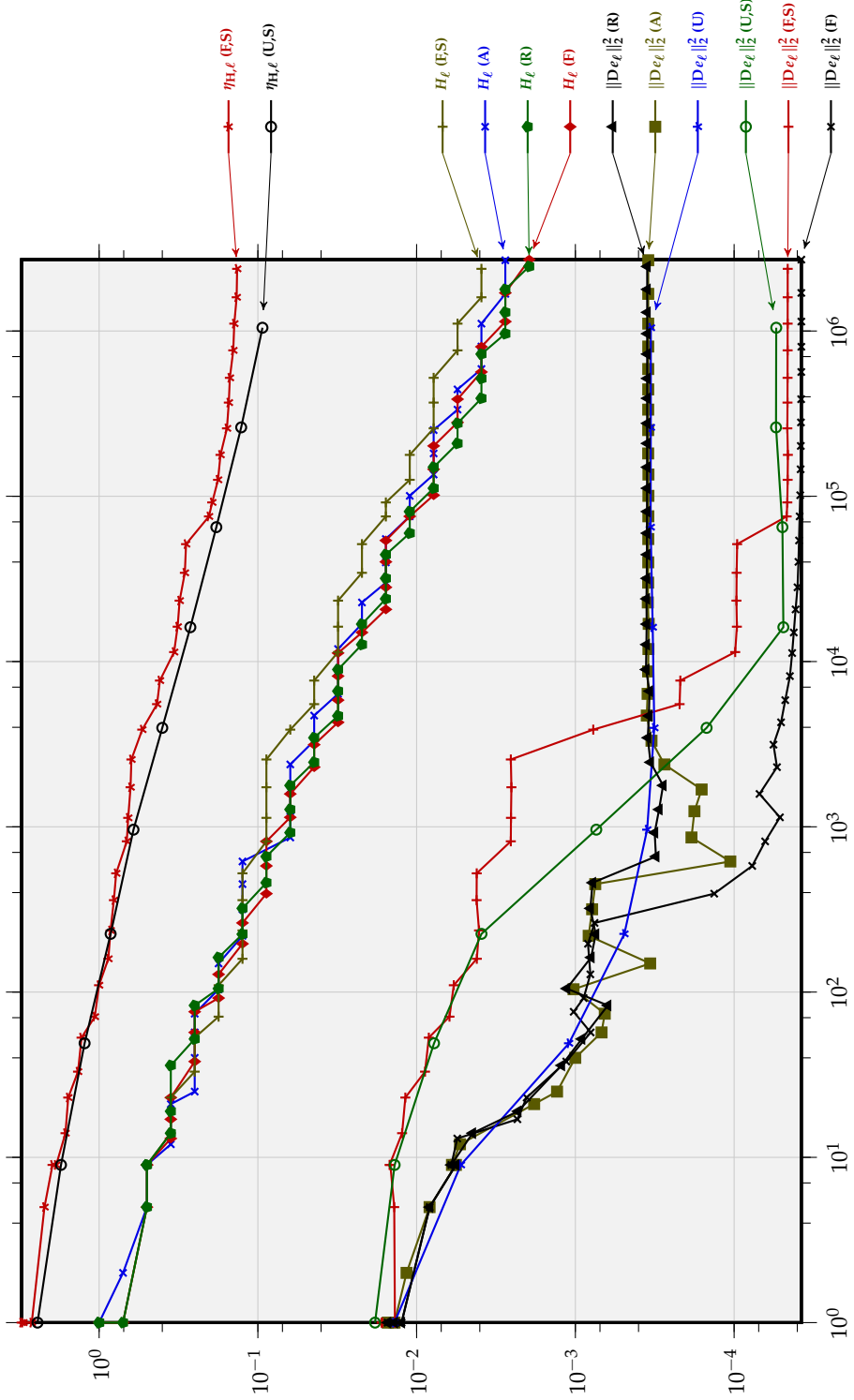

Figure A.10: Convergence graphs of the error $De_\ell := D(u - u_\ell)$, the error estimator $\eta_{H,\ell}$, and of H_ℓ, for the modified optimal design benchmark ("OD-x"), plotted against the number of degrees of freedom. The letters in parentheses denote the refinement indicator (see Table 5.1, page 92) and the use of stabilisation ("S").

B MATLAB Implementation

This appendix chapter introduces the MATLAB code which implements the algorithms and numerical experiments of Chapter 5 and Appendix A. The complete code files are attached to the thesis as Compact Disc. [1]

B.1 Structure of the Implementation

This section outlines the structure of the MATLAB implementation which realises the algorithms of Chapter 5. The data structures are based on finite element code for linear problems (cf. Alberty et al., 1999; Carstensen and Numerical Analysis Group, HU Berlin, 2009). The disc contains 5 338 lines of MATLAB code, including comment lines. The scientific implementation, encompassing the four steps of the AFEM loop, consists of 3 298 lines of MATLAB code, with 362 lines copied or adapted from the AFEM software package (Carstensen and Numerical Analysis Group, HU Berlin, 2009). 2 040 lines of MATLAB code concern data management and plotting of convergence graphs and solutions. Additionally, the code archive contains 443 lines of Python code which prepares data files for convergence graphs and for the Table 5.2 of convergence graphs (page 106).

The following paragraphs provide the prototypes of the majority of the MATLAB functions on the disc, mostly followed by short explanations of usage information and implementation details. Refer to the help comments in the MATLAB function files for additional documentation.

Generic AFEM Loop

The following subroutines organise the numerical realisation of the AFEM loop of Section 5.1 (page 93).

```
function afemLoop(filePrefix,solveFcn,estimateFcn,           ...
                  markType,markLimit,uDFcn,maxLevel,maxNdof, ...
                  c4n0,n4e0,n4sDb0,u0)
```

The function `afemLoop` contains the AFEM loop itself (cf. Section 5.1, page 93). It loads previous numerical results with the function `afemLoadLevel` and stores new results with `afemSaveLevel`. It also implements the step MARK and employs the functions `refineUniformRed` and `refineRGB` for the step REFINE. The user-provided function handles `solveFcn` and `estimateFcn` need to implement SOLVE and ESTIMATE, which are not part of `afemLoop`.

[1] The online version of this document contains the content of the Compact Disc as embedded tar-file. Please use an appropriate pdf viewer to extract the file, such as KDE Okular or Adobe Reader. In contrast to the thesis' text, the code is provided under the terms of the GNU General Public License as published by the Free Software Foundation, either version 3 of the License, or (at your option) any later version. Refer to the file `LICENSE.txt` on the Compact Disc or in the tar-file for more information.

```
function [u,E,niter,nfev,ddEcond] = solveP1Nonlinear(        ...
                        u,W,f,g,alpha,fDegree,gDegree,f2int, ...
                    c4n,n4e,n4sDb,Stab,area4e,P1Grad,optimType)
```

The function `solveP1Nonlinear` prepares the energy functional of the minimisation problem and calls a minimiser with the help of `minWrapper`. It is the core of the solver and explained in Section B.2 with a full code listing.

```
function afemRun(filePrefix,maxNdof,maxLevel,                ...
             c4n,n4e,n4sDb,u,W,p,f,g,alpha,fDegree,gDegree, ...
            markType,markLimit,stabType,stabGamma,stabCoef, ...
                                          estimType,optimType)
```

The function `afemRun` is designed as a wrapper around `afemLoop`. It contains dispatcher functions which redirect to `solveP1Nonlinear` for SOLVE and to one of the estimation functions for ESTIMATE.

```
function afemPostprocess(filePrefix,levels,what,             ...
                u,W,f,g,alpha,uDegree,WDegree,fDegree,gDegree,p)
```

The function `afemPostprocess` reads existing numerical solutions from the filesystem and appends errors and error estimators to the respective data files. Note that `afemRun` only computes and stores the estimator which is required for mesh refinements. `afemRun` does not compute an error estimator at all if uniform mesh refinements are requested.

Problem-Specific Functions

The following functions implement the problems of Sections 2.3, 2.4 and 2.5. Functions for the two-well problem are prefixed with `cckj_`, for the three-well problem with `sb_`, for the optimal design problems with `od_`, and for the Poisson model problem with `poisson_`. Although the Poisson model problem is not subject of this thesis, the MATLAB implementation of the optimal design problem depends on code for the Poisson model problem. Therefore, the latter is also included on the disc.

```
function [f,df,ddf] = cckj_f(x)
function g = cckj_g(x)
function f = sb_f(x)
function f = od_f(x,type)
function f = poisson_f(x,type)
```

The preceding functions implement the lower-order terms of the respective problems.

```
function cckj_run(filePrefix,maxNdof,estimType, ...
                    stabType,stabGamma,stabCoef,geometry,type)
function sb_run(filePrefix,maxNdof,estimType, ...
                        stabType,stabGamma,stabCoef,geometry)
function od_run(filePrefix,maxNdof,estimType, ...
                          stabType,stabGamma,stabCoef,odType)
function poisson_run(filePrefix,maxNdof,estimType,poissonType)
function cckj_pp(filePrefix,levels,what,type)
function sb_pp(filePrefix,levels,what)
function od_pp(filePrefix,levels,what,odType)
function poisson_pp(filePrefix,levels,what,poissonType)
```

The preceding functions call `afemRun` and `afemPostprocess` with the proper, problem-specific function handles as arguments.

```
function [u,du,ddu] = cckj_u(x)
function [u,du,ddu] = sb_u(x)
function [u,du,ddu] = od_u(x,type)
function [u,du,ddu] = poisson_u(x,type)
```

The preceding methods evaluate the exact solution for each of the problems and their first and second derivative.

```
function [w,dw,ddw] = cckj_Wnc(dx)
function [w,dw,ddw] = cckj_W(dx)
function [w,dw,ddw] = sb_W(dx)
function [w,dw,ddw] = od_W(dx,type)
function [w,dw,ddw] = poisson_W(dx)
```

These functions evaluate the convexified energy density of the respective problem and its first and second derivative. As an exception `cckj_Wnc` implements the non-convex energy density of the two-well problem (cf. (2.12), page 25).

Error Estimation

The following functions implement the a posteriori error estimators of Sections 3.3, 3.4 and 4.3. They are referenced by `afemRun`, but actually called by `afemLoop`.

```
function [eta4e,errBnd,sigBnd,rhsBnd] =                          ...
       estimateResidual(u,W,fl,flDegree,p,c4n,n4e,area4e,P1Grad)
function [eta4e,errBnd,sigBnd,divBnd,oscBnd] =                   ...
          estimateFlux(u,W,fl,flDegree,p,c4n,n4e,area4e,P1Grad)
```

These functions implement the residual-based error estimator $\eta_{\mathrm{R},p,\ell}$, the flux error estimator $\eta_{\mathrm{F},p,\ell}$, and the corresponding refinement indicators $\eta_{\mathrm{R},p,\ell}(T)$ and $\eta_{\mathrm{F},p,\ell}(T)$ per triangle T. Amongst the return values are the individual summands which form the error estimator. E.g., `sigBnd` and `rhsBnd` of the residual-based error estimator function `estimateResidual` contain the value of the surface and the volume term, respectively.

```
function eta4e = estimateSigmaAveragingP1(c4n,n4e,u4e,p,      ...
                                                  area4e,area4n)
```

The function `estimateSigmaAveragingP1` returns the averaging refinement indicator $\eta_{\mathrm{A},p,\ell}(T)$ for all elements T. To obtain the value of the averaging error estimator $\eta_{\mathrm{A},p,\ell}$, the code in `afemRun` and `afemPostprocess` computes the ℓ^p norm of the vector in `eta4e`.

Mesh Refinements

The functions `refineRGB` and `refineUniformRed` implement the red-green-blue mesh refinements of Section 5.3. They are called by `afemLoop`. The output variable `Pn4n` is required to prolongate a discrete P_1 conforming function from the original mesh to the refined mesh.

```
function [c4n,n4e,n4sDb,n4sNb,Pe4e,Pn4n] ...
                = refineRGB(c4n,n4e,n4sDb,n4sNb,ms,n4s,s4n,s4e)
function [c4n,n4e,n4sDb,n4sNb,Pe4e,Pn4n]...
       = refineUniformRed(c4n,n4e,n4sDb,n4sNb,n4s,s4n,s4e,mid4s)
```

Generation of Triangulation Data Structures

Functions with the prefix `compute` generate vectors which contain various triangulation-related data. A significant amount of the code therein is copied or derived from the AFEM software package.

```
function e4n = computeE4n(n4e)
function e4s = computeE4s(n4e)
function n4s = computeN4s(n4e)
function s4e = computeS4e(n4e)
function s4n = computeS4n(n4e,n4s)
```

The preceding functions generate matrices of integers that describe the relations between the triangles, the edges and the nodes.

```
function area4e = computeArea4e(c4n,n4e)
function area4n = computeArea4n(c4n,n4e,area4e)
function length4s = computeLength4s(c4n,n4s)
function mid4s = computeMid4s(c4n,n4s)
function normal4s = computeNormal4s(c4n,n4s)
function tangent4s = computeTangent4s(c4n,n4s)
function P1Grad = computeP1Grad(c4n,n4e,area4e)
```

The preceding functions generate real-valued data, like areas of triangles, or unit normal vectors of edges, which are particularly important for error estimators. The three-dimensional array `P1Grad` describes the gradients of nodal basis functions and facilitates fast computation of the energy in `solveP1Nonlinear`.

Stabilisation

The following functions with the prefix `stab` implement the stabilisation terms of Section 3.5 (page 59). Recall that the stabilisation is a bilinear form. Since the MATLAB implementation applies the stabilisation to P_1 conforming finite element functions only, these functions generate matrices `S` which represent the bilinear form in the finite-dimensional space of P_1 conforming functions.

```
function S = stabBCPP1(c4n,n4e,gamma,P1Grad,e4s,length4s)
function S = stabBCPP2(c4n,n4e,gamma,area4e,P1Grad,area4n)
function S = stabBCPP3(c4n,n4e,gamma,area4e,P1Grad)
```

The preceding functions implement the stabilisation functions of Bartels et al. (2004b) (see Section 3.5, page 59).

```
function S = stabWBCC(c4n,n4e,gamma,P1Grad,e4s,maxLength4s)
```

The function `stabWBCC` implements the stabilisation a_ℓ of (3.53) (page 61). See Section B.3 for an explanation with a full code listing.

Plotting

The following methods generate plots of graphs and of functions $v : \Omega \subset \mathbb{R}^2 \to \mathbb{R}$. The plots in this thesis, in particular in Appendix A, are based on these methods. Their purpose is to permit automatic generation of plots and to provide a unified plotting interface for MATLAB as well as Octave.

```
function afemPlot1Ndof(tablefilename,dirprefix,maxndof,      ...
                                          slopeweight,varargin)
function afemPlot1(varargin)
```

The function `afemPlot1` generates two-dimensional plots of curves, e.g., of the convergence graphs of Appendix A. To generate convergence plots based on numerical experiments, `afemPlot1Ndof` reads the data from the filesystem and calls `afemPlot1` to render the plot. The operation of `afemPlot1Ndof` is controlled by a so-called table file. Such files are easily created by hand for simple plots. The table files for the voluminous plots of Appendix A are generated with the Python script `make_afemplot_table.py`. Besides the plot itself, the function `afemPlot1Ndof` returns the approximate convergence rate of each graph it evaluated. The Python script `make_afemplot_tabular.py` transforms these convergence rates into a LaTeX tabular like the one in Table 5.2 (page 106).

```
function afemPlot2(c4n,n4e,u4e,output,color,lines,axes,tics, ...
                                                  view,colorbox)
```

The function `afemPlot2` generates plots of triangulations, e.g. in Figure 5.8 (page 104).

```
function afemPlot3(c4n,n4e,u4n4e,u4e,output,color,lines,     ...
                                                 axes,tics,view)
```

The method `afemPlot3` generates three-dimensional plots of functions of the form $v : \Omega \subset \mathbb{R}^2 \to \mathbb{R}$, e.g. in Figure 2.8 (page 30).

```
function afemPlotCore(type,output,color,axes,tics,view,varargin)
```

Since the implementations of `afemPlot1`, `afemPlot2` and `afemPlot3` share significant amounts of code, these three functions are merely wrappers which call `afemPlotCore`. For three-dimensional plots the function `afemPlotCore` relies on the software `gnuplot` to generate the output file.

Miscellaneous Functions

```
function [x,y,niter,nfev] = minWrapper(f,x,type)
```

MATLAB and Octave ship different methods for the minimisation of nonlinear functionals: `fminunc` for MATLAB, `sqp` for Octave. To provide a generic minimiser with a unified interface, `minWrapper` determines its execution environment and redirects the call to the appropriate function. This ensures compatibility of the numerical codes with Octave.

```
function defaultArgIn(name,def)
```

The function `defaultArgIn` encapsulates boilerplate code for the handling of optional function arguments. Almost all of the other MATLAB functions on the disc use it to fill input variables with default values if the caller does not provide a value.

B.2 Numerical Solution of the Nonlinear Problem

This section presents the function `solveP1Nonlinear`. The function is at the heart of the solution process since it implements the energy functional of (3.10) (page 40), i.e.,

$$E_\ell^{\star\star}(v_\ell) = \int_\Omega \left(W^{\star\star}(\mathrm{D}v_\ell(x)) + \alpha \left| v_\ell(x) - f(x) \right|^2 - g(x)v_\ell(x) \right) \mathrm{d}x + \frac{1}{2} a_\ell(v_\ell, v_\ell)$$

for P_1 conforming finite element functions v_ℓ. The code also implements the first and second derivative of the energy functional to increase the speed of the Newton-Raphson solver: MATLAB's `fminunc` would approximate these derivative otherwise, which is a computationally expensive operation. In spite of this, the implementation is surprisingly short, therefore a complete printout of the code is provided below. The function is also part of the disc which is delivered with the thesis.

The prototype of `solveP1Nonlinear` reads

```
function [u,E,niter,nfev,ddEcond] = solveP1Nonlinear(        ...
                        u,W,f,g,alpha,fDegree,gDegree,f2int, ...
                    c4n,n4e,n4sDb,Stab,area4e,P1Grad,optimType)
```

The function handles `W`, `f` and `g`, and the scalar `alpha` define the energy density and the lower-order terms of the energy functional. The arguments `fDegree` and `gDegree` describe the polynomial degree of the respective functions. This information is used for the quadrature of the lower-order terms. The input vector `u` contains the nodal values of the P_1 conforming finite element function which is the initial guess for the iterative solver. In particular, its values on boundary nodes must correctly represent the Dirichlet boundary values. The arguments `c4n`, `n4e`, and `n4sDb` describe the current triangulation.

The remaining input arguments are optional and may be empty or omitted. `f2int` may contain the value of the integral of $\int_\Omega f(x)^2 \mathrm{d}x$. Since the integral is independent of the triangulation, a precomputed value avoids the recalculation on each level. If the matrix `Stab` is provided, it is used as an additive bilinear form in the energy functional. The function expects a matrix from one of the stabilisation functions above, e.g. from `stabWBCC`. For testing purposes, the exact choice of the minimisation algorithm can be influenced with the argument `optimType`.

The function returns the nodal values of the computed solution in the output argument `u` and its energy value in `E`. The numbers of required iterations and of energy functional evaluations are returned in `niter` and `nfev`. The output argument `ddEcond` contains the condition number of the Hessian matrix of the energy functional in the solution point `u`.

```
1  function [u,E,niter,nfev,ddEcond] = solveP1Nonlinear(        ...
                        u,W,f,g,alpha,fDegree,gDegree,f2int, ...
                    c4n,n4e,n4sDb,Stab,area4e,P1Grad,optimType)
   % solveP1Nonlinear
5  % [u,E,niter,nfev] = solveP1Nonlinear(
   %      u,W,f,g,alpha,fDegree,gDegree,f2int,c4n,n4e,n4sDb,Stab,
   %                                    area4e,P1Grad,optimType)
   %
   % Solves   E(v) = int W(Dv)+alpha*|v-f|^2-gv dx  -->  min
10 %
   % u : Initial solution [#n 1]
   % W : Energy density fctn handle [w,dw,ddw] = W(Dv)
   % (f,g) : fctn handles [f] = f(x)  [g] = g(x), default to @0
   % (alpha) : coefficient, defaults to 0
15 % f/gDegree : Polynomial degrees of f,g for integration
```

```
% (f2int) : int f^2 dx (will be computed if not given)
% c4n, n4e, n4sDb : Grid stuff (c4n=[#n 2])
% (Stab) : sparse stabilization matrix [#n #n]
% (area4e, P1Grad) : More grid stuff
% (optimType) : See minWrapper for types
%
% u : solution [#n]
% E : energy of solution
% niter,nfev : Iteration and f-eval count of optimization
% ddEcond : 2,2-condition of Hessian in final solution point

% (C) 2009--2012 W.Boiger, HU Berlin
% Licensed under GNU GPL 3+. No warranty! See LICENSE.txt .

defaultArgIn('f',[]);
defaultArgIn('g',[]);
defaultArgIn('alpha',0);
defaultArgIn('f2int',[]);
defaultArgIn('Stab',[]);
defaultArgIn('area4e',[]);
defaultArgIn('P1Grad',[]);
defaultArgIn('optimType',[]);
defaultArgIn('M1fg',[]);
defaultArgIn('H',[]);
% H will be the matrix corresponding to the term  int v*v dx
% M1fg will be the vector corresponding to the term
%    int -(2*alpha*f+g)*v
nrNodes = size(c4n,1);
DbNodes = unique(n4sDb);
dof = setdiff(1:nrNodes,DbNodes);
udof = u(dof);
uDbNodes = u(DbNodes);
% Check for special conditions
if alpha==0
  f = [];
  H = sparse(nrNodes,nrNodes);
end
if isempty(f) && isempty(g)
  M1fg = zeros(nrNodes,1);
end
if isempty(f)
  fDegree = 0;
  f2int = 0;
  f = @(x)zeros(size(x,1),1);
end
if isempty(g)
  gDegree = 0;
  g = @(x)zeros(size(x,1),1);
end
% Precompute a lot of things
defaultArgIn('area4e','computeArea4e(c4n,n4e)');
defaultArgIn('P1Grad','computeP1Grad(c4n,n4e,area4e)');
% Compute f2int = int f^2 dx
if isempty(f2int)
  integrandf2 = @(n4p,Gpts4p,Gpts4ref)(f(Gpts4p).^2);
  f2int = integrate(c4n,n4e,integrandf2,2*fDegree,area4e);
  f2int = sum(f2int);
end
% H(i,j) = 2*\int phi_i phi_j dx
% It holds: \int_T phi_i phi_j dx = |T|/12  if i~=j
%                                  = |T|/6   if i==j
if isempty(H)
  H = area4e*[2 2 2 1 1 1 1 1 1 1];
  H = sparse(n4e(:,[1 2 3 1 2 3 1 2 3]),                    ...
             n4e(:,[1 2 3 3 3 2 2 1 1]),H,nrNodes,nrNodes);
  H = (alpha/6)*H;
end
% M1fg(j) = - int (2 alpha f+g) phi_j dx
% ==> dot(M1fg,u) ~~ int -(2 alpha f + g) u dx
if isempty(M1fg)
```

```
    integrandM1fg = @(n4p,Gpts4p,Gpts4ref)                    ...
                              ((2*alpha*f(Gpts4p)+g(Gpts4p))* ...
                          [1-sum(Gpts4ref(1:2)) Gpts4ref([1 2])]);
    M1fg = integrate(c4n,n4e,integrandM1fg,                   ...
                                  max(fDegree,gDegree)+1,area4e);
    M1fg = -accumarray(n4e(:),M1fg(:),[nrNodes 1]);
  end
  % Add Stabilisation to H
  if ~isempty(Stab)
    H = H+Stab;
  end
  clear('Stab');
  % Call core solver
  EffEnergyFcn = @(udof)Energy(udof,uDbNodes,dof,DbNodes,     ...
                                     n4e,area4e,P1Grad,W,M1fg,H);
  [udof,E,niter,nfev] = minWrapper(EffEnergyFcn,udof,optimType);
  u(dof) = udof;
  E = E+alpha*f2int;
  if nargout>4
    [dummy1,dummy2,ddE] = EffEnergyFcn(udof);
    ddEcond = condWrapper(ddE);
  end
end


function c = condWrapper(A)
  % Return condition number of A
  if length(A)<3  % Octave's eigs cannot handle n<3
    A = eig(full(A));
    emax = max(A);
    emin = min(A);
  else
    emax = eigs(A,1,'lm');
    if exist('OCTAVE_VERSION','builtin')
      A = full(A);  % My Octave hasn't umfpack support
    end
    try
      emin = eigs(A,1,'sm');
    catch
      emin = 0;  % eigs fails if cond->Inf
    end
  end
  c = abs(emax/emin);
end


function [E,dE,ddE] =                                         ...
       Energy(udof,uDbNodes,dof,DbNodes,n4e,area4e,P1Grad,W,G,H)
  % G(j) = - int (2f+g)*phi_j dx  = linear part
  % H(i,j) = 2*int phi_i phi_j dx = Hessian (up to W)
  if (nargout==0)
    return;
  end
  u = zeros(size(udof,1)+size(uDbNodes,1),1);
  u(dof) = udof;
  u(DbNodes) = uDbNodes;
  du = dot(P1Grad,reshape([u(n4e);u(n4e)],size(n4e,1),2,3),3);
  switch nargout
    case 1
      w = W(du);
    case 2
      [w,dw] = W(du);
    case 3
      [w,dw,ddw] = W(du);
    otherwise
      error('Can''t satisfy requested number of out arguments');
  end
  E = dot(area4e,w)+dot(G,u)+dot(u,H*u)/2;
  if (nargout<2)
    return;
```

```
    end
    dE = (area4e*[1 1]).*dw;
    dE = reshape([dE dE dE],size(dE,1),size(dE,2),3);
    dE = dot(dE,P1Grad,2);
160 dE = accumarray(n4e(:),dE(:),[size(u,1) 1])+G+H*u;
    dE = dE(dof);
    if (nargout<3)
      return;
    end
165 ddw = (area4e*[1 1 1]).*ddw;
    for k=1:3
      for j=k:3
        h = dot(P1Grad(:,:,k).*P1Grad(:,:,j),ddw(:,[1 3]),2)+  ...
            dot(P1Grad(:,[1 2],k),P1Grad(:,[2 1],j),2).*ddw(:,2);
170     H = H+sparse(n4e(:,k),n4e(:,j),h,size(H,1),size(H,2));
        if k~=j
          H = H+sparse(n4e(:,j),n4e(:,k),h,size(H,1),size(H,2));
        end
      end
175 end
    ddE = H(dof,dof);
  end
```

B.3 Stabilisation

The function `stabWBCC` implements the stabilisation a_ℓ of (3.53) (page 61), i.e.,

$$a_\ell(v_\ell, w_\ell) = H_\ell^{\gamma+1} \sum_{F \in \mathcal{F}_\ell^\Omega} h_F^{-1} \int_F [\mathrm{D}v_\ell]_F : [\mathrm{D}w_\ell]_F \, \mathrm{d}s$$

for $v_\ell, w_\ell \in \mathcal{S}_1(\mathcal{T}_\ell)$.

```
function S = stabWBCC(c4n,n4e,gamma,P1Grad,e4s,maxLength4s)
```

The only required input arguments are `c4n` and `n4e`, which describe the triangulation. The input argument `gamma` defaults to 1. The remaining input parameters are derived from the triangulation data unless the caller provides them explicitely.

```
1  function S = stabWBCC(c4n,n4e,gamma,P1Grad,e4s,maxLength4s)
   % stabWBCC
   % S = stabWBCC(c4n,n4e[,gamma,P1Grad,e4s,maxLength4s])
   %
5  % Computes the matrix representing the bilinear from of the
   % WBCC stabilisation ((2.3) in [BC,2010]):
   %   a(u,v) = max(h_F)^(gamma+1)\sum_F\int_F [Du].[Dv]dx/hF

   % (C) 2009--2012 W.Boiger, HU Berlin
10 % Licensed under GNU GPL 3+. No warranty! See LICENSE.txt .

   defaultArgIn('gamma',1);
   defaultArgIn('P1Grad','computeP1Grad(c4n,n4e)');
   defaultArgIn('e4s','computeE4s(n4e)');
15 defaultArgIn('maxLength4s',...
                'max(computeLength4s(c4n,computeN4s(n4e)))');
   e4s = e4s(logical(e4s(:,2)),:);
   nrNodes = max(n4e(:));
   nrSides = size(e4s,1);
20 s4s = (1:nrSides)'*[1 1 1];
   % Given u4n, Gx*u4n is the jump of the x-element of the
   % gradient of u4n on each side of the grid
   Gx = sparse(s4s,n4e(e4s(:,1),:),                          ...
               squeeze(P1Grad(e4s(:,1),1,:)),nrSides,nrNodes) ...
```

```
        -sparse(s4s,n4e(e4s(:,2),:),                          ...
                squeeze(P1Grad(e4s(:,2),1,:)),nrSides,nrNodes);
    Gy = sparse(s4s,n4e(e4s(:,1),:),                          ...
                squeeze(P1Grad(e4s(:,1),2,:)),nrSides,nrNodes) ...
        -sparse(s4s,n4e(e4s(:,2),:),                          ...
                squeeze(P1Grad(e4s(:,2),2,:)),nrSides,nrNodes);
    S = Gx'*Gx+Gy'*Gy;
    S = (maxLength4s^(1+gamma))*S;
end
```

Remark on the Flux Error Estimator

Due to the additional stabilisation term in the energy functional, the residual of the discrete problem does not satisfy the Galerkin orthogonality. Hence the proofs of reliability of the residual-based error estimator $\eta_{\mathrm{R},q,\ell}$ and the averaging error estimator $\eta_{\mathrm{A},q,\ell}$ do not apply to the stabilised discrete problem (see Section 4.3, page 78, for details). In an effort to provide reliable a posteriori error estimation, the thesis introduces the flux error estimator $\eta_{\mathrm{F},q,\ell}$, whose reliability is independent of the Galerkin orthogonality. The MATLAB implementation minimises a nonlinear functional amongst the space of Raviart-Thomas functions. It contains 373 lines of code and is therefore too long to be displayed in this appendix chapter. Refer to the file `estimateFlux.m` on the disc.

B.4 Content of the Software Archive

The Compact Disc attached to the thesis contains the following files.

```
GNUGPLv3.txt
LICENSE.txt
P0AveragingP1.m
afemLoadLevel.m
afemLoop.m
afemPlot1.m
afemPlot1Ndof.m
afemPlot2.m
afemPlot3.m
afemPlotCore.m
afemPostprocess.m
afemRun.m
afemSaveLevel.m
cckj_W.m
cckj_Wnc.m
cckj_f.m
cckj_g.m
cckj_pp.m
cckj_run.m
cckj_u.m
computeArea4e.m
computeArea4n.m
computeE4n.m
computeE4s.m
computeLength4s.m
computeMid4s.m
computeN4s.m
computeNormal4s.m
computeP1Grad.m
computeS4e.m
computeS4n.m
computeTangent4s.m
defaultArgIn.m
estimateFlux.m
estimateResidual.m
estimateSigmaAveragingP1.m
geometryRectangle.m
getRHSfcn.m
integrate.m
make_afemplot_table.py
make_afemplot_tabular.py
minWrapper.m
od_W.m
od_f.m
od_pp.m
od_run.m
od_u.m
oscillation.m
poisson_W.m
poisson_f.m
poisson_pp.m
poisson_run.m
poisson_u.m
refineRGB.m
refineUniformRed.m
sb_W.m
sb_f.m
sb_pp.m
sb_run.m
sb_u.m
solveP1Nonlinear.m
stabBCPP1.m
stabBCPP2.m
stabBCPP3.m
stabWBCC.m
```

C Common Notation

This appendix chapter describes the notation which is used throughout the thesis.

Theorems, Definitions and alike are numbered consecutively, within their sections, e.g., Theorem (2.2.3) follows Assumption (2.2.2) in Section 2.2. Figures, tables, algorithms and equations are numbered within their chapters, e.g., Equation (3.1) is part of Chapter 3.

The following table lists mathematical symbols which appear regularly in the preceding chapters, along with the number of the page on which they are introduced (where applicable).

Elementary Notation

$\mathbb{N}$		positive integers, i.e., $\{1, 2, \dots\}$
$\mathbb{N}_0$		nonnegative integers, i.e., $\{0, 1, 2, \dots\}$
1	27	the unit element in ring structures with respect to multiplication/ concatenation, e.g., real numbers, matrices or function operators
$]a, b[$		*open* interval $\{x \in \mathbb{R} : a < x < b\}$
$[a, b]$		*closed* interval $\{x \in \mathbb{R} : a \leqslant x \leqslant b\}$
a_+	25	$\max\{0, a\}$
$\lfloor x \rfloor$	18	the largest integer which is less than or equal to $x \in \mathbb{R}$
$\lceil x \rceil$	18	the smallest integer which is greater than or equal to $x \in \mathbb{R}$
$a \cdot b$		ℓ^2 scalar product $\sum_j a_j b_j$ of two vectors $a, b \in \mathbb{R}^d$, irrespective of their orientation
$A : B$		matrix inner product, i.e., $\sum_{j,k} A_{j,k} B_{j,k}$
$\lesssim, \gtrsim$	19	$\leqslant, \geqslant$, up to a positive constant
$\approx$	19	equivalent; $A \approx B \iff A \lesssim B \lesssim A$
$\subset$		subset; equality is permitted
$\lvert X \rvert$		absolute value of a real number $X \in \mathbb{R}$; ℓ^2 norm of a vector $X \in \mathbb{R}^d$; Frobenius-norm $\sqrt{X : X}$ of a matrix X; positive Lebesgue-measure of a set $X \subset \mathbb{R}^d$; finite $(d-1)$-dimensional Hausdorff measure of a set $X \subset \mathbb{R}^d$

Set-Related Notation

$\varnothing$		the empty set
$\#X$		number of elements of the set X (cardinality)
$\operatorname{diam}(X)$	19	diameter of $X \subset \mathbb{R}^d$
$\operatorname{conv} X$		convex hull of $X \subset \mathbb{R}^d$

$\operatorname{int} X$	15	topological interior set of the set X
$\overline{X}$, $\overline{X}^{\|\cdot\|}$		topological closure of the set X with respect to a canonical topology, or the topology of the norm $\|\cdot\|$
∂X	14	topological boundary of X, i.e., $\overline{X}\setminus \operatorname{int}(X)$
n_Γ	14	unit normal vector of surface $\Gamma \subset \mathbb{R}^d$
$[u]_\Gamma$	18	jump of the function u along the surface Γ

Derivatives and Integrals

$\mathrm{D}u$, D^2u	15	first and second derivative of u
Δu		Laplacian of u
$\operatorname{div} u$		divergence of u, that is, the matrix trace of $\mathrm{D}u$
$\fint$	17	mean value integral; $\fint_\Omega u\mathrm{d}x = \int_\Omega u\mathrm{d}x/\lvert\Omega\rvert$

Function Spaces

p', q', r'	20	Hölder conjugate of $p, q, r \in [1,\infty]$; e.g., $1/p + 1/p' = 1$
$\mathcal{C}^k$		space of k times continuously differentiable functions
$\mathcal{C}^{k,1}$	13	space of functions whose k-th derivative is Lipschitz continuous
$\mathcal{D}$	13	space of smooth (infinitely often continuously differentiable) function with compact support
L^p	14	Lebesgue space
L^{s+}	15	space of functions in $L^{s+\varepsilon}$ for $\varepsilon > 0$
$W^{s,p}$	14	Sobolev space (see Definitions (2.1.1), (2.1.2), (2.1.9))
H^s	15	Sobolev space $W^{s,2}$
$H(\operatorname{div})$	15	Sobolev space of function in L^2 whose divergence is also in L^2
H^{s+}	15	space of functions in $H^{s+\varepsilon}$ for $\varepsilon > 0$
P_k	34	space of polynomial functions of degree $\leqslant k$

Triangulations

$\mathcal{T}$, $\mathcal{T}_\ell$	32	triangulation (set of elements), of the level $\ell \in \mathbb{N}_0$
$\mathcal{F}$, $\mathcal{F}_\ell$	32	set of sides (edges if $d = 2$, faces if $d = 3$) of the triangulations $\mathcal{T}$ and $\mathcal{T}_\ell$
$\mathcal{F}^\Omega$, $\mathcal{F}_\ell^\Omega$	32	set of interior sides of the triangulations $\mathcal{T}$ and $\mathcal{T}_\ell$
$\mathcal{F}^{\partial\Omega}$, $\mathcal{F}_\ell^{\partial\Omega}$	32	set of boundary sides of the triangulations $\mathcal{T}$ and $\mathcal{T}_\ell$
$\mathcal{N}$, $\mathcal{N}_\ell$	32	set of nodes of the triangulation $\mathcal{T}$ and $\mathcal{T}_\ell$
ω_z	33	patch of a node $z \in \mathcal{N}_\ell$

ω_F	33	patch of a side $F \in \mathcal{F}$
h_T, h_F	33	diameter of the element $T \in \mathcal{T}_\ell$, diameter of the side $F \in \mathcal{F}_\ell$
h_ℓ	34	mesh size function
H_ℓ	34	global mesh size $\max_{T\in\mathcal{T}_\ell} h_T$
$\mathcal{S}_1$	34	space of conforming P_1 finite element functions
$RT_0(\mathcal{T}_\ell)$	37	space of Raviart-Thomas finite element functions
I_ℓ	35	nodal interpolation operator on $\mathcal{T}_\ell$
Π_ℓ	36	$\mathcal{T}_\ell$-piecewise L^2 projection
Σ_ℓ	36	averaging interpolation operator
$I_{\mathrm{F},\ell}$	38	Fortin interpolation operator
B_ℓ	46	boundary extension operator from Bartels et al. (2004a)
$\operatorname{osc}_{\ell,p}(u)$	37	oscillation of u on $\mathcal{T}_\ell$
$\mathrm{D}^2_\ell u$, $\Delta_\ell u$	35	$\mathcal{T}_\ell$-piecewise second derivative and Laplacian of u
$\mathrm{D}^2_{\ell,\partial\Omega} u$	43	$\mathcal{F}_\ell^{\partial\Omega}$-piecewise $(d-1)$-dimensional second derivative of u on $\partial\Omega$

Minimisation Model Problem

u_D, $u_{D,\ell}$	21, 40	function which encodes Dirichlet boundary conditions
$\mathcal{A}$, $\mathcal{A}_\ell$	21, 40	admissible sets of function for the minimisation model problems
$E^{\star\star}$	21	convex(ified) energy of the minimisation model problem
$W^{\star\star}$, S	21, 21	convex(ified) energy density of the minimisation model problem, and its derivative
f, g	21	lower-order terms of the minimisation model problem
σ, σ_ℓ	21, 40	continuous and discrete stress tensors
Λ, Λ_ℓ	21, 40	derivatives of the lower-order terms of the continuous and discrete minimisation model problem
a_ℓ, $\lvert\!\lvert\!\lvert\cdot\rvert\!\rvert\!\rvert_\ell$	61	stabilisation function and its associated norm

Bibliography

Jochen Alberty, Carsten Carstensen, and Stefan A. Funken. Remarks around 50 lines of Matlab: short finite element implementation. *Numer. Algorithms*, 20(2-3):117–137, 1999.

Sören Bartels. *Numerical Analysis of Some Non-Convex Variational Problems*. Ph.D. thesis, Christian-Albrechts Universität zu Kiel, Kiel, Germany, 2001. `http://eldiss.uni-kiel.de/macau/receive/dissertation_diss_00000519`.

Sören Bartels and Carsten Carstensen. A convergent adaptive finite element method for an optimal design problem. *Numer. Math.*, 108:359–385, December 2007.

Sören Bartels, Carsten Carstensen, and Georg Dolzmann. Inhomogeneous Dirichlet conditions in a priori and a posteriori finite element error anylysis. *Numer. Math.*, 99(1): 1–24, 2004a.

Sören Bartels, Carsten Carstensen, Petr Plecháč, and Andreas Prohl. Convergence for stabilisation of degenerate convex minimsation problems. *IFB*, 6(2):253–269, 2004b.

Wolfgang Boiger and Carsten Carstensen. On the strong convergence of gradients in stabilised degenerate convex minimisation problems. *SIAM J. Numer. Anal.*, 47(6): 4569–4580, 2010.

Wolfgang Boiger and Carsten Carstensen. Stabilised FEM for degenerate convex minimisation problems under weak regularity assumptions. 2012+. Humboldt-Universtiät Preprint 2012-2 `http://www2.mathematik.hu-berlin.de/publ/pre/2012/P-12-02.pdf`. Submitted for publication.

Oskar Bolza. Some instructive examples in the calculus of variations. *Bull. Amer. Math. Soc.*, 9(1):1–10, 1902.

Dietrich Braess. *Finite elements: Theory, fast solvers, and applications in solid mechanics*. Cambridge University Press, 2007.

Susanne Cecelia Brenner and Larkin Ridgway Scott. *The mathematical theory of finite element methods. 2nd ed.* Texts in Applied Mathematics. 15. Berlin: Springer. xv, 361 p, 2002.

Franco Brezzi and Michel Fortin. *Mixed and Hybrid Finite Element Methods*. Springer series in computational mathematics. Springer-Verlag, New York, 1991.

Carsten Carstensen. Quasi-interpolation and a posteriori error analysis in finite element methods. *M2AN Math. Model. Numer. Anal.*, 33(6):1187–1202, 1999.

Carsten Carstensen. Numerical analysis of microstructure. In *Theory and numerics of differential equations (Durham, 2000)*, Universitext, pages 59–126. Springer, Berlin, 2001.

Carsten Carstensen. All first-order averaging techniques for a posteriori finite element error control on unstructured grids are efficient and reliable. *Math. Comp.*, 73(247): 1153–1165, 2004a.

Carsten Carstensen. An adaptive mesh-refining algorithm allowing for an H^1-stable L^2-projection onto Courant finite element spaces. *Constr. Approx.*, 20(4):549–564, 2004b.

Carsten Carstensen. Modelling and simulation of microstructure evolution. Script for EPSRC Summer School June 26–30, 2006, June 2006.

Carsten Carstensen. Finite element method. Yonsei Lectures at the WCU Department Computational Science and Engineering. Yonsei University, 120-749 Seoul, Korea. Unpublished Lecture Notes., 2009.

Carsten Carstensen and Max Jensen. Averaging techniques for reliable and efficient a posteriori finite element error control: Analysis and applications. *CONM*, (383):15–34, 2006.

Carsten Carstensen and Katrin Jochimsen. Adaptive finite element methods for microstructures? Numerical experiments for a 2-well benchmark. *Computing*, 71:175–204, 2003.

Carsten Carstensen and Christian Merdon. Effective postprocessing for equilibration a posteriori error estimators. *Numer. Math.*, pages 1–35, 2012.

Carsten Carstensen and Stefan Müller. Local stress regularity in scalar non-convex variational problems. *SIAM J. Math. Anal.*, 34(2):495–509, 2002.

Carsten Carstensen and Numerical Analysis Group, HU Berlin. AFEM. unpublished MATLAB software package, 2009.

Carsten Carstensen and Petr Plecháč. Numerical solution of the scalar double-well problem allowing microstructure. *Math. Comp.*, 66(219):997–1026, 1997.

Carsten Carstensen, David Günther, and Hella Rabus. Mixed finite element method for a degenerate convex variational problem from topology optimization. *SIAM J. Math. Anal.*, 50(2):522–543, 2012.

José Manuel Cascón, Christian Kreuzer, Ricardo Horacio Nochetto, and Kunibert G. Siebert. Quasi-optimal convergence rate for an adaptive finite element method. *SIAM J. Numer. Anal.*, 46(5):2524–2550, 2008.

Michel Chipot and Lawrence Craig Evans. Linearisation at infinity and Lipschitz estimates for certain problems in the calculus of variations. *Proc. Roy. Soc. Edinburgh Sect. A*, 102 (3–4):291–303, 1986.

Philippe Gaston Ciarlet. *The Finite Element Method for Elliptic Problems*. Society for Industrial Mathematics, April 2002. ISBN 0898715148.

Thomas Frederick Coleman and Yuying Li. On the convergence of interior-reflective Newton methods for nonlinear minimization subject to bounds. *Math. Programming*, 67: 189–224, 1994.

Thomas Frederick Coleman and Yuying Li. An interior trust region approach for nonlinear minimization subject to bounds. *SIAM J. Optim.*, 6(2):418–445, 1996.

Bernard Dacorogna. *Direct methods in the calculus of variations*. Applied Mathematical Sciences 78. Springer., 1989.

Bernard Dacorogna. *Introduction to the calculus of variations*. Imperial College Press, 2004.

Bernard Dacorogna. *Direct methods in the calculus of variations. 2nd ed.* Applied Mathematical Sciences 78. Berlin: Springer. xii, 2008.

Georg Dolzmann. *Variational Methods for Crystalline Microstructure — Analysis and Computation*. Springer, 2003.

Willy Dörfler. A convergent adaptive algorithm for Poisson's equation. *SIAM J. Numer. Anal.*, 33(3):1106–1124, 1996.

Lawrence Craig Evans. *Partial Differential Equations (Graduate Studies in Mathematics, V. 19) GSM/19*. American Mathematical Society, June 1998. ISBN 0821807722.

Lawrence Craig Evans and Ronald Francis Gariepy. *Measure Theory and Fine Properties of Functions*. Studies in Advanced Mathematics. CRC Press, 1992.

Jonathan Goodman, Robert Vita Kohn, and Luis Reyna. Numerical study of a relaxed variational problem from optimal design. *Comput. Methods Appl. Mech. Engrg.*, 57: 107–127, August 1986.

Pierre Grisvard. *Elliptic problems in nonsmooth domains*, volume 24 of *Monographs and Studies in Mathematics*. Pitman (Advanced Publishing Program), Boston, MA, 1985. ISBN 0-273-08647-2.

David Hilbert. Mathematische probleme. In *Nachrichten von der Gesellschaft der Wissenschaften zu Göttingen, Mathematisch-Physikalische Klasse*, volume 1900, pages 253–297, Göttingen, 1900.

Michael Karkulik, David Pavlicek, and Dirk Praetorius. On 2D newest vertex bisection: Optimality of mesh-closure and H^1-stability of L_2-projection. ASC report 10/2012, Institute for Analysis and Scientific Computing, Vienna University of Technology, 2012.

Bernhard Kawohl, Jana Stará, and Gabriel Wittum. Analysis and numerical studies of a problem of shape design. *Arch. Rational Mech. Anal.*, 114(4):349–363, 1991.

Robert Vita Kohn and Gilbert Strang. Optimal design and relaxation of variational problems I–III. *Comm. Pure Appl. Math.*, 39(1–3):113–137,139–182,353–377, 1986.

Christian Kreuzer and Kunibert G. Siebert. Decay rates of adaptive finite elements with Dörfler marking. *Numer. Math.*, 117(4):679–716, 2011.

Mitchell Luskin. On the computation of crystalline microstructure. In *Acta numerica, 1996*, volume 5 of *Acta Numer.*, pages 191–257. Cambridge Univ. Press, Cambridge, 1996.

John Brand Martin. *Plasticity: Fundamentals and General Results*. MIT Press, 1975.

Roy A. Nicolaides and Noel John Walkington. Strong convergence of numerical solutions to degenerate variational problems. *Math. Comp.*, 64(209):117–127, 1995.

Pablo Pedregal. *Parametrized Measures and Variational Principles*. Progress in nonlinear differential equations and their applications. Birkhäuser, 1997.

Andreas Prohl. *Computational Micromagnetism*. Advances in Numerical Mathematics. B.G. Teubner, 2001.

Pierre-Arnaud Raviart and Jean-Marie Thomas. A mixed finite element method for 2-nd order elliptic problems. In Ilio Galligani and Enrico Magenes, editors, *Mathematical Aspects of Finite Element Methods*, volume 606 of *Lecture Notes in Mathematics*, pages 292–315. Springer Berlin / Heidelberg, 1977.

Sergey Igorevich Repin, Stefan Sauter, and Anton Smolianski. A posteriori error estimation for the dirichlet problem with account of the error in the approximation of boundary conditions. *Computing*, 70(3):205–233, 2003.

Tomáš Roubíček. *Relaxation in optimization theory and variational calculus*, volume 4 of *de Gruyter Series in Nonlinear Analysis and Applications*. Walter de Gruyter & Co., Berlin, 1997.

Andrei Nikolaevich Tikhonov, Alexander Vladimirovich Goncharsky, Viacheslav Vasilievich Stepanov, and Anatoly Grigorievich Yagola. *Numerical Methods for the Solution of Ill-Posed Problems*, volume 328 of *Mathematics and its Applications*. Kluwer Academic Publishers Group, Dordrecht, 1995. Translated from the 1990 Russian original by R.A.M. Hoksbergen and revised by the authors.

Jan Valdman. Minimization of functional majorant in a posteriori error analysis based on $H(\mathrm{div})$ multigrid-preconditioned cg method. *Advances in Numerical Analysis*, 2009:15, 2009.

Andreas Veeser and Rüdiger Verfürth. Explicit upper bounds for dual norms of residuals. *SIAM J. Numer. Anal.*, 47(3):2387–2405, 2009.

Rüdiger Verfürth. A posteriori error estimates for nonlinear problems. Finite element discretizations of elliptic equations. *Math. Comp.*, 62(206):445–475, 1994.

Rüdiger Verfürth. *A Review of A Posteriori Error Estimation and Adaptive Mesh-Refinement Techniques*. Advances in numerical mathematics. Wiley-Teubner, 1996.

Laurence Chisholm Young. Necessary conditions in the calculus of variations. *Acta Math.*, 69(1):229–258, 1938.

Laurence Chisholm Young. Generalized surfaces in the calculus of variations. *Ann. of Math. (2)*, 43:84–103, 530–544, 1942.

Laurence Chisholm Young. *Lectures on the calculus of variations and optimal control theory*. W. B. Saunders Co., Philadelphia, 1969.

List of Figures

List of Tables

List of Algorithms

Selbstständigkeitserklärung

Ich erkläre, dass ich die vorliegende Arbeit selbstständig und nur unter Verwendung der angegebenen Literatur und Hilfsmittel angefertigt habe.

Berlin, den 31. Okt. 2012 Wolfgang Josef Boiger